INVESTIGATING THE ROLE OF THE INNER TEGUMENT PROTEINS IN HSV-1 INFECTION

BY

ASHLEY PETER ELLIOT ROBERTS

A THESIS PRESENTED FOR THE DEGREE OF DOCTOR OF PHILOSOPHY

IN THE FACULTY OF BIOMEDICAL AND LIFE SCIENCES

AT THE UNIVERSITY OF GLASGOW

MRC VIROLOGY UNIT
INSTITUTE OF VIROLOGY
CHURCH STREET
GLASGOW
G11 5JR

SEPTEMBER 2009

Abstract

Extensive study of the prototypical alphaherpesvirus, Herpes simplex virus type-1 (HSV-1), has revealed much about its biology and structure. The characteristic virion comprises a DNA containing capsid surrounded by consecutive layers of proteinaceous tegument and lipid envelope. Our understanding of the capsid is relatively advanced compared to that of the tegument. The tegument has previously been thought of as an amorphous accumulation of protein filling the space between the capsid and envelope.

The tegument has been subdivided into the inner and the outer tegument with the proteins pUS3, pUL36 and pUL37 assigned to the inner tegument. A number of studies have pointed to the essential role of both pUL36 and pUL37 in virion morphogenesis by demonstrating a block on secondary envelopment in the absence of either protein. However, the phenotypes attributable to deletion mutants of UL36 and UL37 varied between HSV-1 and the related alphaherpesvirus, Pseudorabies virus (PrV), and between different PrV mutants. In particular the phenotypes of an HSV-1 mutant unable to express functional pUL36 due to an internal deletion between amino acids 362-1555 (KΔUL36) and PrV mutants lacking UL36 showed considerable variation. Both accumulated DNA filled cytoplasmic nucleocapsids, however, those produced by KΔUL36 formed small aggregates within the cytoplasm in contrast to PrV where the capsids were dispersed. UL36 and UL37 deletion mutants were also reported to retain capsids to the nucleus implying a function in nuclear exit.

In order to clarify the seeming disparities between these mutants, novel deletions of both UL36 and UL37 were engineered into HSV-1 17(+). The deletion of UL36 encompassed the entire open reading frame (ORF) while the UL37 deletion removed all but the 3 most C terminal amino acids. Examination by EM revealed that these mutants recapitulate the block on secondary envelopment that is characteristic of inner tegument mutants reported to date, with accumulation of nucleocapsids within the cytoplasm. This examination revealed that the cytoplasmic capsids of the complete UL36 deletion adopted the dispersed phenotype seen in PrV suggesting the phenotype of KΔUL36 is specific to the mutation introduced. Furthermore, this analysis failed to demonstrate a retention of capsids within the nucleus in the absence of either pUL36 of pUL37, indicating that neither has a definitive role in nuclear exit, and the principle function of these proteins is within secondary envelopment.

Work presented within this thesis using IF and Immuno-EM methods shows that pUL36 is associated with the cytoplasmic clusters of capsids produced by a mutant lacking pUL37 suggesting that this may contribute to the aggregation of these capsids. Furthermore, these pUL36-decorated cytoplasmic nucleocapsids appear able to recruit pUL48 but are blocked in secondary envelopment, in contrast to PrV lacking UL37 where virions are formed but at much reduced levels. In the absence of pUL36 no tegument is recruited to cytoplasmic nucleocapsids but both minor capsid associated proteins pUL17 and pUL25 are present.

Cytoplasmic capsids of mutants lacking pUL36 and pUL37 have been isolated and examined biochemically. Cytoplasmic capsids of KΔUL36 were found to be associated with the N terminal fragment (1-361 amino acids) of pUL36 expressed by this virus, implying that a capsid binding activity is present within this region, which is the first demonstration of such an activity outside of the previously mapped activity within the 62 C terminal amino acids of pUL36. The difference in behaviour between KΔUL36 and the complete UL36 deletion also implies that the aggregation of capsids in KΔUL36 is caused by the presence of this fragment.

3 dimensional reconstruction of cytoplasmic capsids from the complete deletion mutants of UL36 and UL37 in HSV-1 17(+) was performed in an attempt to resolve questions over the identity of the density present at the vertices of capsids seen in reconstructions of intact virions. Previous reports had variously implicated pUL36 or pUL17 and pUL25 as the identity of this vertex associated density. This examination has concluded that pUL37 is not part of this density and that the weak density seen at this position in the absence of pUL36 is probably contributed by pUL17 and pUL25. Difficulties in purifying and characterising UL37 minus cytoplasmic capsids mean that the data are inconclusive but they support the proposal that pUL36 contributes to the vertex associated density seen in intact virions and may be part of a heterotrimeric complex with pUL17 and pUL25.

Assembly of L particles, structures consisting of tegument and envelope but lacking capsids, was unaffected by the deletion of either UL36 or UL37. Biochemical characterisation of purified L particles revealed that deletion of pUL36 prevents the incorporation of pUL37 and deletion of pUL37 leads to the absence of pUL36 despite their expression during infection. This suggests that incorporation of inner tegument to L particles, and envelopment of nucleocapsids, requires pUL36 and pUL37 to be present in a complex. The sole exception to this was the incorporation of the N terminal fragment of

pUL36 in KΔUL36 infection into L particles in the absence of pUL37 the mechanism for which is unknown.

Little of the role of the inner tegument proteins in initiating infection has been established. Previous studies have hinted at functions in nuclear pore complex binding and genome release, while a growing body of data implicates pUL36 and pUL37 in cytoplasmic transport of nucleocapsids. As both pUL36 and pUL37 are essential in HSV-1 virion morphogenesis a method was required to establish the defects of inner tegument deletion mutants in the initiation of infection. This was provided by infecting cells at a low multiplicity with mutant viruses (0.01pfu/cell) and subsequently fusing the cells into syncytia, in which several nuclei shared a common cytoplasm. The spread of viral DNA replication in these nuclei was tracked by fluorescence *in situ* hybridisation. In each syncytium the initially infected nucleus produces nucleocapsids that enter the common syncytial cytoplasm and have access to naïve nuclei without needing to undergo secondary envelopment. Using this system the essential role of pUL36 in the initiation of infection was confirmed and it was also shown that pUL37 is dispensable for the initiation of new cycles of viral DNA replication in naïve nuclei. The behaviour of cytoplasmic nucleocapsids within syncytia seems to be equivalent to that of incoming virion derived tegumented nucleocapsids as WT HSV-1 and HSV-1 ΔUL37 infections behaved similarly and were equally affected by treatment with nocodazole suggesting that both are undertaking similar activities.

The work presented here has helped to clarify the roles of the inner tegument proteins during virus assembly and the methods developed have extended our ability to assess the contributions of proteins essential for virion formation, in the initiation of infection. Structural analysis provided support for pUL36 as contributing to the vertex associated density and the studies presented here reinforce the idea that pUL36 may play multiple roles in the initiation of infection.

Table of Contents

Supplementary materials

Roberts, A. P. E., Abaitua, F., O'Hare, P., McNab, D., Rixon, F. J. & Pasdeloup, D. (2009). Differing Roles of Inner Tegument Proteins pUL36 and pUL37 during Entry of Herpes Simplex Virus Type 1. *Journal of Virology* **83**, 105-116.

Appendix A: Supplementary data to Table 4.2

List of tables

Tables follow page stated.

List of figures

Figures follow page stated

Acknowledgements

I would like to begin by thanking my supervisor Dr. Frazer Rixon for the opportunity to work on this aspect of herpes virology and for his unstinting advice, encouragement and not infrequent reminders of the possible throughout the course of this work. As well as for his dedication and thorough critical reading of this manuscript. I am also extremely grateful to (in no particular order) David McNab, Marion McElwee, Joyce Mitchell, Jim Aitken and Dr David Pasdeloup for their willingness to help, giving freely of their time and technical expertise and for making the Unit, and Lab 300 in particular, such an enjoyable place to work for three years. Further thanks are also due to Dr David Bhella and Rebecca Pink for their enthusiastic help and assistance in cryo-EM reconstructions of capsids, and without whom that aspect of this thesis would not have been possible.

I also owe a great deal of gratitude to the many people I know across the country, particularly in York (and those I know from my days at the University of York who have since ventured further afield), Edinburgh and London who have put up with my talking "shop" and being in the lab in mind, if not in body, whilst with them. They have all provided welcome distractions from the lab when needed, and have generously lent their spare rooms for my variously sporadic and last minute visits. Of these, particular thanks must go to Martin, Iain, Kevin and Andy, who have between them provided encouragement and diversions, as well as their own take on a PhD. Further thanks must also be given to Louise, Karl, Andrea, Matt, Nathan, Fiona, Chris, Ben and others too numerous to mention, for their hospitality and making my weekends away a welcome break.

I am also indebted to my fellow PhD students, Dan and Maureen for their advice and help, as well as humour in the course of writing up. Also, Sarah and Rebecca for their frequent hospitality and willingness to break up the day with tea and cake.

Finally, it remains for me to thank my family, whose support, encouragement and assistance have seen me through the course of this work and all that preceded it.

Author's Declaration

All the results presented in this thesis were obtained by the author's own efforts, unless stated otherwise.

Abbreviations

A

Å	Angstrom
Ad	Adenovirus
AlHV-1	Alcelaphine herpesvirus
APS	Ammonium persulphate
ATP	Adenosine triphosphate

B

BAC	Bacterial artificial chromosome
BDMA	Benzyldimethylamine
BHK	Baby hamster kidney
BHV-1	Bovine herpesvirus 1
bp	Base pair
BPP	Basic Phosphoprotein
BSA	Bovine serum albumin

C

˚C	Degrees centigrade
C	Carboxy terminus
CAV	Cell associated virus
CCSC	C capsid specific component
CCV	Channel catfish virus
CKII	Caesin kinase II
cm^2	Square centimeters
CMV	Cytomegalovirus
Cos14	Cosmid 14
cPBS	Complete phosphate buffered saline
cpe	Cytopathic effect
CRV	Cell released virus
Cryo-EM	Cryo-electron microscopy
Cryo-ET	Cryo-electron tomography
CT	Carboxy terminus

D

Da	Dalton
DABCO	1,4-Diazabicyclo[2.2.2]octane
DAPI	4′,6-Diamidino-2-phenylindole dihydrochloride
DMEM	Dulbecco's modified Eagle medium
DMSO	Dimethyl sulphoxide
DNA	Deoxyribonucleic acid
dNTP	2'-deoxynucleoside-5'-triphosphate
ds	Double stranded
DUB	Deubiquitinating enzymes

E

E	Early class gene
E. coli	*Escherichia coli*
EBV	Epstein Barr virus
ECL	Enhanced chemiluminescence
EDTA	Ethylenediamine-tetraacetic acid
EGTA	Ethylene glycol-bis(2-aminoethylether)-*N,N,N′,N′*-tetraacetic acid
EHV	Equid herpesvirus

ElHV	Elephantid herpesvirus
eIF	Eukaryotic initiation factor
EM	Electron microscopy
ER	Endoplasmic reticulum

F

FISH	Fluorescence *in situ* hybridisation

G

GaHV	Gallid herpesvirus
GAM	Goat anti mouse antibody
GAR	Goat anti rabbit antibody
GFP	Green fluorescent protein
GMEM	Glasgow modified Eagle medium
gp	Gene product

H

h	Hour
HA	Haemagglutinin
HeBS	HEPES buffered saline
HCF	Host cell factor
HCMV	Human cytomegalovirus
HEPES	4-(2-Hydroxyethyl)piperazine-1-ethanesulfonic acid
$HFFF_2$	Human foetal foreskin fibroblast
HHV	Human herpesvirus
HIV	Human immunodeficiency virus
HRP	Horse radish peroxidase
HSV	Herpes simplex virus
HVEM	Herpesvirus entry mediator

I

ICP	Infected cell polypeptide
IE	Immediate early
Ig	Immunoglobulin
IgG	Immunoglobulin G
Immuno EM	Immuno electron microscopy
IR_L	Internal repeat long
IR_S	Internal repeat short

K

Kan^R	Kanamycin resistance marker
kb	Kilobase
kbp	Kilobase pair
kDa	Kilo Dalton
KSHV	Kaposi's sarcoma herpesvirus

L

L	Late class
LAT	Latency associated transcript
LB	Luria-Bertani medium (L-Broth)

M

M	Molar
mA	Milliampers
MCP	Major capsid protein

MCS	Multiple cloning site
mg	Milligram
MHV	Murine herpesvirus
miRNA	Micro RNA
ml	Millilitre
mLAT	Minor LAT
mM	Millimolar
mm	Millimeter
MOI	Multiplicity of infection
M_r	Molecular mass
mRFP	Monomeric red fluorescent protein
mRNA	Messenger RNA
MT	Microtubule
MTOC	Microtubule organizing centre
MVE	Multi vesicular endosome

N

N	Amino terminus
ND10	Nuclear domain 10
ng	Nanogram
nm	Nanomolar
Noc	Nocodazole
NPC	Nuclear pore complex
NT	Amino terminus

O

OBP	Origin binding protein
OCT-1	Octamer binding protein-1
OD_{600}	Optical density
oriL	Origin of DNA replication in Long genome segment
oriS	Origin of DNA replication in Short genome segment
ORF	Open reading frame
OsHV-1	Oyster herpesvirus

P

pA	Poly Adenosine tail
PAA	Phosphonoacetic acid
PBS	Phosphate buffered saline
PCR	Polymerase chain reaction
PEM	Microtubule fixation buffer (PIPES-EGTA-magnesium chloride)
Pen/strep	Penicillin, streptomycin antibiotic
PFA	Paraformaldehyde
pfu	Plaque forming units
P hexon	Peripentonal hexon
pi	Post infection
PIPES	Piperazine-N,N'-bis (2-ethansulfonic acid)
PKA	Protein kinase A
PKC	Protein kinase C
PML	Promyelocytic leukaemia protein
PrV	Pseudorabiesvirus
PSSE	Preformed site of secondary envelopment

R

RE	Restriction enzyme

RFP	Red fluorescent protein
RNA	Ribonucleic acid
rpm	Revolutions per minute
RS	Rabbit skin
RSC	Rabbit skin cell

S

s	Second
SDS	Sodium dodecylsulphate
SDS PAGE	Sodium dodecylsulphate polyacrylamide gel electrophoresis
siRNA	Short interfering RNA
ss	Single stranded
STIV	*Sulfolobus* turreted icosahedral virus
SV40	Simian virus 40

T

T	Triangulation number
TBP	TATA box binding protein
TBS	Tris buffered saline
TE	Tris/EDTA
TEMED	N,N,N',N'-tetramethyethylenediamine
TF	Transcription factor
TGN	*Trans*-Golgi network
TNF	Tumor necrosis factor
TPCK	L-(Tosylamido-2-phenyl) ethyl chloromethyl ketone
TR_L	Terminal repeat long
TR_S	Terminal repeat short
ts	Temperature sensitive

U

U	Units
UL	Unique long
UM	Upper matrix protein
US	Unique short
UV	Ultraviolet

V

V	Volt
v/v	Volume/volume
vhs	Virion host shutoff
Vmw	Virion molecular weight
VP	Virion protein
VSV	Vesicular stomatitis virus
VZV	Varicella-zoster virus

W

w/v	Weight/volume
w/w	Weight/weight
WT	Wild type

µg	Microgram
µl	Microlitre
µm	Micrometer

Amino Acid Abbreviations

Amino Acid	Three letter code	One letter code
Alanine	Ala	A
Arginine	Arg	R
Asparagine	Asn	N
Aspartic acid	Asp	D
Cysteine	Cys	C
Glutamine	Gln	Q
Glutamic acid	Glu	E
Glycine	Gly	G
Histidine	His	H
Isoleucine	Ile	I
Leucine	Leu	L
Lysine	Lys	K
Methionine	Met	M
Phenylalanine	Phe	F
Proline	Pro	P
Serine	Ser	S
Threonine	Thr	T
Tryptophan	Trp	W
Tyrosine	Tyr	Y
Valine	Val	V

CHAPTER 1

INTRODUCTION

1. Introduction

1.1. Herpesvirales

Herpesviruses are highly disseminated pathogens known to infect a wide range of (probably all) vertebrates and at least one invertebrate species (Davison *et al.*, 2009; Pellett & Roizman, 2007). The description herpesvirus encompasses a large and diverse group of animal pathogens, which were originally identified and subsequently classified based on morphological features and characteristics of the life cycle. Recently this classification system has been revisited in the light of the availability of molecular sequence data from both viral genomes and amino acid sequences derived from sequenced genomes (section 1.2).

Whilst the *Herpesviridae* family shows a broad host range, each individual virus species has a single host, although hosts may be infected with several distinct herpesviruses (Pellett & Roizman, 2007). To date there are in excess of 100 reported herpesviruses (Davison *et al.*, 2009; Davison *et al.*, 2005a) which must represent only a fraction of the true numbers present in nature. Given the close virus-host species specific occurrence of these viruses it is proposed that they have co-evolved over long periods of time and as such herpesviruses are thought to be particularly well adapted to their hosts (Davison, 2002). Indeed infection of a non natural host by a herpesvirus often results in a more pronounced disease and pathology than would result from infection of the natural host (Davison, 2002).

Historically, the primary means of identifying herpesviruses was based on morphological characteristics predominantly those of the virion structure. Herpes virions are in the order of 200-250 nm in diameter and posses four distinct compartments. The viral genome of linear dsDNA is packaged into an icosahedral protein shell termed the capsid, which is in the order of 125nm in diameter. Surrounding the capsid is a proteinaceous layer called the tegument, which is thought to be relatively amorphous in terms of structure. The tegument and capsid are then ensheathed in a host derived lipid membrane containing numerous viral glycoproteins (Pellett & Roizman, 2007)(Fig. 1.1).

In addition to morphological similarities, herpesviruses share a number of characteristic biological properties, which were also used for classification these being:
i) herpesviruses encode an array of proteins and enzymes for nucleic acid metabolism and DNA synthesis.

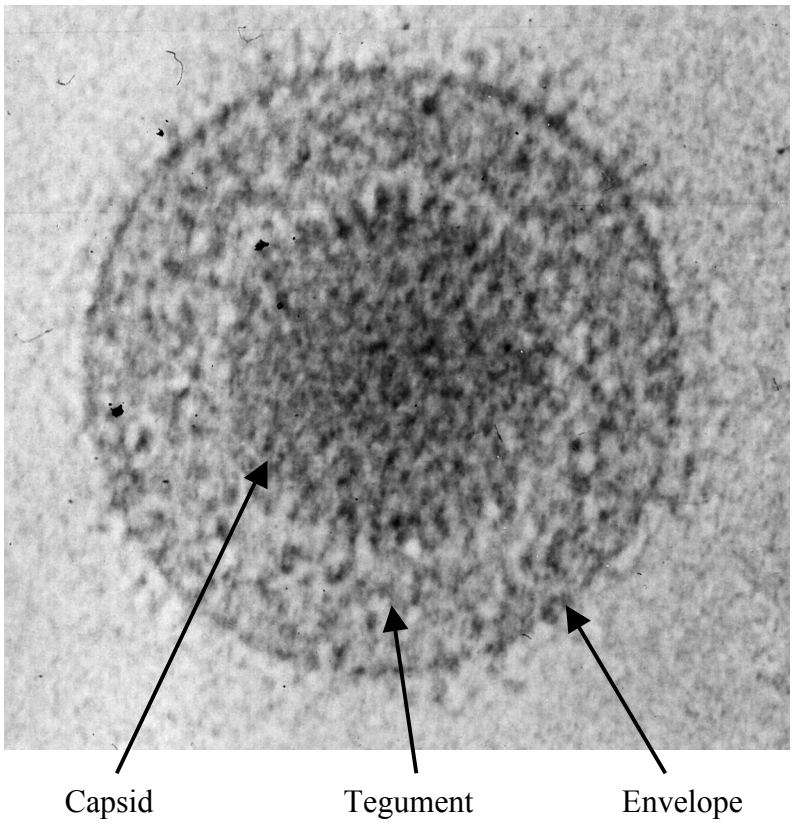

Figure 1.1: Electron micrograph of a frozen hydrated HSV-1 virion.
The virion consists of four compartments: the DNA genome, capsid, tegument and envelope. The DNA genome is contained in the capsid with the densely packaged state of the genomic DNA accounting for the electron-dense appearance of the capsid. The tegument lies between the capsid and the envelope. The envelope is visible as a thin, electron-dense layer surrounding the virion. Glycoprotein spikes protrude from the envelope. The capsid is 1250Å in diameter, while the whole virion is approximately 2000Å in diameter

This figure was reproduced with permission from W. Chiu, Baylor College of Medicine, USA.

ii) replication of viral DNA and formation of capsids occurs in the nucleus of infected cells.
iii) viral replication and release of infectious progeny is cytolytic.
iv) all well studied herpesviruses establish latent infections, in which the virus adopts a dormant state characterised by the expression of only a restricted number of viral genes, and during which no progeny virus is produced.

1.2. Classification of herpesviruses

Herpesvirus taxonomy has traditionally used virion morphological features to guide the classification of viruses as herpesviruses, with lower taxa being assigned based on biological properties. The recent explosion in the availability of molecular sequence data for viral genomes and amino acid sequences derived from those genomes has permitted the existing phylogeny of the *Herpesviridae* to be re-examined based on sequence similarity or divergence. During this re-examination remarkably little of the original classification was altered. However, although taxonomy is an inherently conservative process some alterations were made (reviewed Davison *et al.*, 2009). A notable example is Marek's disease virus-1, which causes tumour like growths in the lymphoid tissues of chickens. Marek's disease virus-1 was classified as a gammaherpesvirus given its tropism for lymphoid tissues, however DNA sequencing has shown it to be more closely related to the *alphaherpesvirinae*, and it has been reclassified accordingly (Buckmaster *et al.*, 1988).

The revised classification has lead to the establishment of the Order *Herpesvirales*, with subdivision to the families; *Herpesviridae* containing the mammalian, avian and reptilian viruses; *Alloherpesviridae* containing the fish and amphibian viruses; and *Malacoherpesviridae* containing the only described invertebrate herpesvirus (Davison *et al.*, 2009)(Fig. 1.2).

Thus within the *Herpesvirales* there are now three distinct lineages, *Herpesviridae*, *Alloherpesviridae*; and the *Malacoherpesviridae*. The majority of known herpesviruses, i.e. those which infect mammals and birds, are classified into the *Herpesviridae*. It is clear that mammalian and avian viruses are related and it is suggested that these viruses have co-evolved with their respective hosts (reviewed Davison, 2002). The *Herpesviridae* is further split into the subfamilies of the alpha-, beta-, and gamma- *herpesvirinae* (Davison *et al.*, 2009).

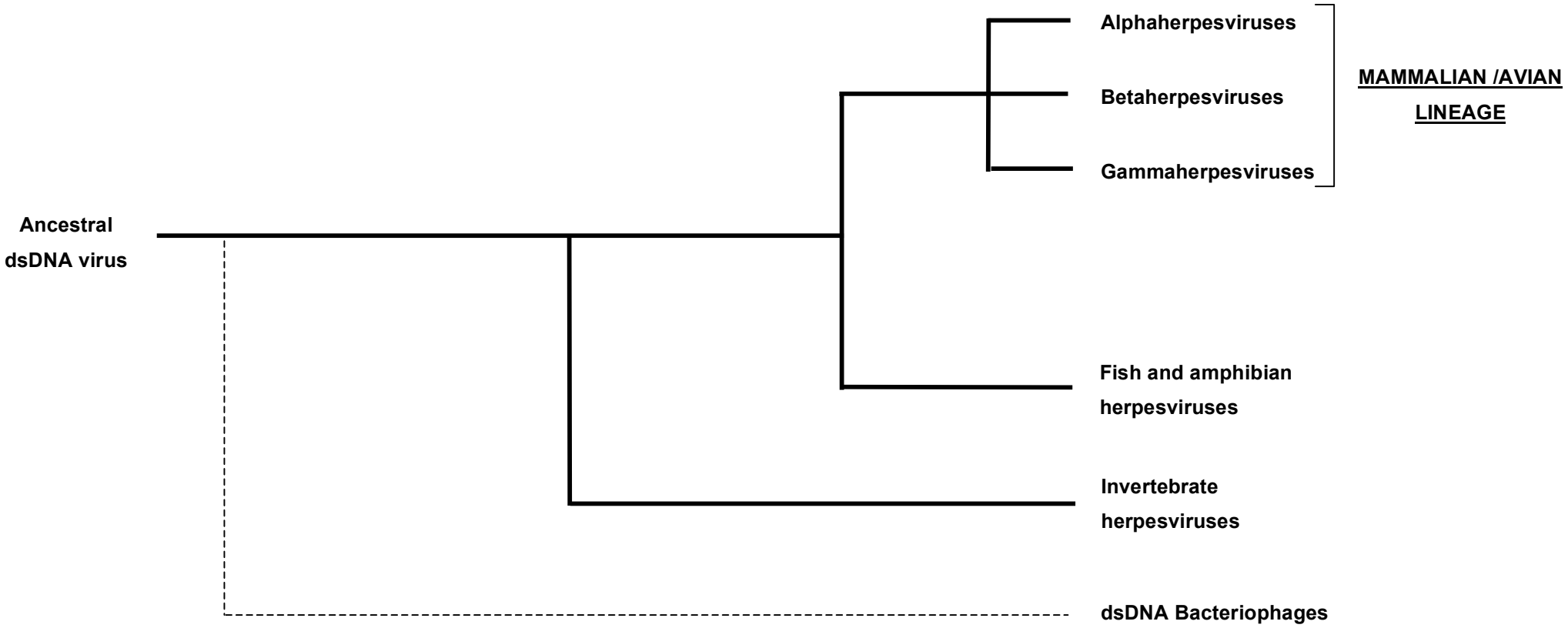
Alphaherpesviruses
Betaherpesviruses
Gammaherpesviruses
MAMMALIAN /AVIAN LINEAGE
Ancestral dsDNA virus
Fish and amphibian herpesviruses
Invertebrate herpesviruses
dsDNA Bacteriophages

Figure 1.2: Lineage map showing the evolutionary divergence of the herpesviruses. Herpesviruses that infect mammalian and avian hosts (*Herpesviridae*) are shown with their division into the alpha, beta, and gamma herpesvirus subfamilies and comprise a single lineage. A second lineage (*Alloherpesviridae*) comprises herpesviruses that infect fish and amphibians. Whilst a third lineage (*Malacoherpesviridae*) comprises the single known herpesvirus that infects an invertebrate host. A potential fourth lineage (broken line) is shown. This reflects the similarities in structure, capsid assembly, and DNA packaging observed between *Herpesvirales* and dsDNA bacteriophages (*Caudovirales*) that suggests both groups share a common ancestor. (Distances not drawn to scale).

1.2.1. Alphaherpesvirinae

Members of this sub family are characterised by their ability to infect a wide range of cell types in tissue culture, by short replication cycles (<24 hours) and efficient destruction of host cells (except for VZV). These viruses characteristically, but not exclusively, establish latent infections in the ganglia of sensory neurons. Within this subfamily there are four genera as follows with notable members listed, *Simplexvirus* containing Herpes Simplex type-1 and type-2 (HSV-1 and HSV-2), *Varicellovirus* containing Varicella-Zoster virus (VZV) and Pseudorabies virus (PrV), *Mardivirus* containing Marek's Disease virus-1 and –2 (GaHV-2 and GaHV-3) and *Iltovirus* containing Infectious laryngo-tracheitis virus (GaHV-1) (Pellett & Roizman, 2007).

1.2.2. Betaherpesvirinae

Members of the *betaherpesvirinae* exhibit a restricted host range in tissue culture, with long reproductive cycles and slow growth. Slow growth in culture leads to the establishment of carrier cultures in which cells survive after infection and infected cells become large (cytomegalia). *In vivo,* latent infection may be established in a wide range of tissues. This subfamily is split into four genera as follows with notable members listed, *Cytomegalovirus* containing Human cytomegalovirus (HCMV), *Muromegalovirus* containing Mouse cytomegalovirus (MHV-1), *Roseolovirus* containing Human herpesviruses type 6 and 7 (HHV-6 and HHV-7), and *Proboscivirus* containing Elephant endotheliotropic Herpesvirus (ElHV-1) (Pellett & Roizman, 2007).

1.2.3. Gammaherpesvirinae

Members of this subfamily display a highly restricted host range in tissue culture, with propagation limited to the family or order of the natural host. They replicate predominantly in lymphoblastoid cells although some are able to enter lytic replication in certain types of epithelial or fibroblastic cell. Infection of the natural host is generally specific for T or B lymphocytes and latent infections are established in lymphoid tissue. This subfamily is split into four genera as follows with notable members listed, *Lymphocryptovirus* containing Epstein-Barr virus (EBV), *Rhadinovirus* containing Kaposi's sarcoma herpesvirus (KSHV), *Macavirus* containing Malignant catarrhal fever virus (AlHV-1), and *Percavirus* containing Equine herpesvirus type-2 (EHV-2) (Davison *et al.*, 2009; Pellett & Roizman, 2007).

1.2.4. Fish, amphibian and invertebrate herpesviruses

Sequence data for non mammalian and avian herpesvirus has become available only comparatively recently. The herpesviruses that have now been isolated from fish and amphibians, as well as an invertebrate species (Oyster herpesvirus, OsHV-1), form two further major lineages, the *Alloherpesviridae*; and the *Malacoherpesviridae* respectively (Bernard & Mercier, 1993; Davison, 1992; 1998; 2002; Davison *et al.*, 2009)(Fig. 1.2). If the assumption is made that the evolutionary separation of these viruses matched that of their hosts it would imply that the fish and amphibian viruses diverged approximately 450 million years ago, and that the invertebrate virus diverged some 1 billion years ago (Kumar & Hedges, 1998; Wray *et al.*, 1996). Herpesviruses of fish and amphibians share a common ancestor based on evidence that they contain a shared subset of genes. The descent of OsHV-1 is much more difficult to ascertain as no other invertebrate herpesvirus has been isolated to which OsHV-1 might be compared. This virus shows a promiscuity unusual among herpesviruses, being apparently not restricted to a particular bivalve species (although this has only been seen in shellfish hatcheries) (Arzul *et al.*, 2001).

1.2.5. Relationships between the herpesviruses

The relationships between viruses within the mammalian/avian and fish/amphibian lineages are much clearer than that between the three lineages. The degree of divergence between these three lineages is so great that comparison of the amino acid sequences shows no obvious links to a common ancestor. All these viruses have a few shared functions that are ubiquitous in living organisms such as DNA polymerase, DNA helicase and protein kinases, all of which could potentially originate by independent capture from the host rather than be derived from a common ancestor. Indeed no herpesvirus specific genes seem to be detectably conserved. Rather surprisingly, in view of the current prevalence of sequence based classification, the basis for a relationship between the disparate mammalian/avian, fish/amphibian and invertebrate lineages rests largely on the historically more important characteristics of shared morphology and replication mechanisms. OsHV-1 and Channel Catfish virus (CCV) are recognised as herpesviruses because of similarities with the HSV-1 capsid structure and, in CCV, their method of DNA packaging requiring the expulsion of a scaffold protein from a preformed capsid (Davison & Davison, 1995; Davison *et al.*, 2005b). If conserved capsid morphology and DNA packaging mechanisms are accepted as a sufficient basis for assigning viruses such as CCV and OsHV-1 as Herpesviruses then it may be inferred that there was a common ancestor

from which all three lineages evolved. Greater investigation of protein structures within the capsid shell, and studies of the mechanisms underlying viral processes are required to provide more confidence to this hypothesis and uncover the evolutionary connections between these viruses.

If this relationship between the mammalian/avian, fish/amphibian and invertebrate lineages is correct then the last common ancestor of these viruses existed prior to the evolution of the first vertebrates, and this ancestral virus would have the unmistakeable morphology of a Herpesvirus (Davison, 2002). The evolution of viruses has proved notoriously difficult to trace, as reflected by the limited depth of taxonomic categories occupied by viruses. At present it remains difficult to unite the different virus families to produce a comprehensive taxonomy charting the relationship between disparate viruses. However, it is becoming increasingly apparent that there are potential relationships between seemingly unrelated virus groups. One such relationship that is becoming more widely apparent is that of dsDNA viruses and dsDNA bacteriophages.

Perhaps one of the most established examples is the relationship between Adenovirus (Ad) and phage PRD1. These two viruses share a common capsid architecture and a structural fold within their major capsid proteins known as a "double jelly roll" (Benson *et al.*, 1999; 2004). The PRD1 – Ad family of viruses has continued to extend with the recent identification of Archaeal proviruses which has expanded the range of host phyla for members of the PRD1-Ad lineage of dsDNA viruses (Krupovic & Bamford, 2008a; b). Parallels exist in capsid structure and assembly, and DNA packaging processes between herpesviruses and ds DNA tailed bacteriophages and have long been noted (Baker *et al.*, 2005; Bamford *et al.*, 2002; Rixon & Chiu, 2003). Recently, these similarities have been extended to the molecular level by identification of characteristic structures and subunit arrangements in the major capsid proteins and portal complexes (Baker *et al.*, 2005; Cardone *et al.*, 2007; Newcomb *et al.*, 2001b). If these observations can withstand greater scrutiny, this would confirm an evolutionary relationship between these viruses and imply that the origins of herpesviruses might predate the separation of the prokaryotic and eukaryotic lineages (section 1.9).

1.3. Herpesviruses as agents of human disease

There are eight known herpesviruses which infect man, causing a range of diseases of varying severity (Table 1.1). These eight viruses cover the spectrum of the three

Virus	Common Name	Subfamily (*Genus*)[1]	Latent site[1]	Primary Associated Illness[2,3,4,5,6,7]	Other Associated Illnesses[3,4,5,6,7]
HHV-1	Herpes simplex virus type 1 (HSV-1)	*Alphaherpesvirinae (Simplexvirus)*	Sensory nerve ganglia	Cold sores	Genital lesions, conjunctivitis, herpetic whitlow, keratitis, encephalitis
HHV-2	Herpes simplex virus type 2 (HSV-2)	*Alphaherpesvirinae (Simplexvirus)*	Sensory nerve ganglia	Genital lesions	Oral lesions, conjunctivitis, herpetic whitlow, keratitis, encephalitis
HHV-3	Varicella-zoster virus (VZV)	*Alphaherpesvirinae (Varicellovirus)*	Sensory nerve ganglia	Chicken pox/fever	Reactivation can lead to shingles
HHV-4	Epstein-Barr virus (EBV)	*Gammaherpesvirinae (Lymphocryptovirus)*	B-lymphocytes	Glandular fever, mononucleosis	Burkitt lymphoma, nasopharyngeal carcinoma
HHV-5	Human cytomegalovirus (HCMV)	*Betaherpesvirinae (Cytomegalovirus)*	Leukocytes, endothelial cells	Congenital abnormalities, mononucleosis, hepatitis	Immuno-compromised individuals suffer from gastro-enteritis and retinitis
HHV-6	Exanthem subitum virus	*Betaherpesvirinae (Roseolovirus)*	T-lymphocytes	Infant rash (exanthema subitum)	Associated with certain malignancies: lymphoma, leukaemia, co-factor in cervical and oral carcinoma
HHV-7	HHV-7	*Betaherpesvirinae (Roseolovirus)*	T-lymphocytes	Febrile illness	-
HHV-8	Kaposi's sarcoma-associated herpesvirus (KSHV)	*Gammaherpesvirinae (Rhadinovirus)*	B-lymphocytes		Kaposi's sarcoma

Table 1.1: Human herpesviruses and their primary and associated illnesses

(1) Roizman *et al*., 1992; (2) Subak-Sharpe and Dargan, 1998; (3) Levy, 1997; (4) Roizman *et al*., 2007; (5) Mocarski *et al*., 2007;

(6) Kieff and Rickinson, 2007; (7) Cohen *et al*., 2007

subfamilies of the *Herpesviridae*. Herpesvirus infection is considered to be ubiquitous in both the developed and developing world. In common with other herpesviruses those infecting humans are able to establish a life long latent infection, in which the viral genome is maintained within the nuclei of infected cells. The cell types in which such reservoirs of latently infecting virus are maintained vary between individual viruses. Latent infections are asymptomatic as only a small subset of viral genes are expressed. However, latent viruses are able reactivate and enter into lytic replication (section 1.8), which may result in physical symptoms. Reactivation seems to require a stimulus although the triggers of reactivation are poorly defined (section 1.8).

Infection with HSV-1, for example, is commonly through the mucosal membranes of the mouth and nose with latent infection established in the trigeminal ganglia. In this latent reservoir the virus may remain undetected by the immune system surveillance until reactivation to the lytic cycle. Reactivation can occur at irregular intervals and results in reappearance of the virus at the site of the initial infection, where it may present as the characteristic cold sore lesion. The other human herpesviruses have equivalent life-cycles although the nature of latency and reactivation will differ. VZV is notable in that it causes two distinct diseases, primary infection results in a generalised infection which produces the characteristic lesions of chicken pox. VZV then maintains a latent infection in the ganglia of the sensory nervous system. Reactivated infection may occur after many years and is not generalised (as per the initial infection) but is restricted to a region of skin associated with a single nerve tract (referred to as a dermatome), resulting in shingles.

1.4. Virion structure of HSV-1

1.4.1. Capsid

The capsid is arguably the most studied and best understood structure within the herpes virion. This depth of understanding is due to the robust nature of this structure and the ease with which it can be purified from the nuclei of infected cells (Liashkovich *et al.*, 2008). Our understanding of the structure of the capsid comes predominantly from cryo electron microscopy (cryo-EM), with biochemical and genetic studies elucidating different aspects of the formation and composition of the capsid (Table 1.2). The capsid structure has been determined to 8.5Å for HSV-1 and seems to be broadly conserved across the families of the *Herpesvirales* (Trus *et al.*, 2001; Yu *et al.*, 2003; Zhou *et al.*, 2000)(Fig. 1.3).

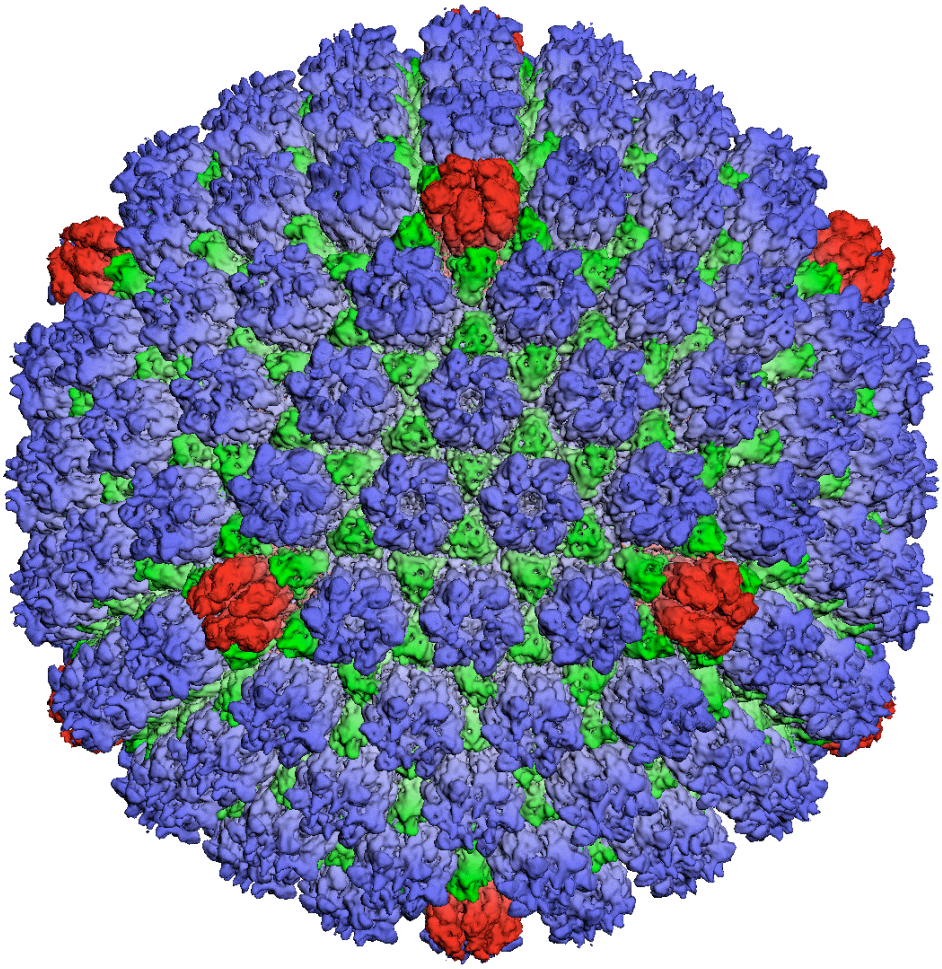

Figure 1.3: Structure of the HSV-1 capsid at 8.5Å.

The capsid is 1250Å in diameter and has a mass of approximately 192 MDa. This reconstruction shows 162 capsomeres: of which 150 are hexons (blue), which form the faces and edges of the capsid and 12 of which are pentons (red), which form the vertices. Between adjacent capsomeres lie the triplexes (green) of which there are 320 copies. The HSV-1 capsid has *T*=16 icosahedral symmetry. Only icosahedrally-ordered structures are shown in this reconstruction. The portal complex which substitutes for one penton vertex is not shown.

This figure was reproduced from Zhou *et al*, (2000).

Gene	Protein	MW (kDa)	Copies per capsid	Location in capsid	Presence in capsids
UL6		74	12	Portal vertex	A, B, C
UL17		74.5		Penton vertex	A, B, C[c]
UL18	VP23	34.2	640	Triplexes	A, B, C
UL19[a]	VP5	149	955[a]	Hexons and Pentons	A, B, C
UL25		62.6		Penton vertex	A, B, C[c]
UL26	VP21	39.8	100[b]	Internal scaffold	B
UL26	VP24	26.6	100[b]	Internal scaffold	A, B, C
UL26.5	VP22a	33.7	1000-1500[b]	Internal scaffold	B
UL35	VP26	12	900	Tips of hexons	A, B, C
UL38	VP19c	50.2	320	Triplexes	A, B, C

Table 1.2: Proteins within HSV-1 A-, B-, and C-capsids.

[a] The UL6 portal protein complex replaces a single penton subunit. As a result 955 copies of VP5 (accounting for the replacement of one penton with the portal) are present whilst the triplexes are unaffected with 5 copies present at the portal vertex (Cardone *et al*., 2007; Chang *et al*., 2007).

[b] Approximate numbers

[c] Proteins present on all capsid types, but most abundant on C capsids, copy numbers not determined (Thurlow *et al*., 2005).

References: Homa and Brown, 1997; McGeoch *et al*., 1989.

The capsid occupies a central position within the virion and contains the viral genome, this structure is designated the nucleocapsid. Several arrangements of the packaged DNA were suggested based on EM of negatively stained and thin sectioned particles. Cryo-EM structures initially suggested a liquid crystalline conformation (Booy *et al.*, 1991). However, it now appears likely to be arranged in a spool conformation similar to that of T7 phage (Cerritelli *et al.*, 1997), in which the DNA appears as concentric layers within the capsid at an interstrand spacing of 26Å for HSV-1 (Zhou *et al.*, 1999). The related betaherpesvirus Human cytomegalovirus (HCMV) packages its genome more tightly than HSV-1 presumably due to the larger size of the HCMV genome (229.3 kbp, Chee *et al.*, 1990), with a modest (17%) increase in capsid volume, resulting in a reduction in interstrand spacing to 23Å (Bhella *et al.*, 2000; Zhou *et al.*, 1999).

The capsid is an icosahedron of some 1,250Å diameter with 20 triangular faces and displaying T=16 symmetry. The constraints of this geometry make the capsid amenable to extensive investigation by cryo-EM reconstruction techniques which exploit the symmetry of the capsid to produce high resolution structures (Zhou *et al.*, 2000). The majority of the capsid structure is formed from the product of the UL19 gene (Desai *et al.*, 1993), designated VP5 or the Major Capsid Protein (MCP). Within the capsid structure VP5 is arranged into two distinct complexes termed capsomers. A 6-subunit arrangement termed the hexon is present in 150 copies forming the faces and edges of the icosahedron, while a 5 subunit arrangement termed the penton occupies the vertices (Wildy *et al.*, 1960; Zhou *et al.*, 2000). Pentons are capable of forming all 12 capsid vertices under experimental conditions, but one vertex is normally occupied by the portal complex (see below) with pentons at the remaining 11 positions (Newcomb *et al.*, 1993; Tatman *et al.*, 1994; Wildy *et al.*, 1960; Zhou *et al.*, 1995)(Fig. 1.3).

1.4.1.1. VP5

VP5 is a large protein (150 kDa) and has been described as having three domains; floor, middle and upper. The floor domain forms a continuous shell around the viral DNA and this is the only domain that interacts to promote inter-capsomer contact (Baker *et al.*, 2003; Zhou *et al.*, 1999). The middle and upper domains rise above the capsid floor forming a projection, termed a turret and retaining the underlying five or six fold symmetry of the floor domain. The upper domain forms the top of the penton and hexon turrets and it is with this structure in the hexon that the small capsid protein VP26 binds, whilst in pentons it is thought to interact with tegument (Booy *et al.*, 1994; Chen *et al.*, 2001; Zhou *et al.*, 1999; Zhou *et al.*, 1995). The crystal structure of the upper domain (designated VP5ud)

was established from a protease resistant fragment of VP5 and was shown to contain a novel fold unrelated to any found in other known viral capsid proteins (Bowman *et al.*, 2003). Bowman *et al*. (2003) modelled the VP5ud into the densities of VP5 within hexon and penton structures derived from cryo EM reconstructions, which showed an altered range of contact residues and buried surfaces and a different charge distribution on the interior surface of the hollow turret. This analysis provides some structural basis for explaining the greater rigidity of the hexons compared to the pentons which are selectively removed from the capsid under treatment with Guanidine hydrochloride (Newcomb & Brown, 1991; 1994). Baker *et al*. (2003) performed a fuller analysis of the structure of VP5 using a bioinformatics approach to model VP5. Using this approach they were able to begin assigning regions of VP5, which were not part of the crystal structure of VP5ud, to structural features from the cryo-EM reconstruction.

1.4.1.2. Small hexon binding protein: pUL35 or VP26

The small capsid protein, VP26, which is encoded by the UL35 gene, binds to VP5 in a 1:1 stoichiometry (Booy *et al.*, 1994). It is not present on pentons but is located at the tips of hexons where it forms a ring of 6 subunits (Zhou *et al.*, 1995). This binding pattern seems to be controlled by the availability of specific binding sites caused by the arrangement of the VP5 monomers within the hexon, which are disrupted by the differing organisation present in the penton (Bowman *et al.*, 2003; Chen *et al.*, 2001; Wingfield *et al.*, 1997). VP26 is not required for virion formation (Desai *et al.*, 1998) and although it has been implicated in contacting cellular motor proteins, capsid transport occurs in its absence (Dohner *et al.*, 2006; Douglas *et al.*, 2004). VP26 seems only to be essential in neuroinvasion in infection of PrV and HSV-1 (Desai *et al.*, 1998; Krautwald *et al.*, 2008).

1.4.1.3. Triplex: VP19C and VP23

A characteristic feature of herpesvirus capsids are the triplexes, which occupy positions at the local 3 fold axes of symmetry between the capsomers and interact with the middle domain of VP5 (Zhou *et al.*, 2000). They are formed from the products of the UL18 and UL38 genes, designated VP23 and VP19C respectively. These proteins interact to form the heterotrimer, which consists of two copies of VP23 and one of VP19C (Newcomb *et al.*, 1993; Zhou *et al.*, 1994) and is present in 320 copies (Fig. 1.3). Both triplex proteins are essential for correct capsid formation (Okoye *et al.*, 2006), however in the absence of VP23 from an *in vitro* capsid assembly system, VP5 and VP19C were shown to form smaller (880Å) capsid like structures with a symmetry of T=7 (Saad *et al.*, 1999). This

suggests that VP19C alone can support interactions between the capsomers and that VP23 has a role in controlling the size and symmetry of the mature capsid (Trus *et al.*, 1996).

1.4.1.4. Portal: pUL6

Given the similarities in architecture and assembly of capsids between herpesviruses and Bacteriophage (section 1.9) it was expected that the herpes capsid would contain a portal structure through which the viral DNA might be packaged and released. Early work showed that pUL6 is present in the capsid as a minor component. Although capsid formation was not prevented by the absence of pUL6, capsids devoid of pUL6 were unable to package DNA (Lamberti & Weller, 1996; Newcomb & Brown, 2002; Newcomb *et al.*, 1994; Patel & Maclean, 1995; Patel *et al.*, 1996; van Zeijl *et al.*, 2000).

pUL6 was shown to be present at a single vertex within the capsid structure by immuno-gold EM labelling and its identity as the portal was suggested when the purified protein was shown to form multimeric rings resembling bacteriophage portals (Newcomb *et al.*, 2001b). The structure of the portal was finally elucidated by cryo-EM reconstruction of portal complexes produced in the heterologous baculovirus expression system, which showed the portal to be a dodecameric ring structure (Trus *et al.*, 2004). Further investigations have resolved the portal within the capsid structure giving some understanding of the association of portal with the VP5 lattice, which supports previous thinking in which one VP5 penton was substituted for a dodecameric ring of pUL6 as the portal (Cardone *et al.*, 2007; Chang *et al.*, 2007).

1.4.1.5. Capsid associated proteins: pUL25 and pUL17

There are two further proteins, pUL25 and pUL17, that are commonly considered to be capsid associated (Ogasawara *et al.*, 2001; Thurlow *et al.*, 2005). These two proteins are known to interact. Neither is essential for capsid formation, but both are important for DNA packaging and are required for virion formation (McNab *et al.*, 1998; Preston *et al.*, 2008; Thurlow *et al.*, 2006). pUL17 and pUL25 associate with procapsids (section 1.5.4.) and the mature capsid forms A (empty), B (scaffold filled) and C (DNA containing) capsids in differing amounts (Thurlow *et al.*, 2005). pUL25 has been localised to the vertices of capsids by Immuno EM as has pUL17 (Thurlow *et al.*, 2006). Recent work has suggested that these minor capsid proteins occupy a position at the penton vertex previously assigned to some of the tegument density present in virions (Trus *et al.*, 2007; Zhou *et al.*, 1999). pUL25 is important for the retention of viral DNA, as in its absence full

length viral genomes are not as effectively retained within capsids, in comparison to WT HSV-1 (Stow, 2001). Interestingly, a ts mutant of pUL25 (ts1249) fails to uncoat the viral genome at the non-permissive temperature, a phenotype displayed by tsB7 at the non-permissive temperature also (Batterson *et al.*, 1983; Preston *et al.*, 2008). These observations have led to the suggestion that pUL25 might act as a cap or plug, holding the DNA inside the capsid (McNab *et al.*, 1998; Preston *et al.*, 2008). pUL17 seems to be important for DNA packaging and is known to promote efficient binding of pUL25 to capsids. In the absence of pUL17, C capsids are not formed and the viral genome is not cleaved to unit lengths (Klupp *et al.*, 2005; Salmon *et al.*, 1998; Thurlow *et al.*, 2006).

Formation of the capsid will be dealt with in section 1.5.4.

1.4.2. Tegument

The herpes virion tegument occupies a region between the capsid and envelope. It is perhaps the most complex section of the virion, and the least well understood. This complexity, together with the flexibility and variation shown in tegument protein composition, and the properties of tegument mutants between individual particles and among related viruses makes analysis of the tegument challenging.

Structurally, the tegument has generally been regarded as amorphous and cryo EM studies on intact virions appear to confirm this view, with the great majority of the tegument not having a consistent structure. Detectable organisation of the tegument seems to be limited to the locations where it interacts with capsids (Grunewald *et al.*, 2003; Zhou *et al.*, 1999) where icosahedrally ordered density can be resolved outside of the capsid radius. The pattern of capsid tegument interaction is a notable point of variation between the alpha-, beta- and gamma- *herpesvirinae* despite the conservation of underlying capsid structure between these three subfamilies. In the alpha-herpesvirus, HSV-1, additional density is restricted to the capsid vertices (Fig. 1.4). This penton associated density was proposed to be pUL36 the largest tegument protein (Zhou *et al.*, 1999) but this assignment is contentious, with recent data attributing much of this material to heterodimers of the minor capsid proteins pUL17 and pUL25 (Trus *et al.*, 2007). For the beta-herpesvirus HCMV, tegument capsid contact appears to form a net like structure over the entire surface of the capsid interacting with penton, hexon and triplexes (Chen *et al.*, 1999). The major proteins involved in HCMV have been suggested to include basic phosphoprotein (BPP, pp150, ppUL32) and upper matrix protein (UM, pp71, ppUL82), which have no counterparts in

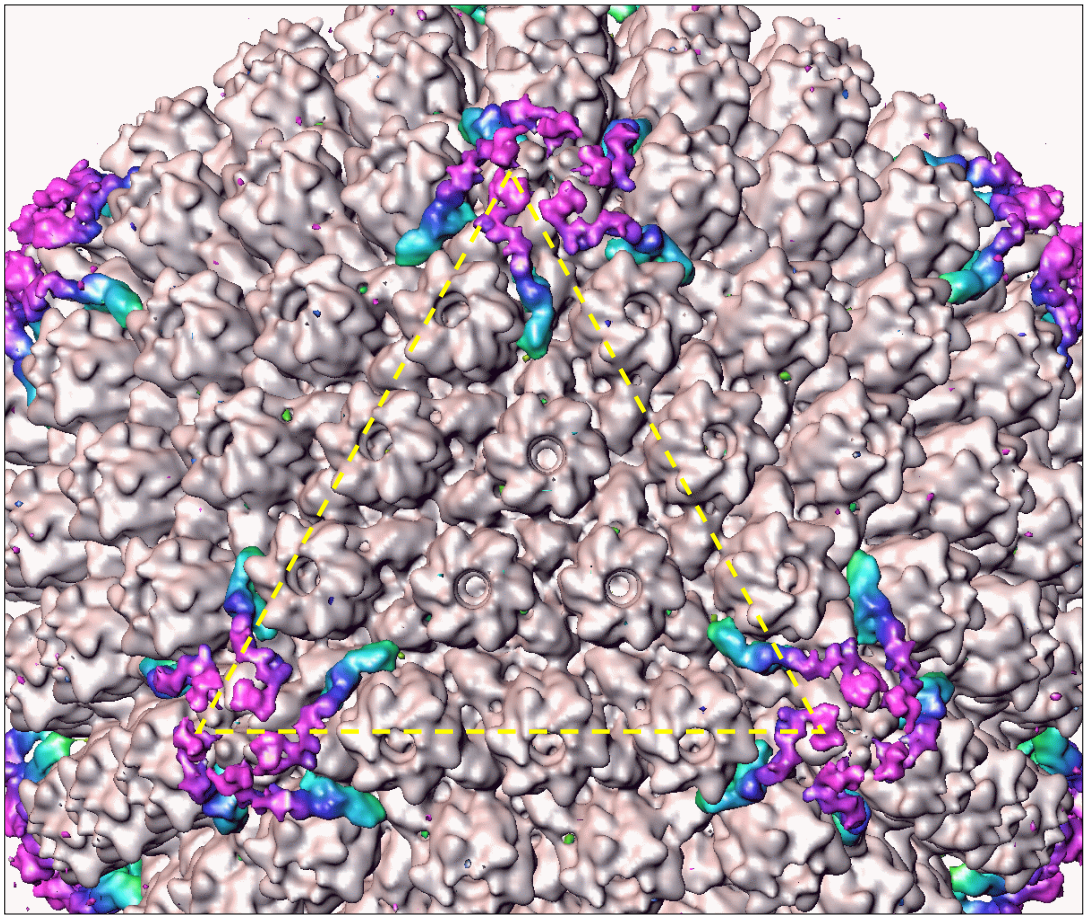

Figure 1.4: Interaction between capsid and icosahedrally ordered tegument density in the intact virion. The structure of the HSV-1 B-capsid is shown in grey. Densities present only on the icosahedral reconstruction of the virion capsid are shown in colour and superimposed on the capsid map. A single icosahedral capsid face is outlined by the broken yellow line. The resolution of this structure is 20 Å. Tegument densities are seen associated with the capsid vertices.

This figure was reproduced from Zhou *et al*, (1999).

the *alphaherpesvirinae* (Chee *et al.*, 1990; Chen *et al.*, 1999). For the gamma-herpesvirus, Murine herpesvirus 68 (MHV-68), there is no indication of icosahedrally ordered tegument density in contact with the capsid, despite the clear presence of capsid/tegument contacts seen by cryo electron tomography (cryo-ET) (Dai *et al.*, 2008).

Recent advances in cryo electron tomography have started to resolve the asymmetric features of HSV-1 virions and initial studies suggested that the tegument is distributed in an asymmetric cap structure with the capsid acentric within the HSV-1 virion, resulting in two distinct poles where large or small quantities of tegument density are seen (Grunewald *et al.*, 2003). The authors suggest that this may be of functional consequence and occur as a result of the process by which tegument is acquired (Grunewald *et al.*, 2003).

The tegument is thought to be composed of some 15 or more viral proteins, and to contain cellular proteins and mRNAs, and viral mRNAs with apparent selection for a subset of viral RNAs (Loret *et al.*, 2008; Michael *et al.*, 2006; Sciortino *et al.*, 2001). The function and consequence of incorporating cellular proteins and mRNAs is unknown, but the incorporation of viral mRNAs (particularly pUL48, Sciortino *et al.*, 2001) would likely prove advantageous in subverting the host cell by allowing immediate *de novo* viral protein synthesis prior to gene expression (McLauchlan *et al.*, 1992; Sciortino *et al.*, 2001; Sciortino *et al.*, 2002). This would supplement the effect of some tegument proteins (VP16, ICP0, vhs), which are known to influence the early stages of viral infection (Cai *et al.*, 1993; Campbell *et al.*, 1984; Fenwick & Everett, 1990; Fenwick & McMenamin, 1984; Kwong *et al.*, 1988). Inclusion of tegument components into virions displays marked variability with some members being present in apparently fixed copy number while others are more flexible in the amount incorporated, with variation apparent even between individual virions (Clarke *et al.*, 2007; del Rio *et al.*, 2005; Leslie *et al.*, 1996; McLauchlan, 1997). The tegument itself has a considerable degree of structural integrity, retaining its form in the absence of both capsid and envelope, although it displays notable "stickiness" resulting in aggregation of particles which have had their envelopes removed (McLauchlan & Rixon, 1992).

Current literature divides the tegument into two regions, the inner and outer tegument (reviewed Mettenleiter *et al.*, 2006). This subdivision has its basis in presumed distribution within the virion and correlates somewhat with biochemical and genetic data. Mettenleiter (2006) places pUS3, pUL36 and pUL37 into the inner tegument, which is closely

associated with the capsid, and all other tegument proteins into the outer tegument, which is thought to be recruited subsequently to the acquisition of the inner tegument.

A more detailed examination of some major tegument components will now be given, focusing on their functions and interactions. As pUL36 and pUL37 are the main subject of this work, their coverage here will be different than that for other tegument proteins as some of their roles will be discussed at greater length in later sections.

1.4.2.1. Inner tegument protein: pUS3

The US3 gene encodes a protein kinase pUS3 that is non essential in tissue culture, and is conserved within the *alphaherpesvirinae* (Daikoku *et al.*, 1993; Frame *et al.*, 1987; Granzow *et al.*, 2004; Nishiyama *et al.*, 1992). pUS3 is a component of both primary and mature virions, being closely associated with the capsid (Granzow *et al.*, 2004). Whilst the kinase activity of pUS3 is dispensable for replication a strong body of data implicates pUS3 in the regulation of pUL31/pUL34 activity and supports a role in nuclear egress (section 1.6.1), by orchestrating events leading to the disassembly of the nuclear lamina and relocalisation of nuclear lamina constituents (Klupp *et al.*, 2001a; Leach *et al.*, 2007; Morris *et al.*, 2007; Mou *et al.*, 2009; Mou *et al.*, 2008). pUS3 is involved in the inhibition of apoptotic responses by the host cell (Benetti *et al.*, 2003; Cartier *et al.*, 2003; Jerome *et al.*, 1999). In the absence of pUS3 large inclusions of capsids form at the inner nuclear membrane, supporting its function in nuclear egress. It has been suggested that pUS3 regulates the fusion of the primary envelope with the outer nuclear membrane by influencing gB activity (Granzow *et al.*, 2004; Wisner *et al.*, 2009). pUS3 phosphorylates pUL12 to regulate its alkaline nuclease activity, and pUS3 also has a role in sustained long distance axonal transport (Coller & Smith, 2008; Daikoku *et al.*, 1995).

1.4.2.2. Inner tegument protein: pUL36

The largest tegument protein pUL36 (VP1/2, VP1-3 or ICP1/2) is encoded by the UL36 reading frame, which is conserved (in function) throughout the alpha- beta- and gamma herpesviruses (McNabb & Courtney, 1992a; Mettenleiter, 2002; Pellett & Roizman, 2007). In HSV-1, this 3164 amino acid protein (calculated Mr 335 kDa) is an essential component of the virion, expressed as a true late (γ2) protein and has been suggested to be responsible for the tegument capsid interaction (Desai, 2000; Fuchs *et al.*, 2004; McNabb & Courtney, 1992b; Szilagyi & Cunningham, 1991; Zhou *et al.*, 1999).

pUL36 is currently thought to be a multifunctional protein possessing a domain capable of interacting with pUL25 at the C terminus that is involved in tegumentation, as well as having proposed roles in genome uncoating, interaction with cytoskeletal components and a DNA binding activity (Batterson *et al.*, 1983; Chou & Roizman, 1989; Coller *et al.*, 2007; Luxton *et al.*, 2006; Shanda & Wilson, 2008; Wolfstein *et al.*, 2006). pUL36 also contains a novel cysteine protease deubiquitinating activity bearing no homology to known deubiquitinating enzymes, and an unusual nuclear localisation signal in the N terminus, (Abaitua & O'Hare, 2008; Kattenhorn *et al.*, 2005; Schlieker *et al.*, 2005; Schlieker *et al.*, 2007).

The first indication of the role of pUL36 came from a mutant designated tsB7, which has a temperature sensitive lesion in the UL36 gene (Knipe *et al.*, 1981; McGeoch *et al.*, 1988; McNabb & Courtney, 1992a). When infections with tsB7 were performed at the non permissive temperature, capsids were seen to accumulate close to the nuclear envelope, where they were frequently seen adjacent to nuclear pores. These capsids retained their genomes and there was no detectable initiation of viral gene expression, (Batterson *et al.*, 1983; Knipe *et al.*, 1981). This led to the proposition that the protein affected by the ts mutation (later shown to be pUL36) was responsible for genome uncoating. Recent work has examined this further and shown that a block on proteolysis of pUL36 in this mutant may be responsible for its phenotype (Jovasevic *et al.*, 2008). Work by Morrison *et al.* (1998a) localised pUL36 to the nuclear rim at early times after infection of vero cells, suggesting that it is retained with the capsid during transport to, and docking with the nucleus. This is supported by more recent work with another alphaherpesvirus, PrV (Luxton *et al.*, 2006) and implies a role for pUL36 in either transport to, recognition of, or interaction with the nuclear pore resulting in genome uncoating. A series of interesting reports have implicated capsid associated pUL36 in interactions with the host cell cytoskeleton, again supporting a role in capsid transport (Luxton *et al.*, 2006; Shanda & Wilson, 2008; Wolfstein *et al.*, 2006). This is discussed further in section 1.5.2.1.

pUL36 also has a role in virion assembly as was demonstrated by construction of a deletion mutant, KΔUL36, which confirmed that pUL36 was essential for the replication of HSV-1 (Desai, 2000). Similar observations were made with PrV (Fuchs *et al.*, 2004; Luxton *et al.*, 2006). In both HSV-1 and PrV, pUL36 was found to be essential for secondary envelopment, with DNA filled capsids accumulating in the cytoplasm in its absence (Desai, 2000; Fuchs *et al.*, 2004). This suggests the pUL36 is required for cytoplasmic secondary envelopment. However, the phenotypes of the HSV and PrV

mutants varied in the disposition of the capsids, with capsids of KΔUL36 accumulating in small clusters in the cytoplasm whilst those of the PrV mutant were dispersed throughout the cytoplasm. This was thought to reflect some biological distinction between HSV-1 and PrV (section 4.5.1). A second PrV mutant with a UL36 deletion was reported to have a defect in nuclear exit of capsids (Luxton *et al.*, 2006), but this was not seen in either the other PrV mutant or the HSV-1 mutant (Desai, 2000; Fuchs *et al.*, 2004).

There is strong evidence that supports a close association of pUL36 with the capsid, and suggests that this interaction is critical to the viral life cycle (Batterson *et al.*, 1983; Coller *et al.*, 2007; Luxton *et al.*, 2006; Morrison *et al.*, 1998a; Wolfstein *et al.*, 2006; Zhou *et al.*, 1999). Currently there is debate over where pUL36 is added to capsids with some reports suggesting a potential for nuclear recruitment (Abaitua & O'Hare, 2008; Bucks *et al.*, 2007). However, if pUL36 is recruited to nuclear capsids this interaction is dispensable for crossing the nuclear membrane (Desai, 2000; Fuchs *et al.*, 2004). One possibility that has been suggested is that pUL36 in the nucleus might represent functional units processed from full length pUL36 which have yet to be characterised (Abaitua & O'Hare, 2008; Coller *et al.*, 2007). A growing body of data suggests that proteolytic processing in infected cells is important for the functions of pUL36 (Jovasevic *et al.*, 2008; Kattenhorn *et al.*, 2005). Indeed the reported deubiquitinating (DUB) activity mentioned earlier, may be regulated by proteolytic cleavage of the functional unit from full length pUL36 (Kattenhorn *et al.*, 2005). Currently the precise function and purpose of the encoded DUB activity in pUL36, which is conserved across pUL36 lineages, remains uncertain with mutants lacking this activity showing minor impairment compared to wild type (Kattenhorn *et al.*, 2005; Schlieker *et al.*, 2005; Wang *et al.*, 2006).

A little studied role proposed for pUL36 is in DNA cleavage and packaging, where it was reported that an equimolar complex of two proteins of 140 kDa and 250 kDa interacted with a DNA fragment containing both DR1 and *Pac*2 sequences. The identity of the 250 kDa fragment was suggested to be VP1-2 due to its recognition by an ICP1 (VP1-2) specific antibody (Chou & Roizman, 1989). To date there is little support for this observation in the literature, save for the reports of nuclear localisation, and nuclear capsid association of pUL36 (Abaitua & O'Hare, 2008; Bucks *et al.*, 2007).

On balance therefore, the evidence available suggests that the major roles of pUL36 are within the cytoplasm, both in secondary envelopment and in processes leading to nuclear pore binding and genome uncoating.

pUL36 is a structural protein and would therefore be expected to interact with other virion proteins. To date, there is no direct evidence for an interaction between pUL36 and the major capsid proteins. All such interactions have been inferred from cryo-EM reconstruction data and stripped virions or partly tegumented capsids (Luxton *et al.*, 2006; Wolfstein *et al.*, 2006; Zhou *et al.*, 1999). An interaction with the minor capsid protein, pUL25, has been identified and shown to involve the C-terminal 62 amino acids of pUL36 (Coller *et al.*, 2007). In contrast, a number of studies have described protein interactions within the tegument. These screens performed using the yeast-2-hybrid systems have suggested an interaction between pUL36 and pUL37, in addition to an interaction between pUL36 and pUL48 (Lee *et al.*, 2008; Vittone *et al.*, 2005). The interaction between pUL36 and pUL37 has since been shown to involve residues F593 and E596 of pUL36. Mutation of either residue (individually) to alanine impaired pUL37 binding. When either F593 or E596, and E580 were replaced by alanine, binding of pUL37 was abolished (Mijatov *et al.*, 2007). The interaction of pUL36 and pUL37 has also been studied in PrV, where a direct interaction has been demonstrated (Klupp *et al.*, 2002). In comparison with HSV-1, PrV pUL36 can function, to a limited extent, in the absence of interaction with pUL37, which may reflect the differing requirements for pUL37 in HSV-1 and PrV, discussed further in section 1.4.2.3 (Fuchs *et al.*, 2004; Klupp *et al.*, 2001b). The binding domain for pUL48 was mapped in the N terminal portion of pUL36 in a yeast-2-hybrid study (Vittone *et al.*, 2005), and has been refined to residues 124-511 (Mijatov *et al.*, 2007).

1.4.2.3. Inner tegument protein: pUL37

The tegument protein pUL37 is encoded by the UL37 reading frame, which is conserved throughout the alpha-, beta-, and gamma herpesviruses (Mettenleiter, 2002; Pellett & Roizman, 2007). In HSV-1, pUL37 is a 1123 amino acid late protein (calculated and apparent Mr ~120 kDa) which is phosphorylated (Albright & Jenkins, 1993; McLauchlan *et al.*, 1994). It is found in virions and is a tegument protein, although its precise localisation remains elusive. Incorporation of pUL37 to the tegument appears to be strictly controlled with the copy number in virions being unaffected by the level of expression in the infected cell. Under conditions where pUL37 was over expressed, incorporation of the protein into virions remained at a fixed level suggesting a strict copy number (McLauchlan, 1997). This was suggested to reflect the availability of a limited number of binding sites, possibly determined by the capsid, although the tight control on incorporation of pUL37 was also seen in L particles (particles which lack the capsid see section 5.2.2) (McLauchlan, 1997).

Much less is known about the functions and importance of pUL37 than is the case for pUL36. This is partly due to the lack of a ts mutant, but also reflects the more limited amount of effort spent in studying this protein. To date the most well supported role for pUL37 is in secondary envelopment, with deletion of the UL37 gene being detrimental to virion formation and large aggregates of DNA filled capsids accumulating in the cytoplasm of infected cells (Desai *et al.*, 2001; Klupp *et al.*, 2001b). Strikingly, however, the requirement for pUL37 varies between HSV-1 and PrV, with pUL37 being absolutely essential for secondary envelopment in HSV-1 but partly dispensable in PrV. Notably, although deletion of pUL37 is detrimental in PrV and results in large accumulations of non-enveloped cytoplasmic capsids, some mature virions are formed and released (Desai *et al.*, 2001; Klupp *et al.*, 2001b).

pUL37 is found predominantly in the cytoplasm and its role in secondary envelopment is consistent with this distribution (Desai *et al.*, 2008; Desai *et al.*, 2001; Klupp *et al.*, 2001b; McLauchlan, 1997; McLauchlan *et al.*, 1994). A recent report has suggested that pUL37 is present on nuclear capsids, although the functional relevance of this remains unknown (Bucks *et al.*, 2007). There has been one report of a nuclear egress defect being linked with the deletion of pUL37 in the HSV-1 mutant KΔUL37. No such defect has been reported for a similar mutant in PrV and with ΔUL37 mutants of both PrV and HSV-1 accumulating large numbers of cytoplasmic capsids it is clear that any role for pUL37 in nuclear egress must be limited (Desai *et al.*, 2001; Klupp *et al.*, 2001b) (section 4.5.2).

Examination of the role of pUL37 in the initiation of infection has been hampered by the lack of a ts mutant and the requirement for this protein in HSV-1 for the formation of virions. Thus the best data available regarding a role in initiation of infection come from PrV, though they must be interpreted with caution given the differences in the requirement for pUL37 between PrV and HSV.

Data from PrV and HSV-1 show that pUL37 is closely associated with capsids, presumably through its interaction with pUL36 (Lee *et al.*, 2008; Luxton *et al.*, 2006; Vittone *et al.*, 2005; Wolfstein *et al.*, 2006). These data are consistent with a role for pUL37 in capsid transport at early times in infection, which is supported by a recent report that PrV virions lacking pUL37 are retarded in transport to the nucleus compared to wild type, inferring that pUL37 may play a role in either contacting cellular motor proteins or in enhancing processivity of motor proteins bound by capsids (Krautwald *et al.*, 2009; Luxton *et al.*, 2006; Wolfstein *et al.*, 2006).

Much of our understanding of the interactions of pUL37 within the tegument is once more derived from yeast-2-hybrid screens. Vittone *et al*. (2005) identified an interaction with pUL36 (section 1.4.2.2) and a self interaction. As described above, data from PrV confirm the pUL36 interaction (Klupp *et al.*, 2002). The self interaction of pUL37 in HSV-1 was recapitulated in a further yeast-2-screen and a novel, although weak, interaction with the capsid protein, pUL38 (VP19C), shown (Lee *et al.*, 2008).

Given the increasing interest in pUL36 there is a commensurate growth of interest in pUL37 as one of its main interaction partners and a major tegument protein. At the start of this project, our understanding of the functions of pUL37 was centred on the defects in secondary envelopment. Because of the absolute requirement for pUL37 in the formation of HSV-1 virions, investigations had not been carried out into the roles of this protein at early times after infection. This was one aim of this project and the findings are described in the Results section of this thesis.

Outer tegument proteins

Because of the large number of outer tegument proteins, the following section will deal only with those which occur in high abundance, or have well studied functions.

1.4.2.4. Outer tegument protein: pUL41

The UL41 ORF encodes the pUL41, or virion host shutoff (*vhs*) protein (calculated Mr 54 kDa apparent Mr 58 kDa). pUL41 has an endoribonuclease activity that is conserved within the alpha-*herpesvirinae*, but homologues are absent from both the beta- and gamma- *herpesvirinae* (reviewed Everly *et al.*, 2002; Smiley, 2004; Taddeo & Roizman, 2006; Taddeo *et al.*, 2006; Zelus *et al.*, 1996). pUL41 is an mRNA specific nuclease capable of degrading both cellular and viral mRNAs (Krikorian & Read, 1991; Kwong & Frenkel, 1987).

Vhs activity is implicated in establishing the superiority of viral gene expression over host gene expression in concert with immediate early gene products such as ICP27. *Vhs* also plays a role in the control of viral gene expression by degrading viral mRNA (Oroskar & Read, 1987; 1989; Read & Frenkel, 1983; reviewed Smiley, 2004). The level of *vhs* activity seems to vary between alpha herpesviruses with some expressing more or less active forms of *vhs*, although the significance of this is not fully understood. *Vhs* activity is not essential in tissue culture but is important in animal models (reviewed Smiley, 2004).

Endonucleolytic cleavage by *vhs* does not require other viral or cellular factors and has an apparent substrate specificity similar to RNaseA (Taddeo & Roizman, 2006; Taddeo *et al.*, 2006). This activity may be governed by an interaction with the cellular translation factor eIF4H. This would ensure recruitment to actively translated mRNAs and would help to account for the apparent selectivity of *vhs* for mRNAs (Feng *et al.*, 2001). *Vhs* activity may be controlled by sequestration into a complex with pUL48 (VP16) which quenches *vhs* activity in a temporally regulated manner that is controlled by the expression kinetics of VP16, thereby permitting viral late gene mRNAs to accumulate (Lam *et al.*, 1996; Smibert *et al.*, 1994). Recent data suggests that pUL49 may also play an important role in the regulation of *vhs*, as mutants deleted for pUL49 accumulated mutations in UL41 which inactivated *vhs* function (Sciortino *et al.*, 2007). Other data suggests that both pUL48 and pUL49 may be required for optimal quenching of *vhs* activity (Taddeo *et al.*, 2007). It is likely that the interaction of pUL41 with pUL48 and pUL49 could also direct its incorporation into virions.

1.4.2.5. Outer tegument proteins: pUL46 and pUL47

The tegument proteins pUL46 (VP11/12) and pUL47 (VP13/14), encoded by genes UL46 and UL47 respectively, are non-essential structural proteins that are expressed as true late genes (Dargan *et al.*, 1995; Dargan & Subak-Sharpe, 1997; Kopp *et al.*, 2002; Zhang *et al.*, 1991; Zhang & McKnight, 1993). Little is known about the functions of these proteins during infection, with limited evidence from HSV-1 and 2 as well as PrV giving some clues to their roles. pUL46 has a purely cytoplasmic distribution, while, pUL47 is found in the nucleus at early times, and at later times post infection in a perinuclear location (Kato *et al.*, 2000; Kopp *et al.*, 2002; Morrison *et al.*, 1998a; Nozawa *et al.*, 2004). Both have been shown to be phosphorylated. Phosphorylation of pUL47 has been implicated in tegument disassembly, while the US3 encoded kinase appears to have a role in stabilising pUL46 (Kato *et al.*, 2000; Matsuzaki *et al.*, 2005; Morrison *et al.*, 1998b; Zahariadis *et al.*, 2008). A number of reports suggest that both proteins may be important for regulating pUL48 (VP16) activity (section 1.4.2.6) (Liu *et al.*, 2005; Zhang *et al.*, 1991; Zhang & McKnight, 1993). Other analyses suggest pUL46 interacts with both capsids and cellular membrane (Murphy *et al.*, 2008), while pUL47 has an important, although not essential, role in virion morphogenesis, with aggregates of capsids accumulating in the cytoplasm of infected cells in the absence of pUL47 (Kopp *et al.*, 2002). Data also show that pUL47 is able to bind RNA, although the purpose of this activity is unknown (Sciortino *et al.*, 2002). There is some evidence suggesting a potential role in neuroinvasion and virulence although

the effect of deleting either pUL46 or pUL47 is not pronounced (Klopfleisch *et al.*, 2006; Klopfleisch *et al.*, 2004).

1.4.2.6. Outer tegument protein: pUL48

The major tegument protein pUL48 (VP16 or Vmw 65) is encoded by the UL48 ORF and is an essential protein in HSV-1 (Dalrymple *et al.*, 1985; Weinheimer *et al.*, 1992). pUL48 is a potent transactivator of viral immediate early gene expression in complex with the cellular proteins OCT-1 and HCF, and is implicated in determining whether the infecting virus enters into latent or lytic replication. Of critical importance is a conserved acidic domain which functions in transcriptional activation (reviewed Goding & O'Hare, 1989; Nevins, 1991; O'Hare, 1993; Wysocka & Herr, 2003). The promiscuity of pUL48 transactivation domains can in some respects be explained by structural investigation, which has shown that these acidic activation domains are unstructured (and the whole protein might be regarded as intrinsically unstructured) which allows for interaction with numerous partners to promote transcription including TBP, TFIIA, TFIIB and components of TFIIF and TFIIH. The unstructured activation domains adopt an ordered conformation on binding of transcritption factors, leading to activation of transcription (Jonker *et al.*, 2005). An example of this is shown by pUL48 binding to a subunit of the transcription factor TFIIH. In this case the unstructured acidic activation domain adopts an alpha helical conformation upon binding, which resembles the situation found when the p53 protein, a potent cellular transcriptional activator, binds to TFIIH (Langlois *et al.*, 2008).

pUL48 is an important structural component of the mature virion (Weinheimer *et al.*, 1992). Indeed, a recent report suggests that it is also a component of primary enveloped HSV-1 virions (Naldinho-Souto *et al.*, 2006), although data from PrV and a recent report of investigations with HSV-1 primary virions do not appear to support this assignment (Fuchs *et al.*, 2002a; Padula *et al.*, 2009). In the absence of pUL48, DNA filled capsids accumulate in the cytoplasm and are not enveloped (Fuchs *et al.*, 2002a; von Einem *et al.*, 2006; Weinheimer *et al.*, 1992). This demonstrates that pUL48 has an important role in secondary envelopment and suggests that pUL48 may be added to capsids undergoing tegumentation within the cytoplasm. This is consistent with the results of fluorescence localisation studies, which show that pUL48 exits the nucleus and accumulates in cytoplasmic foci at late times after infection, suggestive of involvement in secondary envelopment (La Boissiere *et al.*, 2004).

pUL48 has been found to be important for mediating tegument protein interactions, and may be critical to directing the correct assembly of the outer tegument. In the absence of pUL48, cytoplasmic capsids of PrV were shown by immuno EM to localise with pUL36 and pUL37, while L particles formed in the absence of pUL48, lacked both pUL36 and pUL37 although pUL46, pUL47 and pUL49 were present as normal (Fuchs *et al.*, 2002a). This suggests that pUL48 may act as a bridge between the inner and outer tegument components. This idea is reinforced by data from yeast-2-hybrid screens of HSV-1 tegument proteins, which identified interactions between pUL48 and pUL36, pUL46, pUL47 and pUL49 (Vittone *et al.*, 2005). As such the structural role of pUL48 may likely involve its wide variety of interaction partners, which include pUL36, pUL41, pUL46, pUL47 and pUL49. Thus, pUL48 may act as a nexus of interactions that direct incorporation of other outer tegument components. Competition between these proteins for binding sites on pUL48 might account for their variability in incorporation, and may account for the dispensability of some, such as pUL49, in virion formation if the interactions of VP16 and other tegument proteins are multiply redundant for assembly.

1.4.2.7. Outer tegument protein: pUL49

The major tegument protein pUL49 (VP22) is encoded by the UL49 ORF and is expressed as a γ1 gene. It is non-essential in tissue culture, but may be important in animal models of infection (del Rio *et al.*, 2002; Duffy *et al.*, 2006; Elliott *et al.*, 2005; Elliott & Meredith, 1992; Pomeranz & Blaho, 2000). pUL49 is one of the most abundant virion proteins and the copy number in virions can be substantially increased by over expression of pUL49 (Leslie *et al.*, 1996). In this respect it differs from the inner tegument protein pUL37 (section 1.4.2.3)(McLauchlan, 1997). pUL49 is able to assemble into homo-oligomers, which may account for the increased incorporation of pUL49 when over expressed (Hafezi *et al.*, 2005; Leslie *et al.*, 1996; Mouzakitis *et al.*, 2005), and also interacts with pUL48 (Hafezi *et al.*, 2005; Mouzakitis *et al.*, 2005). The domains responsible for pUL48 binding and homo-oligomerisation have both been described as essential for pUL49 packaging to virions, although more recent reports suggest that incorporation of pUL49 to virions may be independent of interaction with pUL48 (Hafezi *et al.*, 2005; O'Regan *et al.*, 2007).

pUL49 is a target of the cellular kinase, casein kinase II (CK II), although only unphosphorylated pUL49 seemed to be incorporated into virions (Elliott *et al.*, 1996). However, a mutant in which the CK II target serine residues were mutated to glutamic acid to mimic permanent phosphorylation, was still capable of packaging pUL49 into virions

(Elliott *et al.*, 1996; Potel & Elliott, 2005). As with pUL47, phosphorylation of pUL49 has been implicated in tegument disassembly and therefore assembly of structurally intact tegument may require the packaging of unphosphorylated pUL49 (Morrison *et al.*, 1998b). The phosphorylation status of pUL49 may affect the incorporation of other tegument resident proteins, namely ICP0 and ICP4. Packaging of ICP0 is abolished when a mutant pUL49 mimicking permanent phosphorylation (serine to glutamic acid substitution described above) is used. Expression of ICP0 may be increased in the presence of phosphorylated pUL49 (Elliott *et al.*, 2005; Potel & Elliott, 2005).

The function of pUL49 during infection remains to be fully elucidated, to date there are reports suggesting a role in viral gene expression and in stabilisation and remodelling of the microtubule cytoskeleton. pUL49 also has the ability to traffic from infected to uninfected cells and can transport mRNA into uninfected cells (Elliott & O'Hare, 1998; Martin *et al.*, 2002; Potel & Elliott, 2005; Sciortino *et al.*, 2002). The biological relevance of any of these activities to viral infection is not yet known although it has been speculated by Sciortino *et al*. (2002), that the ability of pUL49 to traffic into uninfected cells and bind RNA, which is subsequently expressed in those cells, might be of use in priming neighbouring cells for viral infection (Elliott & O'Hare, 1997; Sciortino *et al.*, 2002).

A fuller list of tegument components with known activities and functions is given in Table 1.3.

1.4.3. Envelope

A lipid envelope surrounds the virion and is thought to be derived from the *trans*-Golgi network (TGN) by budding of the tegumented capsid into vesicles (Campadelli *et al.*, 1993; Farnsworth & Johnson, 2006; Harley *et al.*, 2001; Skepper *et al.*, 2001; Sugimoto *et al.*, 2008; Whiteley *et al.*, 1999). The membrane is ~5nm thick varying in diameter between 170 to 200 nm (average = 186 nm). Addition of the glycoproteins raised the diameter to about 225 nm on average (Grunewald *et al.*, 2003). HSV-1 encodes at least 12 glycoproteins that are found in the viral envelope (Table 1.4), which display considerable differences in their requirement during the viral lifecycle. Some such as gD, gH, gL and gB are essential for entry, being important either in cell binding or fusion of the membranes (Cai *et al.*, 1988; Forrester *et al.*, 1992; Herold *et al.*, 1994; Klupp *et al.*, 2008; Klupp *et al.*, 1997; Krummenacher *et al.*, 1998; Pertel *et al.*, 2001; Roop *et al.*, 1993; Whitbeck *et al.*, 1997). Others are not essential, but have helper functions such as gC, which enhances

Gene	Protein	MW (kDa)	Properties and Functions
UL4	-	78	Colocalises with UL3. Function not known.
UL7	-	33	Function not known
UL11	-	10.5	Myristylated, necessary for envelopment and exocytosis
UL13	-	57	Protein kinase, phosphorylates ICP0, ICP22, VP22, vhs, gE etc.
UL14	-	24	Aids in cell to cell spread of virus
UL16	-	40	Function not known
UL21	-	58	Binds microtubules
UL23	TK	41	Wide spectrum nucleoside kinase
UL36	VP1-3	336	Section 1.4.2.2
UL37	-	121	Section 1.4.2.3
UL41	vhs	55	Section 1.4.2.4
UL46	VP11/12	79	Section 1.4.2.5
UL47	VP13/14	74	Section 1.4.2.5
UL48	VP16	54	Section 1.4.2.6
UL49	VP22	32	Section 1.4.2.7
UL50	-	39	dUTPase
UL51	-	25	Function not known
UL55	-	20	Present at sites of virion assembly, function unknown.
RL1	ICP34.5	26.6	Blocks host antiviral responses.
RL2	ICP0	78.5	IE gene transcription regulator
RS1	ICP4	133	IE gene transcription regulator
US3	-	53	Section 1.4.2.1
US10	-	34	Phosphoprotein, function unknown
US11	-	18	RNA binding protein, associates with 60s ribosomal subunit

Table 1.3: HSV-1 tegument proteins and their functions.
References: Roizman *et al*., 2007; Mettenleiter, 2002; Loret *et al*., 2008.

Gene	Protein	MW (kDa)	Properties and Functions
UL1	gL	40	Complexes with gH, required for viral entry and cell fusion
UL10	gM	60	Phosphorylated, important for secondary envelopment
UL20		24	Antifusogenic activity, potential role in nuclear exit
UL22	gH	115	Complexes with gL, required for viral entry and cell fusion
UL27	gB	120	Forms homo-oligomers, required for viral entry and cell fusion, attachment to heparan sulphate
UL43		45	Myristylated integral membrane protein of unknown function
UL44	gC	120	Responsible for initial attachment to heparan sulphate
UL45		18	Type 2 membrane protein, role in gB mediated fusion
UL49.5	gN	9	Interacts with gM
UL53	gK	40	Involved in cell fusion. Potential role in secondary envelopment in the cytoplasm
UL56		21	Type 2 membrane protein, implicated in pathogenesis in mice
US4	gG	60	Required for entry into polarised cells, involved in viral egress and cell to cell spread
US5	gJ	10	Non-essential for viral replication in cultured cells
US6	gD	60	Required for receptor-binding, viral penetration and cell fusion
US7	gI	70	Complexes with gE, important for secondary envelopment
US8	gE	80	Complexes with gI, important for secondary envelopment, involved in cell-to-cell spread forms FcR with gI
US9		10	Type 2 membrane protein

Table 1.4: HSV-1 glycoproteins and their known functions.

References: Subak-Sharpe and Dargan, 1998; Roizman *et al*., 2007; Mettenleiter, 2002; Farnsworth, *et al*, 2003

viral binding and subsequent infection (Herold *et al.*, 1991). While others, such as, gE, gI and gM have roles in virion assembly, although the mechanisms involved remain unclear (Brack *et al.*, 1999; Farnsworth *et al.*, 2003; Farnsworth *et al.*, 2007).

Glycoproteins are distributed around the entire surface of the virion although there are some indications that there may be clustering within the membrane, which may reflect the underlying tegument interactions or functional interactions between different glycoproteins (Grunewald *et al.*, 2003; Handler *et al.*, 1996b). Glycoproteins were found to protrude between 10 and 25 nm from the membrane, with one protruding at a range of angles between 30 and 50˚ (Grunewald *et al.*, 2003). EM analysis suggests that gC is distributed uniformly around the virion, whilst gB and gD appeared to form clusters separately from each other (Stannard *et al.*, 1987). Further analysis using chemical crosslinkers suggested that gB, gC and gD were in close proximity to one another due to the formation of gB-gC, gC-gD and gB-gD hetero-oligomers with a crosslinking agent in which the reactive groups were separated by 11.4Å (Handler *et al.*, 1996b). Recent reports suggest that glycoprotein spikes are separated (centre to centre) by between 9 and 13 nm (Grunewald *et al.*, 2003), consistent with these crosslinking experiments (Handler *et al.*, 1996b). Hetero-oligomers of gH-gL were also detected, as well as hetero-oligomers of gH-gL crosslinked to either gC or gD (Handler *et al.*, 1996b). Another report recapitulated the presence of these hetero-oligomers and, in addition, identified gC-gL and gD-gL hetero-oligomers after crosslinking (Handler *et al.*, 1996a). Estimates, from cryo-ET, of the number of glycoprotein spikes suggest there may be between 595 to 758 (mean 659) per virion while another study suggested the relative ratio of gB:gC:gD:gH in KOS and NS strains, are 1:2:11:16 and 1:1:14:9 respectively, as determined by immunoblotting against purified standards (Handler *et al.*, 1996b).

Our knowledge of the structure of individual glycoproteins is currently limited to that from cryo-tomography of virions and to the crystal structures of gB and gD. From tomograms some structural features of glycoproteins can be seen such as bifurcated (Y shaped) spikes. As were other spikes, which extended straight from the membrane and then subsequently bent such that the upper portion of the spike was at an angle relative to the region immediately protruding from the membrane. Other spikes were observed to maintain a straight conformation but protrude from the membrane at an angle (Grunewald *et al.*, 2003). From the crystal structures of gB trimers there is an apparent structural similarity with VSV G protein, while gD seems to have a core which shows structural similarity to an IgV fold (Carfi *et al.*, 2001; Heldwein *et al.*, 2006).

Envelope glycoproteins are known to interact with the tegument through their cytoplasmic tails, with both gD and gE interacting with pUL49 and pUL11, and interactions between gH and pUL48 having been demonstrated (Chi *et al.*, 2005; Farnsworth *et al.*, 2007; Gross *et al.*, 2003). These interactions are likely key to the acquisition of the envelope by tegumented capsids.

1.5. Viral Replication

1.5.1. Entry

1.5.1.1. Binding and Penetration

The HSV-1 virion represents the extracellular stage of the virus life cycle. In common with all viruses HSV-1 must cross the cellular plasma membrane in order to access and subvert the cellular machinery for viral replication (for a general review of viral entry see Marsh & Helenius, 2006; Poranen *et al.*, 2002). Having acquired a membrane and exited the infected cell HSV-1 is thought to enter new cells predominantly through receptor mediated binding and membrane fusion. Some evidence exists to suggest that HSV-1 might be able to exploit an endocytic pathway, but it is unclear as to whether or not this is a productive entry route (reviewed Marsh & Helenius, 2006; Shukla & Spear, 2001). This overview will cover only the proposed fusion route of entry.

HSV-1 engages molecules on the cellular surface through the glycoproteins present in the viral membrane. HSV-1 encodes a number of glycoproteins, and the function of some have been identified as important for viral entry. Glycoprotein C makes initial contact by binding to the heparan sulfate moieties of the cell surface proteoglycans. gC is non-essential, although its absence leads to a 10-fold decrease in infectivity in culture (reviewed Spear, 2004), and its function can be provided by gB which can also bind heparan sulphate. These interactions are insufficient to mediate viral membrane fusion, and presumably serve to tether the virion to the surface of susceptible cells (reviewed Shukla & Spear, 2001; Spear, 2004; Wudunn & Spear, 1989). HSV-1 can recognise a variety of cell surface entry receptors (reviewed Spear, 2004) including Herpesvirus Entry Mediator (HVEM) a member of the TNF superfamily, nectin1 and 2, and specific sites in heparin sulphate generated by certain 3-*O*-sulfotransferases. More recently the potential of the

paired immunoglobulin like type 2 receptor α as a ligand of gB to act as a coreceptor for HSV-1 and PrV entry by membrane fusion has been highlighted (Arii *et al.*, 2009).

After the virus has bound to these cellular receptors the fusion of the viral and cellular membranes occurs. This results in the deposition of the tegumented nucleocapsid into the cytoplasm, permitting the nucleocapsid and tegument to execute their functions within the newly infected cell (Maurer *et al.*, 2008; Sodeik *et al.*, 1997; reviewed Spear, 2004; Spear & Longnecker, 2003).

Membrane fusion is mediated by the gH/gL complex together with gD and gB (Herold *et al.*, 1994; Johnson & Ligas, 1988; Krummenacher *et al.*, 1998; Pertel *et al.*, 2001; Roop *et al.*, 1993; Shukla & Spear, 2001; Spear, 2004; reviewed Spear & Longnecker, 2003).

Recently, entry of virus into cells by direct membrane fusion has been studied using cryo-ET of frozen infected cells. These studies show the intermediates of viral membrane fusion with the cell (Maurer *et al.*, 2008). They present the first evidence of membrane deformation and support the potential role of glycoprotein conformational changes in cell-viral membrane fusion (Maurer *et al.*, 2008). Thus, viral glycoproteins interacting with cellular receptors undergo conformational changes, at the site where membrane fusion will occur, forming V and Y shaped structures alongside the fusion pore, whilst the membranes are drawn to a distinct point, between these glycoprotein spikes. This brings the membranes into close apposition resulting in the mixing of the viral and cellular membranes and the formation of the fusion pore. After mixing the viral membrane retains its curvature and subsequently gradually adopts a less curved form (Maurer *et al.*, 2008; Sodeik *et al.*, 1997). One further feature this study highlights is the need for the capsid to negotiate the actin cortex present just beneath the cellular membrane, a process that is poorly understood, but must occur (Maurer *et al.*, 2008).

1.5.1.2. Disassembly of tegument

After fusion of the viral and cell membranes, the tegumented nucleocapsid is deposited into the cell (Maurer *et al.*, 2008; Sodeik *et al.*, 1997). In order for the many tegument proteins to exert their functions within the cell they need to be released from this structure. Disassembly of the tegument after infection was shown by immunofluorescence studies of the fate of virion derived proteins, which revealed that tegument proteins were present in different cellular locations by 3 h pi (Morrison *et al.*, 1998a). Such observations are

strengthened by more recent data suggesting that the presence of outer tegument on stripped virions inhibits intracellular microtubule transport (Wolfstein *et al.*, 2006) (section 1.5.2.1). Previous work had suggested that de-enveloped tegument structures produced from purified L particles are stable (McLauchlan & Rixon, 1992), and therefore a mechanism to destabilise this structure to promote disassembly was needed. One interesting feature of the studies reported by Morrison *et al*. (1998a) was the apparent loss of pUL49 signal after infection when using an antibody designated P43 for detection. The authors suggested this might have been due to P43 recognising a phosphorylation sensitive epitope (Morrison *et al.*, 1998a). This implied a role for kinases to induce instability into the tegument structure. Subsequently, Morrison *et al*. (1998b) showed that both viral and cellular kinases could mediate this process, and that addition of phosphatase to an *in vitro*, virion disassembly system, prevented release of pUL49 and pUL47. Furthermore, although phosphorylation promoted the release of pUL49 and pUL47, pUL36 and UL13 kinase remained with the capsid in a manner that was compatible with the locations of pUL49 and pUL47 within the outer tegument, and of pUL36 in inner tegument, where it is tightly associated with the capsid (Morrison *et al.*, 1998b). The absence of UL13 kinase function was associated with retention of pUL49 to the tegument structure, although this could be reversed by the addition of casein kinase II. Casein kinase II was also implicated in phosphorylation of pUL36 and pUL47, while protein kinase A (PKA) phosphorylated both pUL48 and pUL47. The latter was also susceptible to PKC phosphorylation (Morrison *et al.*, 1998b). These phosphorylation events precede viral gene expression, and thus, are likely performed by viral kinases (UL13) packaged into the virions. The potential involvement of cellular kinases (predominantly CK II) may reflect, either an alternative (auxiliary or compensatory) mechanism to be used in the absence of UL13 function or, a means to prevent premature destabilisation of the tegument before entry into the new host cell (Morrison *et al.*, 1998b).

Data from electron microscopy and cryo-ET suggests that tegument disassembly takes place at the plasma membrane immediately after fusion and that detectable parts of the tegument remain with the membrane embedded glycoproteins at the cell surface while an apparently naked nucleocapsid is transported to the nucleus (Maurer *et al.*, 2008; Sodeik *et al.*, 1997). However, the consistency of reports describing retention of inner tegument proteins on capsids as important for downstream functions makes it likely that the nakedness of the capsids seen by both conventional EM and cryo-ET is only apparent (Batterson *et al.*, 1983; Luxton *et al.*, 2006; Morrison *et al.*, 1998a; Morrison *et al.*, 1998b; Wolfstein *et al.*, 2006).

1.5.2. Subversion of the cell

Subversion of the cell likely begins through the activity of pUL41 (*vhs*) released from the infecting virion, which initiates the degradation of mRNAs. Likewise, the presence of pUL48 and ICP0 derived from the infecting virion, produce an environment conducive to viral gene expression. Incorporation of viral mRNAs to the virion would also allow for synthesis of viral proteins in the time immediately after penetration but prior to viral gene expression. However, full subversion of the cell to the expression of the viral gene programme requires the transport of viral nucleocapsids from the periphery of the cell, across the cytoplasm, to the nucleus where they interact with the nuclear pore complex. This results in uncoating of the viral genome and its transport into the nucleus to allow viral gene expression, and thus virus replication, to begin (reviewed Izaurralde *et al.*, 1999).

1.5.2.1. Transport to the nucleus

Viruses must negotiate the interior of cells to access the compartments where different stages of their life-cycles, such as genome replication and particle assembly, take place. Eukaryotic cells are both large and complex with many specialised structures that are spatially separated within the cell. Transport of organelles, vesicles and molecules within a cell therefore require targeting and a dedicated transport system. This system is formed from the microtubule network and the actin cytoskeleton, which are both used as tracks by motor proteins and have been likened to the road network of cities (reviewed Dohner *et al.*, 2005; Greber & Way, 2006; Hirokawa, 1998; Lyman & Enquist, 2009; Poranen *et al.*, 2002; Sodeik, 2000). Viruses, with their need to access particular sites within the cell, are known to exploit cellular transport systems for their own end (Luxton *et al.*, 2006; Mabit *et al.*, 2002; McDonald *et al.*, 2002; Ogawa-Goto *et al.*, 2003; Ohka *et al.*, 2009; Radtke *et al.*, 2006; Sodeik, 2002; Sodeik *et al.*, 1997).

To nuclear replicating viruses the cytoplasm of the cell represents a considerable obstacle, as free diffusion of viral capsids within this compartment is considered highly unlikely (reviewed Sodeik, 2000). The cytoplasm contains many organelles and cytoskeletal structures, and represents a region of molecular crowding that can reach high protein concentrations (in the order of 300mg/ml). This restricts the maximum size of freely diffusing entities to ~500 kDa (reviewed Sodeik, 2002). It has been estimated for HSV-1

that free diffusion of the capsid through 10 μm of cytoplasm would take in the order of 2 hours, making the requirement for engaging the host transport systems paramount for the propagation of large viruses such as HSV-1 and Adenovirus (Sodeik, 2000).

HSV-1 seems to utilise the microtubule network for intracellular transport, although not exclusively. Infection of cells pre-treated with the microtubule depolymerising drug Nocodazole showed infection was retarded but not abolished suggesting that HSV-1 was able to engage a different pathway for transport towards the nucleus. Presumably the actin cytoskeleton is involved as treatment with both Nocodazole and Cytochalasin D (which depolymerises the actin network) showed no residual transport of capsids (Luxton *et al.*, 2006; Sodeik *et al.*, 1997).

Work on *in vitro* reconstitution systems and studies using inhibitory over expression of motor protein components have begun to identify the virus and host components required for capsid transport (Dohner *et al.*, 2002; Wolfstein *et al.*, 2006).

Thus, examining transport of purified HSV-1 capsids or stripped virions (virions treated with detergent and buffers of differing salt concentrations to remove membrane and some tegument components) along purified microtubules has highlighted a potential key role of the inner tegument proteins pUL36 and pUL37 in contacting motor proteins, and through them the microtubule network (Wolfstein *et al.*, 2006). This agrees well with data from live cell work with PrV showing the retention of both pUL36 and pUL37 to the capsid during transport to the nucleus (Luxton *et al.*, 2006). The precise contributions of both pUL36 and pUL37 to this process are uncertain and as yet no microtubule motor protein binding domains have been mapped to either tegument protein. The probable role of the inner tegument in this process is further underscored by analysis of deletion mutants of dispensable tegument proteins, which shows that these deletions (of genes such as UL46/UL47 in a PrV strain) had no impact on cytoplasmic capsid transport in infection (Antinone *et al.*, 2006).

One type of interaction between HSV-1 and microtubules is thought to occur through recruitment of the minus end directed motor proteins dynein and dynactin. HSV-1 capsids have been shown to colocalise with these cytoplasmic proteins in immunofluorescence studies, and their importance for capsid transport towards the nucleus was demonstrated by the suppression of dynein activity following over expression of the dynamitin subunit of dynactin This destabilises the dynactin complex (Dohner *et al.*, 2002), which causes

capsids to remain at, or return to the cell periphery (by plus end directed transport) (Dohner *et al.*, 2002).

The only transport related protein:protein interaction yet demonstrated is that of VP26, the small hexon binding protein, with Tctex1 and RP3 dynein light chains. This interaction appears to be important in neuronal systems but has been shown to be dispensable for capsid transport in non-neuronal cell types (Antinone *et al.*, 2006; Dohner *et al.*, 2006; Douglas *et al.*, 2004). Recent data from PrV suggests that pUL37 has a transport related function in the initiation of infection, as infection by ΔUL37 PrV was retarded by ~1h compared to WT PrV (Krautwald *et al.*, 2009). This retardation may reflect the need for PrV to engage non-microtubule network transport systems (as is the case in nocodazole treated cells, which also show retardation of infection). Alternatively, pUL37 may function as a processivity factor, or in the recruitment of specific motor proteins (Luxton *et al.*, 2006; Sodeik *et al.*, 1997).

HSV-1 bound to microtubules demonstrates unexpected behaviour when imaged using time lapse fluorescence microscopy, in that individual capsids can undergo both anterograde and retrograde movement at different times (reviewed Dohner *et al.*, 2005; Dohner *et al.*, 2002), similar behaviour has also been seen with other viruses including Adenovirus infections (reviewed Dohner *et al.*, 2005; Suomalainen *et al.*, 1999). The current opinion in the field is that HSV-1 capsids bind both plus and minus end directed motors and that the virus is able to regulate the direction of travel by post translational modifications of the motor proteins, presumably through phosphorylation to activate or repress motor activity (Dohner *et al.*, 2005; Dohner *et al.*, 2002; reviewed Greber & Way, 2006).

Initial transport of capsids upon infection is toward the nucleus of the host cell. This involves transport of capsids towards the microtubule organising center (MTOC) and then away from the MTOC towards the nucleus to engage nuclear pores. The mechanism by which HSV-1 apparently switches from minus ended to plus ended transport at the MTOC remains unknown (reviewed Radtke *et al.*, 2006). After assembly within, and release from, the nucleus, capsids must again be transported through the cytoplasm to the site of secondary envelopment. This process is also poorly understood but is becoming the focus of increased research effort (reviewed Lyman & Enquist, 2009).

1.5.2.2. Uncoating

The goal of incoming capsids is to reach a nuclear pore and release their DNA into the nucleus. However the events surrounding interaction of HSV-1 capsids with the nuclear pore complex (NPC) and uncoating of the viral genome are poorly understood even when compared to our understanding of viral intracellular transport (Greber & Fassati, 2003; reviewed Izaurralde *et al.*, 1999; Poranen *et al.*, 2002). Currently data regarding this are confined to ts mutants, which fail to uncoat the viral genome at the NPC under the non-permissive regime and a small number of studies attempting to dissect the molecular interactions in NPC docking and genome release.

Early EM examination of tsB7-infected cells had suggested that incoming HSV-1 capsids associate with nuclear pores (Batterson *et al.*, 1983) and a more recent study confirmed the association of empty WT HSV-1 capsids with nuclear pore structures (Sodeik *et al.*, 1997). These findings were then extended by *in vitro* functional studies using purified nuclei and capsids derived from stripped virions. This work showed that HSV-1 interacted specifically with the NPC, that this interaction could be blocked by antibodies that bound components of the NPC, and that it was dependent on the presence of Importin β. The interaction of HSV-1 with the NPC relied on a viral protein identified as either VP1-3, VP13/14, VP16 or VP22, the function of which was sensitive to trypsin digestion. Release of viral DNA was dependent on host cytoplasmic factors and was an energy dependent process. The authors interpreted these data as implying that components of the NPC have an active role in the binding of capsids and the uncoating of the HSV-1 genome (Ojala *et al.*, 2000).

The viral proteins involved in these processes have remained poorly defined, although work with tsB7 (a mutant of UL36) and a ts mutant of UL25 (ts1249) have suggested roles for these proteins. Both tsB7 and ts1249 display genome uncoating defects following infection in non-permissive conditions, with DNA containing capsids accumulating in the vicinity of the nucleus (Batterson *et al.*, 1983; Preston *et al.*, 2008). This has been interpreted as implicating both pUL36 and pUL25 in the process of genome release. pUL36 and pUL25 are known to interact, suggesting that the defects in tsB7 and ts1249 might affect a common mechanism (Coller *et al.*, 2007; Jovasevic *et al.*, 2008). Previous investigations of null mutants suggested a role for pUL25 in the retention of newly packaged viral DNA within the capsid, supporting the likelihood that this protein may be associated with the DNA packaging/uncoating mechanism (McNab *et al.*, 1998; Stow,

2001). Recent data further suggest that pUL36 must undergo proteolytic processing for genome release to occur (Jovasevic *et al.*, 2008).

There have been recent efforts to dissect the molecular interactions that underlie capsid-NPC interactions and to determine the potential roles of viral proteins in uncoating. One recent investigation using antibodies introduced directly into the cytoplasm has directly implicated pUL36 in NPC binding and has also suggested that the nucleoporins CAN/Nup214 and RanBP2/Nup358 might be the targets of such interaction (Copeland *et al.*, 2009). A second study using siRNA technology, has also demonstrated the importance of CAN/Nup214 for the efficient entry of viral DNA to the host nucleus, suggesting it has a role in either the process of genome import or in capsid binding (Pasdeloup *et al.*, 2009). This investigation used yeast 2-hybrid and immunoprecipitation analyses to identify interactions between pUL25 and the NPC components CAN/Nup214 and hCG1, and between pUL25 and the viral proteins pUL36 and pUL6. The significance of the viral protein interactions is not yet fully understood although Pasdeloup *et al*. (2009) suggest that the interaction of pUL25 and pUL36 at the 11 pentonal vertices of the capsid might be important for virion morphogenesis and egress, while the interaction of pUL25 with pUL36 at the pUL6 portal might place both proteins in the correct position to interact with the NPC to bring about uncoating of the viral genome, thereby explaining the common defect seen with both tsB7 and ts1249.

The viral genome is released through the specialised portal vertex, in a process thought to be equivalent to the release of viral DNA by bacteriophage (section 1.9) (reviewed Poranen *et al.*, 2002). One report has suggested that the DNA passes through the nuclear pore as a condensed rod like structure (Shahin *et al.*, 2006) but the nature of this structure and how this would occur are problematic. The details of the mechanism by which the DNA exits the capsid are currently unknown, but by analogy with bacteriophages it is thought that internal pressure built up during DNA packaging might act as the driving force, at least in part, for the exit of the viral DNA (reviewed Poranen *et al.*, 2002).

1.5.3. Replication

Entry of HSV-1 viral DNA into the nucleus of an infected cell precipitates a chain of events that remodel the nucleus (Simpson-Holley *et al.*, 2005), and result in viral gene expression, genome replication and ultimately virion morphogenesis (Monier *et al.*, 2000). Upon entry viral DNA is thought to adopt an endless configuration consistent with

circularisation (reviewed Boehmer & Lehman, 1997; Strang & Stow, 2005). Other investigations have failed to observe circularised genomes in productively infected cells and have reported that ICP0 inhibits circularisation through interruption of the cellular DNA end joining mechanisms (Jackson & DeLuca, 2003). Jackson and DeLuca (2003) suggested that circularisation of the genome is associated with latent or quiescent infections and that replication in productively infected cells favours linear genomes. This model accounts for the presence of junction fragments (spanning the junction of TR_L and TR_S as would be expected in a circularised molecule) by invoking concatameric genomes, or highly branched replication products, as their source. One feature this model does not explain is how the replication of the terminal ends of a linear molecule would be achieved.

Immediately after entering the nucleus, HSV-1 DNA associates with nuclear substructures termed ND10 or PML bodies and these form the site where transcription and initial replication are thought to occur (Everett & Murray, 2005; Lukonis *et al.*, 1997; Maul *et al.*, 1996; Sourvinos & Everett, 2002; Uprichard & Knipe, 1997). There was some question over whether incoming HSV-1 genomes were targeted to pre-existing ND10 structures or caused the formation of new ND10 structures. Data currently suggest that ND10 structures are highly dynamic and that individual components can be rapidly recruited to incoming viral DNA. This favours the idea that the ND10 structures associated with viral DNA are formed *de novo* from free components within the nucleoplasm (Everett & Murray, 2005).

A growing body of data suggests that ND10 structures must be disrupted to prevent the HSV-1 genome becoming repressed and quiescent and adopting a state akin to latency (Everett *et al.*, 2007; Everett *et al.*, 2008; Everett *et al.*, 2006; Hancock *et al.*, 2006; McMahon & Walsh, 2008; Tavalai *et al.*, 2006). Indeed this seems a principle common to herpesviruses and other DNA viruses suggesting that ND10 structures may represent an innate defence mechanism to counter viruses that replicate in the nucleus (Hancock *et al.*, 2006; Ling *et al.*, 2008; Tavalai *et al.*, 2006; Ullman & Hearing, 2008).

Viruses need to counteract this innate defence mechanism and certain viral proteins are able to alter the composition of ND10 structures in ways which promote lytic infection (Everett *et al.*, 2009; Lukashchuk *et al.*, 2008). In HSV-1, ICP0, an E3 ubiquitin ligase, seems to be highly important for remodelling ND10 structures (Boutell *et al.*, 2002; Everett *et al.*, 2008; Everett *et al.*, 2009; Gu & Roizman, 2009). ICP0 targets PML (an ND10 component) for degradation and so causes the dispersal of ND10 structures (Everett *et al.*, 2006). In addition to their involvement in gene expression, ND10 structures are also

implicated in viral DNA replication. Pre-replicative sites are located at ND10, or ND10 like, structures (Lukonis *et al.*, 1997; Uprichard & Knipe, 1997), and some of these progress to form active replication compartments (Sourvinos & Everett, 2002). The products of genes UL5, UL8, UL52, UL9 and ICP8 (de Bruyn Kops *et al.*, 1998) associate with viral DNA in replication compartments and are able to recruit the viral DNA polymerase (UL30) and accessory factor (UL42) (Liptak *et al.*, 1996), and host factors (Taylor & Knipe, 2004). Active viral DNA replication leads to enlargement of these compartments and the margination of chromatin (Monier *et al.*, 2000).

1.5.3.1. Viral gene expression

As described above, initial viral gene expression occurs close to ND10 structures (Maul *et al.*, 1996), and the expression of genes is by a tightly regulated temporal cascade. Viral gene expression utilises cellular RNA polymerase II (Alwine *et al.*, 1974; Costanzo *et al.*, 1977) and proceeds in 3 waves beginning with the Immediate Early (IE or α) class, then the Early class (E or β) and then finally the Late class (L or γ) (Honess & Roizman, 1974; 1975). Expression of the IE regulatory proteins ICP0, ICP4, ICP22, ICP27 and ICP47 is stimulated by the trans-activating function of virion derived VP16 (Campbell *et al.*, 1984). Of the IE proteins, all but ICP47 play a role in promoting the expression of the E or L proteins (Jones & Roizman, 1979; reviewed Weir, 2001). Expression of the E proteins is independent of viral DNA replication, and the proteins necessary for DNA replication are themselves encoded by E genes (Jones & Roizman, 1979; Roizman *et al.*, 1963). Expression of IE and E genes stimulates the expression of L genes. This class is subdivided into L1 and L2 genes L1 (or leaky late) genes are expressed earlier in infection and expression is stimulated by DNA replication, while L2 (or true late) genes are expressed later in infection and only after viral DNA synthesis has commenced (Conley *et al.*, 1981; Jones & Roizman, 1979; reviewed Weir, 2001). L genes are predominantly structural components with VP5 and pUL36 being examples of L1 and L2 genes respectively. Expression of IE genes is self regulatory, and is also repressed by E and L gene expression (Honess & Roizman, 1975). E gene expression is likewise repressed at the onset of L gene expression. (reviewed Roizman *et al.*, 2007).

1.5.3.2. Viral DNA replication

Replication of the viral genome occurs within the nucleus and is performed by viral gene products. There are 7 key replication proteins, pUL5, pUL8 and pUL52 forming the helicase/primase component, pUL9 the origin binding protein, pUL29 (ICP8) the single

strand DNA binding protein, pUL30 the viral DNA polymerase and pUL42 the DNA polymerase processivity factor (McGeoch *et al.*, 1988; Wu *et al.*, 1988). Viral DNA replication is thought to initiate on the circularised infecting genome at one, or more, of the 3 origins present in the viral genome (Igarashi *et al.*, 1993), of which one is in the U_L region (between UL29 and UL30) and two within the IR_S TR_S inverted repeats (McGeoch *et al.*, 1988; Stow, 1982). Initiation of replication requires unwinding of the DNA to allow access to the replication origin and recruitment of the polymerase. Initially the origin binding protein (OBP) pUL9 (either in isolation or with ICP8) binds to defined sites flanking the central AT rich sequences of the origin and causes looping and distortion of the helix (reviewed Boehmer & Lehman, 1997; Elias & Lehman, 1988; Elias *et al.*, 1986; Olivo *et al.*, 1988; Stabell & Olivo, 1993). pUL9 possesses a helicase activity and begins unwinding the DNA, resulting in the recruitment of ICP8 to ssDNA (Bruckner *et al.*, 1991; Fierer & Challberg, 1992; Lee & Knipe, 1985; Martinez *et al.*, 1992). The helicase-primase complex is subsequently recruited to the origin by interaction with either pUL9, ICP8 or both in complex (reviewed Boehmer & Lehman, 1997). Loading of the helicase-primase (pUL5/pUL8/pUL52) results in further unwinding of the DNA template and synthesis of primers for DNA synthesis (Crute *et al.*, 1988; Crute *et al.*, 1989). Synthesis of viral DNA is performed by the HSV-1 polymerase (pUL30) in combination with the pUL42 processivity factor (Gibbs *et al.*, 1985; Hernandez & Lehman, 1990; Parris *et al.*, 1988). In addition to HSV-1 proteins, cellular proteins might be recruited to achieve DNA synthesis but the identity of such proteins is yet to be confirmed (reviewed Boehmer & Lehman, 1997; reviewed Roizman *et al.*, 2007). Viral DNA replication is thought to begin by a θ mechanism and then switch to a rolling circle replication mechanism that would account for the formation of long concatameric molecules (Stow, 1982). Initiation of DNA synthesis is origin dependent but it becomes origin independent presumably reflecting the switch from θ replication to a rolling circle mechanism (reviewed Boehmer & Lehman, 1997; reviewed Roizman *et al.*, 2007).

1.5.4. Nuclear Capsid assembly and DNA packaging

Assembly of the herpesvirus capsid occurs in the nucleus, and it is into these preformed capsids that the viral genome is packaged. This led to speculation on a relationship between herpesviruses and dsDNA bacteriophages which is dealt with further in section 1.9 (Figure 1.5). The genes encoding the capsid proteins are classified as γ genes. Assembly of functional capsids requires seven proteins, the capsid shell proteins VP5, VP19C, VP23, VP26 (not essential) and pUL6, as well as the products of the UL26 and

UL26.5 reading frames (the protease, which cleaves itself to produce the proteins VP21 and VP24, and preVP22a respectively) that act as a scaffold around which the capsid shell is formed (Desai *et al.*, 1993; Newcomb & Brown, 2002; Tatman *et al.*, 1994; van Zeijl *et al.*, 2000; Zhou *et al.*, 1995). Translated capsid and scaffolding proteins must enter the nucleus, and preVP22a and VP19C contain nuclear localisation signals (Adamson *et al.*, 2006; Nicholson *et al.*, 1994). Interaction of preVP22a with VP5 and of VP19C with VP23 ensures nuclear localisation of these proteins. Interaction of preVP22a with pUL6 is believed to be responsible for the localisation of pUL6 to the nucleus (Newcomb *et al.*, 2003).

The process of capsid assembly is currently thought to begin with the interaction of pUL6 and preVP22a to form a portal structure on a preVP22a scaffold (Newcomb *et al.*, 2003). Incorporation of VP5 into the procapsid structure is thought to be by addition of preVP22a complexed VP5 to the growing scaffold, nucleated on the preVP22a complexed portal, with subsequent recruitment of the triplex proteins (Newcomb *et al.*, 1999; Newcomb *et al.*, 2003). The initial product of capsid assembly is the spherical procapsid that matures to the characteristic angular herpes capsid following cleavage of the scaffolding protein by the VP24 viral protease (Figure 1.5). The procapsid displays the five and six fold symmetries of the mature capsid but the shell is much less integrated and the procapsid is also much less stable than the mature capsid (Newcomb *et al.*, 1996; Newcomb *et al.*, 1999). The procapsid was identified as an intermediate of capsid assembly in both *in vitro* capsid assembly systems and in infection with mutants such as ts1201 where maturation of the capsid is blocked by the inactivity of the mutant protease (Newcomb *et al.*, 1996; Newcomb *et al.*, 2001a; Newcomb *et al.*, 2000). Assembly of the procapsid does not require the presence of pUL6, as seen in the heterologous baculovirus expression system (Newcomb *et al.*, 1999). However, capsids lacking pUL6 cannot package DNA.

Maturation of the procapsid to the mature form requires the activity of the VP24 viral maturational protease as shown by the effect of the ts lesion in ts1201 or the similar mutant tsProtA which results in the accumulation of procapsids at the non permissive temperature (Gao *et al.*, 1994; Preston *et al.*, 1983; Preston *et al.*, 1992). VP5 interacts with scaffold through defined domains of both scaffolding protein and VP5 (Thomsen *et al.*, 1995; Walters *et al.*, 2003; Warner *et al.*, 2001). VP24 protease cleaves the C terminal 25 amino acids, which contain the VP5 binding domain, from preVP22a, resulting in the formation of VP22a. This cleavage releases VP5 from the underlying scaffold and triggers the rearrangement of the shell proteins (Heymann *et al.*, 2003). Mutations in either of the VP5

or preVP22a interaction domains are detrimental to capsid assembly. In virus mutants where the maturational cleavage site has been removed, escape mutants have been isolated with compensatory changes in VP5 that weaken binding of the scaffolding protein (Desai & Person, 1999).

Angularisation can occur in the absence of DNA packaging, and this process leads to the formations of three distinct and separable species of capsid. A capsids are empty lacking both internal scaffold and viral DNA, B capsids contain a protein core of cleaved scaffolding protein (VP22a). C capsids lack the internal protein scaffold but do contain a unit length viral genome.

Replicated viral DNA is thought to be packaged in a manner similar to that of dsDNA bacteriophages (Figure 1.5). In dsDNA bacteriophages viral DNA is packaged into preformed procapsids through the portal, which substitutes in place of one penton vertex within the capsid shell (Tang *et al.*, 2008). HSV-1 likewise assembles preformed capsids and viral DNA is thought to be packaged into the capsids through a specialised portal vertex (Cardone *et al.*, 2007; Chang *et al.*, 2007). The portal is a dodecameric ring of pUL6 containing a central channel through which DNA is thought to enter the capsid shell (Trus *et al.*, 2004). The structure of the HSV-1 portal is similar to that seen in dsDNA bacteriophages (Tang *et al.*, 2008). DNA packaging in bacteriophage requires energy, and one model suggests that a symmetry mismatch between the five fold vertex and the 12 fold portal complex permits the portal to rotate in order to package DNA although this has been cast into doubt by experiments which appear to show that the bacteriophage portal is fixed in the capsid (reviewed Hugel *et al.*, 2007; Meijer *et al.*, 2001).

Further similarity to dsDNA bacteriophages is seen in genome packaging. Viral DNA is packaged into the capsid by the action of a complex called the terminase, which contains pUL15 pUL33 and pUL28. The precise mechanism by which DNA is packaged is unknown. It is thought that the terminase loads onto specific sequences on the viral DNA and associates with the portal complex. The DNA is then translocated into the capsid in an energy dependent process requiring the hydrolysis of ATP (Dasgupta & Wilson, 1999). The packaging reaction is terminated by the recognition of a specific termination signal, contained in the a sequence, which is present between the long and short repeat sequences. The terminase cleaves the dsDNA concatameric genome to release the unit length genome. Retention of the DNA within the capsid is thought to involve the binding of pUL25 to the capsid, and possibly also pUL17 (McNab *et al.*, 1998; Salmon *et al.*, 1998).

1.6. Exit

1.6.1. Nuclear egress

The exit of capsids from the nucleus of infected cells has long been an area of controversy. Two major models were originally proposed for the escape of capsids from the nucleus; an envelopment, de-envelopment, re-envelopment model, or a single envelopment model (reviewed Mettenleiter, 2002). The double envelopment model, in which a capsid gains and then loses an envelope at the inner and outer nuclear membranes before gaining a final envelope in the cytoplasm, is currently the most widely accepted based on an accumulation of data and will be discussed in detail below. The single envelopment model proposed that the virion envelope is derived from the nuclear membrane and retains its integrity until the particle is released through the secretory pathway (reviewed Mettenleiter, 2002). This model implies that envelopment at the inner nuclear membrane results in the formation of intact mature virions, which contain a full complement of tegument and envelope proteins.

More recently a study has proposed that capsids may exit the nucleus through dilated nuclear pores to access the cytoplasm. However, the biological significance of this observation is unclear (Wild *et al.*, 2009). Indeed a report of experiments performed to establish the integrity of the nuclear membrane and the size discrimination of the pores, suggests that even at late times after infection the integrity of the nuclear structure is not compromised (Hofemeister & O'Hare, 2008).

The evidence supporting the envelopment, de-envelopment, re-envelopment model of viral morphogenesis is extensive. It includes the following: direct evidence from EM of capsids undergoing envelopment in the cytoplasm (Granzow *et al.*, 2001); differences between the lipid content of the virion envelope and the nuclear membrane (van Genderen *et al.*, 1994); the identification of tegument and glycoprotein mutants that accumulate unenveloped capsids in the cytoplasm, thereby demonstrating that these proteins affect a later, cytoplasmic maturation step, after the capsids have passed through both nuclear membranes (Brack *et al.*, 1999; Desai *et al.*, 2001; Desai, 2000; Farnsworth *et al.*, 2003). Furthermore retargeting of glycoprotein gD to the ER results in gD being incorporated to the primary virion and is subsequently found to be absent from the mature virion, suggesting that the primary envelope is shed, and a second one acquired prior to egress of mature virion from the cell (Skepper *et al.*, 2001; Whiteley *et al.*, 1999).

Enveloped capsids are frequently seen in the perinuclear space in electron micrographs of infected cells (Mettenleiter *et al.*, 2006; Naldinho-Souto *et al.*, 2006). Since budding of interphase nuclear membranes is not a normal process, this envelopment step requires modification of the nuclear membrane and the underlying lamina. There is now considerable evidence demonstrating the nature of these modifications. A number of structural elements such as Emerin and lamin A/C are affected (phosphorylation of Emerin has been shown in HSV-1 infection leading to delocalisation) and recruitment of Protein Kinase C (PKC) to the inner nuclear membrane to destabilise the nuclear lamina has been shown in HCMV infection (reviewed Lyman & Enquist, 2009; Morris *et al.*, 2007; Muranyi *et al.*, 2002; Simpson-Holley *et al.*, 2004). The result of these changes is that the lamina is disassembled thereby facilitating access of the nucleocapsid to the nuclear membrane. (Morris *et al.*, 2007; Reynolds *et al.*, 2004; Scott & O'Hare, 2001). Two viral proteins involved in this process are pUL31 and pUL34, which form a complex. Independent deletions of UL31 and UL34, which are conserved throughout the *Herpesviridae*, show large deficits in nuclear egress, with these deletions resulting in abrogation of virion morphogenesis (Fuchs *et al.*, 2002c; Klupp *et al.*, 2000; Reynolds *et al.*, 2001). Another protein, pUS3, appears to be important for localisation of the pUL31/pUL34 complex (Reynolds *et al.*, 2001). The absence of pUS3 activity results in the accumulation of enveloped nucleocapsids between the nuclear membranes, which supports a role for pUS3 in primary de-envelopment (Klupp *et al.*, 2001a; Reynolds *et al.*, 2002).

1.6.2. Tegumentation

The site and sequence of tegument addition is still largely unresolved. Some tegument proteins have been reported as associated with nuclear capsids (Bucks *et al.*, 2007) and immuno EM has identified the presence of pUL48 in primary enveloped capsids in the perinuclear space, although the precise composition of these particles is not yet firmly established (Naldinho-Souto *et al.*, 2006; Padula *et al.*, 2009). However, tegumentation is presumed to occur, primarily in the cytoplasm of infected cells based on data from investigation of primary virion composition suggesting that most common tegument proteins are absent from these virions, as well as ultrastructural EM observations of virion morphogenesis which suggested cytoplasmic acquisition of tegument (Granzow *et al.*, 2001; Padula *et al.*, 2009). Investigation of inner tegument mutants such as KΔUL36 (Desai, 2000) and similar mutants, in both HSV-1 and PrV, showed that either apparently tegument free, or minimally tegumented unenveloped capsids accumulated within the

cytoplasm (Desai *et al.*, 2001; Fuchs *et al.*, 2002a). Such an accumulation argues in favour of the site of tegument acquisition being within the cytoplasmic compartment of the cell in concert with the apparent absence of tegument from primary virions and ultrastructural investigation showing presumed tegument acquisition in the cytoplasm.

The order and location of acquisition of tegument proteins is poorly understood, but there is data to suggest that tegumentation can begin in two distinct places, and is driven by the network of interactions between the tegument proteins. Some tegument components, namely the proteins pUS3, pUL36 and pUL37 are thought to assemble directly onto capsids after they have exited from the nucleus. These are typically described as inner tegument proteins (reviewed Mettenleiter, 2002). However, the majority of the tegument proteins, designated the outer tegument proteins and including pUL48 and pUL49 (VP16 and VP22), are believed to associate first with the viral glycoproteins at the site of virion envelopment at Golgi derived vesicles (reviewed Mettenleiter, 2002). Evidence for this model of assembly comes from several sources. Thus, capsids of mutants lacking outer tegument proteins are associated with the inner tegument components (Fuchs *et al.*, 2002a) and particles consisting solely of tegument and envelope (L particles) can still form under conditions where capsids are not present or are incapable of forming virions (Dargan *et al.*, 1995; Klupp *et al.*, 2001b; Rixon *et al.*, 1992). An interesting insight into the assembly process was gained from the identification of L particles, which contain a full spectrum of tegument proteins (Szilagyi & Cunningham, 1991). Their existence implies that capsids are not required for the tegument to associate with the membrane and glycoproteins and to form structures that are competent to bud (Rixon *et al.*, 1992). Rather, they suggest that the assembly and envelopment processes are intrinsic to the tegument/glycoprotein complex and that these may drive the incorporation of the capsid to form the infectious virion. Interestingly, the inner tegument proteins pUL36 and pUL37 are both found in L particles, showing that they can interact independently with either the capsid or the tegument, and recent work has suggested that these proteins may be directly responsible for targeting the capsids to the site of virion formation on membranes of the *trans*-Golgi network (Desai *et al.*, 2008; D. Pasdeloup pers. comm.). As such it may be possible to speculate that L particles represent failed or abortive attempts at envelopment of capsids, and that there are precursors to L particles; these being sites to which glycoprotein tails recruit outer tegument proteins. These would represent sites primed for envelopment, which are competent to bud when a capsid coated in inner tegument becomes available. Division of the process of tegumentation between two sites would reduce the need for extensive coordination in the stepwise addition of tegument components.

The network of interactions between tegument proteins that is thought to drive tegument formation and result in secondary envelopment has been studied in yeast-2-hybrid systems and with deletion mutants (Lee *et al.*, 2008; Vittone *et al.*, 2005). At the base of this network is the interaction between pUL36 and pUL25, which is thought to form the link by which capsid acquires tegument (Coller *et al.*, 2007; Pasdeloup *et al.*, 2009). Analysis of the tegument interaction network is difficult owing to the redundancy of interactions between proteins and the tendency for the outer tegument components in particular, to form multiple interactions. An interaction between the inner tegument proteins, pUL36 and pUL37, has been documented. In terms of interactions between the inner and outer tegument proteins, pUL36 has been shown to interact with pUL48. However, there is some evidence to suggest that pUL36 and pUL37 normally interact with other tegument components as a complex. Thus, a mutant lacking pUL36 failed to localise pUL37GFP to the proposed site of secondary envelopment (Desai *et al.*, 2008). More evidence for the importance of the pUL36/pUL37 interaction is presented in this thesis. Given the proposition that pUL36 and pUL37 are acquired by capsids, and that in the absence of either, acquisition of outer tegument appears to be blocked, this would suggest that the complex of pUL36 and pUL37 is necessary to target cytoplasmic nucleocapsids to sites containing outer tegument components. As well as interacting with pUL36, pUL48 seems to be a nexus of many interactions between outer tegument components including pUL41, pUL46, pUL47 and pUL49, which is in agreement with its critical importance in virion morphogenesis in HSV-1 (Lee *et al.*, 2008; Mossman *et al.*, 2000; Vittone *et al.*, 2005).

As noted previously, the inner and outer tegument seem to differ in their sensitivity to changes in the abundance of their component proteins. Thus, deletion of either pUL36 or pUL37 results in the accumulation of unenveloped cytoplasmic capsids, whereas many outer tegument proteins are not necessary for formation of infectious virions (Desai *et al.*, 2001; Desai, 2000; Fuchs *et al.*, 2004; Kopp *et al.*, 2002; Pomeranz & Blaho, 2000). pUL46, pUL47 and pUL49 may be deleted with no apparent detriment to virion morphogenesis. Interestingly, although, as described earlier, the amount of pUL37 incorporated into virions seems to be fixed (McLauchlan, 1997), pUL49, in contrast, may be incorporated at greatly increased levels when over expressed (Leslie *et al.*, 1996). Indeed, there is some evidence suggesting natural variation in the incorporation of pUL49 into tegument between individual virions (del Rio *et al.*, 2005). These findings imply that the outer tegument displays a greater plasticity and redundancy than the inner tegument and are suggestive, once again, that tegumentation nucleates at two spatially distinct and

separate places, with the nucleation points of the outer tegument being either more numerous or capable of binding multiple components (Farnsworth *et al.*, 2003; Farnsworth *et al.*, 2007; Fuchs *et al.*, 2002a; Fuchs *et al.*, 2002b).

1.6.3. Secondary Envelopment

A range of experiments with deletion mutants and mutants expressing tagged proteins suggests that secondary envelopment occurs at the *trans*-Golgi network (TGN) (Campadelli *et al.*, 1993; Desai *et al.*, 2008; Farnsworth & Johnson, 2006; Harley *et al.*, 2001; Skepper *et al.*, 2001; Sugimoto *et al.*, 2008; Whiteley *et al.*, 1999; D. Pasdeloup pers. comm.). A recent report also implicates Multivesicular endosomes (MVE) in HSV-1 envelopment (Crump *et al.*, 2007). Notably, MVEs can receive cargoes from the TGN (Raiborg *et al.*, 2003). Experiments retargeting the localisation of viral glycoproteins to different membrane systems, such as the ER, lead to their absence from the mature virion, supporting a role for the Golgi, or Golgi derived structures, in secondary envelopment (Whiteley *et al.*, 1999). Compounds such as Monensin and Brefeldin A which can disrupt the membrane systems of the cell, and block glycoprotein trafficking and processing, also block secondary envelopment (Cheung *et al.*, 1991; Dasgupta & Wilson, 2001; Ghoshchoudhury *et al.*, 1987). However, the precise mechanism of envelope formation remains obscure, and the role of viral glycoproteins in this process remains to be fully elucidated. gD and the gE/gI complex are known to have redundant but essential roles in virion envelopment. Deletion of both gD and gE impaired secondary envelopment and resulted in a major reduction in numbers of enveloped virions, whereas deletion of gD and gI impaired envelopment to a lesser extent. A triple deletion of gD, gE and gI resulted in a even greater impairment of envelopment than the gD and gE deletion (Farnsworth *et al.*, 2003). The authors suggested that the cytoplasmic domains of these glycoproteins are necessary and sufficient for tethering the tegumented capsid to the membrane site of envelopment, and the accumulation of tegumented capsids, which was observed within the cytoplasm of cells infected with these mutants, might reflect the lack of preformed sites of secondary envelopment, which presumably require gD, gE and gI to form correctly.
Some evidence exists to implicate glycoproteins in determining the site of viral release, with gE/gI apparently important for directing cell-to-cell spread of infection by inducing transport of virions to cell junctions (Farnsworth & Johnson, 2006).

In the model presented here, HSV-1 must bud from the cytoplasmic surface of a vesicle into the lumen to acquire a membrane and enter the exocytic pathway. Within the cell

budding events of this nature are unusual and appear restricted to the multivesicular endosome (MVE). Indeed studies with the related betaherpesvirus, Human CMV, showed virions present in organelles displaying MVE like morphology (Fraile-Ramos *et al.*, 2002). Similarly, it seems that other viruses such as HIV make use of the MVE budding machinery for virion formation, suggesting this may be a common route of virion formation exploited by viruses (reviewed Bieniasz, 2006; Demirov & Freed, 2004; Morita & Sundquist, 2004).

The MVE budding machinery is composed of three multiprotein complexes, Endosomal sorting complexes required for transport (ESCRT) -1, -2 and -3 with accessory proteins (reviewed Hurley & Emr, 2006). The normal function of this complex is in targeting ubiquitinated proteins for degradation at the lysosome (Slagsvold *et al.*, 2006). HIV has been shown to interact with the ESCRT pathway through domains within structural proteins termed Late domain motifs (L-domain) (reviewed Bieniasz, 2006; Demirov & Freed, 2004; Morita & Sundquist, 2004). L-domains (PS/TAP, PPxY and YPxL) interact with the ESCRT complexes and such motifs are present in a range of HSV-1 proteins including VP5, VP16, pUL36 and the cytoplasmic tail of gE (Crump *et al.*, 2007). This abundance of L-domains was suggested to reflect the importance of engaging the ESCRT pathway and the functional redundancy of some of these proteins in virion morphogenesis. The frequency of L-domains was suggested as a means to tolerate the potential loss of individual L-domains due to the functional redundancy of the proteins in which they occur. (Crump *et al.*, 2007). The authors suggest that conservation of a single L-domain within pUL36 in all three subfamilies of the *Herpesviridae*, and the essential role of this protein in envelopment, point to the potential for this to be important for recruiting the ESCRT machinery (Crump *et al.*, 2007). However data from PrV suggests that pUL36 might be dispensable for envelopment, as pUL36 is absent from L particles produced by a UL48 deletion mutant (Fuchs *et al.*, 2002a). Therefore the L-domains within both pUL36 and pUL48 appear to be potentially dispensable for engaging the ESCRT pathway, unless the production of these particles exploits another mechanism for formation.

The precise interactions of HSV-1 with the ESCRT pathway are currently subject to investigation. To date only one component of this pathway has been identified as essential for HSV-1 morphogenesis. Expression of a dominant negative mutant of Vps4, which is required to recycle the components of the ESCRT pathway, has been shown to inhibit this process (Babst *et al.*, 1998; Bishop & Woodman, 2000; Slagsvold *et al.*, 2006). In HSV-1 infection, expression of the dominant negative Vps4EQ inhibited the envelopment of HSV-

1. Tegumented nucleocapsids were present in the cytoplasm and were partially wrapped in membrane, but the membrane ends failed to fuse to complete the envelopment process (Crump *et al.*, 2007). From this it is evident that Vps4 is important for the final stages of envelopment, either to recycle or release the ESCRT complex from the membrane, or in some other process that is required to permit the closure of the virion envelope.

Another aspect of secondary envelopment is that enveloped HSV-1 particles accumulate in the TGN and are exposed to a low pH in this organelle (Harley *et al.*, 2001). In the absence of this low pH, infectivity of the derived enveloped particles is lowered, suggesting a role for low pH in virion formation or maturation (Harley *et al.*, 2001). pH dependent maturation is seen in members of the *Flaviviridae* (West Nile virus, Dengue fever virus) (reviewed Mukhopadhyay *et al.*, 2005). As such the possibility that a low pH might be needed for final processing or maturation of the intact HSV-1 virion cannot be discounted.

1.7. Axonal transport and assembly in neurons

Infection of differentiated neuronal cells poses special problems for herpesviruses as the progeny particles have to be transported considerable distances from the cell body to the termini of axons. Two models have been proposed for this process. In the first, virus assembles in the cell body and is transported along the axon as an intact virion (reviewed Ch'ng & Enquist, 2005; del Rio *et al.*, 2005; Diefenbach *et al.*, 2008). In the second, capsids are transported separately from envelope components and are brought together for final envelopment at the termini of the axon (reviewed Diefenbach *et al.*, 2008; Holland *et al.*, 1999; Penfold *et al.*, 1994). This debate is fuelled by conflicting evidence from EM and confocal fluorescence microscopy studies showing the presence of structures that might confirm either model. Such microscopic data has, to date, proven hard to analyse definitively as there has been no reliable means to discern input from progeny virus in these assay systems. A recently developed microfluidic system capable of separating neuronal cell bodies and axon termini for live cell imaging has provided a means to resolve this matter (Liu *et al.*, 2008). Lui and colleagues (2008) examined neuronal transport of progeny PrV capsids (by VP26 mRFP label) and tegument (by VP22 GFP label) produced after infection of the cell body. In this system red, green and yellow (colocalised) punctae were observed. The authors' interpreted individual red punctae as capsids which were predominantly transported in the anterograde direction, although they could also travel in the retrograde direction in absence of VP22. Individual green punctae were interpreted as L particles, and were observed to undergo anterograde transport, while capsid associated

with tegument (yellow punctae denoting virions) were seen to move predominantly in the anterograde direction, with these punctae accounting for the majority of capsids. These data suggest therefore, that intact virions rather than subassemblies are transported in axons (Liu *et al.*, 2008). Other evidence from PrV seems to support the proposition that virions are assembled in the cell body for subsequent transport (del Rio *et al.*, 2005). There is also evidence from PrV that tegument proteins may not traffic independently of capsids in axons, as they are able to regulate the directionality of capsid transport (Luxton *et al.*, 2005). However, in HSV-1 there is accumulating evidence which suggests that capsids, tegument and envelope components might be transported independently, or in subassemblies, to the axon growth cones and varicosities for secondary envelopment and subsequent exit (Miranda-Saksena *et al.*, 2009; Saksena *et al.*, 2006). It is not clear yet whether these represent genuine differences between these two viruses or reflect the present uncertainty in the experimental models.

1.8. Latency

A characteristic of all herpesviruses is their ability to establish a latent infection, which are notable in that there is minimal expression of viral gene products. HSV-1 typically establishes latency through the sensory neurons that innervate the area around the mouth, resulting in a latent infection of the trigeminal ganglion. Latent infection allows a population of healthy carriers to be produced in whom reactivation from latency occurs sporadically under the influence of a range of poorly understood triggers including exposure to UV light, stress, suppression of the immune system and injury (reviewed Efstathiou & Preston, 2005). Reactivation from latency can lead to asymptomatic shedding of virus or symptomatic infection, facilitating spread of infection to new hosts. As such, latency forms a strategy for long term propagation within a population (Roizman *et al.*, 2007).

Latency is considered to have three stages, establishment, maintenance and reactivation (Roizman *et al.*, 2007). How latency is established remains to be conclusively shown but current thinking suggests that it results from a failure of IE gene expression (Efstathiou & Preston, 2005; Marshall *et al.*, 2000; Preston & Nicholl, 1997). In this scenario, the cellular environment of the neuron is considered to be intrinsically restrictive to viral gene expression. The reasons for this are thought to include the failure of the VP16 transcription factor to be transported along the axon to the nucleus after disassembly of the tegument at the axonal terminus, and lack of VP16 activity as a result of the cytoplasmic distribution of

the VP16 transcription cofactor, host cell factor (HCF) (Kristie *et al.*, 1999; Lu & Misra, 2000a). Both these effects would tend to block VP16 mediated transcription of IE genes that would otherwise lead to productive infection (Efstathiou & Preston, 2005). Furthermore, ICP0 expression can be reduced by the activity of a cellular transcription factor Zhangfei, that is able to bind host cell factor (HCF) preventing it from activating the ICP0 promoter (reviewed Jones, 2003; Lu & Misra, 2000b). Yet another factor affecting IE gene expression is the deposition of histones on IE promoters and their modification to prevent IE gene expression. Normally VP16 would recruit chromatin remodelling factors to IE promoters to relieve this repression and even exclude histone from actively transcribing promoters. In latency, IE and E gene promoters (particularly the ICP0 promoter) show a reduced association with acetylated H3, which is suggestive of a repressive chromatin conformation, whilst the LAT promoter is found to be enriched for acetylated H3, indicating active chromatin (reviewed Efstathiou & Preston, 2005; Kubat *et al.*, 2004a; Kubat *et al.*, 2004b).

In acute infection not all neurones are latently infected, with some actively expressing viral proteins although the subsequent fate of those cells expressing HSV-1 proteins is unclear. Many of the cells latently infected with HSV-1 harbour multiple copies of the viral genome, which may be derived from multiple input virions or result from accumulation of replicated viral genomes after gene expression with a subsequent block on cell death (Efstathiou & Preston, 2005; Thompson & Sawtell, 2000). One hallmark of latency is the expression of a viral transcript, LAT, which maps within the long repeat sequences and is transcribed antisense to ICP0 and ICP4. The LAT transcript occurs in several forms including one of ~8.3kb, referred to as mLAT, from which the other LATs are spliced. mLAT is the least abundant of the LAT transcripts and contains an intron. The splicing of this intron from mLAT generates the major LAT species of 2.0kb which is further spliced to a 1.5kb species. Expression of the 1.5kb LAT is restricted to neurons whilst the 2.0kb transcript is detectable in both neurons and productively infected cells late in infection (Efstathiou & Preston, 2005; Roizman *et al.*, 2007). The 2.0kb LAT is thought to be an unusually stable intron that exists as a lariat structure. It is capable of inhibiting transactivation of gene expression by ICP0 although the mechanism for such repression remains unclear (Efstathiou & Preston, 2005; Farrell *et al.*, 1991; Thomas *et al.*, 2002).

As yet there are no reports of a peptide being translated from the HSV-1 LAT (Efstathiou & Preston, 2005; Jones, 2003). However, it has been suggested that LAT can be processed to release functional microRNA (miRNA) (reviewed Grey *et al.*, 2008). Four such

miRNAs have been described within the LAT transcript. One has been shown to decrease the abundance of ICP0 and one to decrease ICP4 abundance (Umbach *et al.*, 2008) with further miRNAs suggested to affect the γ1 34.5 gene. One function of mLAT, therefore, seems to be to produce miRNAs capable of interfering with IE gene expression by suppressing levels of ICP0 and ICP4. Again, this fits with a model based on entry to latency being determined by a failure of IE gene expression. The LAT promoter contains neuron specific response elements and LAT has been implicated in the maintenance of latency by blockage of IE gene expression and through anti-apoptotic functions which ensure the survival of latently infected neurons (Efstathiou & Preston, 2005; Jones, 2003).

Our understanding of the factors needed to achieve reactivation from latency is incomplete. Gene expression during reactivation from latency must occur in a viral protein (VP16) independent manner, and reactivation appears to represent a failure of the repressive systems which allows cellular factors access to IE promoters leading to subsequent expression of the viral gene cascade. The principal viral function involved is presumably ICP0 which is a promiscuous activating factor (Coleman *et al.*, 2008; Efstathiou & Preston, 2005).

1.9. Relationships between Herpesviruses and bacteriophage

The existence of deep evolutionary relationships between large dsDNA viruses and bacteriophages has become increasingly apparent. These relationships are not seen in either genome or amino acid sequence comparisons but rather in the conservation of structural or mechanistic features. The first of these relationships to be fully established was that between adenovirus and bacteriophage PRD1. It was based on the conservation of a protein fold termed a double jelly roll, in the major capsid proteins of adenovirus and PRD1 and was supported by further similarities between the composition and architecture of their capsids (reviewed Belnap & Steven, 2000). This structurally defined relationship was subsequently shown to include a number of other virus families including the iridoviruses, phycodnaviruses, and *asfarviridae*, and probably, mimiviruses and poxviruses, and was also shown to extend to the archeal virus Sulfolobus turreted icosahedral virus (STIV) thereby encompassing all three kingdoms of life (Benson *et al.*, 2004; Krupovic & Bamford, 2008b).

A relationship between the *Herpesvirales* and the *Caudovirales* (tailed bacteriophage) had long been suspected based on shared structural and mechanistic features. Initially the main

point of similarity was considered to be the packaging of DNA into a preformed capsid that is assembled around an internal scaffold (Fig. 1.5). Subsequently, a number of other common features have been recognised. Thus, in common with the *Caudovirales* HSV-1 forms an immature intermediate capsid species termed the procapsid, (Newcomb *et al.*, 1996; Rixon & Chiu, 2003; Rixon & McNab, 1999). Phage procapsid assembly typically initiates on the portal structure and proceeds by sequential addition of the individual capsid proteins in association with scaffolding proteins. Similar processes are now believed to occur in HSV-1 where assembly initiates on a portal and scaffold bound VP5 is incorporated into the procapsid (Newcomb *et al.*, 1999; Newcomb *et al.*, 2003; reviewed Rixon & Chiu, 2003). Notably in both tailed phages and herpesviruses the procapsid is significantly more sensitive to disruption than the mature angularised form and in both cases procapsids can disassemble at low temperatures (reviewed Newcomb *et al.*, 2000; Rixon & Chiu, 2003). Another common feature is that the scaffold is transient and is removed from the procapsid during DNA packaging in a process that triggers the substantial rearrangements associated with capsid maturation.

Recently, the *Herpesvirales* and the *Caudovirales* have been found to share a diagnostic protein fold within their major capsid proteins. This, fold was seen in the major capsid proteins of HK97, P22, T4 and HSV-1 and showed a highly conserved arrangement of secondary structural elements despite the low amino acid sequence conservation among all these proteins (Baker *et al.*, 2005) (Fig. 1.6). The fold is unique to these viruses and its distinctive nature is probably related to the extensive reorganisation that this part of the capsid shell undergoes during maturation (Heymann *et al.*, 2003). Entry of DNA into a preformed capsid requires a specialised mechanism and this function is fulfilled by the phage portal. The identification of a similar portal in HSV provided further strong evidence for a relationship between these viruses. In both cases the portal is composed of a dodecameric ring of identical subunits (reviewed Newcomb *et al.*, 2001b; Rixon & Chiu, 2003; Trus *et al.*, 2004), which occupy one capsid vertex (Cardone *et al.*, 2007; Chang *et al.*, 2007; Trus *et al.*, 2004). The portal ring has a channel running through the centre through which the DNA passes (Cardone *et al.*, 2007; reviewed Rixon & Chiu, 2003; Trus *et al.*, 2004). In HSV-1 DNA packaging is an energy dependent process and is driven by an ATPase which appears to be distantly related between the *Caudovirales* and *Herpesvirales*, once more adding to the weight of evidence suggesting a deep evolutionary link between these virus groups (reviewed Krupovic & Bamford, 2008b).

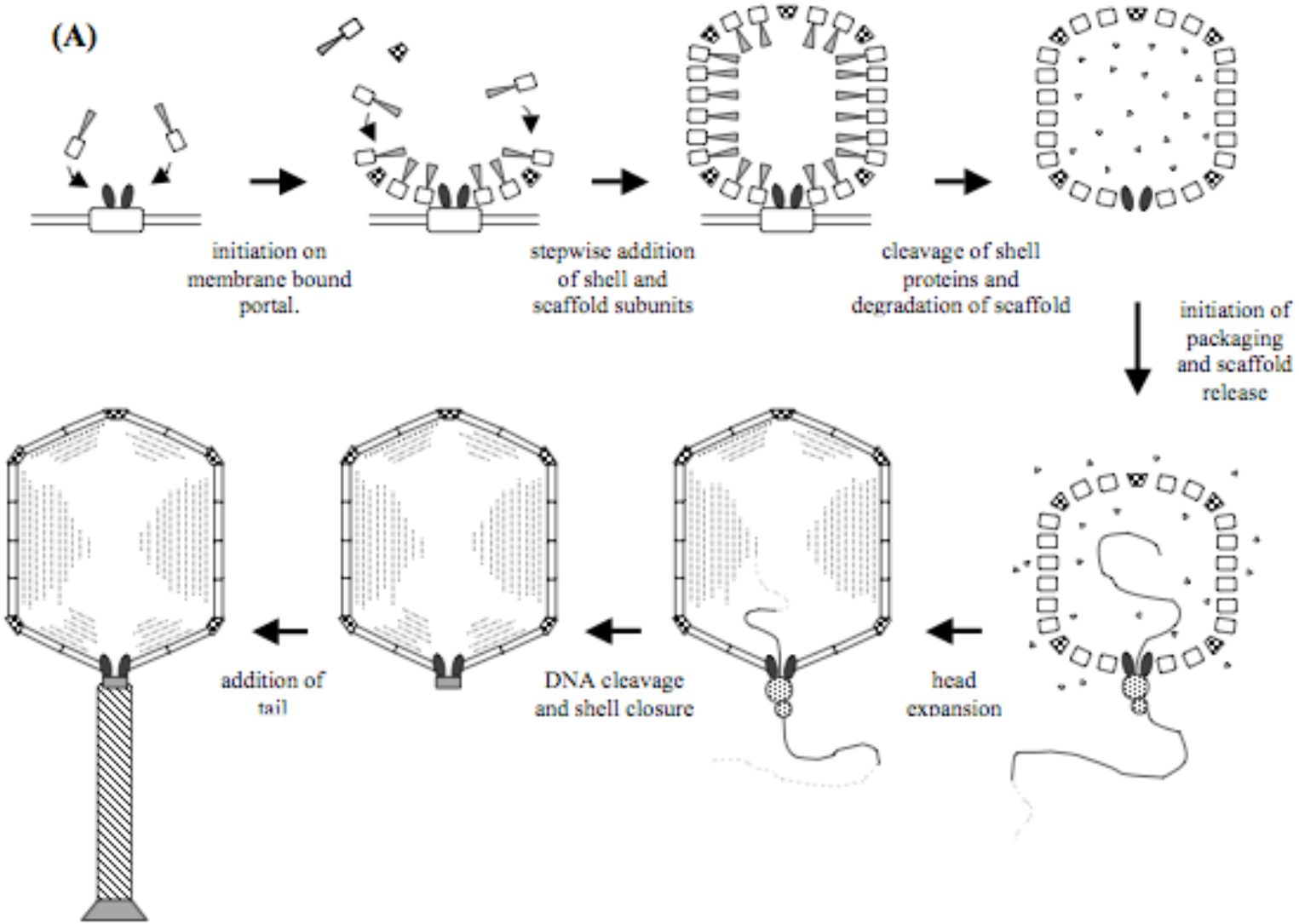
(A)
initiation on membrane bound portal.
stepwise addition of shell and scaffold subunits
cleavage of shell proteins and degradation of scaffold
initiation of packaging and scaffold release
head expansion
DNA cleavage and shell closure
addition of tail

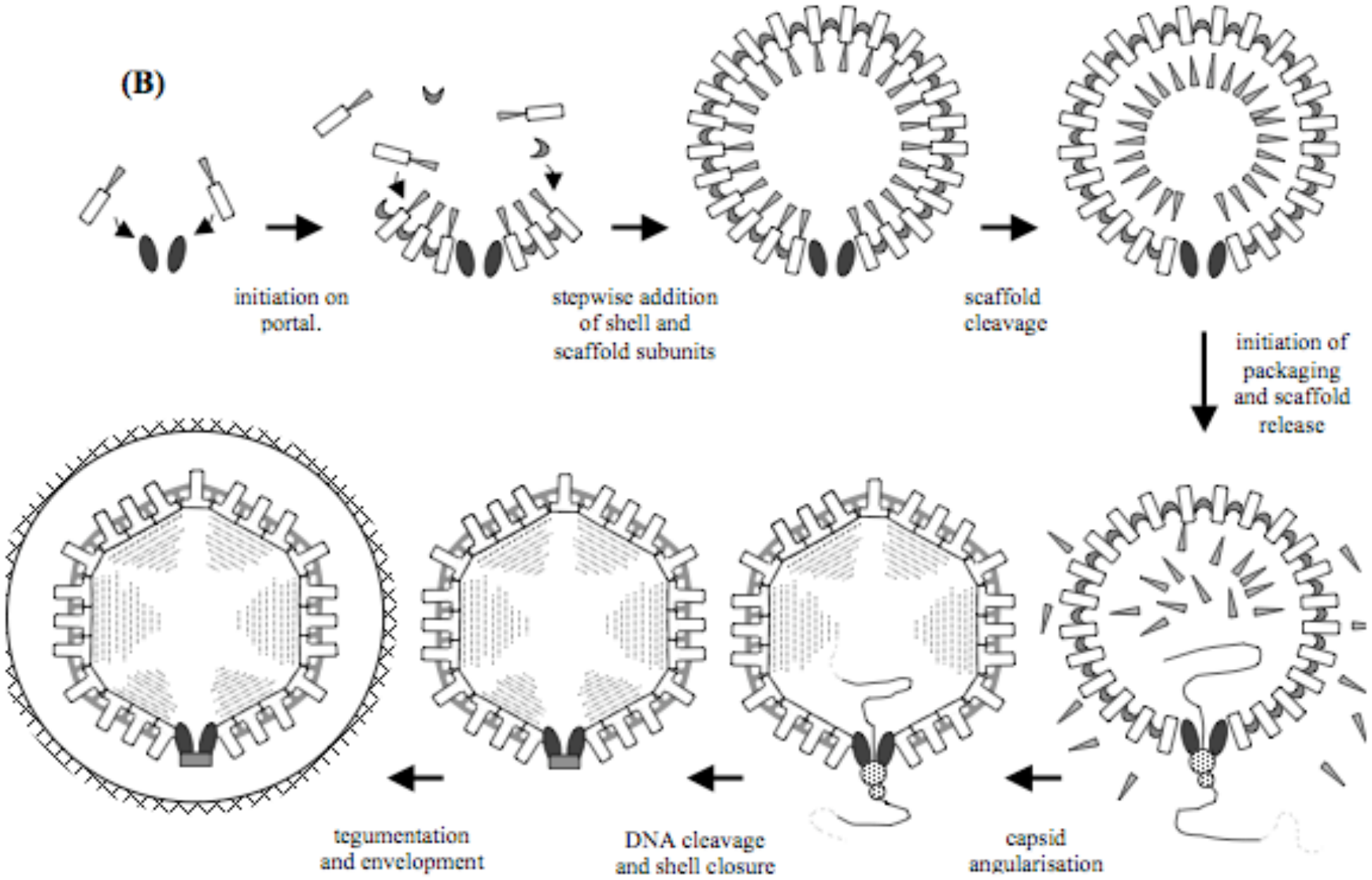
(B)
initiation on portal.
stepwise addition of shell and scaffold subunits
scaffold cleavage
initiation of packaging and scaffold release
capsid angularisation
DNA cleavage and shell closure
tegumentation and envelopment

Figure 1.5: Comparison of virion assembly in bacteriophage and HSV-1.
Stages within the assembly and maturation of phage T4 (A) and HSV-1 (B) are shown. Major capsid proteins forming HSV-1 pentons and hexons and T4 hexons are shown as open boxes, T4 penton proteins as hatched trapeziums. HSV triplexes are shown as crescents, with scaffold as triangles in both cases. The exact mechanisms for some stages are incompletely understood and may differ from those shown here.

Reproduced from Rixon and Chiu (2003)

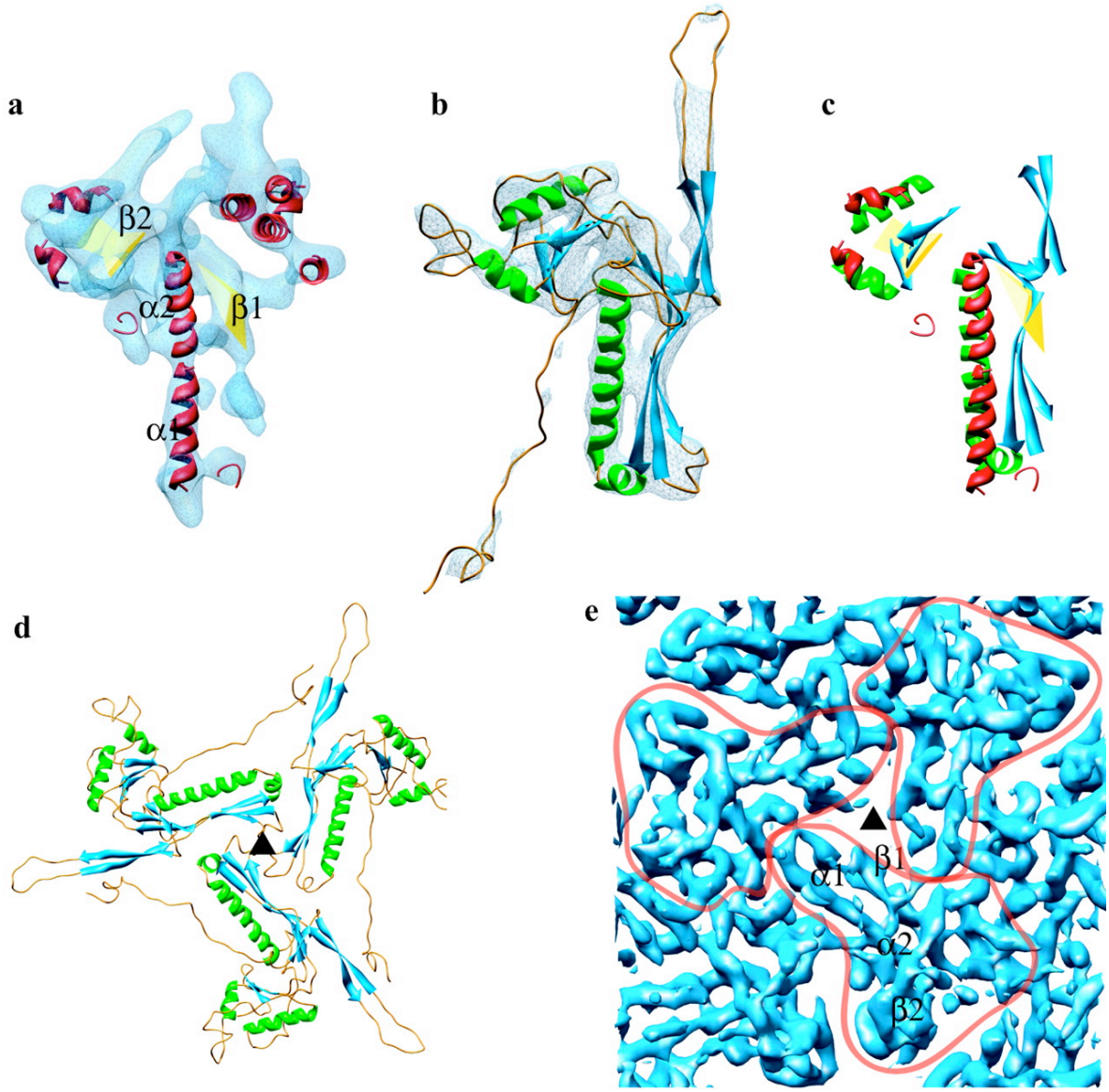

Figure 1.6: The secondary structures of HSV-1 VP5 and HK97 gp5 and their organisation in capsids.

(a) The VP5 floor domain (blue), viewed from outside the capsid. Structural analysis of cryo-EM reconstructions has identified two long α-helices (α1 and α2 highlighted in red) adjacent to a large β sheet (β1 highlighted in yellow), as well as a second β sheet (β2 highlighted in yellow), and several smaller helices flanking α1 and α2. **(b)** The crystal structure of HK97 gp5 shown in the same view reveals a similar arrangement. **(c)** Alignment of secondary structural elements demonstrates a match between the floor domain of VP5 and gp5. **(d)** Arrangement of gp5 subunits around a local three-fold axis (denoted with a black triangle) in the HK97 capsid, as viewed from within the capsid. **(e)** Organisation of the HSV-1 capsid floor shown as for gp5 in (d). Individual VP5 subunit floor domains are highlighted, with the long α-helices, α1 and α2 and associated β sheets, β1 and β2 are marked for one subunit.

Figure reproduced from Baker *et al.*, 2005.

All these shared features point to evolutionary relatedness and while any one feature could be explained in terms of convergent evolution between these viruses, in combination they provide an overwhelming case in favour of a common ancestry for these groups of otherwise seemingly unrelated viruses (reviewed Rixon & Chiu, 2003). If such an argument is accepted then the possibility that the *Herpesvirales* and *Caudovirales* share a common history suggests that their ancestor predates the split of the prokaryotic and eukaryotic cellular lineages. This means that the herpesvirus lineage has survived and diversified from that time to the present day, which would account for the presence of herpesviruses in so many species. It is notable, that the areas of apparent commonality between *Herpesvirales* and *Caudovirales* are associated with the capsid, the structure and function of which is fundamental to the virus and which forms the unit most likely to be transmitted to progeny generations.

Our understanding of herpesviruses, though growing, remains incomplete. One of the least understood aspects being tegument, namely acquisition and the functions of the inner tegument at early times post infection. Currently our knowledge of the role of these proteins in virion morphogenesis is comparatively advanced, although conflicting data from both model alpha-herpesviruses (HSV-1, PrV) confounds our understanding. Work presented in this thesis describes the creation of novel complete deletions of both inner tegument genes UL36 and UL37 in HSV-1. Characterisation of these mutants was performed to assess the biological basis of the disparate phenotypes exhibited by existing HSV-1 and PrV mutants. Additionally biochemical analysis of L particles was performed to assess the role of pUL36 and UL37 in assembly of tegument into extracellular viral structures. Cryo-EM studies, using cytoplasmic C capsids from pUL36 and pUL37 deletion mutants, were performed to clarify the nature of the penton vertex associated density contentiously attributed to pUL36. Furthermore, the roles of pUL36 and pUL37 in the initiation of infection were probed using a syncytial model of infection which allowed the need for the production of mature virions in the absence of either essential inner tegument protein to be circumvented. This has allowed the role of both pUL36 and pUL37 to be assessed by the effect of their deficit on the spread of viral DNA replication within syncytia.

CHAPTER 2

MATERIALS AND METHODS

2. Materials and Methods

2.1. Materials

2.1.1. Chemicals

Reagents and chemicals used for EM analysis were purchased from TAAB laboratories. All other chemicals and reagents were sourced from either Sigma-Aldrich, BDH Chemicals UK or Fischer unless otherwise noted.

Acrylamide:bis acrylamide (30% w/v 37.5:1)	Biorad
Ammonium Persulphate (APS)	Biorad
Chloroform	Prolab
ECL	Amersham Biosciences
S.O.C	Invitrogen
Nocodazole	Calbiochem
G418 Sulphate	Calbiochem

2.1.2. Oligonucleotides

Oligonucleotides were sourced from either TAGN, or Eurogentec. Cy3 5' labelled oligonucleotides were sourced from MWG (Table 2.1).

2.1.3. Enzymes

Restriction enzymes and DNA modifying enzymes were sourced from New England Biolabs or Roche.

2.1.4. Cell lines

Baby hamster kidney-21 C13 (BHK C13): A fibroblast cell line isolated from hamster kidneys (Macpherson & Stoker, 1962).
Human foetal foreskin fibroblasts ($HFFF_2$): A fibroblastic cell line derived from a 14-18 week old human Caucasian foetus. Supplied by ECACC.
Rabbit skin cells (RS cells): A fibroblast cell line isolated from the skin of a rabbit (Baines & Roizman, 1991).

Name	Sequence
pApVBstBI F	* CTAGAACGGATCCGTCGACTTCGAAC
pApVBstBI R	* GATCGTTCGAAGTCGACGGATCCGTT
UL36rm_loxFAS_F	TTGCGTTTAATGTCGTGTTTATTCAAGGGAGTGGGATAGGATAACTTCGTATATACCTTT- -CTATACGAAGTTAT**GGCCTGGTGATGATGGCGGGATCG**
UL36rm_loxFAS_R	AGACAGACAAACGCAGCTCGGTTTTTGGGAAGCGATCACCATAACTTCGTATAGAAA- -GGTATATACGAAGTTAT**TCAGAAGAACTCGTCAAGAAGGCG**
UL37rm_loxFAS_R	ATGCCGGGACTTAAGTGGCCGTATAACACCCCGCGAAGACATAACTTCGTATAGAAA- -GGTATATACGAAGTTAT**TCAGAAGAACTCGTCAAGAAGGCG**
UL36seqF	CTGCGGCGCACCTATTCACC
UL36seqR	CGAGGACGACGAGATGATCC
UL37seqR	CTCCGGTGGGTTGTGTTGGC
Pseudobank F	**AGTCGACGGTACCGC
Pseudobank R	**GTGGATCCCGGGCCC
UL36_HA_Nterm	*TCTAGA*GGC**ATG*TACCCTTACGACGTGCCTGACTACGCT***AGATCTGGTGGCGGAAACAACACTAACC
UL36CTBamHIF24886	ATGTCGTCGTCATCTTCTTCGG
OriLseq_F	CCTGCGAGAGGCACAGATGC
OriLseq_R	GGTGGGATGGCAAAATTACC
US1-2 BAC F	TGGCCGATACCAGCTCCGTGGAAC
US1-2 BAC R	TCACATCTGCTATCCGGTTACCAC

Table 2.1: Oligonucleotides used within this work. Modifications: * 5’ phosphorylation, ** 5’ Cy3 fluorescent conjugate.

Rabbit skin cells expressing pUL19 (UL19RSC): In UL19RSC the parental RSC line has been transformed to express pUL19 encoding the major capsid protein VP5 in a pApV based construct. Supplied by Dr. V. Preston.
Rabbit skin cells expressing pUL36 (HAUL36), pUL37 (80CO2) or both pUL36 and pUL37 (4C) are described in section 3.2.

2.1.5. Tissue culture medium

Tissue culture media and supplements were sourced from Invitrogen, except pooled human serum which was sourced from Cellect. The media requirements of each cell line were as follows:
BHK-21 cells: Glasgow Modified Eagle's Medium (GMEM) supplemented with 10% tryptose phosphate broth and 10% newborn calf serum.
RS cells and derivatives: Dulbecco's Modified Eagle's Medium (DMEM) supplemented with 10% foetal calf serum and 1% non-essential amino acids. For complementing cells G418 selection was at 1mg/ml every 5^{th} passage.
$HFFF_2$ cells: Dulbecco's Modified Eagle's Medium (DMEM) supplemented with 10% foetal calf serum.

2.1.6. Other media

Optimem: A commercial medium formulation specified for use with Liposome transfection protocols.
Overlay medium: Glasgow Modified Eagle's Medium supplemented with 10% tryptose phosphate broth and 10% newborn calf serum, 1% penicillin/streptomycin and 1.125% carboxymethylcellulose.

2.1.7. Viruses

Wild type HSV-1 strain 17 syn^+ (Brown *et al.*, 1973).
K5ΔZ: A mutant strain of HSV-1 (KOS) in which the UL19 gene is disrupted by the insertion of the lacZ gene (Desai *et al.*, 1993).
KΔUL36: A mutant strain of HSV-1 (KOS) in which the UL36 gene is disrupted by the deletion of sequences between residues 79456-75877 equivalent to amino acids 362 to 1555 out of 3,164 total residues (Desai, 2000). This deletion causes the ORF to become out of frame after the deletion and brings 42 fusion codons into frame prior to a termination signal.

ARΔUL36, FRΔUL37 and ARΔUL36ΔUL37 are described later in section 3.3.

2.1.8. Bacterial culture medium

L-Broth (LB)	10 g/L NaCl, 10 g/L Bacto™ peptone, 5 g/L Bacto™ yeast extract
L-Broth agar (LB agar)	L-Broth with 1.5% (w/v) Bacto™ agar.
LB/LB agar + antibiotic	LB/LB agar supplemented with Ampicillin at 50 μg/ml, Chloramphenicol at 15 μg/ml, tetracycline at 2μg/ml or kanamycin at 30 μg/ml.

2.1.9. Bacterial Strains

DH5α: An *E. coli* strain carrying the *endA*$^-$ and *recA*$^-$ mutations. These mutations remove endonuclease I activity (endA) and reduce homologous recombination (recA). This allows for improved quality of plasmid DNA preparations and improved stability of plasmids respectively.

Genehogs: Commercial transformation competent DH10B derivative (Invitrogen) specifically prepared for use with large plasmid DNAs such as pBAC SR27 exhibiting a high level of transformation efficiency.

2.1.10. Plasmids

pApV: An expression plasmid containing the HSV-1 ICP6 (UL39) promoter and the simian virus 40 (SV40) polyadenylation sequence (Lamberti & Weller, 1998).

pET28a: A T7 expression vector (Novagen).

pUC19: A high copy number cloning plasmid vector for *E. coli* (NEB).

pDsRed-Monomer vector: A plasmid encoding the monomeric form of RFP, DsRed-Monomer. (Clontech)

GFPemd: A plasmid encoding a variant of GFP (Packard).

pGEMT-Easy: A vector supplied as a linear DNA with single 3' A overhangs for use in cloning PCR products generated with Taq polymerase (Promega).

pSC101-BAD-gbaA^{tet}: the Red/ET expression plasmid for λRED recombination. This plasmid carries the λ phage *redγβα* operon and *recA* gene as a polycistronic operon under the control of the arabinose inducible promoter P_{BAD}. This construct is supported by the pSC101 replicon backbone which contains a temperature sensitive origin of replication (Genebridges GmbH).

pRpsl-neo: a plasmid bearing the rpsl-neomycin selection cassette used for λRED recombination and subsequent selection (Genebridges GmbH).

pSV2Neo: A plasmid used to confer G418 resistance to mammalian cells (Clontech).

pC1-Neo: A plasmid used to confer G418 resistance to mammalian cells (Promega).

pBAC SR27: A bacmid clone of the HSV-1 genome. In this bacmid the BAC backbone and a mammalian expression Cre recombinase are flanked by loxP sites and are inserted between the genes US1 and US2 in the HSV-1 genome. The HSV-1 genome present in this construct is a derivative of strain 17. Supplied by Charles Cunningham (NCBI FJ593289).

Cosmid 14: A subgenomic cosmid containing HSV-1 sequences between 54445 and 90477 residues (Cunningham & Davison, 1993).

pGX336: A pUC118 based plasmid containing the HSV-1 BamHI H fragment between 79,441 and 86,980b residues. Supplied by Dr V. Preston

pUL373: A plasmid based on the pGEM-1 vector containing a 3.5Kb ClaI – HindIII fragment (residues 84171 – 80707) in the AccI-HindIII sites of pGEM-1. Subsequently modified by insertion of an oligonucleotide to destroy the HindIII site, generating a BamHI site at the 3' end of the ORF. Supplied by Dr J. McLauchlan.

HSV-1 genomic DNA pseudo bank: A collection of pEGFP-C1 plasmids containing 200-500bp SacII fragments of the HSV-1 genome derived from a Bacmid clone and used to generate probes for fluorescence *in situ* hybridisation. The plasmids are maintained as a mixed population. Supplied by Dr D. Pasdeloup.

2.1.11. Antibodies

2.1.11.1. Mouse monoclonal antibodies

DM1A: directed against chicken embryo brain α tubulin (Sigma Aldrich).

DM165: directed against the HSV-1 major capsid protein (VP5) (McClelland *et al.*, 2002).

#E12-E3: directed against an N terminal fragment of HSV-1 pUL36 (VP1/2). Supplied by Dr. P. O'Hare.

mAb4846: directed against HSV-1 glycoprotein D. Supplied by Susan Graham (McLauchlan *et al.*, 1994).

HA-7: directed against an influenza Haemagluttinin (HA) epitope (Sigma)

MCA406: directed against the HSV-1 scaffold protein (VP22a) (Serotec).

UL17: directed against HSV-1 pUL17 (Thurlow *et al.*, 2005). Supplied by Dr. V. Preston.

UL25: directed against HSV-1 pUL25 (Thurlow *et al.*, 2005). Supplied by Dr. V. Preston.

VP16 (1-21): directed against an epitope spanning residues 456-490 of HSV-1 VP16 (Santa Cruz).

2.1.11.2. Rabbit polyclonal antibodies

AGV031: directed against HSV-1 VP22 (Hafezi *et al.*, 2005).

αVP1-2NT1r: directed against an N terminal fragment of HSV-1 pUL36 (VP1/2) (Abaitua & O'Hare, 2008). Supplied by Dr. P. O'Hare.

M780: directed against HSV-1 pUL37 as described by Shelton *et al.*, (1994). Supplied by Dr. F. Jenkins.

191A: directed against the HSV-1 major capsid protein (VP5).

2.1.11.3. Other antibodies

GAM_{488}: Goat anti mouse antibody conjugated to Alexafluor 488 (Molecular probes).

GAM_{568}: Goat anti mouse antibody conjugated to Alexafluor 568 (Molecular probes).

GAR_{488}: Goat anti rabbit antibody conjugated to Alexafluor 488 (Molecular probes).

GAR_{568}: Goat anti rabbit antibody conjugated to Alexafluor 568 (Molecular probes).

GAM_{HRP}: Goat anti mouse antibody conjugated to horseradish peroxidase (HRP) (Sigma).

GAR_{HRP}: Goat anti rabbit antibody conjugated to horseradish peroxidase (HRP) (Sigma).

2.1.12. Buffers and Solutions

General

TE: 10mM Tris 1mM EDTA pH8.0

DNA loading buffer: 40% (w/v) sucrose, TE, 0.01% bromophenol blue

EPT: 154mM NaCl, 3mM Na_2HPO_4, 2.4mM KH_2PO_4

PBS A: 170mM NaCl, 3.4mM KCl, 10mM Na_2HPO_4, 1.8M KH_2PO_4, pH7.2

PBS Complete (cPBS): PBS A + 6.8mM $CaCl_2$, 4.9mM $MgCl_2$

PFA fix: 4% (w/v) PFA in EPT

PEM: 10 mM PIPES (piperazine-N,N'-bis (2-ethanesulfonic acid)), 5 mM EGTA (ethylene glycol-bis (b-aminoethylether)-N,N,N',N'-tetraacetic acid), and 2 mM $MgCl_2$, pH 6.8,

Microtubule fix: PEM, 4% formaldehyde, 0.2% Triton X-100

TAE: 40mM Tris, 20mM glacial acetic acid, 1mM EDTA pH8.0

TBE: 90mM Tris, 90mM boric acid, 1mM EDTA

TBS: 20 mM Tris, 0.15 M NaCl pH 8.0

TBS Tween: TBS + 1% Tween20

Tryptose phosphate broth: 10% (w/v) tryptose phosphate dissolved in PBS

Versene: 600mM EDTA dissolved in PBS A containing 0.0002% phenol red

Capsid preparation

NTE: 500mM NaCl, 20mM Tris.HCl (pH8.0), 1mM EDTA (pH8.0)

NTE suspension buffer: NTE + 1% (v/v) Igepal + Roche complete protease inhibitor

cPBS stripping buffer: cPBS + 1% (v/v) Igepal + Roche complete protease inhibitor

Sucrose gradient solutions

40% Sucrose cushion: 40% (w/v) sucrose in NTE

20% Sucrose: 20% (w/v) sucrose in NTE

50% Sucrose: 50% (w/v) sucrose in NTE

10% Sucrose: 10% (w/w) sucrose in NTE

40% Sucrose: 40% (w/w) sucrose in NTE

Acid washing

Wash solution: 0.14M NaCl

Acid solution: 0.14M NaCl, 0.1M glycine pH3

DNA preparation

Solution 1: 25mM Tris (pH8.0), 10mM EDTA, 50mM glucose

Solution 2: 0.2M NaOH, 1% SDS

Solution 3: 3M potassium acetate (pH5.0)

Phenol Chloroform: phenol/chloroform (1:1) saturated with 10mM Tris (pH8.0)

PEG/NaCl buffer: 20% (w/v) PEG6000, 2.5M NaCl

Cell Fusion

PEG fusion buffer: 50 % PEG1500 in 75 mM Hepes (pH 8) (Roche)

DMSO wash: Unsupplemented DMEM + 15% DMSO

Overlay: DMEM + 10% pooled human serum (Cellect)

Virion and L Particle preparation

5% Ficol: 5% (w/v) Ficol 400 in Eagles A+B without phenol red

15% Ficol: 15% (w/v) Ficol 400 in Eagles A+B without phenol red

Fluorescence *in situ* hybridisation

Fix: 95% ethanol, 5% glacial acetic acid

Hybridisation buffer: 50% Formamide, 10% Dextran sulfate, 4x SSC

2xSSC: 0.3M NaCl, 0.03M sodium citrate

CellMask stain: 0.5µg/ml CellMask Deep Red (Invitrogen) in cPBS

Protein gel electrophoresis

Resolving gel buffer: 0.75M Tris-HCl (pH8.0), 1% SDS

Stacking gel buffer: 0.125M Tris-HCl (pH6.7), 0.1% SDS

3x SDS loading buffer: Stacking gel buffer: 25% SDS:β mercaptoethanol:glycerol (10:8:5:10)

Tank buffer: 50mM Tris, 50mM glycine, 0.1% SDS

Western blotting

Transfer buffer: 25mM Tris, 192mM glycine, 0.1% SDS, pH8, 20% (v/v) ethanol

Block: TBS-Tween + 5% (w/v) Marvel milk powder

Stripping buffer: 100mM β mercaptoethanol, 2% SDS, 62.5mM Tris-HCl (pH7.0)

Calcium phosphate transfection

HeBS: 137mM NaCl, 5mM KCl, 0.7mM Na_2HPO_4, 5.5mM D-glucose, 21mM HEPES

Calcium Chloride: 2M $CaCl_2$

Carrier DNA: Calf thymus DNA in TE at 3mg/ml

2.1.13. Commercial Kits:

QIAquick 8	Qiagen
Sephaglas Bandprep Kit	Amersham Pharmacia Biotech Inc
Midi prep Kit	Qiagen
pGEM-T Easy	Promega
Expand High fidelity PCR system	Roche
Nucleobond AX kits	Macherey Nagel
Taq DNA polymerase	New England Biolabs
Geneclean turbo kit	Qbiogene

2.1.14. Miscellaneous reagents

Hybond membrane	Amersham
Lipofectamine 2000	Invitrogen
dNTPs	Roche
Pre stained protein molecular weight marker	Amersham
100bp and 1Kb DNA ladders	New England Biolabs
CellMask Deep Red	Invitrogen
Thin walled polycarbonate centrifuge tubes	Beckman
Electroporation cuvettes	Apollo

2.2. Methods

2.2.1. DNA gel electrophoresis

2.2.1.1. Analytical agarose gel electrophoresis of DNA

Agarose gel electrophoresis was carried out in a mini gel apparatus. Agarose gels were prepared by mixing agarose (1% w/v) in TBE and heating in a microwave until all the agarose was in solution. This solution was then cooled to 50˚C before the addition of

ethidium bromide at 0.5μg/ml after which the gel was cast. Once the gel had set it was covered with TBE, the comb and dams were removed and samples were mixed with loading buffer at a ratio of 2:1 and loaded onto the gel alongside appropriate size markers. The samples were electrophoresed at 100V for ~40mins. Samples were examined and photographed by short wave UV transillumination.

2.2.1.2. Preparative agarose gel electrophoresis of DNA

Gels were prepared as described above, with TAE replacing TBE. Gels were loaded similarly as for analytical electrophoresis, but electrophoresed at ~60V for up to 90 mins. DNA was examined under long-wave UV transillumination, Fragments were excised with a sterile scalpel and retained in 1.5ml reaction vials at 4°C until purification.

2.2.2. DNA cloning and manipulation

2.2.2.1. Polymerase chain reaction

Amplification of fragments for sequencing or cloning was performed with the Expand High Fidelity system (Roche), whilst colony screening for inserts or deletions was performed using the Taq DNA polymerase (NEB).

Reactions were set up as described below where the volumes given are for an individual reaction. Where bacterial colony material was to be screened the colonies were introduced to the reaction mix using a sterile toothpick and the sample volume replaced with deionised water.

Component	Expand High fidelity	Taq DNA polymerase
Reaction Buffer with $MgCl_2$	10μl (5x)	5μl (10x)
dNTPs (10mM)	2μl	1μl
DMSO (GPR)	2.5μl	2.5μl
Forward primer (100μM)	0.25μl	0.25μl
Reverse primer (100μM)	0.25μl	0.25μl
Template	1μl	1-5μl or colony material
DNA polymerase	1μl	0.5μl
H_2O	33μl	to 50μl final volume

In all cases reactions were made up in thin wall 0.2ml PCR tubes (Abgene) and reactions were performed according to the following PCR profile:

Step 1:	1 cycle	94°C for 3 mins
Step 2:		94°C for 30s
	30 cycles	50°C for 30s
		72°C for 3 mins
Step 3:	1 cycle	72°C for 7 mins
Step 4:		4°C constant temperature

Primer annealing temperatures were varied between 50 and 65˚C as required for primer pairs. For cloning purposes PCR products were routinely gel purified after preparation before ligation to the vector.

2.2.2.2. Fluorescence In Situ Hybridisation probe

Fluorescent DNA for in situ labeling of infected cells was produced using a PCR based method. A pseudo bank containing 200-500bp SacII fragments of the HSV-1 genome cloned into pEGFP-C1 was used as a template. Primers (MWG) were homologous to the regions flanking the SacII site of pEGFP-C1 and had Cy3 fluorophores linked to their 5' ends. PCR amplification of the pseudo library was performed with the Expand High Fidelity DNA polymerase kit.

A typical reaction was made up as follows:

5x reaction buffer without $MgCl_2$	10µl
$MgCl_2$ (25mM)	8µl
dNTPs (10mM)	1µl
DMSO (GPR)	5µl
Forward primer	50 pmoles
Reverse primer	50 pmoles
Template (pseudo-bank DNA)	100ng
DNA polymerase	0.75µl
H_2O	to 50µl

Reactions to amplify the HSV-1 fragments from the pseudo bank were run according to the following PCR profile:

Step 1:	1 cycle	94°C for 5 mins
Step 2:		94°C for 30s
	30 cycles	52°C for 30s
		72°C for 1 min
Step 3:	1 cycle	72°C for 5 mins
Step 4:		4°C constant temperature

After PCR the reactions were subjected to gel purification on 1.5% TAE agarose gels and bands of 200-500bp size excised under long wave UV transillumination. This was done as quickly as possible to avoid bleaching of the Cy3 fluorophore. After excision DNA was extracted using the Geneclean turbo kit which retains small fragments more efficiently. Probe DNA was routinely protected from direct light and stored at 4°C.

2.2.2.3. Restriction enzyme digestion

For analytical digests, 0.2-0.5μg of plasmid DNA was digested in a total volume of 20μl including appropriate restriction buffers, BSA (100μg/ml) where specified and 10 units of restriction enzyme. Digest reactions were typically incubated for 1 hour at the recommended temperature.

For multiple restriction digests, where all enzymes have compatible buffer and temperature requirements the most appropriate buffer and temperature was selected and supplemented with BSA if required, and incubated at the specified temperature. Digests with enzymes having compatible buffers but differing temperatures of incubation were carried out sequentially. However, in cases where both the buffer and temperature requirements were incompatible DNA from the first reaction was ethanol precipitated and resuspended directly into suitable restriction endonuclease digest mixture before addition of the second enzyme.

Typically preparative digests followed the principles of analytical digest, except for the use of larger quantities of plasmid DNA (1-10μg or greater) and a concomitant increase in the

number of restriction endonuclease units present (20-50U) and reaction volume (at least 10 times the volume of restriction endonuclease added). For preparative digests, reactions were commonly longer, 3 hours or more, and progress was assessed by removal of aliquots for analytical gel electrophoresis.

2.2.2.4. De-phosphorylation of digested DNA

Digested DNA was dephosphorylated with Antarctic Phosphatase (NEB) following the manufacturer's protocol. Following heat inactivation of the phosphatase, the digested DNA was normally used for subsequent procedures with no further purification.

2.2.2.5. Purifying DNA fragments from gels

DNA fragments were recovered from agarose/TAE gel slices by use of the Sephaglas^{TM} Bandprep Kit following the specified protocol. DNA recovery was determined by both analytical agarose gel electrophoresis and by UV spectrophotometry.

2.2.2.6. Determination of DNA yield by UV spectrophotometry

DNA concentration was measured on an Eppendorff Biophotometer with dilution as appropriate.

2.2.2.7. Annealing oligonucleotides

Complementary oligonucleotides were annealed by mixing in a 1:1 molar ratio with addition of 20µl of 10mM $MgCl_2$ to 10µl oligonucleotides, and heated in a PCR machine to 99°C for 5 mins then, 95°C for 10mins after which the temperature was decreased by 0.5°C per 30s until held at 4°C (Correnti *et al.*, 2002).

2.2.2.8. Standard ligation

Ligation of inserts to plasmids was performed using both purified digested insert and vector which had been dephosphorylated after digest with compatible restriction enzymes. Insert to vector ratio was 3:1 or greater depending on the size of the insert. Reactions were performed with either T4 DNA ligase and buffer system (NEB) for 2 hours at room temperature, or with pGEM-T Easy DNA ligase and buffer system (Promega) and held at

4°C overnight. Ligation reactions were typically performed in 20µl volumes with 1µl of ligase.

2.2.2.9. Ligation of PCR products

Ligation of PCR products into pGEM-T Easy was performed following the manufacturer's protocol with between 1 and 5µl of purified PCR product after assessment of concentration by analytical electrophoresis of the purified product. PCR insert identity was confirmed by restriction digest and sequencing where required.

2.2.2.10. Ethanol precipitation of DNA

DNA was routinely precipitated in the presence of 300mM sodium acetate and 2.5 volumes of 100% ethanol and held at -20°C for at least 30 min, precipitated DNA was pelleted at 13,000 rpm for 5 min or more and washed in 70% ethanol before resuspension of the dried pellet.

2.2.2.11. Small scale plasmid DNA preparation ('miniprep')

Small scale preparation of plasmid DNA was by either QIAprep 8 or by NaCl/PEG precipitation on 1.5ml of bacterial suspension. For QIAprep8 bacteria were pelleted at 13,000 rpm for 5 min before lysis and downstream processing as recommended by the manufacturer, using a QIAvac 6S vacuum manifold and a KNF vacuum pump (model number N022AN.18).

For preparation of plasmid DNA by NaCl/PEG precipitation 1.5ml of bacterial suspension was centrifuged at 13,000 rpm for 5 min before removal of the supernatant. 100µl of solution 1 was added, the pellet was then resuspended by vigorous mixing and allowed to stand at room temperature. After 10 min freshly made solution 2 was added (200µl), mixed by inversion and incubated on ice for 10 min. 150µl of solution 3 was then added and incubated on ice for a further 10mins. The white precipitate of cell debris was pelleted by centrifugation at 13,000 rpm for 5 min and the supernatant was transferred to a fresh reaction vial. One volume of phenol:chloroform was added and mixed by inversion for 5 min using a rotating table. Aqueous and organic phases were separated by centrifugation at 13,000 rpm for 5 min and the aqueous layer was transferred to a fresh reaction vial. Two volumes of 100% ethanol were added, mixed and incubated for 30mins at room temperature. Precipitated DNA was pelleted by centrifugation (13,000 rpm, 5 min) and

resuspended in 100µl of TE containing RNaseA at 100µg/ml and further incubated for 30 mins at 37°C. After digestion of RNA 120µl of PEG/ NaCl solution was added and mixed by inversion. This solution was incubated at 4°C for at least 1 hour. DNA was pelleted by centrifugation at 13,000 rpm for 5 min. The supernatant was removed and the pellet washed with 70% ethanol before drying and resuspension in 50µl of TE or deionised distilled water.

2.2.2.12. Large scale plasmid DNA preparation ('midiprep')

Large scale preparation of plasmid DNA was performed using the Qiagen Midi kit or the Macherey Nagel Nucleobond AX kit as per the manufacturer's instructions. For pBAC SR27 and derivatives, or plasmids of 20kbp or greater the following modifications were required. For purification of DNA pBAC SR27 and derivatives were grown as 200ml cultures and the volume of lysis solutions 1, 2 and 3 were increased to 10ml. For all large plasmid DNAs the elution buffers were pre warmed to 65°C before use and administered to the columns in two separate 2.5ml washes. In all cases after isopropanol precipitation, the DNA pellet was resuspended in 200µl of deionised distilled water, transferred to a sterile 1.5ml reaction vial, and made up to 300mM sodium acetate. After addition of 2.5 volumes of 100% ethanol and incubation at -20°C for at least 4 hours or overnight, precipitated DNA was pelleted at 13,000 rpm for 10 min and washed with 70% ethanol before air drying. Dry pellets were reconstituted in 50µl of deionised distilled water and stored at 4°C.

2.2.2.13. Preparation of viral genomic DNA

Viral genomic DNA was prepared from either purified virions or cell-released virus (see section 2.2.5.3). In all cases the volume was made up to around 500µl and to a final concentration of 1% SDS and 300mM sodium acetate. Addition of SDS disrupts the virion releasing the genome from the capsid. To this viral lysate an equal volume of TE saturated phenol:chloroform was added and mixed gently by rolling to prevent shearing of genomic DNA. Following centrifugation at 13,000 rpm for 5 min, the upper aqueous phase was transferred to a fresh reaction vial and subjected to repeat phenol:chloroform extraction until no further protein precipitate was observed at the interface between aqueous and organic layers. After the final extraction, two volumes of 100% ethanol were added to the aqueous phase and mixed gently by rolling until DNA was observed to precipitate. The sample was stored at -20°C for 15 mins or longer and the precipitated DNA was pelleted at

13,000 rpm for 5 min. The pellet was washed with 70% ethanol, air dried and resuspended in TE. Viral genomic DNA concentration was then determined by UV spectrophotometry.

2.2.2.14. Oligonucleotides

All oligonucleotides from commercial suppliers were delivered as lyophilized powder, which were resuspended in the volume of distilled deionised water required to achieve a final concentration of 100μM.

2.2.2.15. DNA Sequencing

DNA sequencing was performed by either the Molecular Biology Support Unit at Glasgow University, the Sequencing Service at the University of Dundee, or by Claire Addison at the MRC Virology Unit, Glasgow. Sequence data quality was confirmed by examination of electroferograms using sequence trace analysis software Chromas.

2.2.3. Bacterial methods

2.2.3.1. Bacterial culture

(a) Large scale culture
For standard plasmids and cosmids or derivatives, 50ml of LB Broth supplemented with appropriate antibiotics was inoculated with either a single picked colony or stab from glycerol stock and incubated at 37°C in an orbital shaker at approximately 180rpm overnight. For pBAC SR27 the volume of LB Broth was increased to 200ml.

(b) Small scale culture
For standard plasmids, cosmids, pBAC SR27 and derivatives 5ml of LB broth supplemented with appropriate antibiotics was inoculated with either a single picked colony or stab from glycerol stock and incubated at 37°C in an orbital shaker at approximately 180rpm overnight.

pHAUL36 must be propagated at 30°C to avoid deletions within the plasmid, and strains hosting pSC101-BAD-gba^{tet} must also be grown at 30°C to maintain this temperature sensitive plasmid.

2.2.3.2. Preparation of electrocompetent E. coli

At all stages cells were grown in LB without antibiotics. A 10ml starter culture of *E. coli* was set up and inoculated with a stab from a glycerol stock. This culture was allowed to grow for 2 h at 37°C with shaking and then used to inoculate a 100ml overnight culture, this 100ml culture was then used to inoculate a 1 litre culture which was grown to OD_{600} of 0.5 to 0.6. The resulting culture was transferred into pre-chilled 250ml Falcon tubes and incubated on ice for at least 30 mins before centrifugation at 5,000 rpm for 15 mins at 0°C in an SLA –1500 rotor. The supernatant was removed before addition of 50 ml of sterile water, chilled to 4°C, to each pellet. Cells were kept on ice at all times and resuspended by shaking with further addition of sterile ice cold water to a total volume of 160ml. The cells were then pelleted at 3,500 rpm for 15 mins at 0°C, the supernatant was removed and the cells resuspended in a total volume of 500ml ice cold sterile water. They were split into three equal aliquots and centrifuged once more at 3,500 rpm for 15mins at 0°C. The supernatants were again removed and the three cell pellets resuspended in a total of 40ml of ice cold sterile 10% glycerol. The cells were pelleted at 5,800 rpm for 15 mins at 0°C using an SS34 rotor and the supernatant was removed. Finally the pellet was resuspended in 2ml of ice cold sterile 10% glycerol and aliquoted into 40µl volumes for storage in 1.5ml reaction vials at -70°C.

2.2.3.3. Transformation of E. coli by electroporation

Electro-competent E. coli cells exhibit lowered transformation efficiency with repeated freeze-thawing. Individual aliquots of electrocompetent cells were thawed slowly on ice immediately prior to use.

Transformations were typically carried out using 1 - 10ng of plasmid DNA, or 1µl of ligation reaction or 1µl of linear DNA containing the λRED selection cassette. Electro-competent cells were thawed and aliquoted into prechilled 500µl microfuge tubes to which the appropriate DNA was added and mixed by brief pippetting and stirring. This suspension was transferred to an electroporation cuvette (Apollo). The cuvette was placed into a Hybaid Cell Shock set to 1800V and activated. After electroporation, cells were mixed with 500 - 1000µl of S.O.C. medium (Invitrogen) transferred to a 15ml Falcon tube and incubated at 37°C in an orbital shaker for 1 hour. Of this suspension, 100µl was plated to LB agar plates containing the appropriate antibiotics and incubated overnight at 37°C unless otherwise stated.

2.2.3.4. Formation of glycerol stocks

1.5ml of bacterial culture, transferred to a 1.5ml reaction vial, was centrifuged at 13,000 rpm for 5 mins and the supernatant discarded. The cell pellet was subsequently resuspended in 250µl 2% Bacto^{TM} peptone (Difco) and 250µl 80% glycerol was added solutions were well mixed before storage at -70°C.

2.2.3.5. Recovery of glycerol stocks

Cultures to be recovered were kept on dry ice and a small sample withdrawn using a sterile tooth pick for inoculation into LB Broth containing appropriate antibiotics.

2.2.3.6. λRED recombination

Primers for PCR to amplify the selection cassette and flank it with HSV-1 sequences were designed according to the manufacturer's instructions. See section 3.3.1.

DNA selection cassette was amplified by PCR as described previously (section 2.2.2.1) using pRpslneo as a template. PCR product was purified by gel electrophoresis (section 2.2.1.2), and recovered and concentration determined as previously described.

Recombination of the selection cassette into pBAC SR27 was by a λRED based method. Firstly *E. coli* (genehogs) carrying pBAC SR27 were rendered electro-competent by subculture of an overnight culture, grown to OD_{600} ~0.4 at which 1.5ml was withdrawn and centrifuged at 13,000 rpm and the supernatant discarded. Cells were resuspended in ice-cold sterile deionised distilled water and subsequently pelleted at 13,000 rpm for 5 mins. This was repeated once more on which occasion about 20µl of supernatant was retained. Cells were briefly resuspended by flicking, and 1µl of pSC101-BAD-gbaA^{tet} was added. Cells were transferred to an electroporation cuvette and treated as described in section 2.2.3.3. Notably cells carrying the pSC101-BAD-gbaA^{tet} plasmid must be grown at 30°C to ensure retention of the temperature sensitive plasmid. Colonies resistant to both chloramphenicol (15µg/ml) (pBAC SR27) and tetracycline (2µg/ml) (pSC101-BAD-gbaA^{tet}) were picked and grown up as indicated for small scale preparations from which glycerol stocks were formed for further use. To perform λRED mediated recombination *E. coli* hosting both pBAC SR27 and pSC101-BAD-gbaA^{tet} were grown overnight with antibiotics as described for small scale culture at 30°C before subsequent subculture to

1.5ml of fresh LB with antibiotics and cultured to OD_{600} ~0.3 - 0.4. At which time the arabinose inducible promoter P_{BAD} was activated by addition of l-arabinose to a final concentration of 0.3-0.4%. For each experiment two subcultures were set up, of which only one was treated with l-arabinose. Both cultures were incubated at 37°C for no more than 1 hour to promote expression of the polycistronic operon containing the recombination proteins.

After incubation at 37°C both induced and uninduced cells were rendered electro-competent as described previously in this section and subsequently electroporated with 1-2μl of purified linear DNA selectable marker cassette. In a modification of the manufacturer's method the electroporated bacteria were resuspended in 1000μl S.O.C. and incubated at 37°C for 70mins, after which 100μl was plated to LB agar plates containing chloramphenicol (15μg/ml) and kanamycin (15μg/ml) and incubated overnight at 37°C. This selects for only the modified pBAC SR27 with inserted selection cassette and favours the loss of pSC101-BAD-gbaA^{tet} from the host.

2.2.4. Cell culture methods

2.2.4.1. Mammalian cell culture

(a) Routine passage

BHK-21 cells were routinely cultured in 850cm^2 roller bottles and passaged at confluence. Cells were seeded into roller bottles at 2x10^7 cells/vessel in 100ml of medium, gassed with 100% CO_2 to a final concentration of 5% and cultured by rotation at 0.5 rpm at 37°C. To harvest cells, growth medium was removed, the cells were washed twice in versene and then overlaid with 20ml of trypsin (10x) /versene (100μl in 20ml versene) and incubated in a minimal volume (~3ml) at 37°C until detached. Detached cells were resuspended directly into 20ml of complete GMEM and then used to seed subsequent vessels. Cells remained viable in suspension for up to one week at 4°C.

Rabbit skin cells and $HFFF_2$ were passaged routinely in 150cm^2 flasks using the method described for BHK-21 cells. If these cells were to be expanded to 850cm^2 roller bottles an entire large flask was used to seed the roller bottle, which was treated as described previously.

(b) Storage of cell stocks

To form stocks of cells, large flask cultures were harvested by trypsinisation (as described for routine passage) and were pelleted by centrifugation at 1,000 rpm for 5 mins at 4°C in a Sorvall RT7 centrifuge. The supernatant was discarded and the resultant pellet resuspended in 3ml of 'freezing medium' 90% calf serum and 10% DMSO (tissue culture tested) per flask. 1ml aliquots of the suspension were dispensed into cryo-vials and these were stored in a polystyrene container at -70°C overnight prior to transfer to liquid nitrogen for long term storage.

(c) Recovery of frozen cell stocks

Vials of cells were thawed at 37°C and diluted in ~20ml growth media. They were centrifuged at 1,000 rpm at 4°C for 5mins to pellet the cells. The supernatant was discarded and cell pellet resuspended in 1ml of growth medium before being transferred to a large flask with 50ml of growth medium and incubated at 37°C overnight. The medium was replaced the following day and the cells were then passaged as normal upon reaching confluence.

2.2.4.2. Transfection of mammalian cells: Calcium phosphate

Transfection of mammalian cells by Calcium phosphate precipitate was essentially as described by Stow and Wilkie (1976) and was used where transfection of multiple DNAs was required. Briefly, cells were plated at a density of ~$2x10^5$ per 35mm plate and cultured at 37°C. The following day cells of ~60% confluence were selected for transfection. A total of 3μg of target DNA, was combined with 22.5μg carrier DNA in 1ml of HeBS, and mixed by gentle shaking. Next 35μl of 2M $CaCl_2$ was added, mixed by gentle shaking and allowed to stand for 5 min at room temperature to form the calcium phosphate precipitate. The growth medium was removed and the cells were rinsed twice with unsupplemented medium. Cells were then overlaid with 400μl of calcium phosphate precipitate per plate and incubated at 37°C. After 40 min, 2ml of growth medium with supplements was added to each plate and incubated for a further 4 h at 37°C. Each plate was then washed twice with 2ml of unsupplemented growth medium. The cells were overlaid with 1ml of 22.5% DMSO in HeBS for 4min at room temperature with periodic shaking. DMSO/HeBS was removed and the cells carefully washed twice with 2ml of unsupplemented growth medium before being overlaid with a final 2ml of growth medium containing 1% Pen/strep and 0.1% Gentamicin and incubated as required for subsequent use.

2.2.4.3. Transfection of mammalian cells: Liposome

Transfection with lipofectamine 2000 was performed in accordance with the manufacturer's protocol. Briefly, 35mm plates of cells were seeded with $1x10^6$ cells to achieve a confluency of ~90% after overnight incubation at 37°C. Cells were washed with growth medium and overlaid with fresh growth medium. Target DNA was diluted in Optimem (250µl/plate). Typically only 1µg/plate of DNA was transfected using 2.5µl of Lipofectamine 2000 diluted in 250µl of Optimem per plate. After 5 min diluted Lipofectamine 2000 was mixed with diluted target DNA and incubated at room temperature. After 20min, 500µl of the Lipofectamine/DNA suspension was added to each plate and mixed with the 2ml of growth medium by rocking. Cells were then returned to 37°C and incubated overnight or as required for downstream applications. Where cells were to be superinfected after lipofectamine 2000 transfection the growth medium containing Lipofectamine 2000 was replaced at 8-9 hours after addition. The cells were initially washed with 2ml of growth medium then overlaid with a further 2ml of growth medium and cultured as normal overnight. Superinfection was performed after overnight incubation in fresh growth medium.

2.2.4.4. Superinfection

Cells transfected as previously described, were superinfected at a suitable time post transfection (typically 24 h). Cells were briefly washed with growth medium and then infected with the desired virus, in a volume of 100µl and incubated for 1 h, before being overlaid with 2ml growth medium.

2.2.5. Generation of virus mutants

2.2.5.1. Isolation of complementing cell lines

To generate complementing cell lines RS cells were plated and treated as described for calcium phosphate mediated transfection. These cells were co-transfected with plasmids expressing HSV gene constructs and either pSV2Neo or pCI-Neo to allow selection using G418. At 24 hours post transfection cells were removed with trypsin (section 2.2.4.1) and plated at low densities into 24 well plates and 35mm dishes in growth medium. G418 (100mg/ml in deionised distilled water, 0.2µm filtered) was added at a final concentration of 1mg/ml and the medium supplemented with G418 was changed every three days.

Cytotoxicity was monitored and this regime maintained until outgrowth of resistant colonies was evident. Resistant colonies were isolated from one another into individual wells of a 24 well plate under continuing G418 selection. In cases were two colonies of resistant cells were present in the same well, the colonies were separated using small squares of Whatman filter paper sterilized by immersion in alcohol and air dried under UV illumination. Filter papers were soaked in trypsin/versene solution (section 2.2.4.1) normally used for harvesting cells and placed onto the colony of cells. The cells were incubated at 37°C in the presence of this trypsin/versene soaked filter paper for 5 – 10min before the filter paper was recovered and used to inoculate a well of a 24 well plate with the detached cells. When confluent, cells were harvested with trypsin and transferred to 35mm dishes followed by expansion into small flasks. Once sufficient cells were available they were tested for their ability to complement virus mutants. Successful lines were expanded and stored in liquid nitrogen.

2.2.5.2. Isolation of virus mutants by plaque picking

Following transfection of virus or BAC DNA, plaques were either picked directly as they became apparent, or the cells were left until they showed complete cpe then harvested and used to infect further monolayers after serial dilution (as described for the determination of titre). For lethal mutants, virus was titrated on both complementing and non-complementing cell lines. Well separated plaques were picked into 300µl of growth medium and subjected to two freeze-thaw cycles before being titrated once more. Each virus underwent at least two cycles of plaque purification to ensure homogeneity.

2.2.5.3. Preparation of virus stock

Confluent monolayers of BHK-21 or RS cells typically in 10 850cm^2 roller bottles were used to grow high titre stocks of WT HSV-1. Virus mutants were grown on the appropriate complementing cell line. Monolayers were commonly infected with 0.03 to 0.05 pfu/cell in 40ml of growth medium and incubated with rotation (0.5 rpm) at 31°C or 37°C until the cells were easily dislodged into the medium by shaking. Cells and medium were transferred to 250ml Falcon tubes and collected by centrifugation at 2,000 rpm at 4°C for 10 min in a Sorval RT7 centrifuge. The resultant supernatant was decanted and retained, whilst the cell pellet was resuspended in 5ml of growth medium. Virus stocks were prepared from both these fractions:

Cell-associated virus (CAV): Mature virus was released from the pooled cell pellet by sonication using a Kerry Ultrasonic Bath until all visible bodies of cellular material had dissipated. The resultant suspension was clarified by centrifugation at 3,000 rpm, at 4°C for 10 min, before the supernatant was removed, aliquoted into 1.5ml cryo-vials and stored at -70°C. This is a relatively dirty extract which contains both mature virus particles, virus capsids and cell debris.

Cell-released virus (CRV): The clarified supernatant medium from the infected cells contains released virus particles, comprised of both virions and L particles and as such is a cleaner extract. Virus was concentrated from the supernatant medium by centrifugation at 12,000 rpm for 2 hours at 4°C in a Sorval SLA 3000 rotor. The resultant supernatant was discarded and the pellet overlaid with 2ml of medium. The pellet was allowed to resuspend overnight on ice. Any residual material was dispersed by pipetting gently if required, aliquoted into 1.5ml cryo-vials and stored at -70°C.

2.2.5.4. Determination of titre

35mm dishes of cells were set up to achieve a confluence of 80% or greater after overnight incubation at 37°C. For mutant viruses both complementing and non-complementing cells were used to assess the degree of reversion in these stocks. Virus stocks were serially diluted in 10 fold steps by addition of 100µl of each dilution into 900µl of fresh medium. The medium was removed from the cells and replaced with 100µl of each virus dilution. The plates were incubated at 37°C for 1 h with periodic agitation to ensure the monolayer remained hydrated. The inoculum was removed and replaced with 2ml of overlay medium containing methylcellulose and incubated for a further 3 days at 37°C until plaques were visible. Plates were stained with Giemsa (BDH) after removal of the overlay medium for at least 2 hours before washing in copious quantities of water. Stained monolayers were examined under a dissecting microscope and plaques were counted to determine the titre of the virus stock.

2.2.5.5. Determination of single step growth kinetics

Confluent monolayers of cells, on 35mm plates, were infected with 10 pfu/cell of virus in a 100µl of medium. After 1 hour the inoculum was removed and the cells were rinsed twice in 500µl washing solution. After rinsing, the cells were exposed to 500µl of acid solution for 1 min with gentle agitation. The acid solution was then removed and the cells washed

twice with 1ml cPBS before being overlaid with growth medium and incubated at 37°C. For each virus, one plate was used per time point and was harvested by scraping cells into the culture medium. Harvested samples were kept on ice at 4°C until all samples were collected before being sonicated to disrupt cells prior to determination of titre.

2.2.6. Immunofluorescence

All cells intended for fluorescence microscopy were grown on coverslips, sterilized with alcohol and placed in the bottom of a suitable plate.

Infected cells on coverslips were washed twice, briefly, in cPBS before fixation. For visualization of microtubules, fixation was in Microtubule fixation buffer at room temperature for 5 min after which the fixative was removed, and cells incubated with methanol for 5 min at -20°C (Vielkind & Swierenga, 1989). For detection of VP5 with DM165, fixation was performed with methanol alone for 5 min at -20°C. After incubation at -20°C, methanol was removed and the cell monolayers air dried prior to rehydration in cPBS. Samples could then be stored at 4°C until required. For other antibodies, cells were washed twice in cPBS, then overlaid with PFA fixative. After 30 min incubation at room temperature the fixative was removed and the cells were exposed to 0.01% Triton X100 in cPBS for 15 mins. The cells were then washed twice and overlaid with cPBS before storage at 4°C until required.

In all cases the primary antibodies were diluted in cPBS to a dilution that had previously been established as suitable for immunofluorescence detection. Each coverslip was overlaid with 100µl of primary antibody solution and incubated in a humidified atmosphere for 1 h at room temperature. The coverslips were washed extensively in three changes of 2ml cPBS, before incubation with the secondary antibody solution. Secondary antibodies were commonly diluted at 1:1000 as recommended by the supplier. 100µl of secondary antibody solution was used to overlay each coverslip and incubated for 1 h at room temperature in a humidified atmosphere. After incubation cells were washed extensively in cPBS and were then washed once in deionised water. After draining coverslips were mounted onto microscope slides using Mowiol mounting medium (Harco) containing 2.5% DABCO (Sigma) and 1µg/ml DAPI (Sigma) if required. Coverslips were examined in a Zeiss LSM 510 confocal microscope using the Diode (405nm), Argon (488nm), and HeNe (543 and 633nm) lasers and the 63x oil immersion objective lens. For immunofluorescence filter sets BP 420-480, BP 505-550 and LP filter 560 were used,

while for FISH filter sets BP 560-615 and LP 650 were used to ensure separation of the cy3 and cy5 signals. Channels were scanned sequentially on 512x512 (average 4). Images were captured with LSM510 software (version 4, SP2) and exported from LSM Image browser.

2.2.7. Cell fusion for syncitia

Cell fusion was performed using a method based on that of Lewis and Albrechtbuehler (1987). $HFFF_2$ cells for fusion into syncitia were plated at low density onto 22mm square coverslips and cultured as previously described until ~80% confluent (typically overnight at 37°C after plating at $5x10^5$ cells/dish). Assuming a total cell count of $1x10^6$, cells were infected at 0.01 pfu/cell with either WT or mutant virus in ~300µl of medium. At 1 h post infection cells were fused by treatment with PEG fusion buffer (Roche). The virus inoculum was removed and the cells were washed twice in 2ml of unsupplemented medium. Monolayers that were not required for fusion were overlaid with DMEM supplemented with 10% pooled human serum (Cellect). Monolayers to be fused were overlaid with 1ml of PEG fusion buffer (50% PEG1500 in 75mM Hepes (pH8), Roche). All solutions for cell fusion were maintained at 37°C. After 1 min of exposure the PEG fusion buffer was removed and the monolayers briefly washed 3 times in 1 ml of DMEM supplemented with 15% DMSO. The monolayers were then washed twice more with 2ml of unsupplemented DMEM to remove all traces of the DMSO, before being overlaid with 2ml of DMEM supplemented with 10% pooled human serum (Cellect) and incubated to 24 h post infection. In certain experiments Nocodazole was added at 3 h post infection to a final concentration of 0.5µg/ml. On duplicate plates, the equivalent volume of DMSO carrier solution was added as a control.

2.2.8. Fluorescence in situ hybridization (FISH)

At 24 h post infection cells were washed twice in cPBS before being overlaid with 1ml of FISH fixative (95% ethanol, 5% acetic acid) and incubated at -20°C for 5 min. After 5 min the fixative was drained and coverslips allowed to air dry before rehydration in 2ml of cPBS for at least 30 min. (Samples could then be stored at 4˚C for several days if required). To prepare monolayers for hybridization the cPBS overlay was removed, replaced with 1ml of hybridization buffer and incubated at 37°C for at least 30 min. Excess buffer was removed and the coverslips were transferred to individual microscope slides

with the monolayers facing upwards. 8μl of probe (1μl HSV-1 probe labeled with Cy3, 0.5μl salmon testis DNA (10mg/ml) in 8.5μl hybridization buffer) was added to each coverslip and the slides incubated at 95°C for 2 min in a Memmert hybridisation oven. The slides were retrieved and the coverslips inverted (cell side down) onto a clean area of the same slide before transfer to a humidified hybridization chamber (Cambrex) and incubation at 37°C overnight. 2xSSC was pre-equilibrated to 65°C overnight. After overnight incubation coverslips were transferred carefully to 35mm dishes with the monolayers upwards. The coverslips were washed and incubated twice in 2xSSC at 65°C for 5 min per wash. After a further wash in 2xSSC at room temperature for 5 min, the coverslips were rinsed in cPBS, and overlaid with 2ml of cPBS before further processing. If CellMask staining was required, the monolayers were incubated for 30 min in CellMask stain. The coverslips were then washed 3 times in 2ml of cPBS. All cells were rinsed in deionised water and mounted on slides as described for Immunofluorescence.

2.2.9. Preparation of Capsids

For the production of both nuclear and cytoplasmic capsids confluent monolayers of BHK-21 cells in 850cm^2 roller bottles were infected at 5 pfu/cell with WT HSV-1 or mutant virus in 40ml of growth medium. Typically 10 roller bottles were used per virus infection, and washed twice with 50ml cPBS at 3 h post infection. At 22-24 h post infection the growth medium was decanted into 250ml falcon tubes. Detached cells were pelleted by centrifugation at 2,000 rpm for 10min at 4°C and added back into the procedure described below. If required for virion and L particle production, the clarified medium was treated as described for CRV in section 2.2.5.3.

Cells were collected by adding 10ml of stripping buffer (cPBS + 1% Igepal + protease inhibitors) to one roller bottle. The roller bottle was rotated until all the cells had entered the buffer, which was then transferred to the next roller bottle. A second 10ml of stripping buffer was added to the first roller bottle to wash out residual cells. This process was continued until all the cells had been harvested. The two 10ml samples were then pooled. Nuclear and cytoplasmic fractions were separated by centrifugation in a 50ml centrifuge tube at 3,000 rpm for 10 mins at 4°C. The cytoplasmic extract (supernatant) was decanted to a fresh 50ml centrifuge tube and the nuclear pellets resuspended in 30ml of NTE resuspension buffer. The nuclei were disrupted using a Branson soniprobe at a power setting of 5-6 and frequency of 60% until the solution was homogeneous. Both nuclear and cytoplasmic fractions were centrifuged at 3,000 rpm and 4°C. Cleared supernatants were

transferred to AH629 tubes and underlayed with 5ml of 40% (w/v) sucrose cushion. The samples were balanced and centrifuged for 1 h at 25,000 rpm and 4°C in a Sorvall Pro 80 or Discovery 90SE. The supernatants were discarded and the pellets were washed with 5ml of either NTE resuspension buffer for nuclear capsids or cPBS stripping buffer for cytoplasmic capsids. Excess buffer was removed by blotting and the pellets overlaid with 500µl of NTE resuspension buffer (nuclear) or cPBS stripping buffer (cytoplasmic). Pellets were stored on ice at 4°C overnight then resuspended using a Kerry Ultrasonic bath, before loading onto preformed sucrose gradients. For preparations of up to 5 roller bottles 15ml TH641 10-40%(w/w) sucrose gradients were used, for larger preparations 36ml AH629 20-50% (w/v) sucrose gradients were used. Gradients were formed using a Gradient Master (Biocomp). After sample loading, they were then balanced and subjected to centrifugation. For 10-40% gradients this was at 40,000 rpm for 20 min at 4°C, whilst for 20-50% gradients this was at 25,000 rpm for 1 h at 4°C. After centrifugation, capsid bands could be visualized by overhead illumination. They were collected by fractionation as described below or by side puncture and collecting the visible bands using an 18 gauge needle and a syringe. Isolated bands were diluted to 30ml in NTE and the capsids recovered by centrifugation at 25,000 rpm for 1 h. The pellets were washed with 5ml of cPBS, before resuspension on ice over night in up to 100µl of cPBS.

2.2.9.1. Fractionation of gradients

Fractionation of gradients was performed to allow assessment of the protein composition of the material in each fraction. Fractionation was performed by insertion of an 18 gauge needle at the position of the seam present at the base of each tube to provide a consistent location. Fractions were collected into pre marked 15ml Falcon tubes or 1.5ml microfuge tubes as required. In all cases material present in each fraction was pelleted by centrifugation at 50,000 rpm at 4°C in a TLA 100.2 or 100.3 rotor (Beckman).

2.2.10. Preparation of Extracellular virions and L Particles

Extracellular virus was collected from growth medium as described for preparation of CRV. To prepare virions and L particles the resuspended pellets of extracellular material were sonicated briefly in an Ultrasonic bath to disperse large aggregates before being loaded onto preformed 5-15% Ficol gradients. Ficol gradients were prepared from 5% and 15% Ficol in Eagles medium without phenol red. Gradients were formed in AH629 tubes using a Gradient Master (Biocomp). After sample loading they were balanced and

centrifuged at 12,000 rpm for 2 h at 4°C. After centrifugation virion and L particle bands could be visualized by overhead illumination, they were collected by fractionation as described above or by side puncture and collecting the bands using an 18 gauge needle and syringe. The bands were then diluted to 30ml in Eagles A+B the virions and L particles were collected by centrifugation at 12,000 rpm for 1 h at 4°C, before resuspension on ice over night in 100µl of Eagles A+B.

2.2.11. Electron microscopy

2.2.11.1. Preparation of samples for electron microscopy

Thin section:

Confluent monolayers of cells were infected at 5 pfu/cell for 24 h with either WT HSV-1or appropriate mutant viruses. At 24 h post infection, the medium was removed and the cells were gently washed twice in cPBS. Cells were then fixed in 2.5% glutaraldehyde in cPBS and kept at 4°C for at least 1 hour. The monolayers were washed twice in cPBS and overlaid with ~200µl of osmium tetroxide for 1 h. The monolayers were again washed twice and scraped into 1ml of cPBS. The cells were pelleted at 2,000 rpm for 5 min. The cell pellets were resuspended in 500µl of 2% low melting point agarose in cPBS at 50°C, and were pelleted at 5,000 rpm for 5 min in a vertical axis rotor (Microfuge 12, Beckman). The cell pellets were examined and if suitably compact were chilled at 4°C for at least 1 h. The agarose containing the cells was isolated using a single edged razor blade and subdivided into 2mm cubes after removing excess agarose. The cubes of cells were then dehydrated through a graded series of alcohol (30, 50, 70, 90, 100, 100%) for 1 h per step before being transferred to a BEEM capsule and submerged in EPON 812 resin (TAAB) mixed with 150µl of BDMA hardener per 10ml resin. The cells float in the resin but following overnight infiltration with resin they sink to the bottom of the BEEM capsule. The resin was removed by inverting the BEEM capsule on a paper towel and fresh resin added. An indelible label was submerged in the resin which was then placed in an oven maintained at 65°C for at least 2 days to polymerise the resin.

Immuno EM:

Subconfluent monolayers of $HFFF_2$ cells were infected at 10 pfu/cell with WT HSV-1 or mutant viruses. At 24 h post infection the cells were washed twice in cPBS before fixation with 4% PFA and 0.1% glutaraldehyde in EPT at 4°C for at least 1 h. After removal of fix the monolayers were washed twice with cPBS, and scraped into 1 ml of cPBS. The cells

were pelleted through agarose as described above. The cubes of agarose containing the cells were dehydrated through a graded alcohol series, as described above except that the alcohol dilutions were precooked to 4°C and each step was carried out at 4°C for 1 h. Cells were then transferred to BEEM capsules and submerged in a 1:1 mix of 100% ethanol:Unicryl resin at -20°C for at least 1 h. The ethanol:Unicryl mix was then replaced with 100% Unicryl and left overnight at -20°C. The following day this resin was replaced with fresh 100% Unicryl for at least 1 h. Indelible labels were submerged into the resin and the resin was polymerised by exposure to UV for 3 days at -20°C.

2.2.11.2. Analysis of ultra-thin sections by transmission electron microscopy

Thin section:
Specimens for thin section analysis were cut using a Leica EM UC 6 ultramicrotome and mounted onto 400 mesh copper grids (Gilora). Sections were allowed to dry before staining with heavy metals for contrast. Heavy metal staining was performed by submerging the grids in 50µl drops of saturated Uranyl acetate in 50% ethanol for 1 h. They were washed in 3x 50µl drops of deionised water for 5 mins each then submerged in 50µl drops of lead citrate (Reynolds, 1963) for 1 min before washing once more as described above. Sections were dried before being viewed on a JEOL 1200EX microscope.

Immuno EM:
Specimens for Immuno EM were cut as described for thin section, but were mounted on nickel grids. Sections were allowed to dry onto grids before antibody staining. Grids were immersed in 50µl drops of cPBS supplemented with 0.05% Tween20 to hydrate them. They were then transferred to a 50µl droplet of cPBS/Tween20 containing the appropriate antibody at a dilution determined suitable for Immuno EM. After 1 h they were washed 3 x 5 min each in cPBS/Tween20 and transferred to cPBS/Tween20 containing 10nm gold conjugated goat anti rabbit or goat anti mouse IgG (1:100) for 1 h. The grids were washed 3x in cPBS/Tween20 and once in deionised water before drying. The sections were exposed to osmium tetroxide vapour for 1 h and stained with Uranyl acetate and visualised as described for thin sections.

2.2.12. Cryo-Electron microscopy

Sample grids were prepared for cryo-electron microscopy either manually or using a Mark IV vitrobot (FEI, Oregan). For manual preparation freshly glow discharged Quantifoil

holey carbon support film grids (R2/2 Quantifoil Micro Tools GmbH, Jena, Germany) were held in needle tip forceps and inserted into the manual plunging apparatus. 5µl of capsid suspension was added to the grid and blotted with filter paper to produce a thin film on the grid. Samples were vitrified by plunging into liquid nitrogen cooled ethane slush and subsequently transferred to storage containers in liquid nitrogen.

Preparation using the Mark IV vitrobot (FEI, Oregan) was essentially as described for manual preparation, with the following modifications. The vitrobot was set to 100% humidity and 22˚C. Blotting of samples was performed automatically for 4s using filter paper on rotating foam pads, changed after 16 cycles or between different samples before vitrification as described for manual preparation.

Grids were mounted in a 914 cryo-stage (Gatan, California) and transferred to a JEOL 2200 FS cryo-microscope. Suitable fields of capsids were identified and imaged at a magnification of 50,000x (corresponding to a pixel size of 2.2Å) with energy filtering and a slit width of 20 eV. Images were captured using an ultrascan 4k x 4k charge-coupled device camera (Gatan, California) image pairs were taken at close to focus (~1µm under focus) and further from focus (~ 2-3µm under focus). Particles were selected from the image pairs were then processed using X3D to correct low frequency variations in intensity. For each micrograph defocus values were calculated with BSOFT and images were subsequently corrected for the effects of contrast transfer function with CTFMIX after which the focal pairs were merged. Origin and orientation information was determined by the polar Fourier transform method and reconstructions were refined using cross common lines. Resolution was assessed by division of the data set into two equal subgroups and independent reconstructions were generated, with subsequent comparison using indices of similarity including the Fourier shell correlation and spectral signal to noise ratio approaches. Final visualization of reconstructions was in UCSF Chimera and surface contoured to mean plus one standard deviation of density.

2.2.13. Protein analysis

2.2.13.1. SDS-polyacrylamide gel electrophoresis for protein separation

Proteins were separated by electrophoresis through SDS polyacrylamide gels essentially as described by Laemmli (1970). Typically 10% acrylamide gels were prepared from Acrylamide:bisacrylamide solution (Biorad), resolving gel buffer and deionised water.

Polymerisation of the acrylamide solution was by addition of APS and TEMED. Acrylamide solution containing APS and TEMED was poured between clean pre assembled gel plates. Resolving gel was poured to a depth of 1cm below the comb, and overlaid with 70% ethanol. After polymerisation of the resolving gel the ethanol overlay was removed and residual ethanol removed by blotting and the stacking gel was then prepared from acrylamide:bisacrylamide solution, stacking gel buffer, deionised water, APS and TEMED. Stacking gel containing APS and TEMED was then poured on top of the resolving gel, avoiding air bubbles, and the comb inserted. The comb was removed upon polymerisation and wells washed with tank buffer and emptied before loading. Samples were prepared by mixing with boiling mix at 1x final concentration, and heated to 95°C for 5min. Likewise protein molecular weight standards were prepared as specified by the manufacturer. Electrophoresis was performed with the Biorad Miniprotean II or III kit or the Biorad criterion kit according to the manufacturer's instructions. Gels were run at ~100V until the dye front reached the bottom of the gel.

2.2.14. Western blotting

2.2.14.1. Protein transfer

Transfer of protein to a nitro-cellulose membrane was performed by wet transfer. Following SDS PAGE (section 2.2.13.1) the stacking gel was removed, and the resolving gel was placed into the gel holder cassette of a trans blot system (Biorad). Gels were set on top of a fibre pad and one sheet of Whatman 3mm paper both of which were pre-soaked in transfer buffer and held in transfer buffer whilst loading. Nitrocellulose membrane was placed on top of the gel and air bubbles removed to ensure good contact between gel and membrane. A second sheet of Whatman 3mm paper and the second fibre pad, were placed on top before the assembly was sealed and loaded into the electrode cassette. The tank was filled with transfer buffer and the Bio-ice cooling unit was inserted. Transfer was performed at 230mA constant current for 3 hours.

2.2.14.2. Detection of bound proteins

Following protein transfer, membranes were incubated with 5% (w/v) Marvel milk powder in TBS-Tween for at least 30 min at room temperature to block non-specific binding of antibody. The membranes were then rinsed in TBS-Tween and the primary antibody was added in 5ml of 1% Marvel in TBS-Tween. Typically incubation with the primary antibody was carried out overnight at 4°C, but in some cases incubation at room

temperature for 2 hours was used. The membrane was washed 3 times in TBS-Tween before addition of either GAM_{HRP} (1:1000) or GAR_{HRP} (1:5000 or 1:10,000) secondary antibody in 5ml of 1% Marvel in TBS-Tween. Blots were incubated at room temperature with shaking for 1-2 h, the blots were then washed 3 times in TBS-Tween. Immunodetection was performed using ECL (Amersham) in accordance with manufacturer's instructions, equal volumes of reagent 1 and 2 were mixed to prepare fresh ECL solution and membranes were incubated in this for 2 min before excess ECL was removed. Visualisation of ECL fluorescence was performed using UV sensitive Kodak X-OMAT film. Where required for reprobing membranes were treated with Stripping buffer at 50°C for 30 min with periodic agitation. After stripping, membranes were washed in TBS-Tween 3x 10 min, then blocked as described above before incubation in fresh primary antibody. Where multiple assays were performed on the same membrane, initial immunodetection was targeted against the least abundant species.

CHAPTER 3

CONSTRUCTION OF INNER TEGUMENT MUTANT VIRUSES, COMPLEMENTING CELL LINES AND ISOLATION OF REVERTANTS

3. Construction of inner tegument mutant viruses, complementing cell lines and isolation of revertants

3.1. Construction of plasmids used for generation of UL36, UL37 and UL36-UL37 expressing cell lines

Deletion mutants of UL36 and UL37 have been made in two alpha-herpesviruses, HSV-1 and PrV, while a temperature-sensitive (*ts*) mutant in UL36 has also been described for HSV-1. Previous studies with these mutant viruses have highlighted the essential nature of the products of both genes in HSV-1 (Desai *et al.*, 2001; Desai, 2000). In PrV UL36 is also essential (Fuchs *et al.*, 2004) whilst UL37 is non-essential, deletion severely impairs virus production (Klupp *et al.*, 2001b). Since both genes are essential in HSV-1, deletion mutants must be propagated in cell lines capable of supplying the protein required to complement the defect. Previously established HSV-1 cell lines (Desai *et al.*, 2001; Desai, 2000) have been made with DNA fragments, which have included extensive flanking sequences. Because these sequences extend well beyond the limits of the virus deletions, they allow recombination to take place between virus and cell DNAs leading to a high rate of reversion in the virus stock. This was especially noticeable for the mutant KΔUL36 and its complementing cell line HS30 (Desai, 2000). As such it was desirable to produce new complementing cell lines, which contained more limited viral sequences without extensive flanking sequences. In combination with virus mutants deleted for the entire ORF, such a strategy minimises the opportunity for homologous recombination and reversion. Similarly, a complementing cell line containing only the UL36 and UL37 ORFs was needed to support growth of a UL36-UL37 double mutant.

3.1.1. Modification of pApV for cloning of the UL36 ORF

Lamberti and Weller (1998) described an expression plasmid, pApV, which has the HSV-1, ICP6 (UL39) promoter and an SV40 polyadenylation sequence flanking a multiple cloning site (MCS) and cloned into a pUC118 backbone. The use of the ICP6 promoter means that the cloned gene is induced under conditions of HSV-1 infection ensuring high levels of expression when required. For cloning of the UL36 ORF it was necessary to modify the MCS to introduce a BstBI restriction enzyme site downstream of the existing

XbaI site to generate a new vector designated pApVB. A schematic representation of the strategy used to construct pApVB is shown in Figure 3.1. Modification of the MCS in pApV was performed using a pair of complementary 5' phosphorylated oligonucleotides pApVBstBIForward and pApVBstBIReverse, which were annealed to produce the ds oligonucleotide pApVBstBI following the protocol of Correnti *et al.*, (2002) as described in section 2.2.2.7.

pApVBstBIForward
5'-CTAGAAC*GGATCC*GTCGAC**TTCGAA**C
pApVBstBIReverse
5'-GATCG**TTCGAA**GTCGAC*GGATCC*GTT

pApVBstBI:

5'-CTAGAAC*GGATCC*GTCGAC**TTCGAA**C
TTG*CCTAGG*CAGCTG**AAGCTT**GCTAG-5'

The cohesive ends designed to regenerate the XbaI site and remove the BamHI site are underlined. Italics highlight the new BamHI site, double underlining the SalI site and the BstBI site is in bold.

Annealed oligonucleotides were purified by gel electrophoresis and subsequent gel extraction as described in sections 2.2.1.2 and 2.2.2.5 respectively. 1.6μg of pApV was digested sequentially with 10U of XbaI and BamHI and subjected to dephosphorylation (Fig. 3.2). The linker was ligated to the prepared vector and transformed into competent DH5α cells which were subsequently grown on ampicillin selection plates. Individual colonies were isolated and DNA prepared for analytical digest.

To assay for incorporation of pApVBstBI, DNA from individual colonies was screened by XbaI and BamHI co-digestion and then by SalI and XmnI co-digestion (Figs. 3.3 (A) and 3.3 (B)). An XmnI site was present in the pUC118 vector sequences. No SalI sites were present in pApV but one was introduced with pApVBstBI. Therefore, the appearance of two bands (~2.1Kbp and ~1.8Kbp) following XmnI and SalI co-digestion confirmed that the ligation of pApVBstBI with pApV was successful. Three positive colonies were identified and were subjected to further analytical restriction digestions with SalI, BstBI

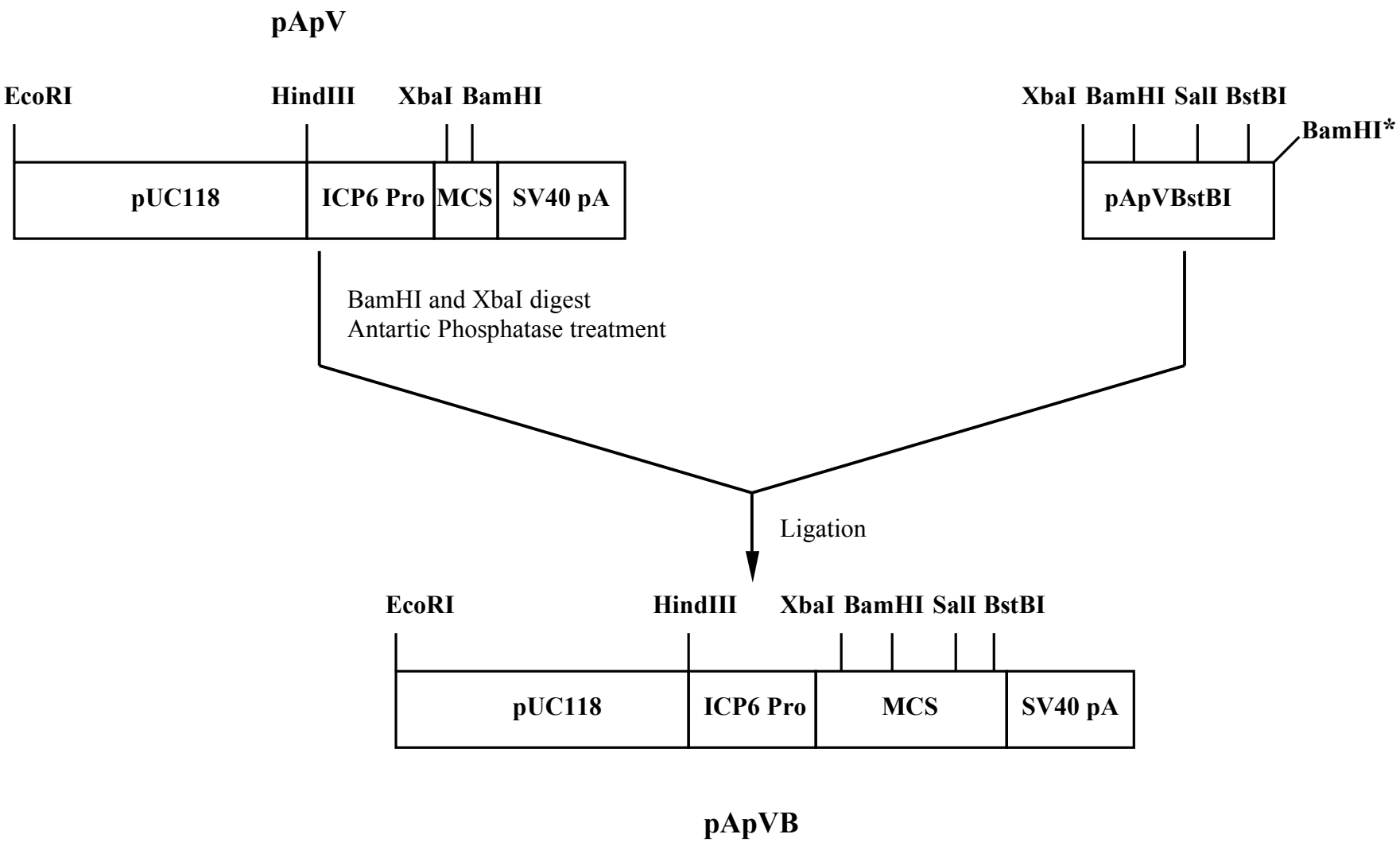
pApV
EcoRI
HindIII
XbaI BamHI
pUC118
ICP6 Pro
MCS
SV40 pA
XbaI BamHI SalI BstBI
BamHI*
pApVBstBI
BamHI and XbaI digest
Antartic Phosphatase treatment
Ligation
EcoRI
HindIII
XbaI BamHI SalI BstBI
pUC118
ICP6 Pro
MCS
SV40 pA
pApVB

Figure 3.1: Schematic representation of the cloning strategy used to produce pApVB.
The structure of pApV is shown with the locations of the pUC118, HSV-1 UL39 promoter (ICP6 Pro), SV40 polyadenylation signal (SV40 pA) and MCS sequences indicated (not to scale). The relative positions of the XbaI and BamHI restriction enzyme (RE) sites in the MCS are marked. The ds oligonucleotide (pApVBstBI) is shown with the relative positions of RE sites indicated. BamHI* represents the terminal sequences that anneal to but fail to regenerate a BamHI site. pApVBstBI was ligated with BamHI and XbaI digested pApV to generate pApVB.

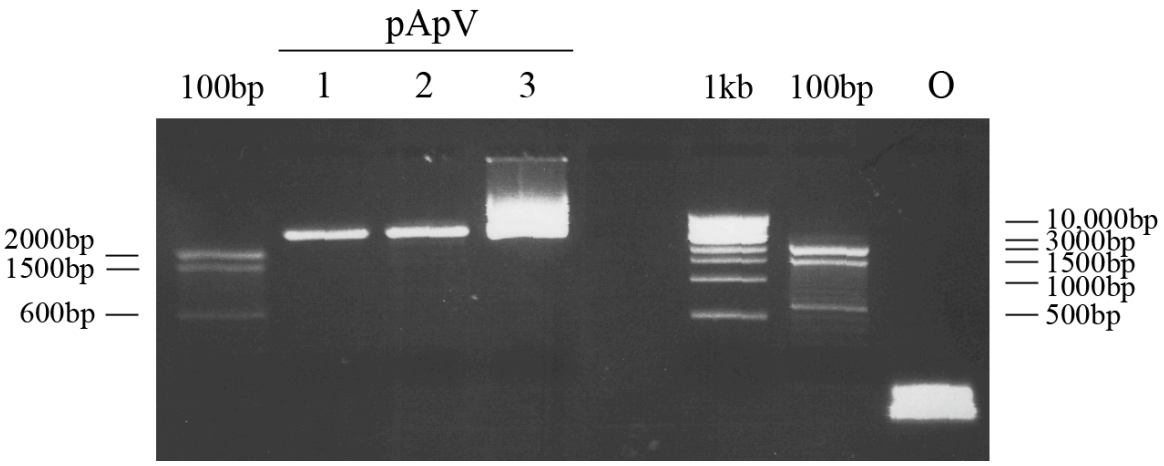

Figure 3.2: Construction of pApVB

pApV was digested sequentially with XbaI and BamHI (Lane 2). This produces two fragments of 3,908 and 6 bp, the smaller of which is not visible. XbaI digested (lane 1) and undigested (lane 3) pApV were run as controls. Lane O shows 5µl of the annealed oligonucleotide pApVBstBI.

DNA ladders are 100bp or 1kb (1Kbp) from NEB.

(A)

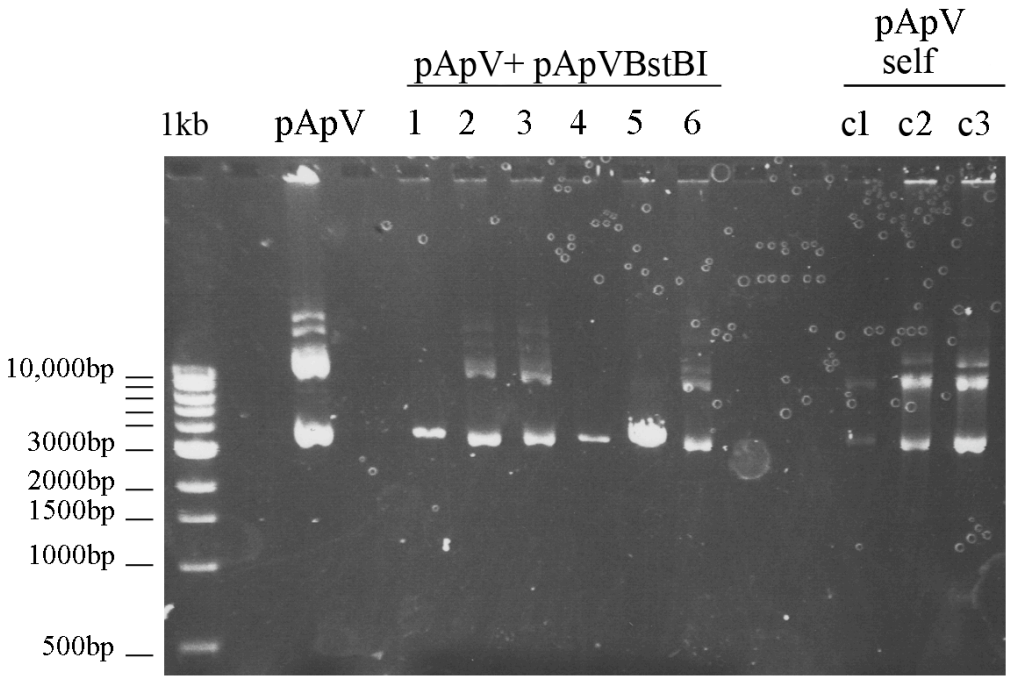
pApV+ pApVBstBI
pApV self
1kb
pApV
1
2
3
4
5
6
c1
c2
c3
10,000bp
3000bp
2000bp
1500bp
1000bp
500bp

(B)

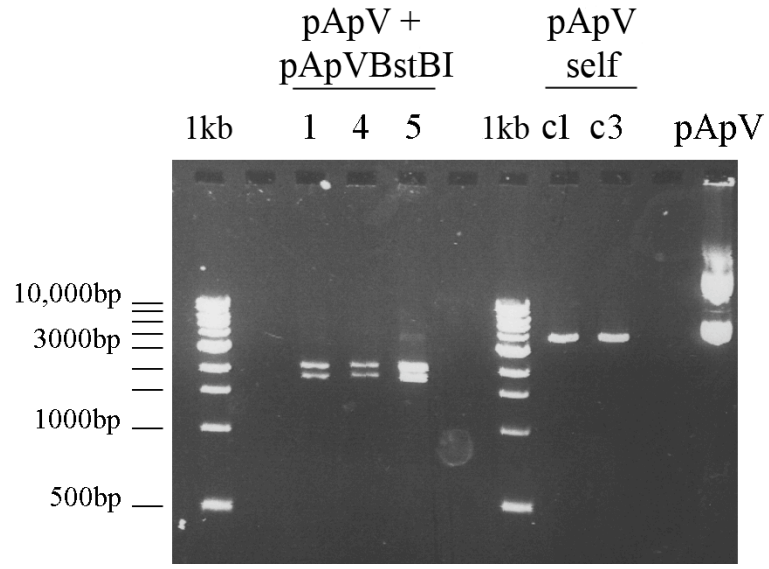
pApV +
pApVBstBI
pApV
self
1kb
1
4
5
1kb
c1
c3
pApV
10,000bp
3000bp
1000bp
500bp

(C)

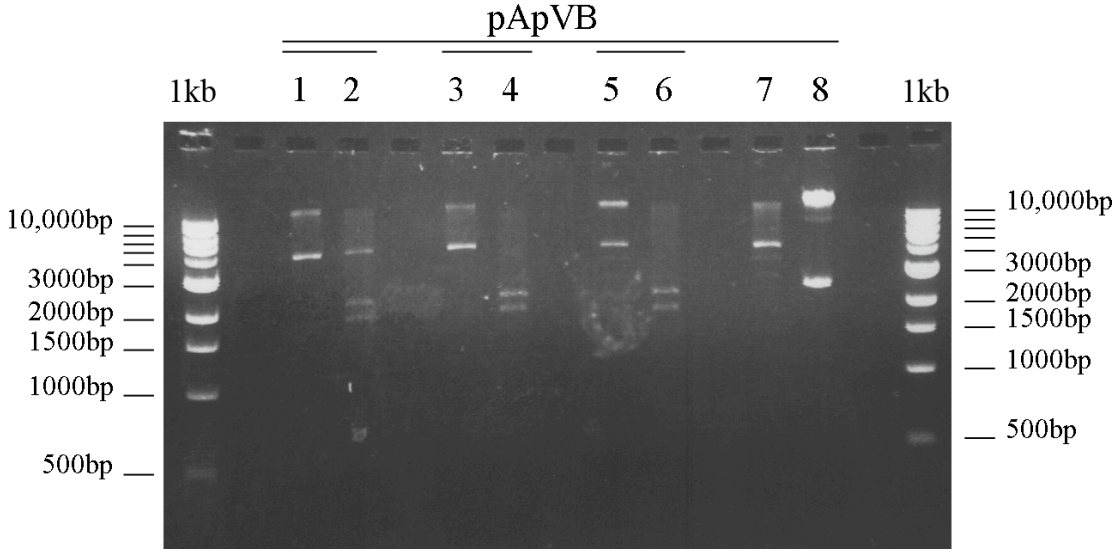
pApVB
1kb
1
2
3
4
5
6
7
8
1kb
10,000bp
3000bp
2000bp
1500bp
1000bp
500bp
10,000bp
3000bp
2000bp
1500bp
1000bp
500bp

Figure 3.3: Analysis of pApVB clones.

(A) DNA from six colonies (1-6) from the ligation of XbaI/BamHI digested pApV (Fig. 3.2 lane 2) to pApVBstBI (Fig. 3.2 lane O) and three colonies (c1-c3) from self ligation of XbaI/BamHI digested pApV were digested with XbaI and BamHI. A digestion product of the expected size (3926 bp) is present in lanes 1,4, and 5. pApV shows undigested pApV DNA used as a control.

(B) SalI and XmnI analytical codigests of putative pApVB clones. DNA from colonies 1,4 and 5 (A) were digested with SalI and XmnI. XmnI cuts within the pUC118 vector sequence of pApV, and a SalI restriction site was present in pApVBstBI. Therefore ligation of pApVBstBI in XbaI/BamHI digested pApV should result in 2 fragments of 1815 bp and 2119 bp as seen in lanes 1,4 and 5. A single 3934 bp band is seen in lanes c1 and c3 reflecting the presence of the XmnI site in the pUC118 vector. pApV shows undigested pApV DNA used as a control.

(C) Clone 5 from (B) was selected for further analysis by digestion with SalI, SalI and XmnI (lanes 1and 2), BstBI, BstBI and XmnI (lanes 3 and 4), XbaI, XbaI and XmnI (lanes 5 and 6), XbaI and BstBI (lane 7) or left undigested (lane 8). Digestion with SalI, BstBI and XbaI produce a 3934 bp band (lanes 1,3 and 5) and co-digestion with XmI produced bands of ~1800 bp and ~2100 bp (lanes 2,4 and 6) confirming the incorporation of pApVBstBI.

In all cases 1kb denotes a 1Kbp DNA ladder (NEB).

and XbaI individually or together with XmnI co-digestion, such as that in Fig. 3.3 (C). One isolate, clone 5, was selected, designated pApVB and used for subsequent cloning steps.

3.1.2. Construction of the UL36 expression vector pHAUL36

Initial attempts were made to clone the full length UL36 ORF by direct ligation of an SpeI-BstBI fragment derived from cosmid 14 (Fig. 3.4) into pApVB digested with XbaI and BstBI. However, this approach proved unsuccessful and an alternative cloning strategy was adopted as summarised in schematic form in Figure 3.5. pApVB was linearised by BamHI digestion, dephosphorylated and gel purified. The 9.2Kbp BamHI fragment (residues 70168-79441; (McGeoch *et al.*, 1988) of UL36 was derived by BamHI digestion of cosmid 14. It was gel purified and ligated into the BamHI digested pApVB. Following transformation into DH5α cells, DNA from individual colonies was analysed by BamHI digestion (Fig. 3.6 (B). Plasmids producing fragments of the expected sizes were digested with BstBI to determine the orientation of the inserts (Fig. 3.6 (A)). Those having the correct orientation produced two fragments of ~860bp and ~12.3Kbp (Fig. 3.6 (A) lanes 1, 3 and 10), whilst those in the incorrect orientation gave bands of ~8.4Kbp and ~4.7Kbp. One positive clone was selected (clone 10) and designated pApVB36C. pApVB36C DNA was digested with BstBI and the ~12.3Kbp fragment was purified from an agarose gel. This fragment, which contains the vector sequences, was self ligated and transformed into DH5α cells. The resulting plasmids should contain the ~8.4Kbp C terminal region of the UL36 ORF as a BamHI-BstBI fragment cloned into the MCS of pApVB with just 32bp of HSV-1 flanking sequence between of the UL36 termination codon and the BstBI site. DNA from individual colonies was subject to analytical restriction enzyme digestion with BamHI, BstBI, SphI and XbaI, an example of which is shown in Figure 3.7, this analysis was performed to confirm the loss of second sites for both BstBI (Fig. 3.7 compare lanes 1 and 5) and BamHI (Fig. 3.7 compare lanes 3 and 7) after BstBI digestion and self ligation. One clone was selected for use in further cloning steps and was designated pApVB36CBs.

To supply the N terminal end of the UL36 ORF the missing sequences were generated by PCR amplification from a cosmid 14 template using the following primers:

UL36_HA_Nterm (Forward)

XbaI BglII

5'-*TCTAGA*GGC**ATG*TACCCTTACGACGTGCCTGACTACGCT***AGATCTGGT GGCGGAAACAACACTAACC

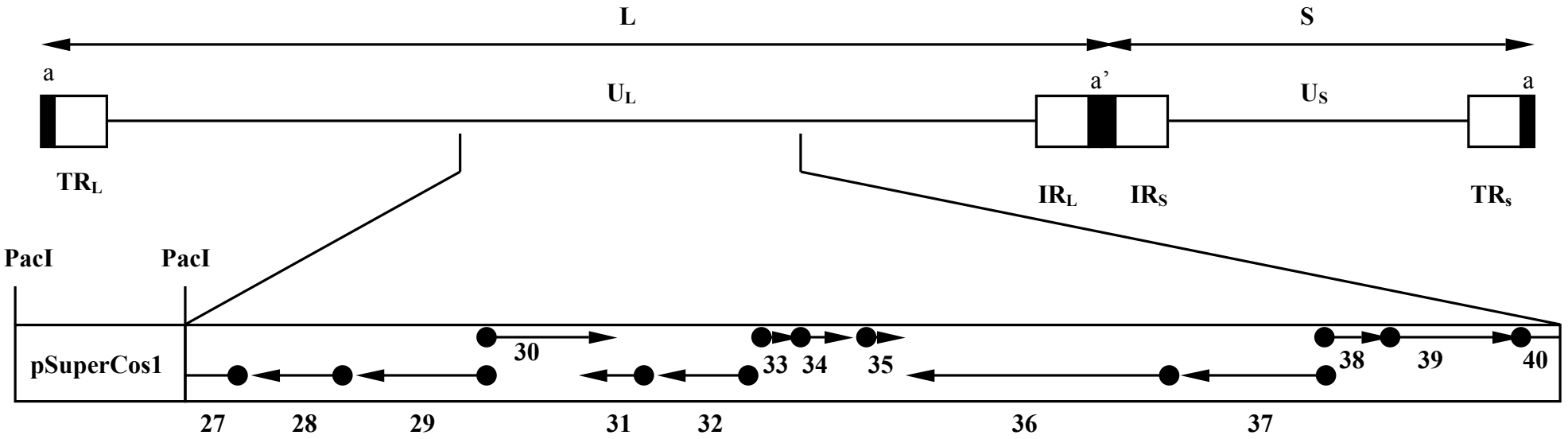

Figure 3.4: Schematic representation of the HSV-1 genome organisation and the structure of Cosmid 14.

A conventional representation of the HSV-1 genome (not shown to scale). The long (L) and short (S) genome regions are indicated with the unique (U_L and U_S) sequences shown as solid lines, and major repeat elements (TR_L, IR_L, IR_S and TR_S) as open boxes. The terminal a sequences and internal a' sequence are marked by filled boxes.

A schematic representation of Cosmid 14 is shown below, highlighting the PacI restriction sites of pSuperCos1 into which the HSV-1 genome fragment spanning residues 54445 to 90477 (McGeoch *et al*., 1988) of the prototypical arrangement was cloned (Cunningham and Davison, 1993). The fragment of the HSV-1 genome present in Cosmid 14 spans ORFs UL27 to UL40 (both truncated). The order and direction of the ORFs present are show as arrows, start positions are indicated as filled circles and arrowheads indicate orientation

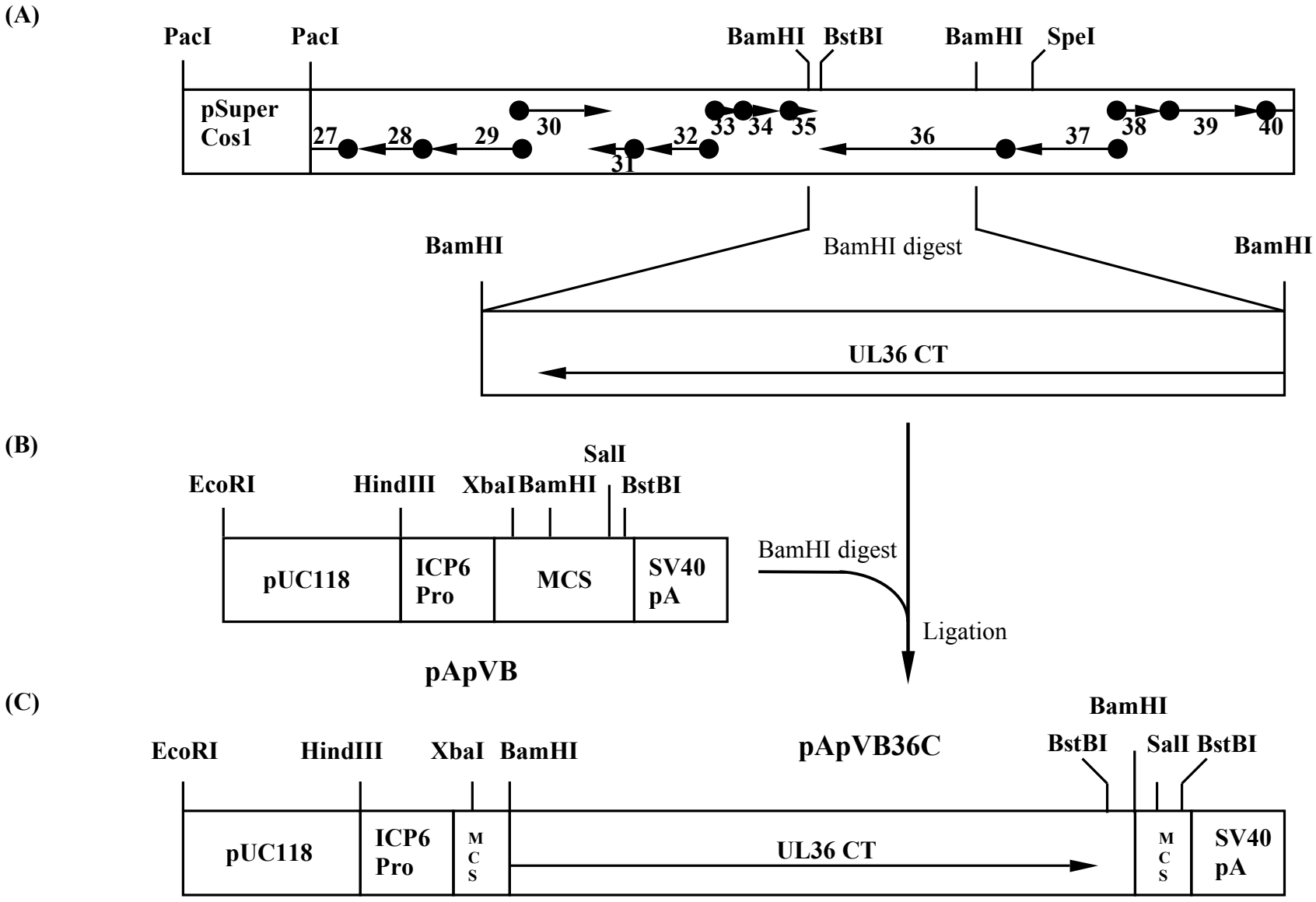
(A)
PacI
PacI
BamHI
BstBI
BamHI
SpeI
pSuper
Cos1
27
28
29
30
31
32
33
34
35
36
37
38
39
40
BamHI
BamHI digest
BamHI
UL36 CT
(B)
SalI
EcoRI
HindIII
XbaI
BamHI
BstBI
pUC118
ICP6
Pro
MCS
SV40
pA
BamHI digest
Ligation
pApVB
(C)
BamHI
EcoRI
HindIII
XbaI
BamHI
pApVB36C
BstBI
SalI
BstBI
pUC118
ICP6
Pro
M
C
S
UL36 CT
M
C
S
SV40
pA

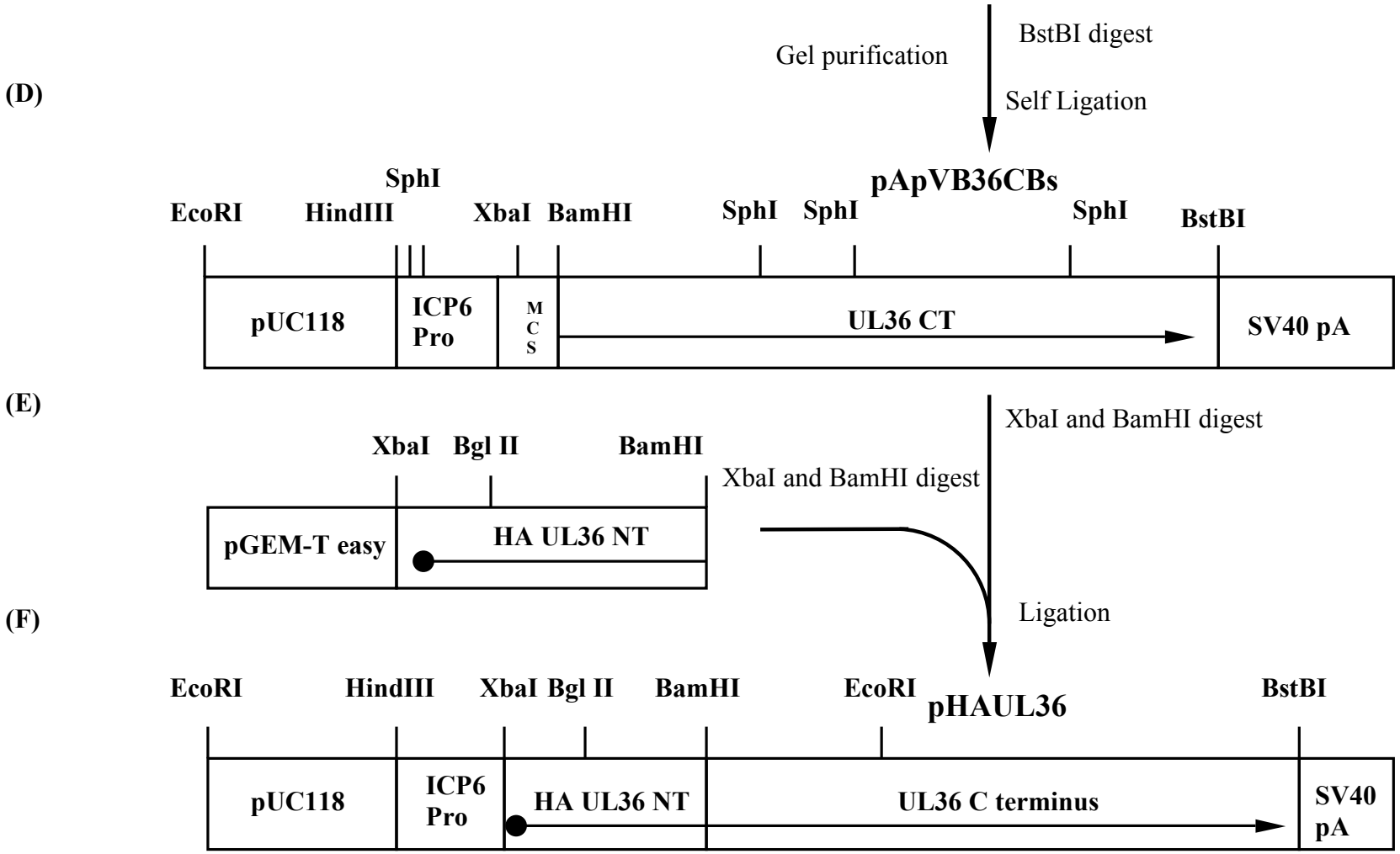

Fig 3.5: A schematic representation of the cloning strategy used to produce a pUL36 expression vector.

Figure 3.5: Schematic representation of the cloning strategy used to produce the pUL36 expression vector, pHAUL36.

(A) A schematic representation of Cosmid 14. The BamHI D fragment which spans the C terminal ~8.4Kbp of the UL36 ORF with ~850bp of flanking sequence downstream of the ORF (shown enlarged), was isolated from Cosmid 14 DNA by BamHI digestion and gel purification.

(B) A schematic representation of pApVB as shown previously in Figure 3.1. pApVB was linearised by digestion with BamHI and ligated with the BamHI D fragment.

(C) pApVB36C was produced by the ligation of the BamHI D fragment to pApVB. This shows the product in the correct orientation for further cloning to repair the UL36 ORF.

(D) pApVB36C was digested with BstBI to remove the HSV-1 sequences downstream of the UL36 ORF and to remove the BamHI site which denotes the end of the HSV-1 insert. Religation generates pApVB36CBs which retains just 32bp of HSV-1 flanking sequence after the UL36 stop codon and has a unique BamHI site downstream from the ICP6 promoter.

(E) The missing 5' region of UL36 was generated by PCR against a Cosmid 14 DNA template and cloned into pGEM-T easy. The primers for this reaction are described in Table 2.1. The primer specifying the N terminal end of the UL36 ORF contained an XbaI site and had sequences encoding the influenza Haemagluttinin (HA) epitope fused in frame upstream of codon 2 of UL36. A BglII site separated the HA tag and the UL36ORF. As a consequence the N-terminus of the encoded protein (HA-UL36) has the sequence:

M **YPYDVPDYA** RS GGGNNTN (with the HA epitope in bold and the pUL36 residues underlined). The HA-UL36 N terminal sequences were released from pGEMT-easy by XbaI and BamHI digestion and ligated to XbaI and BamHI digested pApVB36CBs.

(F) A schematic representation of pHAUL36, which has the full length UL36 ORF containing an HA tag and under control of the ICP6 promoter and SV40 polyA signal.

In all panels ORFs are marked by arrows, the start position of each is indicated with a filled circle and arrowheads indicate the orientation of the reading frame. Constructs are not shown to scale

(A)

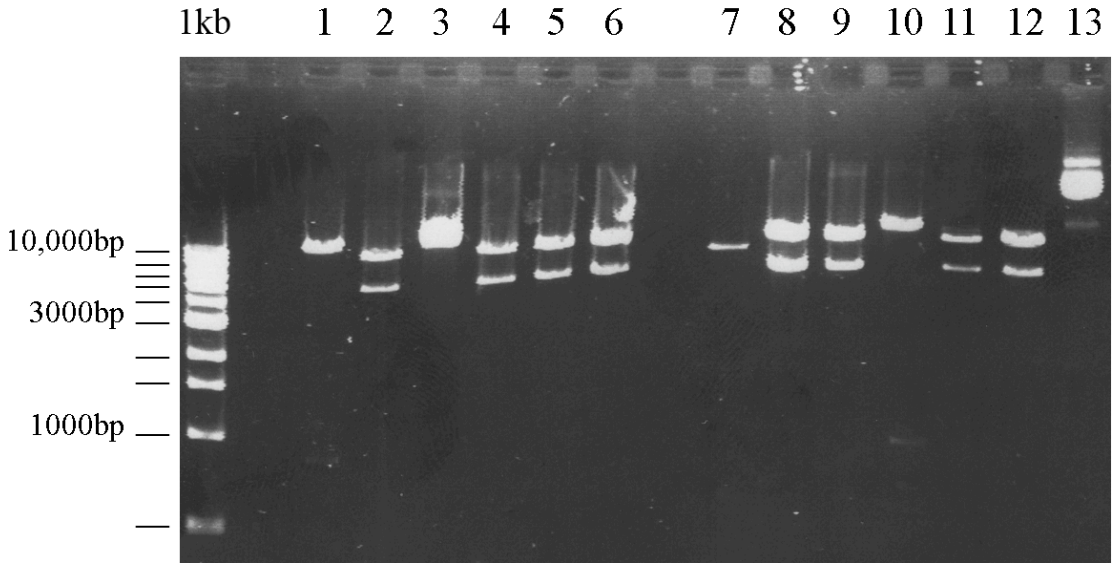
1kb
1
2
3
4
5
6
7
8
9
10
11
12
13
10,000bp
3000bp
1000bp

(B)

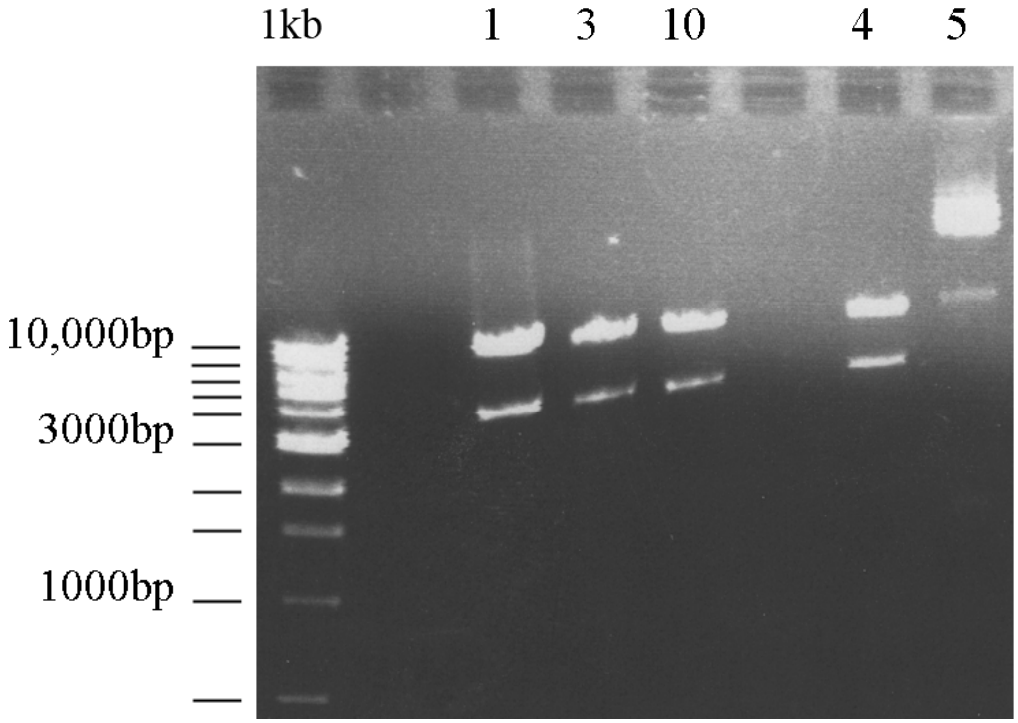
1kb
1
3
10
4
5
10,000bp
3000bp
1000bp

Figure 3.6: Analysis of pApVB36C constructs.

(A) Individual pApVB36C DNAs were digested with BstBI to determine the orientation of the BamHI insert. Clones in lanes 2,4,5,6,8,9,11 and 12 produced bands of ~4.7Kbp and ~8.4Kbp, showing that the BamHI fragment was in the incorrect orientation. Lanes 1,3 and 10 had bands of >10 Kbp and ~1 Kbp showing that the BamHI insert was in the correct orientation. Clone 10 was selected for use in further work.

(B) DNAs from clones 1,3,10 and 4 were digested with BamHI to confirm the integrity of the BamHI insert. Lane 5 shows undigested clone 4 DNA as a control. All clones release a band of ~4 Kbp (pApVB) and one of >10 Kbp (the BamHI fragment spanning the UL36 C terminus).

In all cases 1kb denotes a 1Kbp DNA ladder (NEB).

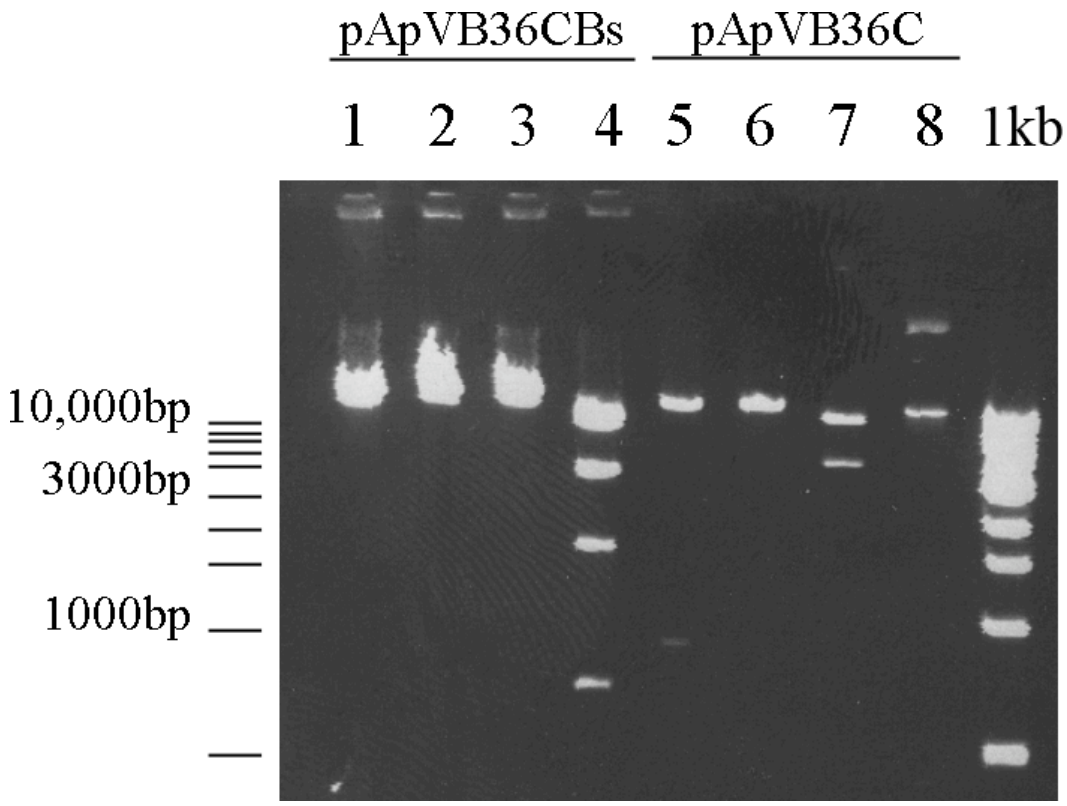

Figure 3.7: Analysis of pApVB36CBs.

The UL36 C-terminal flanking sequence in pApVB36C, were removed by digestion with BstBI to produce pApVB36CBs (Fig. 3.5). Digestion of pApVB36C with BstBI (lane 5) and BamHI (lane 7) produced bands of 12348 bp and 859bp and of 9273 bp, and 3934 bp, respectively. Digestion with XbaI linearised the plasmid as expected (lane 6), while digestion with SphI was incomplete (lane 8). Digestion of pApVB36CBs with BstBI (lane 1), XbaI (lane 2) and BamHI (lane 3) confirmed the unique nature of each of these sites. Digestion with SphI (lane 4) produced the expected bands of 6856 bp, 3228 bp, 1549 bp, and 681 bp, confirming the gross structural integrity of pApVB36CBs.

1kb denotes the 1Kbp DNA ladder (NEB).

Amino acid sequence: **M*YPYDVPDYA***RSGGGNNTN

UL36CTBamHIF24886 (Reverse)
5'-ATGTCGTCGTCATCTTCTTCGG

As an antibody against pUL36 was unavailable at this time, sequences encoding an epitope from the influenza virus haemaglutinin were included (HA; shown in bold italics). These were placed upstream from the sequences for codons 2-8 of the UL36 ORF (HSV-1 sequences are underlined). A BglII site was included between the HSV-1 and HA sequences and an XbaI site was added at the 5' end to allow cloning into the XbaI site of pApVB36CBs. The reverse primer lies 95bp downstream from the BamHI site that forms the boundary of the HSV-1 sequences in pApVB36CBs.

The amplified PCR product (Fig. 3.8 (A)) was ligated into pGEM-T Easy and transformed into DH5α cells. DNA from individual colonies was assessed for the presence of a ~1.2Kbp insert by digestion with XbaI and BamHI (Fig. 3.8 (B)). One positive clone was selected and designated pGEMUL36 NT HA. pGEMUL36 NT HA was digested with BamHI and XbaI and the ~1.2Kbp fragment containing the UL36 N-terminal sequences was gel purified and ligated into BamHI-XbaI digested pApVB36CBs. Following transformation into DH5α cells, DNA from individual colonies was subject to analytical restriction enzyme digestion with BglII and EcoRI (BglII was chosen as the PCR product introduces a unique site at the 5' end of the ORF). 3 colonies exhibited the expected digestion pattern, producing bands of 5626bp, 4165bp and 3688bp (Fig. 3.8 (C) Lanes: HA, pHAUL36 1 and 2). One clone was selected and designated pHAUL36. Expression of pUL36 from pHAUL36 was verified by western blotting of extracts from RS cells transfected with pHAUL36 and superinfected with WT HSV-1 or FRΔUL37. Immunodetection was performed on the HA epitope (Fig. 3.9).

3.1.3. Construction of the UL37 expression vectors pGX336GFP and pApV-UL373

pGX336GFP and pApV-UL373 were produced prior to the work presented here. They are described briefly here because they were used to generate cell lines needed for isolating and propagating the UL37 minus mutant, FRΔUL37, which was used extensively in the studies described later in this thesis.

(A)

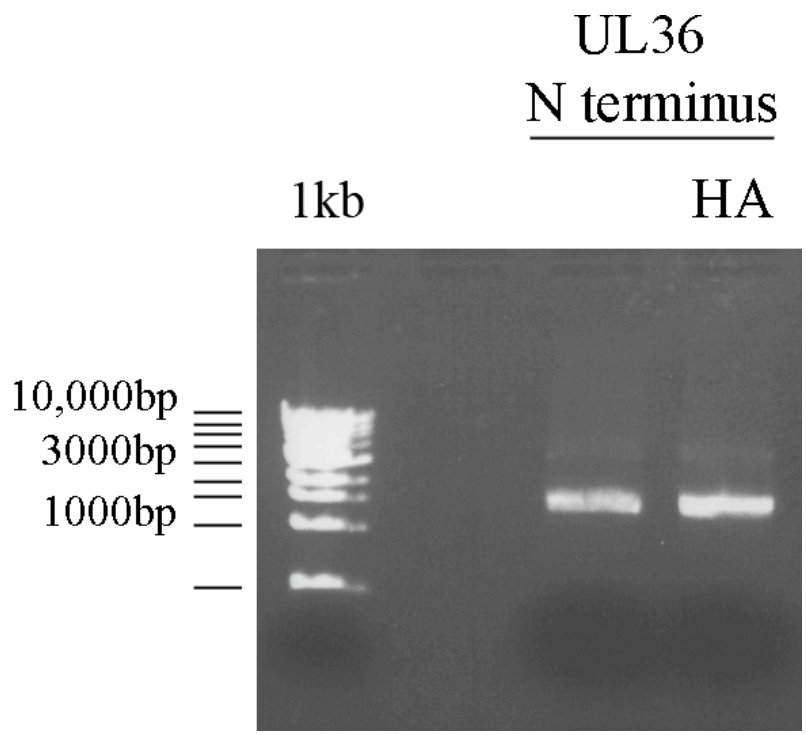
UL36
N terminus
1kb
HA
10,000bp
3000bp
1000bp

(B)

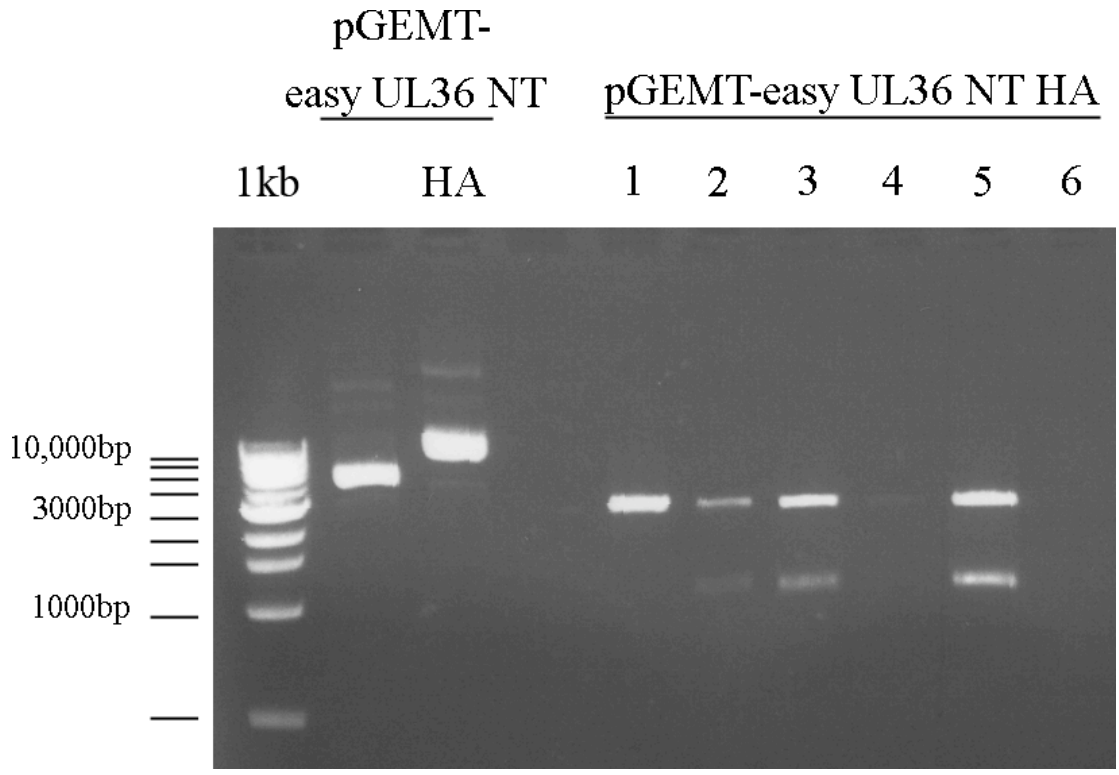
pGEMT-
easy UL36 NT
pGEMT-easy UL36 NT HA
1kb
HA
1
2
3
4
5
6
10,000bp
3000bp
1000bp

(C)

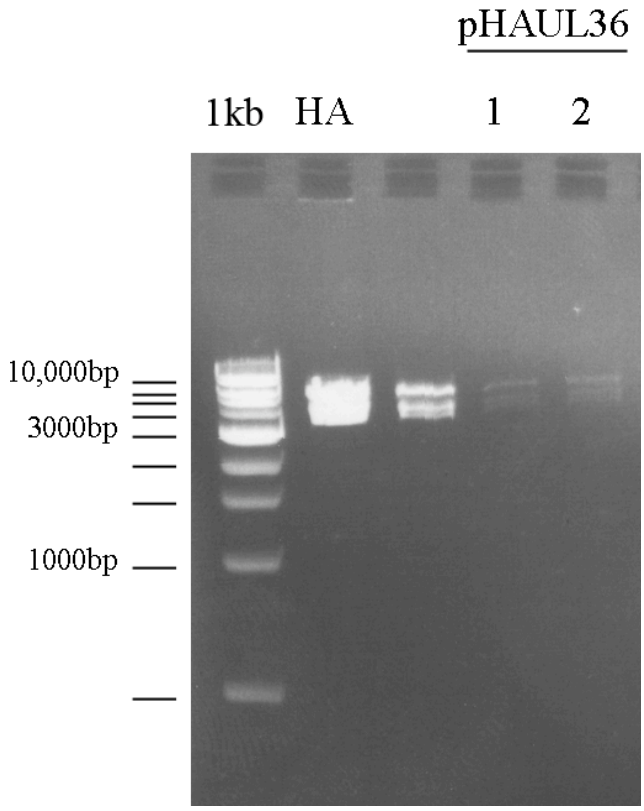

Figure 3.8: Cloning of the UL36 N terminus and construction of pHAUL36 (Fig. 3.5).
(A) Preparative gel showing the ~1.1Kbp PCR product containing the HA tagged N terminal sequences of the UL36 ORF amplified from cosmid 14 DNA.
(B) Analytical gel showing individual clones of pGEMUL36 NT HA co-digested with XbaI and BamHI (lanes 1-6). Lanes 2, 3 and 5 contain a fragment of ~1.1Kbp corresponding to the HA tagged UL36 N terminus. HA = undigested control.
(C) Analytical gel showing individual clones of pHAUL36 co-digested with BglII and EcoRI. Three diagnostic bands of 5626bp, 4165bp and 3688bp are clearly visible in lanes HA, 1 and 2.

Unlabeled lanes in panels A,B and C contain pUL36 N terminal constructs with a pp65 epitope fused in frame as described for HA. These constructs were not used in any further work.

In all cases 1kb denotes the 1Kbp DNA ladder (NEB).

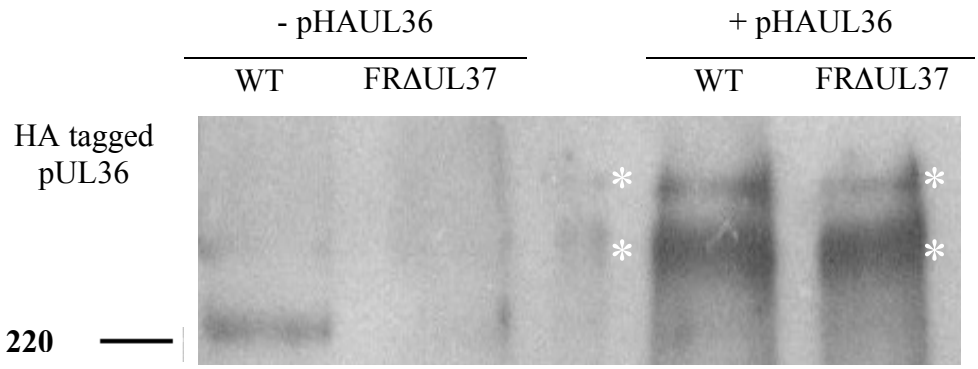

Figure 3.9: Expression of HA tagged pUL36 from pHAUL36

Untransfected RS cells (-pHAUL36) or cells transfected with pHAUL36 (+pHAUL36) were superinfected with 5 pfu/cell of either WT HSV-1 or FRΔUL37. After incubation at 37˚C for 24 h, the cells were harvested and the proteins were separated on a 10% polyacrylamide gel and transferred to nitrocellulose membrane. Expression of HA tagged pUL36 was detected by western blotting using HA-7 antibody directed against the HA epitope. pUL36 related bands are indicated (*).

3.1.3.1. pGX336GFP:

Briefly, the GFP ORF from GFPemd (Packard) was flanked with SpeI sites by PCR as described previously (Roberts *et al.*, 2009). This was cloned into the unique SpeI site that is present two codons upstream of the UL37 termination codon in pGX336 to generate an in frame fusion between the UL37 and GFP ORFs as shown schematically in Figure 3.10.

3.1.3.2. pApV-UL373:

Because the cell lines generated with pGX336GFP contain extensive HSV-1 sequences flanking the UL37 ORF, recombination between the virus and cell can rescue the deletion in FRΔUL37. Therefore, alternative complementing cell lines were produced that contained minimal flanking sequences. To do this, the BamHI fragment from pUL373 that contains the UL37 ORF (McLauchlan, 1997) was cloned into the BamHI site of pApV as shown schematically in Figure 3.11 (Roberts *et al.*, 2009).

3.1.4. Construction of UL36 and UL37 dual expression vectors pETNhe6 and pUCNhe4

To support the replication of a UL36-UL37 double deletion mutant, a cell line expressing both UL36 and UL37 was required. The easiest method to create such a cell line was to use a DNA fragment spanning both UL36 and UL37. Such a fragment can be generated from cosmid 14 by NheI digestion, which releases a ~16.6 Kbp fragment spanning residues 68662 to 85304 and containing all of genes UL33 to UL37 and the N terminal portion of UL38 (McGeoch *et al.*, 1988). The construction of pETNhe6 and pUCNhe4 is shown schematically in Figure 3.12. The NheI fragment was isolated from a preparative gel (Fig. 3.13 (A)) and ligated into XbaI digested and dephosphorylated pET28a(+) vector (XbaI and NheI produce complementary 5' overhangs). The ligated DNA was transformed into DH5α cells and DNA from individual colonies was analysed by EcoRI digestion (Fig. 3.13 (B)). Two clones, designated pETNhe1 and pETNhe6, were identified (one from each orientation of the insert; inverse and genomic orientation respectively) and grown up for further use. The purified NheI fragment from cosmid 14 was also ligated into XbaI digested pUC19 to produce pUCNhe4 and pUCNhe5 (Fig. 3.13 (C)).

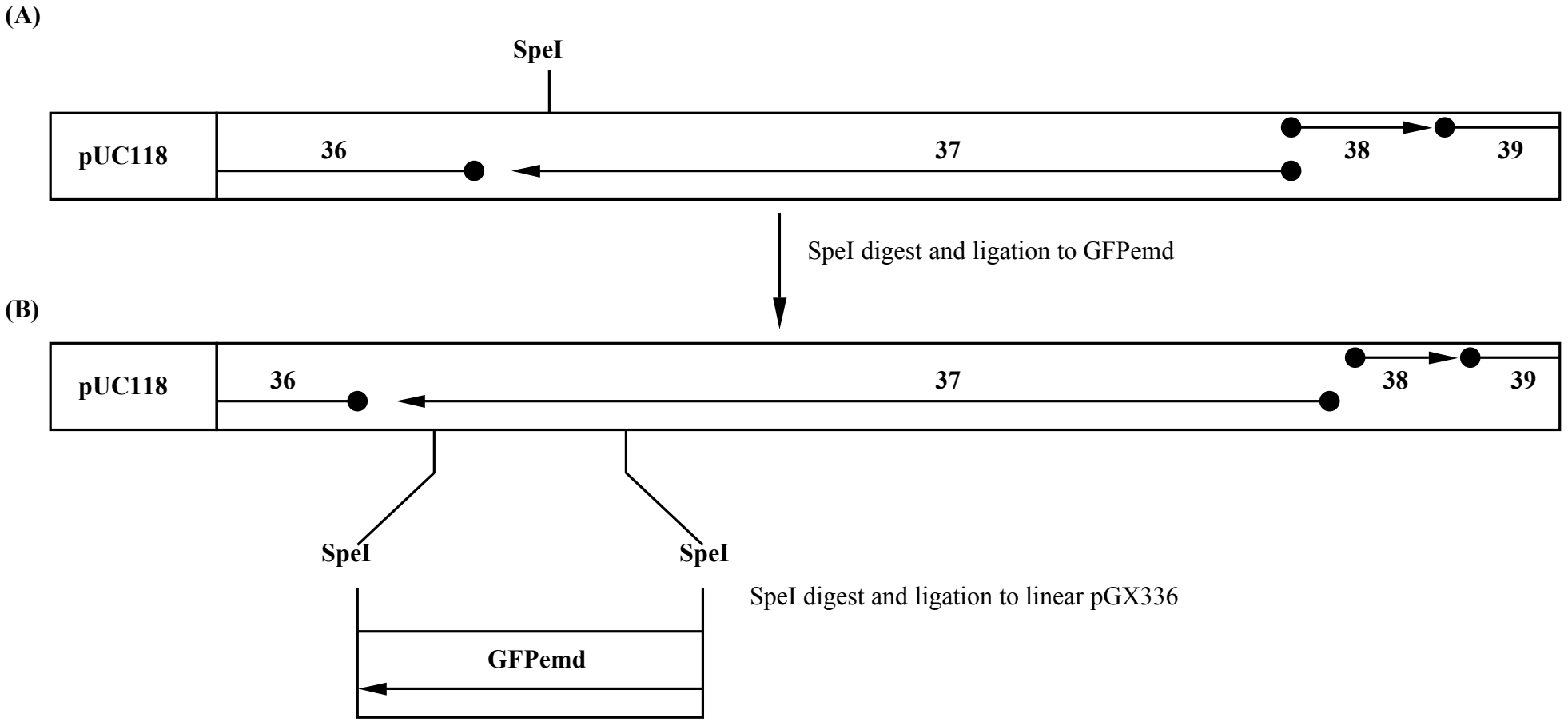
(A)
SpeI
pUC118
36
37
38
39
SpeI digest and ligation to GFPemd
(B)
pUC118
36
37
38
39
SpeI
SpeI
SpeI digest and ligation to linear pGX336
GFPemd

Figure 3.10: Schematic representation of the cloning strategy used to produce pGX336GFP.

(A) A schematic representation of pGX336, which contains the BamHI H fragment cloned into pUC118. BamHI H contains ORFs UL37 and UL38 and parts of UL36 and UL39. The location of the unique SpeI site present at the 3' end of the UL37 ORF is indicated. This SpeI site is 3 codons upstream of the UL37 stop codon.

(B) A schematic representation of pGX336GFP showing the GFPemd ORF sequences inserted into the SpeI site to yield pUL37 with GFP fused to its C terminus.

In both panels, ORFs are marked by arrows, the start position of each indicated with a filled circle and arrowheads indicating the orientation of the reading frame. Constructs are not shown to scale

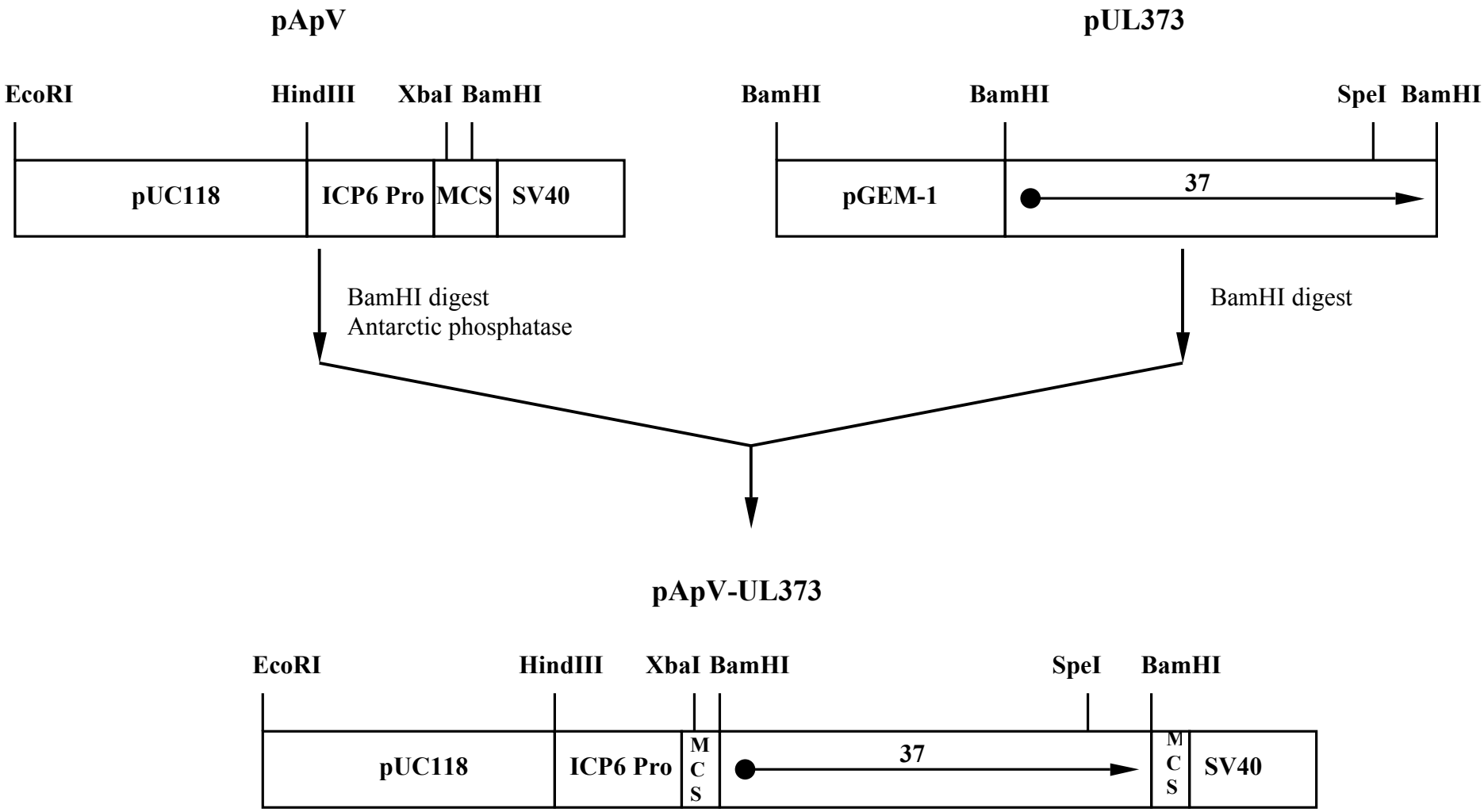
pApV
EcoRI
HindIII
XbaI
BamHI
pUC118
ICP6 Pro
MCS
SV40
pUL373
BamHI
BamHI
SpeI
BamHI
pGEM-1
37
BamHI digest
Antarctic phosphatase
BamHI digest
pApV-UL373
EcoRI
HindIII
XbaI
BamHI
SpeI
BamHI
pUC118
ICP6 Pro
M
C
S
37
M
C
S
SV40

Figure 3.11: Schematic representation of the cloning strategy used to produce pApV-UL373.

The structures of pApV (Fig. 3.1) and pUL373 (McLauchlan, 1997) are shown with the locations of relevant restriction enzyme sites marked (not to scale). The UL37 ORF was released from pUL373 as a BamHI fragment and ligated with BamHI digested pApV to generate pApV-UL373.

Constructs are not shown to scale

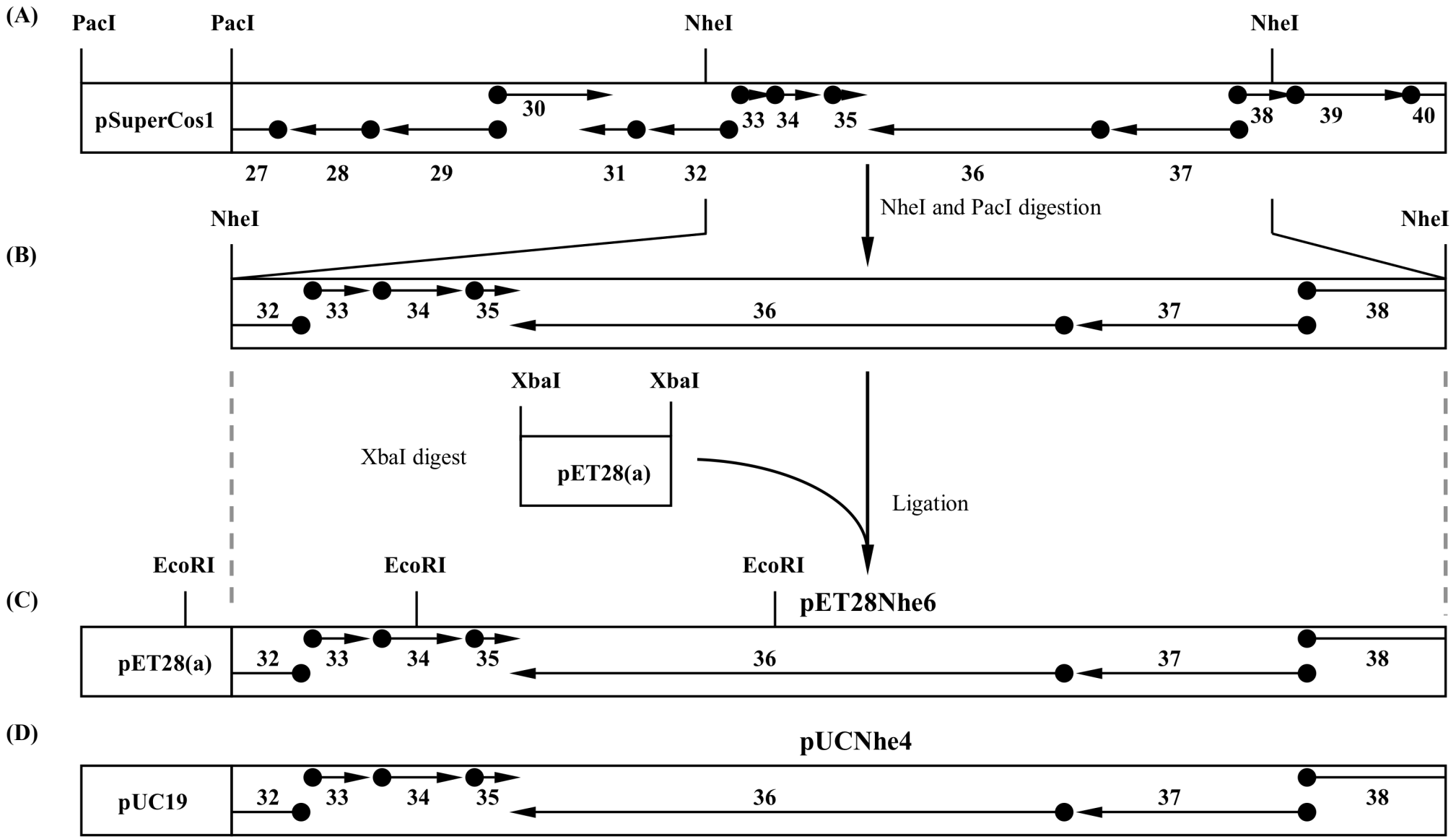
(A)
PacI
PacI
NheI
NheI
pSuperCos1
30
33
34
35
38
39
40
27
28
29
31
32
36
37
NheI and PacI digestion
(B)
NheI
NheI
32
33
34
35
36
37
38
XbaI
XbaI
XbaI digest
pET28(a)
Ligation
EcoRI
EcoRI
EcoRI
(C)
pET28Nhe6
pET28(a)
32
33
34
35
36
37
38
(D)
pUCNhe4
pUC19
32
33
34
35
36
37
38

Figure 3.12: Schematic representation of the cloning strategy used to produce pET28Nhe6 and pUCNhe4.
(A) A schematic representation of Cosmid 14 as shown previously in Figure 3.4 in which the NheI fragment spanning ORFs UL32 to UL38 is indicated.
(B) An expanded representation of the 16,642bp NheI fragment isolated from Cosmid 14, which contains ORFs UL33 to UL37 and parts of ORF UL32 and UL38. pET28(a) was linearised by digestion with XbaI and ligated to the purified NheI fragment. Ligation of the NheI and XbaI compatible ends destroys both the NheI and XbaI restriction sites.
(C) A schematic representation of pET28Nhe6.
(D) A schematic representation of pUCNhe4. The NheI fragment shown in (B) was ligated to XbaI digested pUC19 as described for pETNhe6.

In all panels ORFs are marked by arrows, the start position of each indicated with a filled circle and arrowheads indicating the orientation of the reading frame. Constructs are not shown to scale

(A)

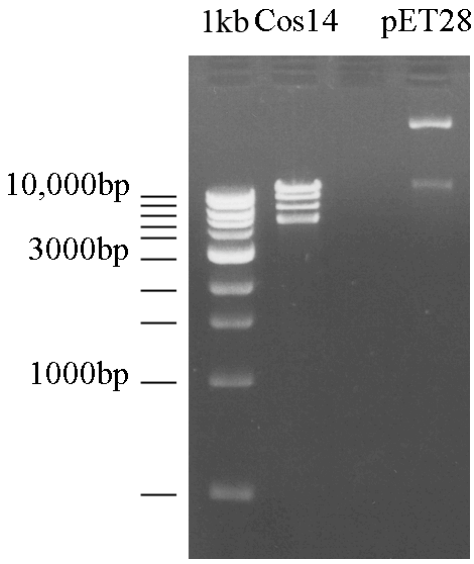
1kb Cos14 pET28
10,000bp
3000bp
1000bp

(B)

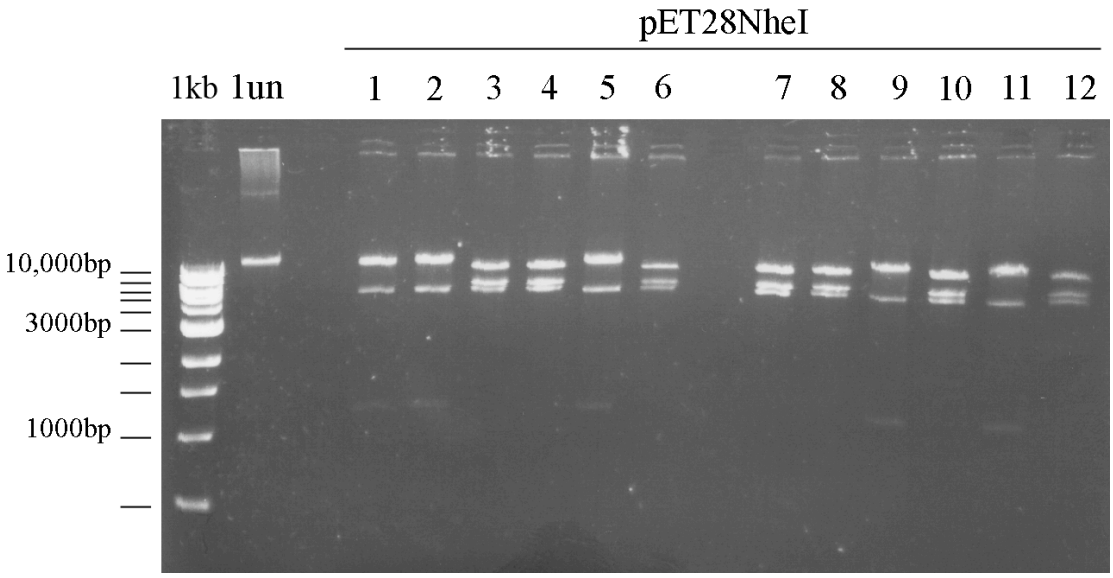
pET28NheI
1kb 1un 1 2 3 4 5 6 7 8 9 10 11 12
10,000bp
3000bp
1000bp

(C)

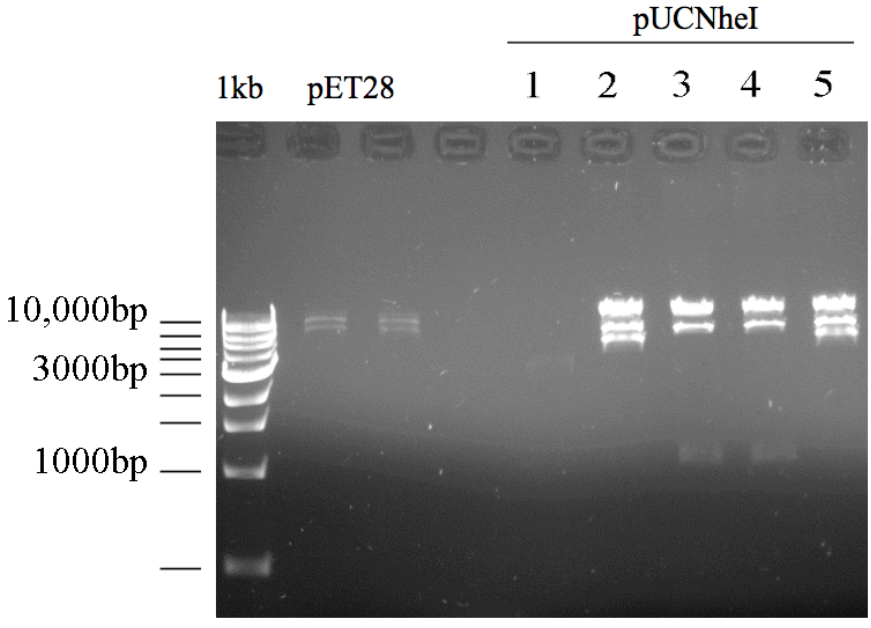
pUCNheI
1kb pET28 1 2 3 4 5
10,000bp
3000bp
1000bp

Figure 3.13: Construction of pET28Nhe6 and pUCNhe4.

(A) Isolation of the NheI fragment spanning UL33-UL37. This fragment was derived from cosmid 14 DNA (Fig. 3.12) after co-digestion with PacI and NheI. The required fragment is a band of ~16.6 Kbp and is the slowest migrating species present (lane Cos14). Undigested pET28 is shown in lane pET28.

(B) Analytical digests of putative pET28NheI clones. The NheI fragment from (A) was ligated into XbaI linearised pET28. Lanes 1-12 contain putative pET28NheI clone DNAs, digested with EcoRI. EcoRI cuts twice within the insert and once within the vector and provides a guide to the orientation of the fragment within the plasmid. Clones 1,2,5,9 and 11 are in the same orientation whilst clones 3,4,6,7,8,10 and 12 are in the opposite orientation. Lane 1un contains undigested DNA from the same clone as lane 1.

(C) Analytical digests of putative pUCNheI clones. The NheI fragment from (A) was ligated into XbaI linearised pUC19. Lanes 1-5 contain putative pUCNheI clone DNAs, digested with EcoRI. EcoRI cuts twice within the insert and once within the vector and provides a guide to the orientation of the fragment within the plasmid. Clones 2 and 5 are in the same orientation whilst clones 3 and 4 are in the opposite orientation.

In all cases 1kb denotes the 1Kbp DNA ladder (NEB).

3.2. Production of expressing cell lines

3.2.1. Isolation of UL36 cell line

To produce a cell line capable of supporting the replication of UL36 deletion mutants, pHAUL36 (section 3.1.2) was co-transfected with pSV2Neo (Clontech) into RS cells by Calcium phosphate precipitation as described in section 2.2.4.2. RS cells were chosen for their ability to support HSV-1 replication and their resistance to senescence in culture such that any derived line is available over multiple passages. 24 h after transfection, cells were passaged and plated at low density in 24 well plates and 35mm dishes. After overnight incubation at 37°C, the medium was removed and replaced with complete growth medium supplemented with G418 at 1mg/ml. G418 is toxic to both prokaryotic and eukaryotic cells, and acts by inhibiting protein synthesis. As such G418 can be used to select for cells transfected with DNA which incorporates a G418 resistance marker such as in pSV2Neo. Under G418 selection, cells not harbouring an integrated copy of pSV2Neo were killed. The medium containing G418 was changed every three days until the sensitive cells were lost and colony outgrowth from individual resistant cells was observed. When they had reached sufficient size, resistant colonies were harvested and subcultured into fresh 24 well plates. Colonies that grew well were expanded to large flasks and at the same time were tested for their ability to support the replication of KΔUL36 (Desai, 2000). 35mm dishes of each clone were set up and infected at a low MOI with KΔUL36 (section 2.1.7). Cells were incubated at 37°C and monitored for the formation of plaques. Resistant clones that were capable of supporting the replication of KΔUL36 were stored away as cell stocks. One clone was selected on the basis of good growth characteristics and ability to support efficient KΔUL36 growth and was designated HAUL36(1)1. Western blotting using the anti-pUL36 antibody (#E12-E3) confirmed that HAUL36(1)1 expressed pUL36 following infection with HSV-1 (ARΔUL36ΔUL37) (Fig. 3.14 lane HA). HAUL36(1)1 was used for isolating the UL36 deletion mutant ARΔUL36 and for maintaining ARΔUL36 and KΔUL36 (see section 3.3.1).

3.2.2. Isolation of UL37 cell lines

The cell line 1.40(2), which expresses a GFP tagged form of pUL37 under control of its own promoter, was isolated prior to this work and was produced by co-transfection of pGX336GFP (section 2.1.10) and pSV2Neo into RS cells as described for formation of UL36 complementing cells (section 3.2.1). Colonies of cells resistant to G418 were

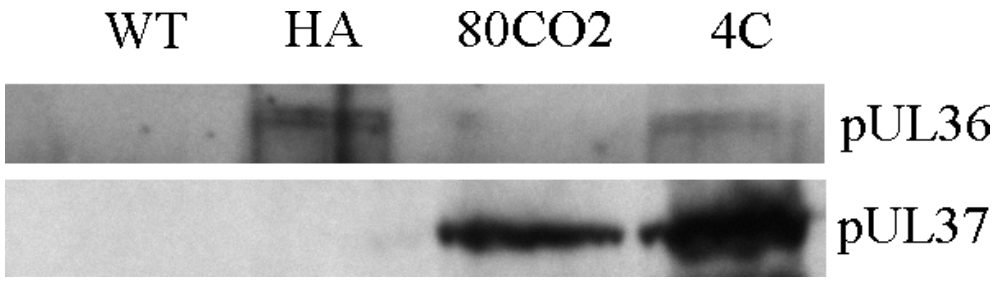

Figure 3.14: Expression of pUL36 and pUL37 by complementing cell lines.
Complementing cell lines constructed by co-transfection of RS cells with pHAUL36 and pSV2Neo (HAUL36 (HA)), or pApV-UL373 and pCI-Neo (80CO2) or with pHAUL36, pApV-UL373 and pCI Neo (4C) were examined for expression of the transgene constructs. Cells were superinfected with 5 pfu/cell of ARΔUL36ΔUL37. After incubation at 37^{o}C for 24 h, the cells were harvested and the proteins were separated on a 10% polyacrylamide gel and transferred to nitrocellulose membrane for western blotting. Expression of pUL36 was detected using #E12-E3 antibody (upper panel) and expression of pUL37 using M780 antibody (lower panel). In both panels untransformed RS cells (WT) are included as a non-complementing cell line.

screened for the stable integration of the pUL37 expression vector pGX336GFP. As no ΔUL37 mutant was available for screening an alternative strategy was pursued. G418 resistant clones were co-transfected with HSV-1 17+ virion DNA and pFRΔUL37, a clone of pGX336 in which UL37 is deleted and replaced with RFP (sections 2.1.10 and 3.3.3). Red fluorescent plaques were isolated and subjected to repeated cycles of infection on G418 resistant clones, and RS cells, selecting for red fluorescence and inability to propagate on parental RS cells. One G418 resistant clone capable of complementing such red fluorescing plaques (section 3.3.3) was selected and designated 1.40(2) as previously described (Roberts *et al.*, 2009).

pGX336GFP contains extensive HSV-1 sequences which increases the potential for reversion by recombination between the virus and cellular sequences. To avoid this, another cell line was generated using the more limited UL37 ORF sequences present in pApV-UL373 (section 3.1.3.2). RS cells were transfected with pApV-UL373 and pCI-Neo by Calcium phosphate precipitation and were treated essentially as described previously (section 3.2.1). In this case G418 resistant cells were screened for their ability to complement the defect in FRΔUL37. One clone was isolated and designated 80CO2. This cell line was used for all further work involving FRΔUL37. Expression of pUL37 was verified by western blot following infection with ARΔUL36ΔUL37 (Fig. 3.14 lane 80CO2)

3.2.3. Isolation of UL36-UL37 dual expressing cell lines

To produce a cell line capable of supporting the replication of a deletion mutant lacking both UL36 and UL37, pET28Nhe6 (section 3.1.4) was co-transfected with pSV2Neo into RS cells by Calcium phosphate precipitation. The transfected cells were passaged at low density and selected for growth in medium containing G418 as described above. Resistant colonies were tested for their ability to support the replication of KΔUL36 and FRΔUL37 (section 2.1.7 and section 3.3.3). One was selected for further use, expanded and stocks laid down. This line was designated RSC14 and was used initially to make the UL36 and UL37 deleted virus (ARΔUL36ΔUL37) (section 3.3.2). However, when ARΔUL36ΔUL37 was passaged in RSC14 cells a high rate of reversion was seen.

To produce a cell line in which recombination leading to reversion would be unlikely, the constructs pHAUL36 and pApV-UL373 were co-transfected with pCI-Neo (Promega) into RS cells as outlined above. As before colonies were selected based on G418 resistance and complementation of the deletions in both KΔUL36 and FRΔUL37. One line was selected

for further work and designated 4C. These cells lack the extensive flanking sequences which promoted recombination in RSC14 cells. In 4C cells both the UL36 and UL37 ORFs are under the control of the ICP6 promoter and activated only under conditions of viral infection. Expression of pUL36 and pUL37 was verified by western blot following infection with ARΔUL36ΔUL37 (Fig. 3.14 lane 4C)

3.3. Production of HSV-1 deletion mutants

3.3.1. Generation of an HSV-1, UL36 minus mutant

The existing UL36 deletion mutant, KΔUL36, was produced by restriction enzyme digestion and religation of a plasmid containing the UL36 ORF followed by marker transfer of the resulting deletion into HSV-1 virus DNA. This generated a mutant with an internal deletion of 3,600bp in UL36 (amino acids 362-1555), but left 1083bp of sequence (3' of the deletion) corresponding to amino acids 1-361 and 4809bp of sequence (5' of the deletion) corresponding to amino acids 1556-3164 intact. As a result the N terminal 361 codons of UL36 were fused to a further 42 codons arising from the frameshift caused by the deletion (Desai, 2000). Consequently this existing mutant is possibly best viewed as a truncation rather than a deletion of pUL36.

Because KΔUL36 contained only a partial deletion of the UL36 ORF, a second, complete deletion mutant was made using the HSV-1 bacterial artificial chromosome (BAC) pBAC SR27 (supplied by C. Cunningham). In pBAC SR27, loxP recombination sites flank the bacterial maintenance sequences and a Cre recombinase gene, which are inserted between genes US1 and US2. The Cre recombinase is expressed only in mammalian cells and results in the loss of the bacterial sequences, leaving a single loxP site between US1 and US2 (Smith & Enquist, 2000). The UL36 ORF was removed from pBAC SR27 using a variation on the λRED/ET recombination system (Genebridges, GmbH). In this system, all recombination steps are carried out in the host bacteria carrying the DNA of interest. Initially, a cassette consisting of a kanamycin resistance gene and a streptomycin sensitivity gene flanked by HSV-1 sequences is introduced into a defined location on the target DNA by homologous recombination, and colonies are selected for their ability to grow on agar medium containing kanamycin. The marker can then be excised by a second round of homologous recombination followed by counter selection on agar medium containing streptomycin. However, when this procedure was attempted with pBAC SR27, the counter selection step consistently produced large, non-specific deletions. Fortunately,

the presence of the Cre recombinase gene in pBAC SR27 provided an alternative method to excise the kanamycin resistance cassette by Cre/lox recombination. In order to avoid recombination with the existing loxP sites in pBAC SR27 variant sites were used. The variant site chosen was loxFAS, which has been shown to have a low level of heterologous recombination with the archetypal loxP WT (Siegel *et al.*, 2001). Therefore, PCR was carried out on the rpsL-neo template supplied with the λRED/ET kit, using primers UL36rm_loxFAS_F and UL36rm_loxFAS_R.

UL36rm_loxFAS_F
5'-TTGCGTTTAATGTCGTGTTTATTCAAGGGAGTGGGATAGG*ATAACTTCG*
*TATATACCTTTCTATACGAAGTTAT***GGCCTGGTGATGATGGCGGGATCG**

UL36rm_loxFAS_R
5'-GACAGACAAACGCAGCTCGGTTTTTGGGAAGCGATCACC*ATAACTTCGTATA*
*GAAAGGTATATACGAAGTTAT***TCAGAAGAACTCGTCAAGAAGGCG**

HSV-1 sequences are underlined, rpsL-neo sequences are in bold and the LoxFAS sequences are in italics.

The resulting PCR product contains the neomycin cassette flanked by nested FAS sites and HSV-1 sequences from upstream and downstream of the UL36 ORF. Insertion of this cassette into pBAC SR27 deletes the entire UL36 ORF between residues 71006-80589.
The PCR product was purified on agarose gels and stored at –20^{o}C until needed.

To begin the λRED mutagenesis procedure, Genehog bacteria (Invitrogen) were transformed with pBAC SR27 DNA and selected for chloramphenicol resistance. Genehog bacteria were used as a host strain for pBAC SR27 due to the efficiency with which they can be transformed with large DNA constructs. A single colony was isolated and used to form a glycerol stock. This clone was grown and rendered electrocompetent by the method recommended by Genebridges (GmbH) (section 2.2.3.6), transformed with pSC101-BAD-gba^{tet} and selected for resistance to both chloramphenicol and tetracycline. pSC101-BAD-gba^{tet} is a thermo-sensitive plasmid that contains the RED/ET recombination proteins under the control of an arabinose inducible promoter P_{BAD} (Guzman *et al.*, 1995).

To perform λRED mutagenesis, genehogs hosting both pBAC SR27 and pSC101-BAD-gba^{tet} were grown to stationary phase overnight at 30°C. They were then subcultured into

1.5 ml of fresh LB supplemented with chloramphenicol (15μg/ml) and tetracycline (2μg/ml) and grown to an $O.D_{600}$ of ~0.3. The cultures were then split into two groups, one of which was induced to express the RED/ET recombination proteins by addition of l-arabinose and both the induced and uninduced cultures were shifted to 37°C for 1 h. The cells were then made electrocompetent and transformed with the PCR amplified selection cassette described above. After growth at 37°C for 70 min to allow recombination to occur, aliquots of both induced and uninduced cultures were plated onto LB agar containing chloramphenicol and kanamycin, and grown at 37°C overnight, which causes the thermo-sensitive plasmid pSC101-BAD-gba^{tet} to be lost.

Comparison of the plates from the induced and uninduced cultures showed the expected ~100:1 ratio in colony numbers, and 6 colonies from the induced sample were grown as 5 ml cultures in LB containing chloramphenicol and kanamycin. To confirm that the rpsl/neo cassette had replaced the UL36 ORF, the BAC DNA was isolated and analytical PCR was performed using primers sited outside of the deleted region (Fig. 3.15 (A)). All six clones gave PCR products of the size expected for the rpsl/neo cassette.

DNA was prepared from the six BAC clones and transfected into complementing, HAUL36-1, cells (section 3.2.1) using lipofectamine 2000. Cell monolayers were monitored for signs of plaque formation. Only two of the six BAC clones were found to be infectious and these were harvested when the cell monolayers showed extensive cpe. The two virus stocks were then titrated on HAUL36-1 and non-complementing, RS, cells to assess their growth phenotypes. Both virus stocks failed to propagate on parental RS cells with viral propagation and plaque formation limited to HAUL36-1 cells. Individual plaques were picked from HAUL36-1 cell monolayers and subjected to two cycles of repeated titration and plaque purification on HAUL36-1 cells. All plaques were also titrated on RS cells to screen for the presence of revertant or wild type virus (section 2.2.5.4). One isolate was selected for further work, designated ARΔUL36, a virus stock was expanded and stored at –70^{o}C.

3.3.2. Generation of an HSV-1, UL36-UL37 minus mutant

Creation and isolation of a double null mutant was by the same method as described for the ΔUL36 mutant, ARΔUL36. However, the mutagenesis cassette used to produce the UL36 and UL37 double null mutant was generated from the rpsL-neo template by PCR using the UL36rm_loxFAS_F primer (section 3.3.1) and a second primer, UL37rm_loxFAS_R,

(A)

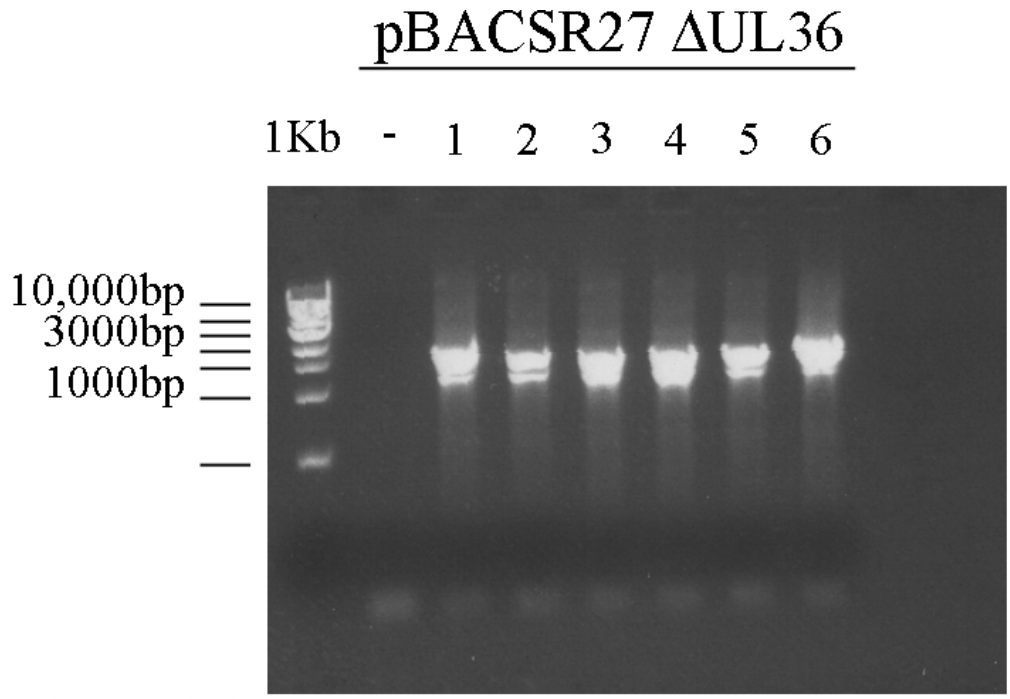
pBACSR27 ΔUL36
1Kb - 1 2 3 4 5 6
10,000bp
3000bp
1000bp

(B)

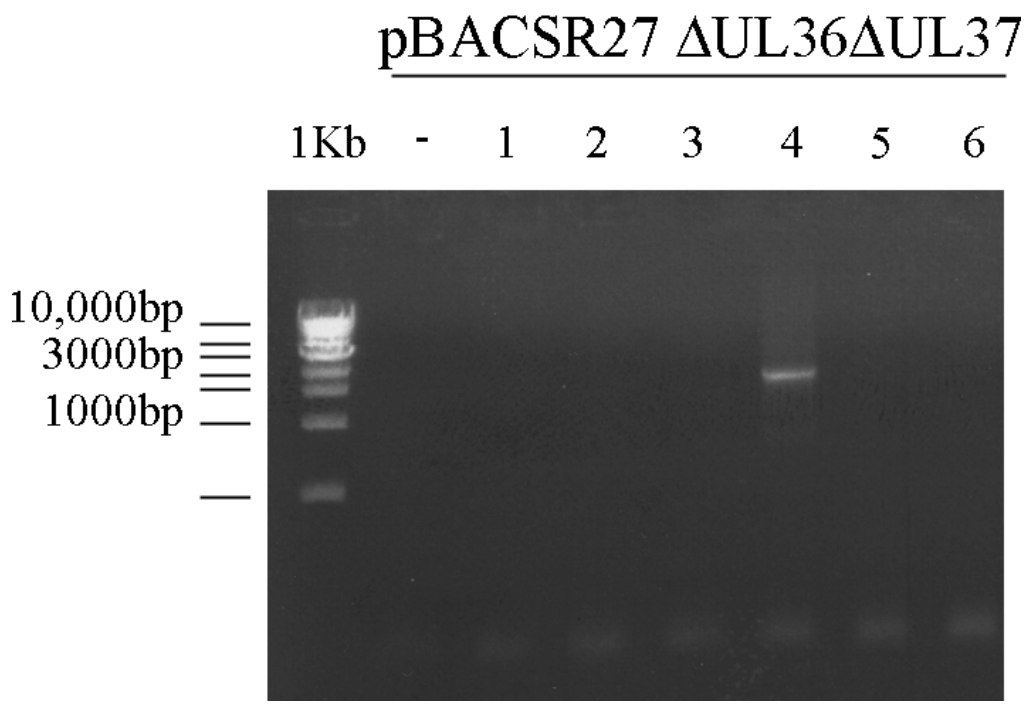
pBACSR27 ΔUL36ΔUL37
1Kb - 1 2 3 4 5 6
10,000bp
3000bp
1000bp

Figure 3.15: Analytical PCR for the λRED kan^R selection cassette insertion into UL36 or UL36 and UL37.

(A) Individual pBACSR27 ΔUL36 clones were subject to PCR amplification using primers seqUL36 F and R (Table 2.1), which flank the UL36 locus. The ~1.6 Kbp product demonstrates that in all 6 clones examined the UL36 ORF (~9.5Kbp) has been replaced with the λRED selection cassette.

(B) Individual pBACSR27 ΔUL36ΔUL37 clones were subject to PCR amplification using primers seqUL36 F and seqUL37 R (Table 2.1), which flank the UL36-UL37 loci. The ~1.6 Kbp product in lane 4 demonstrates that the λRED mediated recombination has been successful in only this one instance.

In all cases 1Kb refers to a 1Kbp ladder (NEB) and – is a negative control lacking template DNA.

which contained HSV-1 sequences from upstream of the UL37 ORF. This results in the deletion of both UL36 and UL37 between residues 71006-84226.

UL37rm_loxFAS_R

5'-ATGCCGGGACTTAAGTGGCCGTATAACACCCCGCGAAGAC*ATAACTTCGTAT AGAAAGGTATATACGAAGTTAT***TCAGAAGAACTCGTCAAGAAGGCG**

HSV-1 sequences are underlined, rpsL-neo sequences are in bold and the LoxFAS sequences are in italics.

Although six colonies were analysed, only one (clone 4) gave the correct profiles following analytical PCR and BamHI digestion. Initially this mutant (clone 4 Fig. 3.15 (B)) was propagated on RSC14 cells (section 3.2.3) but under large scale culture it showed a high level of reversion as determined by titration on non-complementing, RS, cells. Given the nature of the pET28NheI DNA construct, which contained extensive HSV-1 sequences flanking the UL36 and UL37 ORFs used to generate the RSC14 cell line, reversion to wild type is unsurprising. Furthermore, because rescuant viruses are likely to retain some growth advantage over the deletion mutant, even when propagated in complementing cells, their accumulation during virus propagation is also not surprising.

To rectify this situation the 4C cell line was isolated as described previously (section 3.2.3). In this cell line the DNA constructs pHAUL36 and pApV-UL373 used to produce HAUL36 and 80CO2 cells respectively, were used (sections 3.2.1 and 3.2.2). In both pHAUL36 and pApV-UL373, there is no overlap between the HSV-1 ORF sequences introduced into the cells and sequences retained in the virus deletion mutant. As a consequence, homologous recombination between the mutant viral genome and the integrated constructs within the complementing cells cannot occur, thereby preventing rescue. pBAC SR27 deleted for both UL36 and UL37, pBAC SR27 Δ36Δ37(4), was transfected into 4C cells and the resultant virus, designated ARΔUL36ΔUL37, was isolated as described for ARΔUL36. At all times virus harvests were screened on parental RS cells HAUL36, 80CO2 and 4C cells to establish the phenotype of the mutant. (section 2.2.5.4) After preparation of a high titre stock, the virus was again titrated on the same spectrum of cells. However, with the combination of ARΔUL36ΔUL37 and the 4C cell line, there was no evidence for the reversion seen previously with RSC14 cells.

3.3.3. Production of an HSV-1, UL37 minus mutant

Modification of the HSV-1 genome to remove the UL37 ORF was performed prior to this work using the method described in Roberts *et al*. (2009). Briefly, the UL37 ORF was deleted from pGX336 by digestion with HpaI and ClaI, which removes all but the 3 final C terminal amino acids. The ClaI site was rendered blunt ended by treatment with T4 DNA polymerase and the linear vector self-ligated forming pGX336-37minus. pGX336-37minus was subsequently modified by insertion of RFP as an XbaI/NheI fragment isolated from pDsRed-monomer-N1 (Clontech) into the unique SpeI site present in the residual UL37 sequences (Fig. 3.16). The resulting plasmid, pFRΔUL37, contains the RFP ORF under control of the UL37 promoter. pFRΔUL37 and wild type HSV-1 strain 17+ virion DNA were co-transfected into 1.40(2) cells and red fluorescent plaques were selected. Individual isolates were screened for the differential ability to grow on 1.40(2) cells and not on non-complementing cells. One isolate, designated FRΔUL37, was selected for further use and was amplified to large-scale.

3.4. Isolation of revertants of ARΔUL36, FRΔUL37 and ARΔUL36ΔUL37

To ensure that the behaviour of the HSV-1 deletion mutants was not affected by the presence of deleterious second site mutations within the viral genomes, revertants of ARΔUL36, FRΔUL37 and ARΔUL36ΔUL37 were isolated. RS cells were transfected using lipofectamine 2000 with pUCNhe4 (section 3.1.4) and superinfected with 1pfu/cell of each mutant. pUCNhe4 contains the NheI fragment (68662-85304) which includes UL36 and UL37 and has extensive flanking sequences to permit recombination. Each virus isolate was subjected to two cycles of plaque picking on non-complementing RS cells to ensure homogeneity. One plaque isolate, from each original mutant, capable of growth on parental RS cells was selected and used to generate large-scale stocks. The revertant viruses were designated ARΔUL36R, FRΔUL37R and ARΔUL36ΔUL37R respectively.

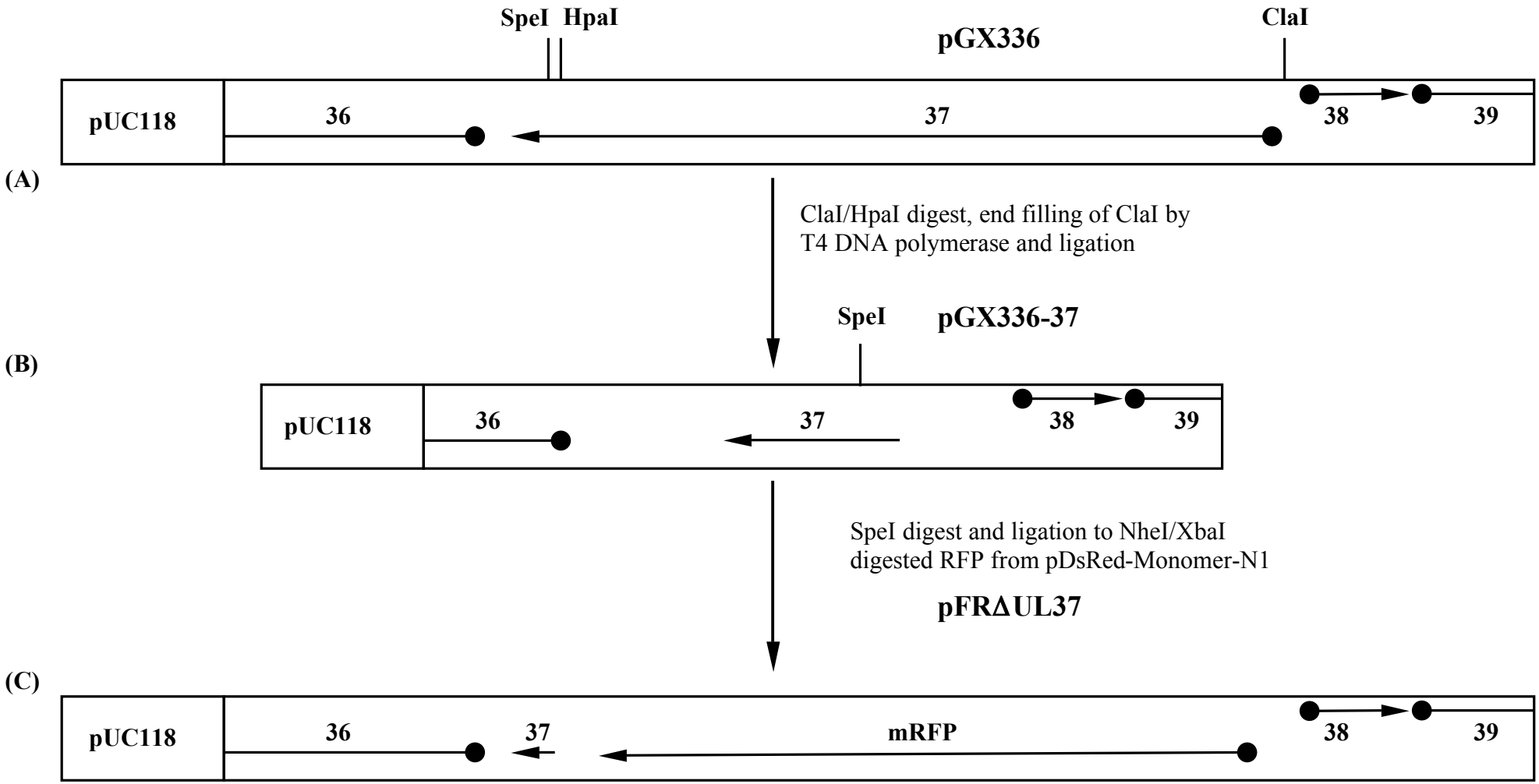
SpeI
HpaI
pGX336
ClaI
pUC118
36
37
38
39
(A)
ClaI/HpaI digest, end filling of ClaI by
T4 DNA polymerase and ligation
SpeI
pGX336-37
(B)
pUC118
36
37
38
39
SpeI digest and ligation to NheI/XbaI
digested RFP from pDsRed-Monomer-N1
pFRΔUL37
(C)
pUC118
36
37
mRFP
38
39

Figure 3.16: Schematic representation of the cloning strategy used to produce pFRΔUL37. (A) A schematic representation of pGX336, which contains the BamHI H fragment cloned into pUC118. BamHI H contains ORFs UL37 and UL38 and parts of UL36 and UL39. The location of the unique SpeI, HpaI and ClaI sites are indicated. The SpeI site is 3 codons upstream of the UL37 stop codon.
(B) A schematic representation of pGX336-37. Digestion of pGX336 with ClaI and HpaI removes the majority of UL37, leaving 3 codons at the C terminal end of the UL37 ORF.
(C) A schematic representation of pFRΔUL37. The mRFP ORF released from pDSRed-Monomer-N1 as an NheI/XbaI fragment was ligated into SpeI digested pGX336-37, placing mRFP under control of the UL37 promoter.

In all panels, ORFs are marked by arrows, the start position of each indicated with a filled circle and arrowheads indicating the orientation of the reading frame. Constructs are not shown to scale

CHAPTER 4

CHARACTERISATION OF THE MUTANTS ARΔUL36, FRΔUL37 AND ARΔUL36ΔUL37

4. Characterisation of the mutants ARΔUL36, FRΔUL37 and ARΔUL36ΔUL37

4.1. Phenotypes of alphaherpesvirus inner tegument mutants

Mutations of the genes UL36 and UL37 in the alphaherpesviruses HSV-1 and PrV have been described previously. Early work in this area was conducted with the temperature sensitive mutant tsB7, which was mapped between 0.46 and 0.52 map units, by complementation with HSV-2 restriction enzyme DNA fragments (Knipe *et al.*, 1981), in a position later shown to contain the UL36 ORF (McGeoch *et al.*, 1988). EM examination of tsB7-infected cells suggested a defect in uncoating of the viral genome at the non-permissive temperature, with DNA containing capsids accumulating at nuclear pores (Batterson *et al.*, 1983).

The first deletion mutant to be described for either UL36 or UL37 was KΔUL36 (Desai, 2000). In KΔUL36 a section corresponding to amino acids 362-1555 (of 3164 residues) was removed from the centre of the UL36 ORF. Studies with KΔUL36 showed that full-length pUL36 was essential for the formation of mature virions, and that in its absence, C capsids were trapped in the cytoplasm and were not enveloped. These cytoplasmic C capsids formed small clusters or aggregates in the cytoplasm. A PrV mutant (PrV-ΔUL36F) has also been made, which has a complete deletion of UL36, and as with HSV-1, was found to have a block on envelopment of cytoplasmic C capsids. However, the cytoplasmic capsids of PrV-ΔUL36F did not aggregate but adopted a more dispersed phenotype (Fuchs *et al.*, 2004). While in another PrV mutant, PRV-GS678, deletion of UL36 was linked to a defect in egress of capsids from the nucleus (Luxton *et al.*, 2006).

The construction of a deletion mutant of UL37 (KΔUL37), lacking amino acids 86-1120 of 1123 residues, showed that this inner tegument protein was also essential for virion formation, with large aggregates of unenveloped C capsids accumulating in the cytoplasm of infected cells (Desai *et al.*, 2001). This study also reported a nuclear egress defect associated with the deletion of UL37, suggesting that C capsids were retained in, or retarded in exit from, the nucleus (Desai *et al.*, 2001). In contrast, UL37 was shown to be non-essential in the PrV mutant, PRV-ΔUL37, although its deletion severely attenuated production of extracellular virions and also resulted in large accumulations of cytoplasmic C capsids (Klupp *et al.*, 2001b). A second PrV UL37 deletion mutant (PRV-GS993) was

reported to have a defect in nuclear egress of capsids leading to low numbers in the cytoplasm. This mutant was also non-lethal but had a severe impact on viral growth (Luxton *et al.*, 2006). It can be seen from this description that the phenotypes of the existing inner tegument mutants are diverse and divergent, agreeing mainly in the respect that deletion of either inner tegument protein gene leads to the accumulation of unenveloped C capsids within the cytoplasm of infected cells, although some mutants exhibited a defect in nuclear egress. Therefore, the work detailed here was carried out to characterise the phenotypes of the independent HSV-1 UL36 and UL37 deletion mutants and of the UL36-UL37 double deletion mutant described in section 3.3.

4.2. Characterisation of viral DNA structure in ARΔUL36 and ARΔUL36ΔUL37

To confirm the mutations in ARΔUL36 and ARΔUL36ΔUL37, viral DNA was isolated from cell-released virus (section 2.2.2.13) and the UL36 and UL36-UL37 loci were amplified by PCR. In addition, as the U_L origin of replication (oriL) has been shown to be unstable in bacteria and the BAC vector maintenance sequences are designed to be removed by Cre/lox recombination in mammalian cells, the status of these two genome regions was also established by PCR amplification (Table 2.1).

λ RED recombination replaces the UL36 ORF between residues 70966 and 80590 with 1320 bp corresponding to the rpslneo kan^R cassette. If the replacement had occurred, PCR of this region using the flanking primers UL36seqF and UL36seqR (positions 70845 and 80766) should give rise to a product of 1657 bp. In pBAC SR27 Δ36(1), the PCR gave a product of ~1.6 Kbp, confirming the replacement of the UL36 ORF with the kan^R selection cassette (Fig. 3.15(A)). Following transfection into HAUL36(1) cells and isolation of ARΔUL36, PCR with UL36seqF and R gave a product of ~500 bp. This demonstrated the removal of the kan^R selection cassette and confirmed that the Cre recombinase encoded within the BAC vector is expressed and functional in mammalian cells (Fig. 4.1 (A)). The Cre recombination should leave only a single lox FAS site in place of the UL36 ORF and this was verified by sequencing of the PCR product (Fig. 4.2 (A)).

Similar analyses were preformed on pBAC SR27 Δ36Δ37(4) and produced similar results. In pBAC SR27 Δ36Δ37(4) both UL36 and UL37 were replaced with the rpslneo kan^R cassette (corresponding to insertion between positions 70966 to 84227). PCR with the

(A)

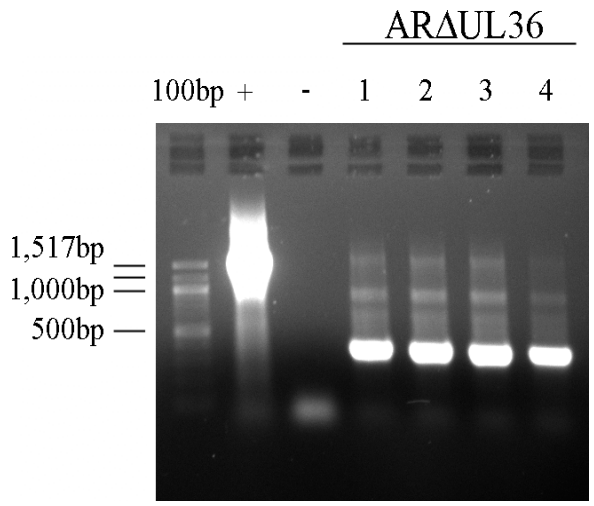
ARΔUL36
100bp + - 1 2 3 4
1,517bp
1,000bp
500bp

(B)

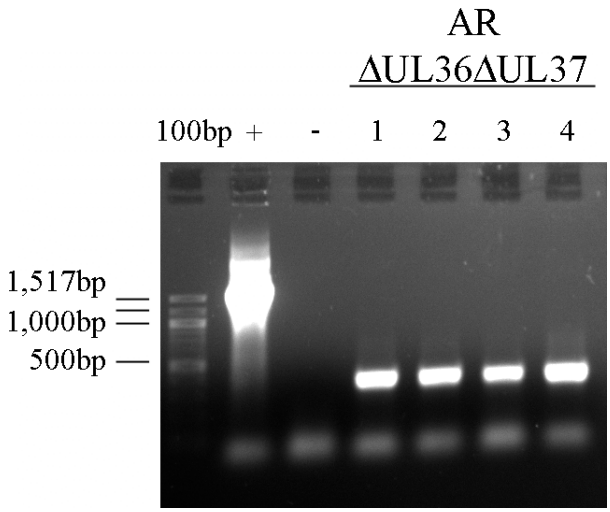
AR
ΔUL36ΔUL37
100bp + - 1 2 3 4
1,517bp
1,000bp
500bp

(C)

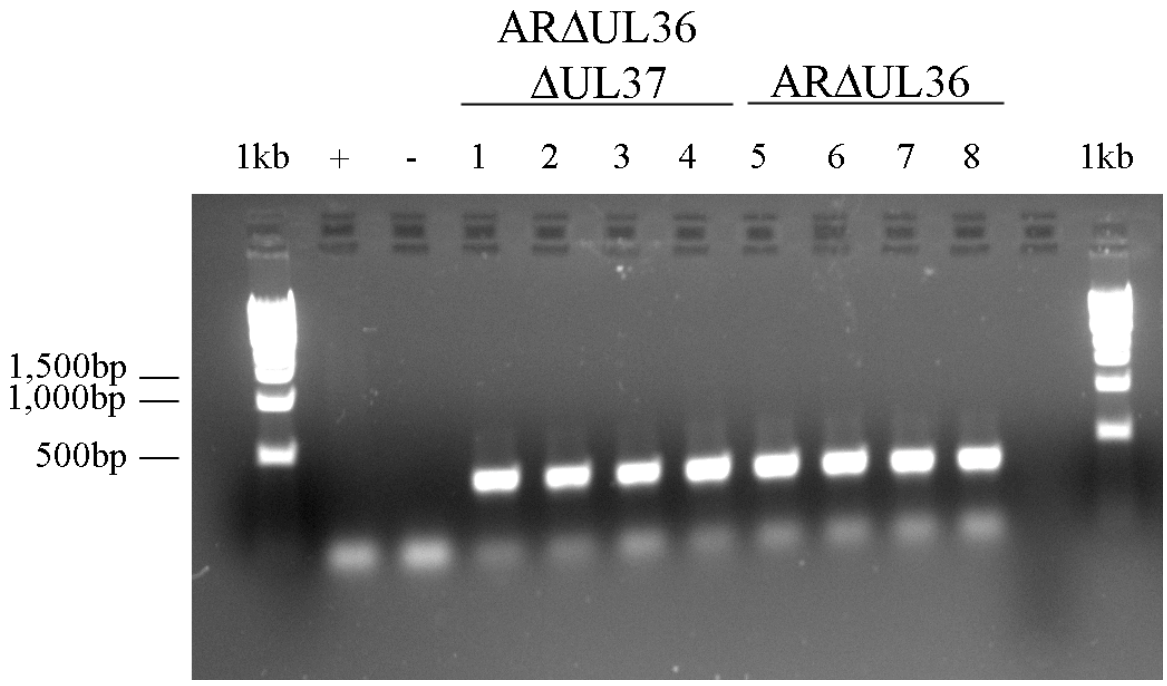
ARΔUL36
ΔUL37
ARΔUL36
1kb + - 1 2 3 4 5 6 7 8 1kb
1,500bp
1,000bp
500bp

Figure 4.1: Analytical PCR on deletion mutant virus DNAs.

(A) PCR to establish the status of the UL36 locus in viral DNA. Virion DNAs from individual plaque isolates of ARΔUL36 were subjected to PCR using primers seqUL36 F and R (Table 2.1), which flank the UL36 locus (lanes 1-4). Lane + contains the product of PCR against pBAC SR27 Δ36(1) (Fig. 3.15), and lane – shows a control PCR carried out in the absence of DNA template. The 1657 bp band in lane + reveals the presence of the kan^R rpsl/neo cassette. The 337 bp bands in lanes 1-4 confirm the Cre mediated excision of the loxFAS flanked kan^R rpsl/neo cassette.

(B) PCR to establish the status of the UL36 and UL37 loci in viral DNA. Virion DNAs from individual plaque isolates of ARΔUL36ΔUL37 were subjected to PCR using primers seqUL36 F and seqUL37 R (Table 2.1), which flank the UL36 and UL37 loci (lanes 1-4) Lane + contains the product of PCR against pBAC SR27 Δ36Δ37(4) (Fig. 3.15), and lane – shows a control PCR carried out in the absence of DNA template The 1654 bp band in lane + reveals the presence of the kan^R rpsl/neo cassette. The 334 bp bands in lanes 1-4 confirm the Cre mediated excision of the loxFAS flanked kan^R rpsl/neo cassette.

(C) PCR to establish the status of the BAC vector sequences in viral DNA. Virion DNAs from individual plaque isolates of both ARΔUL36 and ARΔUL36ΔUL37 was subjected to PCR using primers US1-2 BAC F and R (Table 2.1), which flank the US1 – US2 junction into which the loxP flanked BAC vector was inserted (lanes 1-8). Lane + contains the product of PCR against pBAC SR27, and lane – shows a control PCR carried out in the absence of DNA template. No product band is seen in lane +. In all lanes 1-8 the amplification of a product of ~500 bp indicates the Cre mediated excision of the BAC vector sequences from between US1 and US2.

(A)

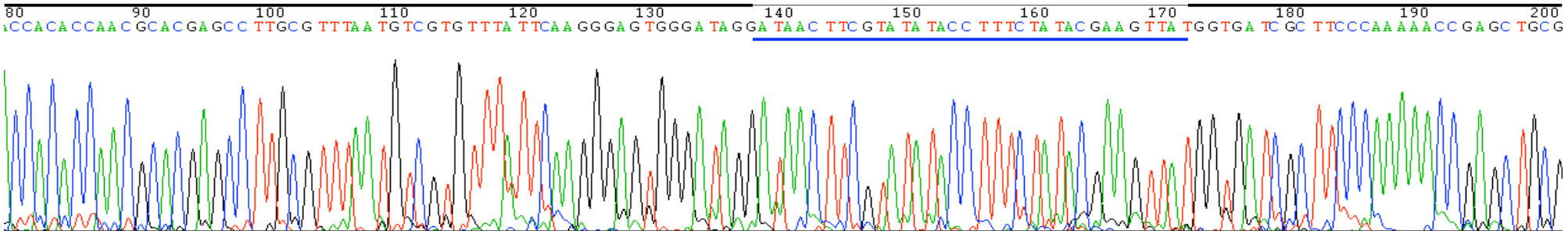
80 90 100 110 120 130 140 150 160 170 180 190 200
ACCACACCAACGCACGAGCCTTGCGTTTAATGTCGTGTTTATTCAAGGGAGTGGGATAGGATAACTTCGTATATACCTTTCTATACGAAGTTATGGTGATCGCTTCCCAAAAACCGAGCTGCG

(B)

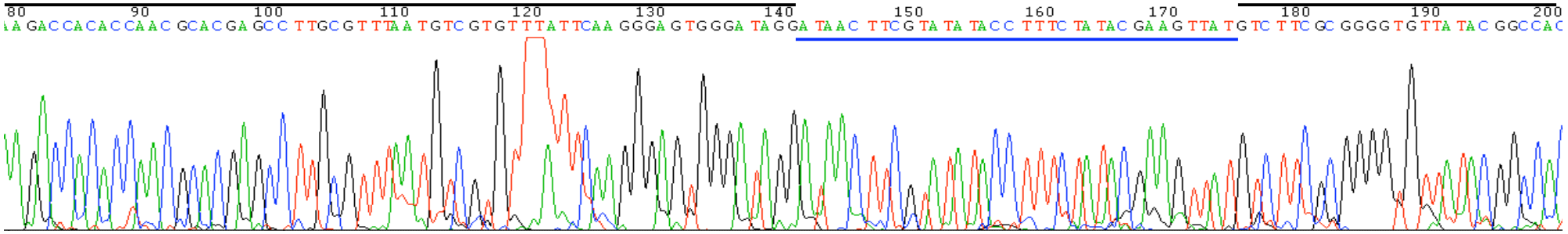
80 90 100 110 120 130 140 150 160 170 180 190 200
AAGACCACACCAACGCACGAGCCTTGCGTTTAATGTCGTGTTTATTCAAGGGAGTGGGATAGGATAACTTCGTATATACCTTTCTATACGAAGTTATGTCTTCGCGGGGGTGTTATACGGCCAC

(C)

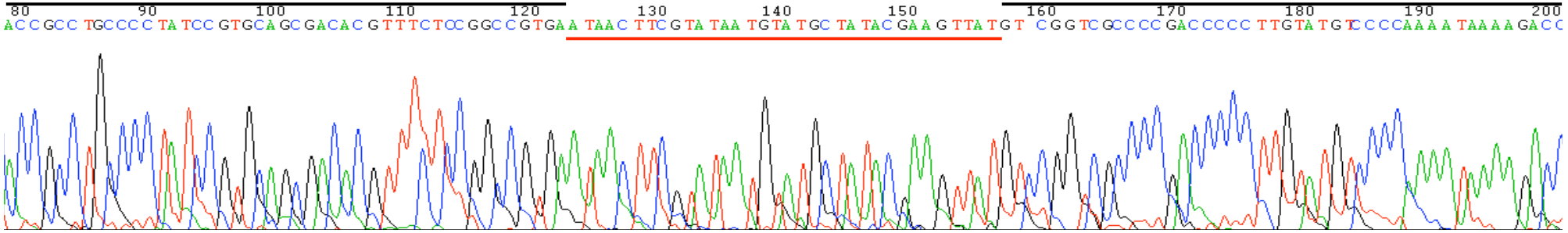
80 90 100 110 120 130 140 150 160 170 180 190 200
ACCGCCTGCCCCTATCCGTGCAGCGACACGTTTCTCCGGCCGTGAATAACTTCGTATAATGTATGCTATACGAAGTTATGTCGGTCGCCCCGACCCCCTTGTATGTCCCCAAAATAAAAGACC

Figure 4.2: Sequencing of the deletion sites in ARΔUL36 and ARΔUL36ΔUL37

The UL36 ORF in ARΔUL36 (A), and a region encompassing the UL36 and UL37 ORFs in ARΔUL36ΔUL37 (B), were replaced by a single loxFAS site following Cre/lox recombination. In both ARΔUL36 and ARΔUL36ΔUL37, the BAC vector maintenance sequences were replaced by a single loxP site (C). The UL36 and UL36-UL37 deletions were confirmed using primers seqUL36 F and seqUL36 R, and seqUL36 F and seqUL37 R respectively (Table 2.1) and the BAC vector sequence deletions, using primers US1-2 BAC F and R (Table 2.1). The lox P and flanking sequences from ARΔUL36 and ARΔUL36ΔUL37 were identical, so only that from ARΔUL36 is shown here.

Black bars above the nucleotide numbers highlight the extent of HSV-1 genomic sequence. Blue bars underneath the sequence in (A) and (B) highlight loxFAS sites, while a red bar underneath the sequence in (C) highlights the loxP site.

flanking primers UL36seqF (used previously) and UL37seqR (position 84399) showed the presence of a product of ~1.6 Kbp similar to that seen for pBAC SR27 Δ36(1) with an expected size of 1653 bp (Fig. 3.15 (B)). Following transfection into complementing cells and isolation of ARΔUL36ΔUL37, PCR with UL36seqF and UL37seqR gave a product of ~500 bp akin to that seen with ARΔUL36 and sequencing confirmed the removal of the kan^R cassette by Cre mediated recombination (Figs. 4.1 (B) and 4.2 (B)).

PCR of the locus containing the vector sequences necessary for maintaining the BAC in the bacterial host with primers US1-2 BAC F and R (Table 2.1), shows that this also was deleted by the activity of the Cre recombinase giving rise to a band of <500 bp rather than the ~13 Kb expected for the parental BAC (Fig. 4.1 (C) and 4.2 (C)). The control reaction in lane + (Fig. 4.1 (C)) should amplify the BAC vector but under the conditions used the time allowed for amplification was too short for product formation. This resulted in the absence of a product band from this lane.

In both ARΔUL36 and ARΔUL36ΔUL37, PCR was also carried out to determine the status of oriL. OriL is a palindromic sequence and is often lost in bacterial culture (Collins, 1981). PCR of the oriL loci, using primers OriLseq_F and R (Table 2.1) of WT HSV-1 viral DNA gave rise to two bands of ~450 bp (full length) or ~300 bp (deleted) (Fig. 4.3), the 300bp variant presumably lacks the pallindromic sequence located between residues 62403 and 62548 of the prototypical genome arrangement (McGeoch *et al.*, 1988). ARΔUL36 and ARΔUL36ΔUL37 viral DNAs produced only a ~300 bp band (Fig. 4.3). Thus, in WT HSV-1 there would appear to be a mixed population of full length and deleted versions of oriL, while in the BAC derived mutants all the oriL loci are of the deleted form.

Virus can be recovered from cells by transfection of cosmids containing overlapping genome fragments (Cunningham & Davison, 1993). In their experiments Cunningham and Davison (1993) showed that when cosmids containing a full oriL were used for this all derived viruses contained a complete oriL. If the cosmids used were heterogeneous for full or deleted oriL this was reflected in the progeny virus, which was likewise heterogeneous for oriL. If oriL was present only in the deleted form in the cosmid set, then virus could still be recovered but it lacked a full oriL sequence. Deletions in oriL have been reported to result in reduced growth in tissue culture (Nagel *et al.*, 2008). However, the viruses derived from pBAC SR27 showed at most only a slight delay in growth kinetics when compared to the WT HSV-1 (section 4.4). The revertants of ARΔUL36 and ARΔUL36ΔUL37, like the

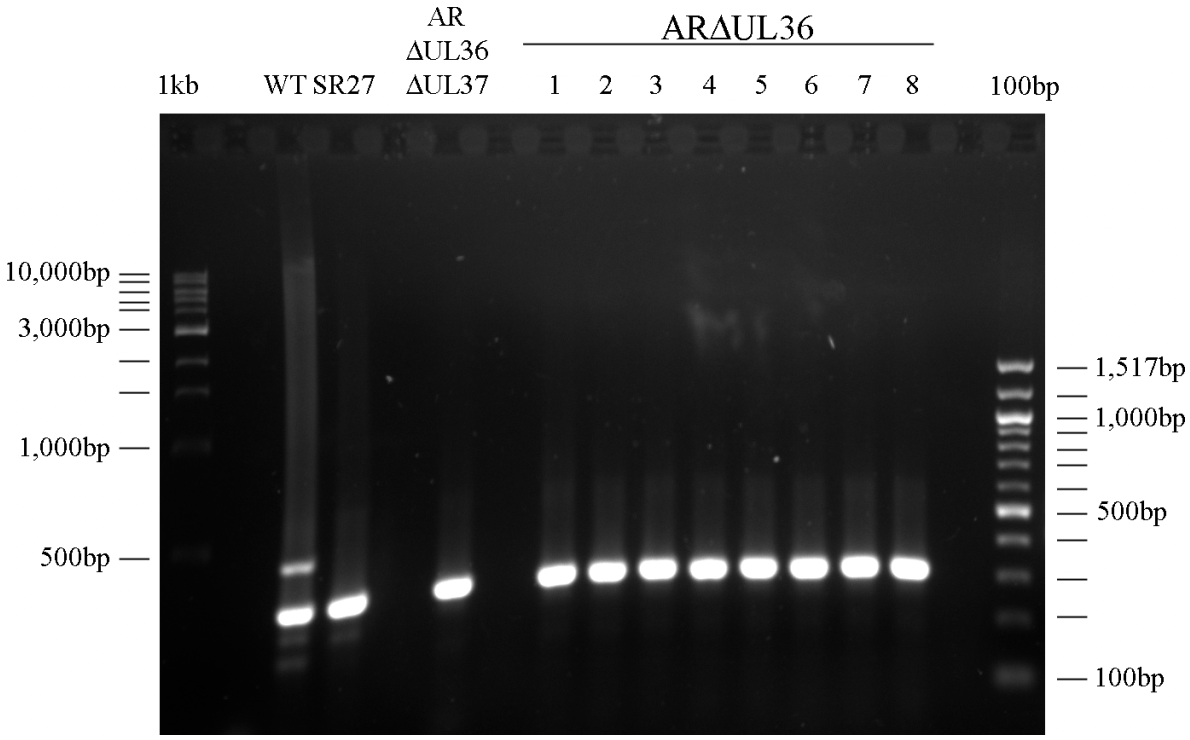

Figure 4.3: Analytical PCR examination of oriL in BAC derived viruses.

Viral DNA was subjected to PCR with primers OriLseq_F and R (Table 2.1), which flank the oriL locus. The PCR templates used were isolated virion DNAs from WT HSV-1 (lane WT), ARΔUL36ΔUL37 and from individual plaque isolates of ARΔUL36 (lanes 1-8), and pBAC SR27 DNA (SR27). Lane WT contained two major bands of 457 bp (indicative of intact oriL) and ~300bp (suggestive of oriL deletion). Only the ~300bp band was present in lanes containing products generated from BAC or BAC derived templates.

parental viruses, lack full-length oriL and grow with WT HSV-1 like kinetics. OriL is absent from pUCNhe4 which was used for the recombination to repair the lethal deletions. pUCNhe4 contains sequences from UL33-UL38 only (residues 68662-85304) and so was unable to supply a potentially WT oriL to these mutants, but was suitable to repair the lethal defects introduced to these mutants. This suggests that the absence of oriL from these viruses does not have a significant impact on *in vitro* replication and is unlikely to have affected the results described below.

4.3. Expression of viral proteins by HSV-1 WT, K5ΔZ and the tegument mutants KΔUL36, ARΔUL36, FRΔUL37 and ARΔUL36ΔUL37.

To analyse the protein expression profiles of the mutants K5ΔZ, KΔUL36, ARΔUL36, FRΔUL37 and ARΔUL36ΔUL37 monolayers of non-complementing cells were infected at 5 pfu/cell with either WT HSV-1 or the mutant viruses. Protein extracts were prepared, separated by PAGE and transferred to nitrocellulose membranes for western blotting. The blots were probed with antibodies against the major capsid protein pUL19 (VP5), the inner tegument proteins pUL36 (VP1/2) and pUL37, and two representative outer tegument proteins, pUL48 (VP16) and pUL49 (VP22) (Fig. 4.4).

Probing the blot with the anti-pUL19 antibody confirmed that the protein was present in all samples except K5ΔZ where UL19 is disrupted by insertion of lacZ at the N terminus of the UL19 ORF (Desai *et al.*, 1993). In KΔUL36, ARΔUL36 and ARΔUL36ΔUL37 where the UL36 ORF was disrupted or absent, no full-length pUL36 was seen. However, a novel 43 kDa species was present in the KΔUL36 sample. The antibody αVP1-2NT1r is directed against an N terminal fragment of pUL36 (Abaitua & O'Hare, 2008) and the 43 kDa band corresponds to the size predicted for the N terminal fragment encoded by the truncated UL36 ORF in KΔUL36. Bands present in all samples presumably represent non-specific binding by the antibody, while bands present only in HSV-1 WT, K5ΔZ and FRΔUL37 represent N terminal breakdown products of full length pUL36. Similar results were obtained using a mouse anti serum against pUL36 (Roberts *et al.*, 2009). As expected, no pUL37 was present in FRΔUL37 or ARΔUL36ΔUL37, while pUL48 (VP16) and pUL49 (VP22) were detected at similar levels in all samples.

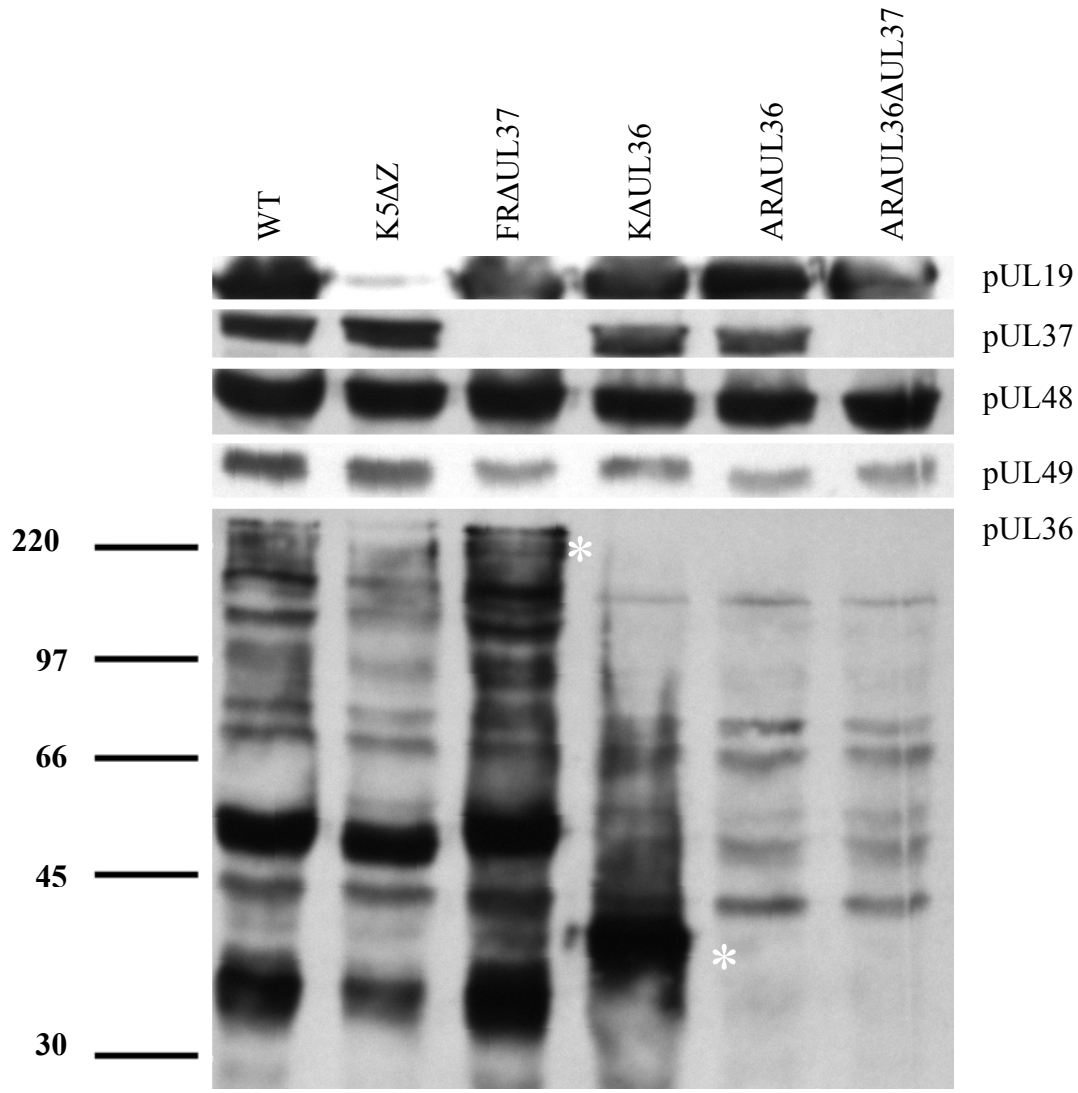

Figure 4.4: Protein expression profiles of WT HSV-1, K5ΔZ and tegument mutants on non-complementing cells.

RS cells were infected with 5 pfu/cell of WT HSV-1 (WT), K5ΔZ or with a tegument mutant virus. After incubation at 37^{o}C for 24 h, the cells were harvested and the proteins were separated on a 10% SDS polyacrylamide gel and transferred to nitrocellulose membrane for western blotting. Protein expression was examined using the following antibodies: pUL19 (DM165), pUL36 (αVP1-2NT1r), pUL37 (M780), pUL48 (VP16 (1-21)) and pUL49 (AGV031). Full length pUL36 and the 43 kDa N terminal fragment are marked (*). Molecular weight standards are indicated to the left of the lower panel.

4.4. Growth characteristics of the tegument mutants ARΔUL36, FRΔUL37, ARΔUL36ΔUL37 and their revertants.

Growth of the tegument mutants KΔUL36, ARΔUL36, FRΔUL37 and ARΔUL36ΔUL37 was compared on complementing and non-complementing cells. As expected, titration of virus stocks showed that the WT HSV-1 and the rescuants FRΔUL37R, ARΔUL36R and ARΔUL36ΔUL37R grew equally well on both cell types. In contrast all the mutants showed reductions in titer of $>10^5$ between complementing and non-complementing cells (Table 4.1). This analysis also showed that spontaneous reversion of the mutant phenotype is a rare event as no plaques were detected on non-complementing cells (at dilutions of 10^{-3} and lower the cell monolayers showed complete cpe).

Because of their lethal phenotypes, single step growth analysis of the mutants could only be carried out on complementing cells. Therefore, single step growth kinetics were established by infecting 35mm plates of the appropriate complementing cells with K5ΔZ, KΔUL36, ARΔUL36, FRΔUL37 and ARΔUL36ΔUL37 and by infecting RS cells with WT HSV-1 and the rescuants, FRΔUL37R, ARΔUL36R and ARΔUL36ΔUL37R. All infections were at 10 pfu/cell and unabsorbed input virus was inactivated by an acid wash (Stow, 2001). At 3, 6, 12, and 24 h post infection one plate per virus was harvested, by scraping the cells into the medium, and stored on ice. Once all time points had been collected, the samples were sonicated to release cell-associated virus. The samples were then serially diluted and plated onto appropriate complementing cells to determine their titres. In this analysis the mutants also showed single step growth kinetics that were similar to or only marginally slower than for WT HSV-1 (Fig. 4.5 (A) and (B)) and the revertants grew as well as WT HSV-1 (Fig. 4.5 (C)). As each complementing cell line contains only the relevant HSV-1 ORF needed for trans complementation it is possible to infer that there are no second site mutations within the mutant genomes that are detrimental to viral growth. This is confirmed by the WT HSV-1-like growth of the revertants FRΔUL37R, ARΔUL36R and ARΔUL36ΔUL37R.

It is notable that the absence of full-length oriL from the mutant and rescuant viruses derived from pBAC SR27 seems not to be detrimental to virus growth in culture when compared with WT HSV-1 and whilst there may be an indication of slightly slower growth kinetics, these mutants seem less affected than those reported by Nagel *et al*. (2008). The

(A)

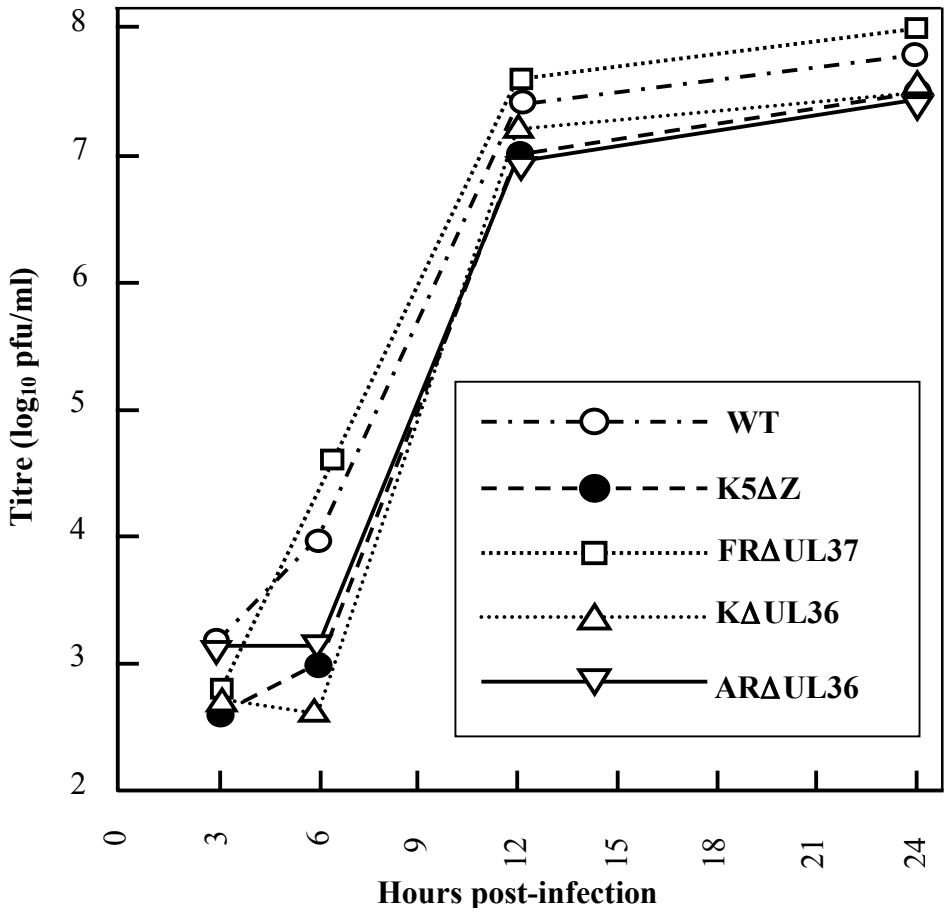
Titre (log_{10} pfu/ml)
Hours post-infection
WT
K5ΔZ
FRΔUL37
KΔUL36
ARΔUL36

(B)

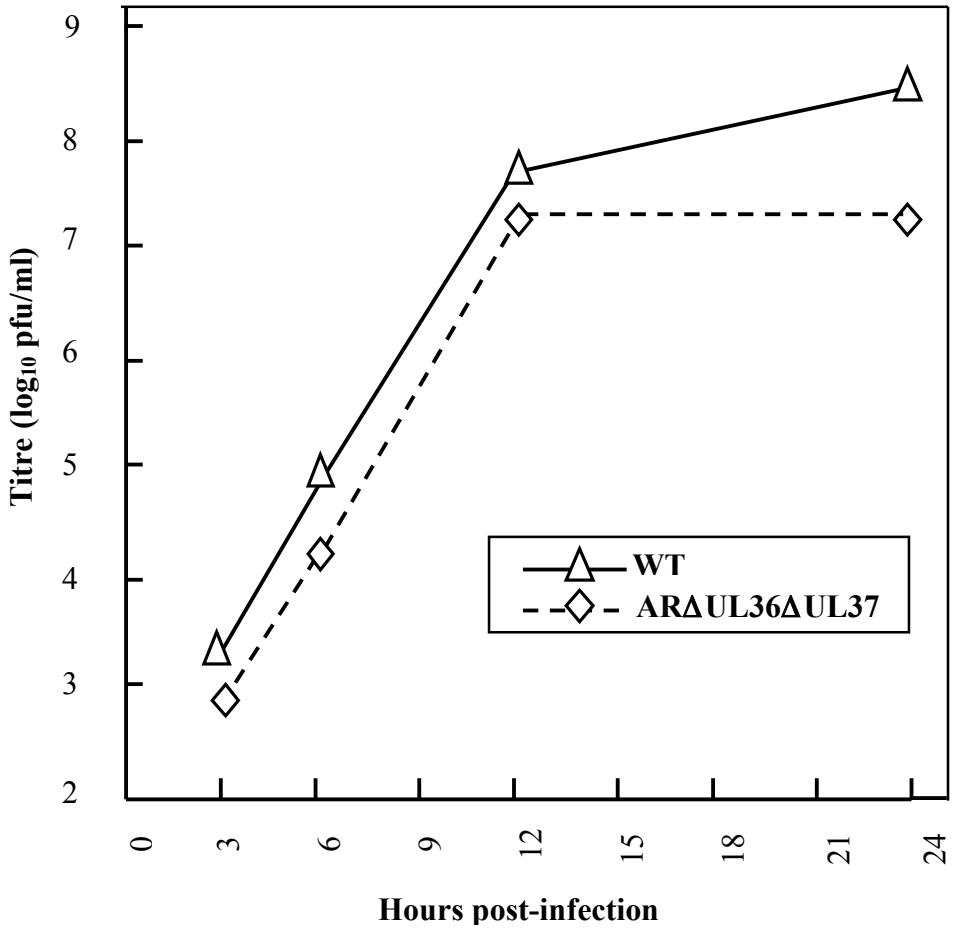
Titre (log_{10} pfu/ml)
Hours post-infection
WT
ARΔUL36ΔUL37

(C)

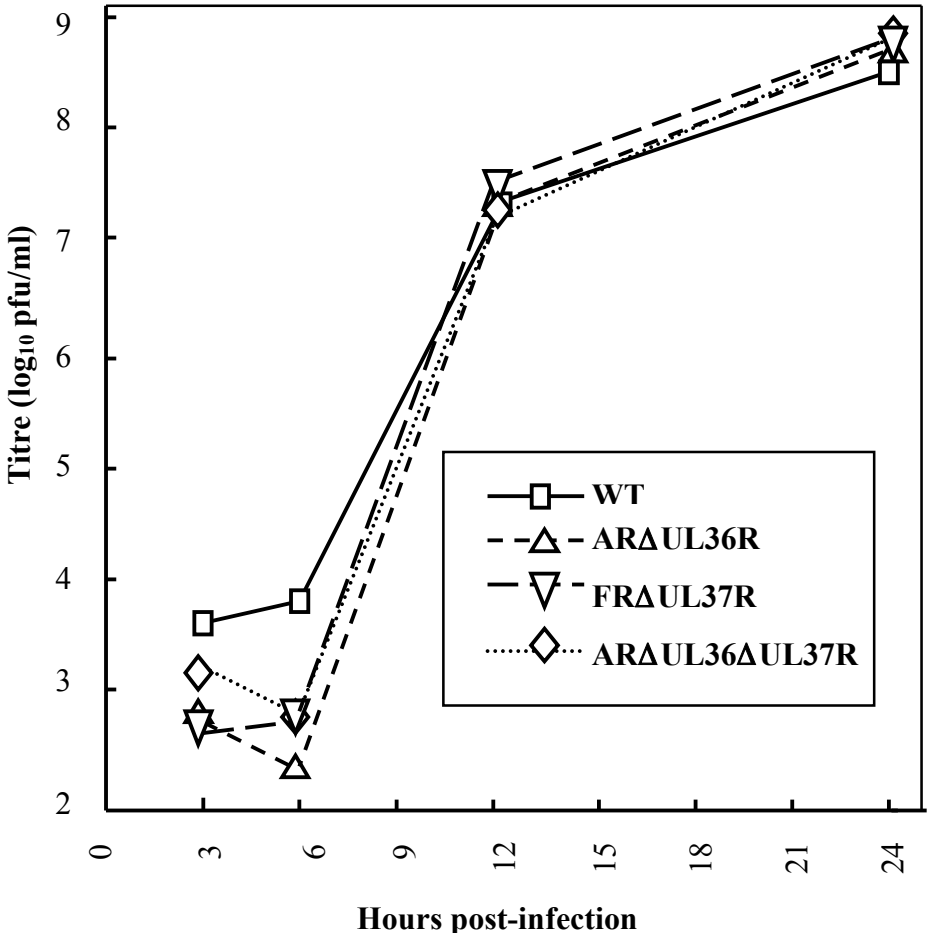

Figure 4.5: Determination of the single step growth kinetics for WT HSV-1, K5ΔZ, the inner tegument mutants and their rescuants.

Replicate dishes of complementing RS cells were infected with 10 pfu/cell of: (A) K5ΔZ, FRΔUL37, KΔUL36 or ARΔUL36, or (B) ARΔUL36ΔUL37. Replicate dishes of non complementing RS cells were infected in an identical fashion with (A,B,C) WT HSV-1 (WT), or (C) the rescuant viruses, ARΔUL36R, FRΔUL37R or ARΔUL36ΔUL37R. After 1 h at 37°C, the cells were washed at low pH to remove residual input infectivity and overlaid with 2 ml of DMEM, and incubation was continued at 37°C. At 3, 6, 12, and 24 h after infection, the cells were harvested by scraping into the supernatant medium, and the progeny virus was titrated on complementing cells.

Virus	Non-complementing	Complementing
WT HSV-1	$1.8x10^{10}$	$1.2x10^{10}$ [a], $1.4x10^{10}$ [b], $1.2x10^{10}$ [c]
K5ΔZ	$<10^4$*	$1.6x10^9$
FRΔUL37	$<10^4$*	$1.9x10^9$
FRΔUL37R	$6.2x10^{10}$	$9x10^{10}$
KΔUL36	$<10^4$*	$3.1x10^9$
ARΔUL36	$<10^4$*	$2.0x10^9$
ARΔUL36R	$2.5x10^{10}$	$2.4x10^{10}$
ARΔUL36ΔUL37	$<10^4$* [a,b]	$2x10^{10}$
ARΔUL36ΔUL37R	$4.3x10^{10}$	$2.8x10^{10}$

Table 4.1: Comparison of titres of WT HSV-1, K5ΔZ, tegument mutants and rescuants on non-complementing and complementing cell lines.

* ARΔUL36, KΔUL36, FRΔUL37 and ARΔUL36ΔUL37 show only cpe at dilutions of 10^{-3} or less.

a titre on HAUL36 cells

b titre on 80CO2 cells

c titre on 4C cells.

precise functions and requirement of oriL remain poorly understood. Data from animal model systems is contradictory, suggesting that oriL may or may not be required for efficient growth, whilst being dispensable in tissue culture (Balliet & Schaffer, 2006; Polvinobodnar *et al.*, 1987).

4.5. Electron microscopic analysis of mutant infected cells

4.5.1. Analysis of capsid distribution in infected cells

Virus morphogenesis has been examined previously in the inner tegument mutants of both HSV-1 and PrV. A general finding is that these mutants accumulate unenveloped DNA filled capsids (C capsids) within the cytoplasm of infected non-complementing cells (Desai *et al.*, 2001; Desai, 2000; Fuchs *et al.*, 2004; Klupp *et al.*, 2001b); although one UL36 mutant of PrV has been reported as releasing very few capsids of any type from the nucleus (Luxton *et al.*, 2006). However, there is conflicting evidence from both HSV-1 and PrV mutants regarding cytoplasmic capsid aggregation (Desai, 2000; Fuchs *et al.*, 2004) and nuclear retention of capsids (Desai *et al.*, 2001; Fuchs *et al.*, 2004). The work described here was intended to address these inconsistencies.

EM examination of thin sections of WT HSV-1 infected cells revealed a characteristic distribution of capsid species. Thus, A (empty), B (containing scaffold) and C (DNA filled) capsids, were present within the nucleus, while C capsids in the cytoplasm, were frequently associated with membrane structures. Indeed most C capsids within the cytoplasm were present as virions or were in the process of envelopment, and mature virions were seen on the cell surface (Fig. 4.6).

In cells infected with KΔUL36 the numbers and distribution of capsid within the nuclei were similar to those of WT HSV-1 (Table 4.2). However, in agreement with previous studies of this mutant (Desai, 2000), numerous C capsids were seen within the cytoplasm (Fig. 4.7). These capsids formed aggregates, and none were observed in the process of envelopment. As would be expected in the absence of envelopment, there were no virions on the cell surface.

Cells infected with ARΔUL36 also contained cytoplasmic C capsids. However, in contrast to KΔUL36, ARΔUL36 cytoplasmic C capsids did not accumulate into aggregates, but were dispersed throughout the cytoplasm (Fig. 4.8). This is in keeping with the phenotype

reported for the PrV mutant PrV-ΔUL36F (Fuchs *et al.*, 2004). Once again, no virions were seen on the surface of cells infected with this mutant.

FRΔUL37 infected cells also exhibited the characteristic presence of A, B and C capsids within the nuclei of infected cells, and in agreement with the previously reported phenotype for KΔUL37 (Desai *et al.*, 2001) and PrV-ΔUL37 (Klupp *et al.*, 2001b) this mutant accumulated large aggregates of unenveloped C capsids within the cytoplasm. No enveloped virions were present on the cell surface (Fig. 4.9). Examination of micrographs provided no evidence to support the proposition of nuclear retention of capsids in ΔUL37 infections (Desai *et al.*, 2001). This aspect will be addressed further in section 4.5.2.

As might be expected for a virus lacking both pUL36 and pUL37, cells infected with ARΔUL36ΔUL37 accumulated C capsids within the cytoplasm and none were seen in the process of envelopment, nor were virions observed on the cell surface (Fig. 4.10). The cytoplasmic C capsids were not aggregated as in FRΔUL37, but had a dispersed distribution resembling that of ARΔUL36. An interesting feature of some cells infected with this mutant was the extensive rearrangement of the nuclear membrane. The sections appear to show the formation of numerous membrane bounded structures present within the perinuclear space, or in close juxtaposition to the external leaflet of the nuclear membrane (Fig. 4.10). Densely staining material was associated with the membrane surrounding these structures, which in rare cases contained C capsids. No such phenotype has been reported for any single deletion of an inner tegument protein, although there are numerous reports of nuclear membrane alterations in HSV-1 infection (reviewed Dargan, 1986). To determine whether this was a consistent feature, infected RS, $HFFF_2$ and BHK-21 cells were examined. In the great majority of BHK-21 cells there was little apparent rearrangement of the nuclear membrane although isolated examples similar to the situation seen in $HFFF_2$ cells were observed (Fig. 4.11 (A) and (B)). Some rearrangement of the nuclear membrane was seen in RS cells although much less frequently than encountered in $HFFF_2$ cells (Fig. 4.11 (C) and (D)) This suggests that the effect of this mutation on nuclear membrane morphology may be, at least partly, influenced by the cell type.

From the analysis performed here it is clear that although they share the block on envelopment previously seen in the absence of pUL36 or pUL37, both ARΔUL36 and FRΔUL37 show differences in comparison with the reported phenotypes of their direct HSV-1 counterparts, KΔUL36 and KΔUL37. The EM images of KΔUL36 infected cells in Desai (2000) show that deletion of pUL36 leads to the cytoplasmic accumulation of C

(A)

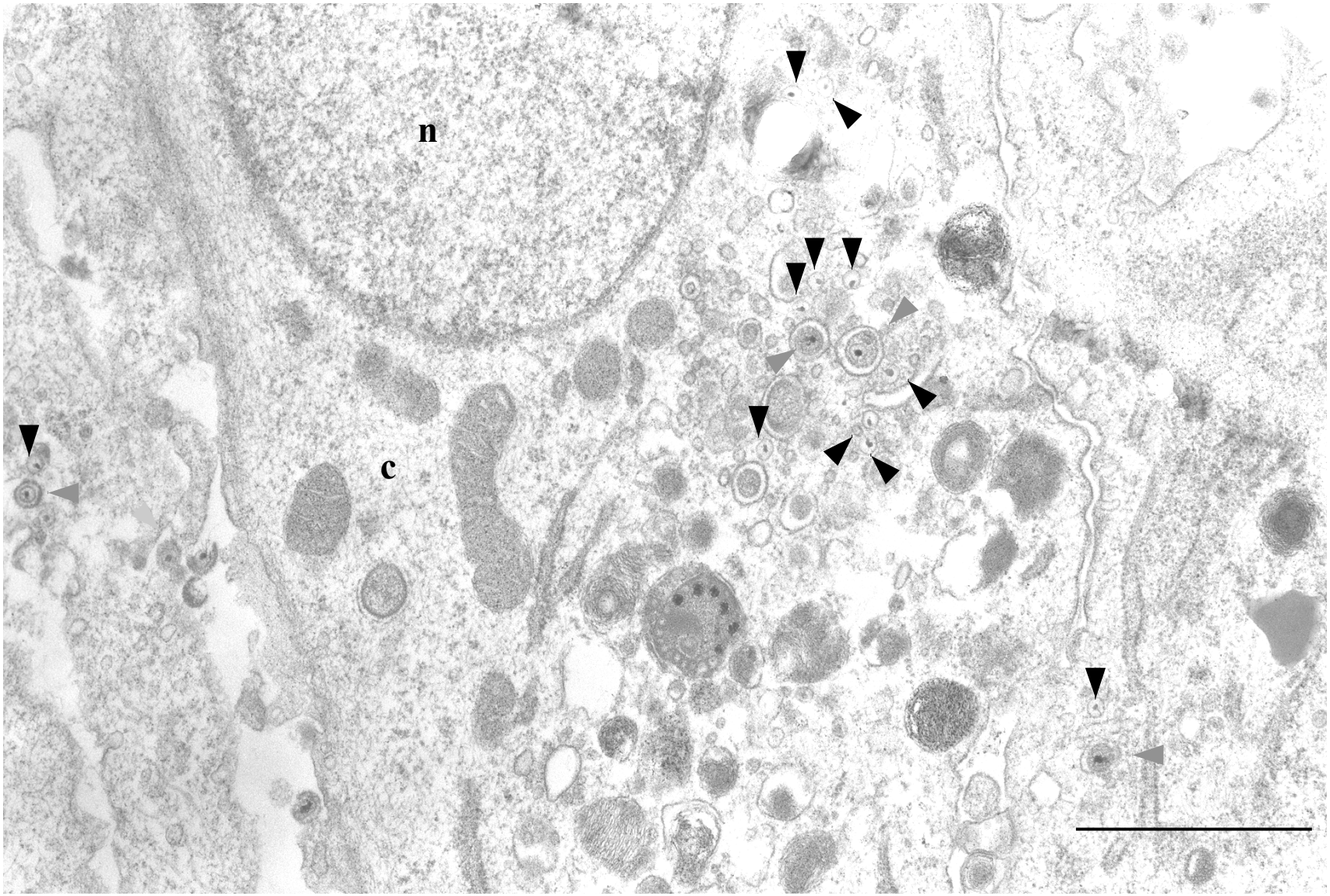

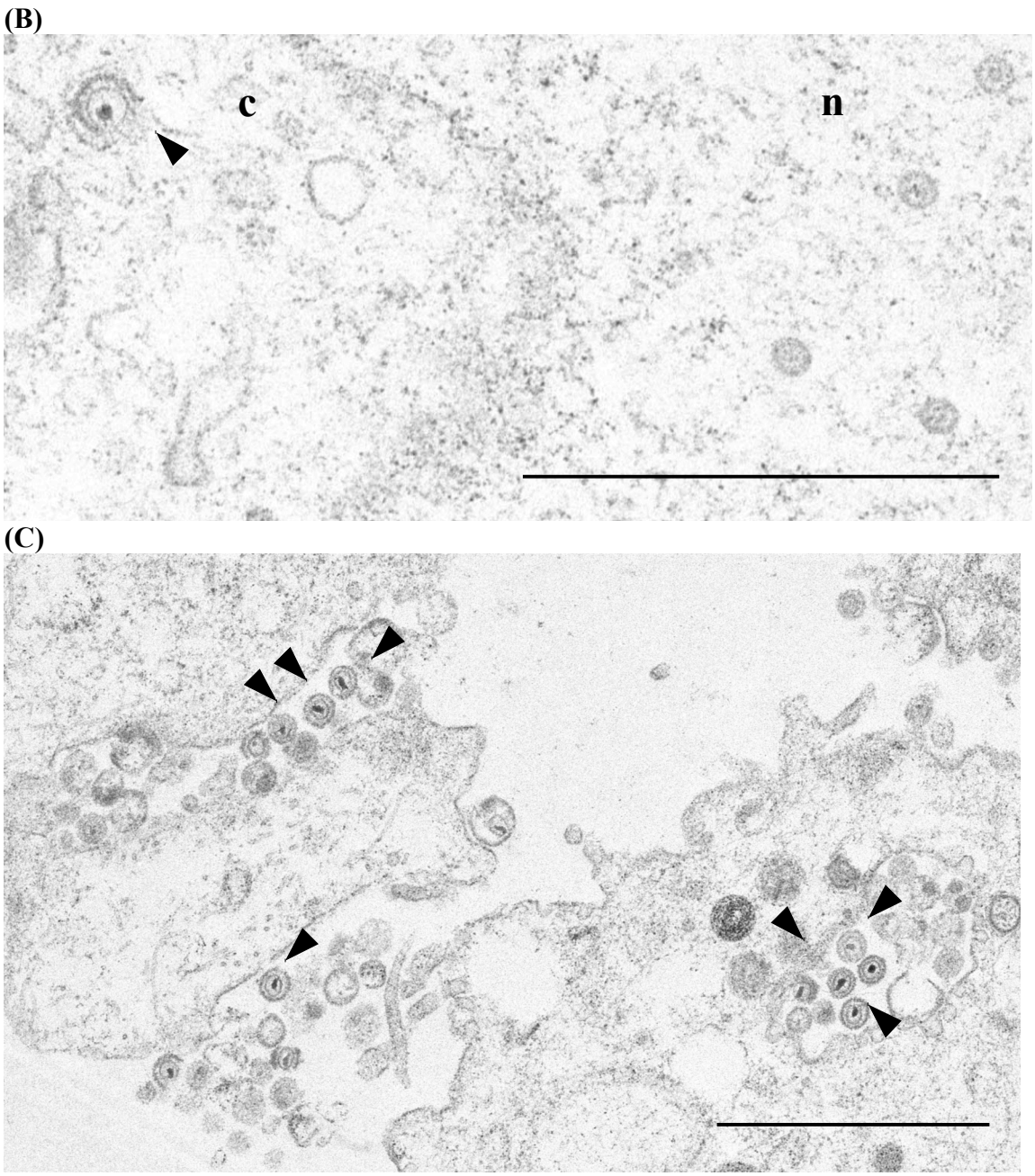

Figure 4.6: Electron microscopic analysis of $HFFF_2$ cells infected with WT HSV-1

A monolayer of $HFFF_2$ cells was infected with 5 pfu/cell of WT HSV-1. Cells were fixed and prepared for electron microscopy at 24 h postinfection.

(A) Electron micrograph of a WT HSV-1 infected cell showing both naked (black arrowheads) and enveloped (grey arrow heads) capsids in the cytoplasm.

(B) Section showing a C capsid undergoing envelopment in the cytoplasm (black arrowhead) and B capsids in the nucleus (right).

(C) Section showing extracellular virions and enveloped capsids inside a cytoplasmic vesicle (black arrowheads).

Nuclear (n) and cytoplasmic (c) compartments are labeled. Bar = 1μm.

(A)

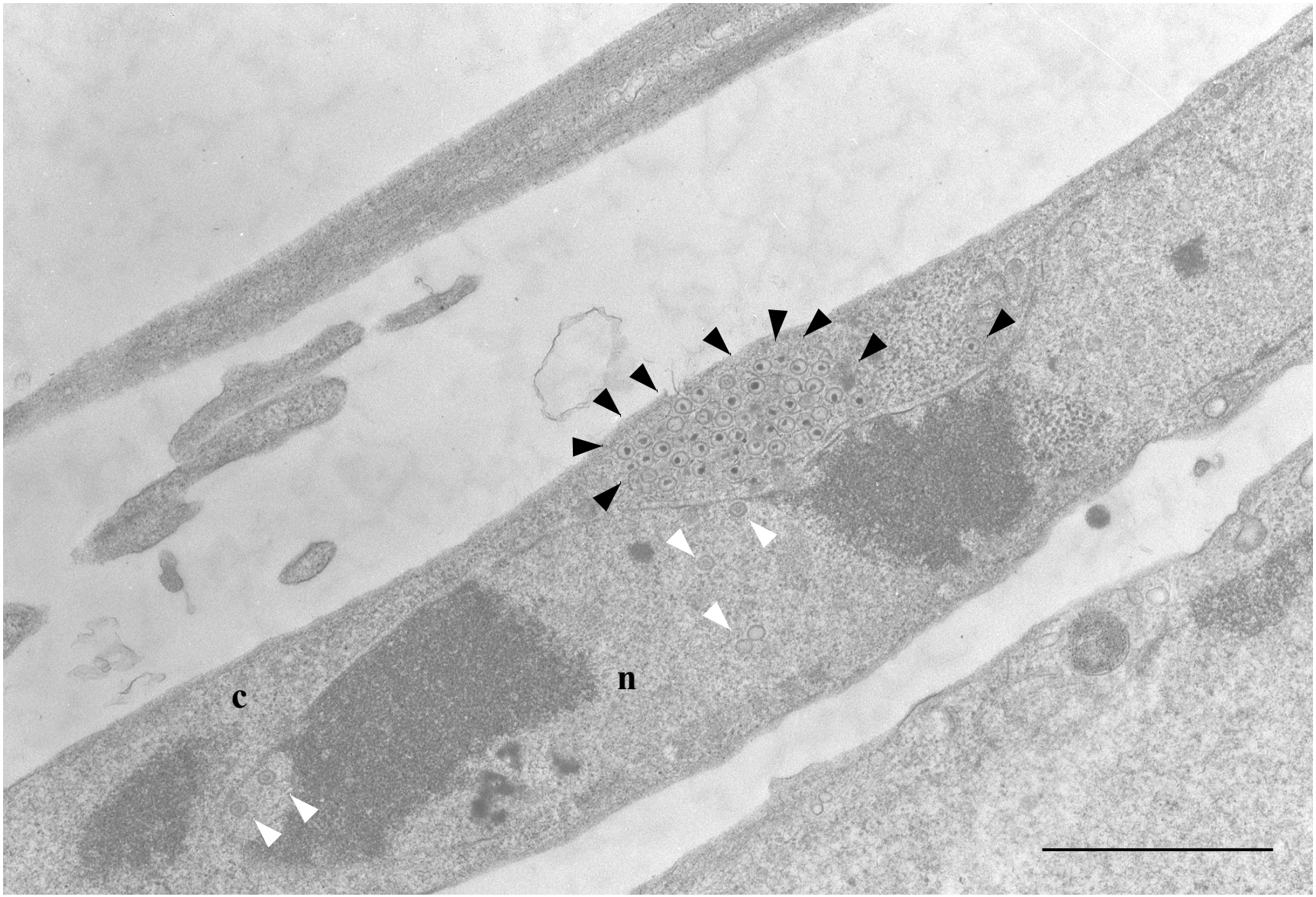

(B)

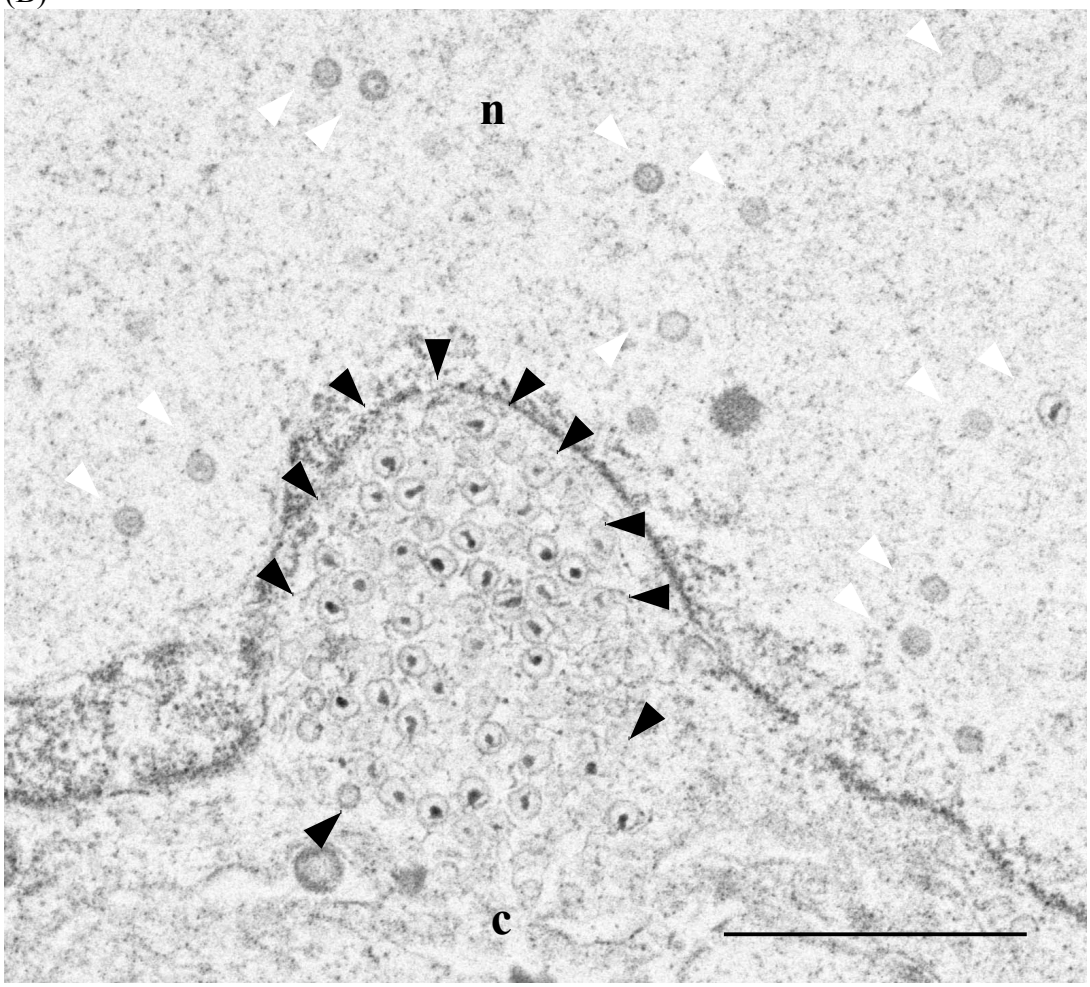

Figure 4.7: Electron microscopic analysis of $HFFF_2$ cells infected with KΔUL36

A monolayer of $HFFF_2$ cells was infected with 5 pfu/cell of KΔUL36 and prepared for EM as for Fig. 4.6.

(A) Electron micrograph of a KΔUL36 infected cell. A and B capsids (white arrowheads) are present in the nucleus (centre) Within the cytoplasm, C capsids are present in aggregates (black arrow heads). No enveloped virions are present on the surface of the cell.

(B) A section showing aggregated and individual cytoplasmic C capsids. A, B and C capsids are seen within the nucleus.

Nuclear (n) and cytoplasmic (c) compartments are labeled. Bar = 1μm.

(A)

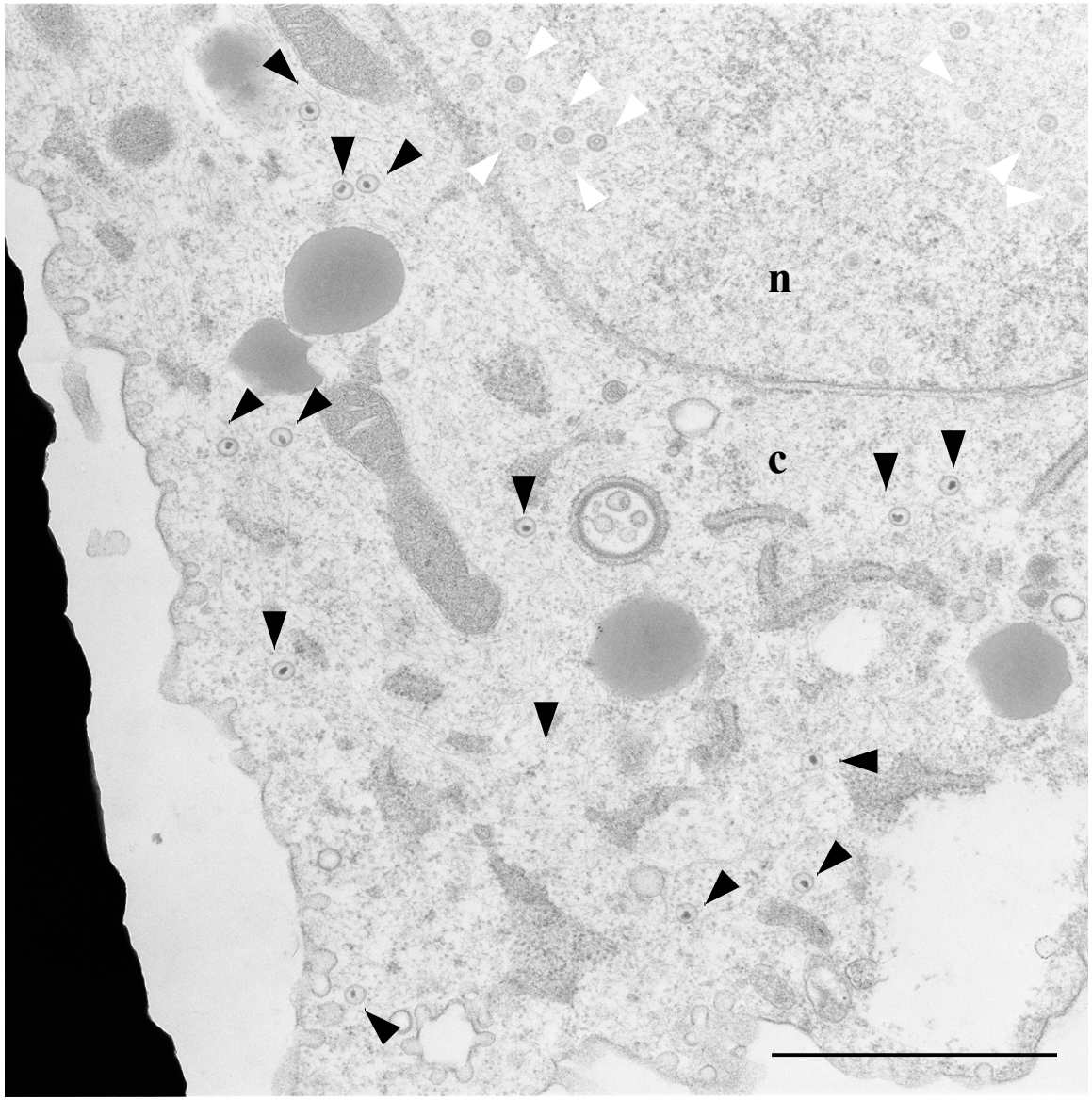

Figure 4.8: Electron microscopic analysis of $HFFF_2$ cells infected with ARΔUL36

A monolayer of $HFFF_2$ cells was infected with 5 pfu/cell of ARΔUL36 and prepared for EM as for Fig. 4.6.

(A) Electron micrograph of an ARΔUL36 infected cell. B capsids are present in the nucleus (white arrowheads) Within the cytoplasm, C capsids (black arrow heads) are dispersed throughout the cytoplasm. No enveloped virions are present on the surface of the cell. Cytoplasmic capsids are not seen in close proximity to membrane structures.

Nuclear (n) and cytoplasmic (c) compartments are labeled. Bar = 1μm.

(A)

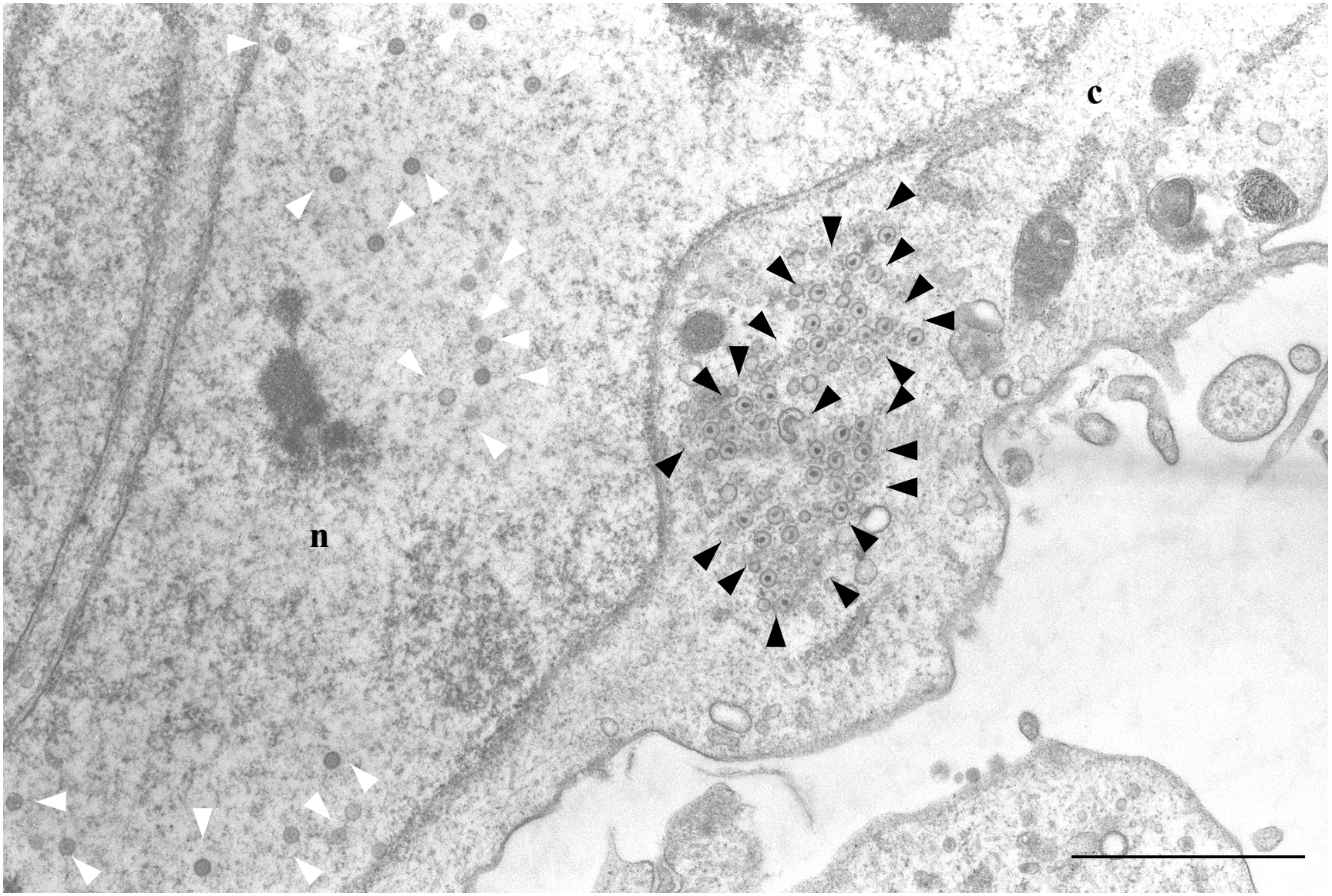

(B)

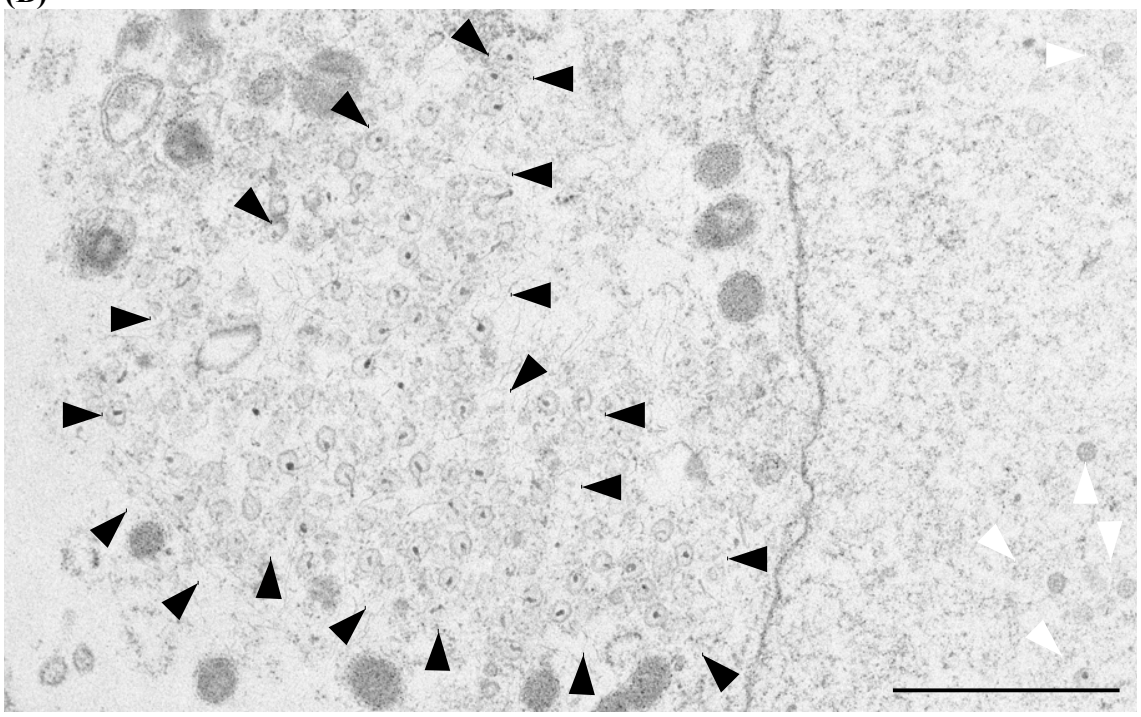

Figure 4.9: Electron microscopic analysis of HFFF cells infected with FRΔUL37

A monolayer of $HFFF_2$ cells was infected with 5 pfu/cell of FRΔUL37 and prepared for EM as for Fig. 4.6.

(A) Electron micrograph of an FRΔUL37 infected cell. A and B capsids are present in the nucleus (white arrowheads) Within the cytoplasm aggregates of C capsids are present (black arrowheads). No enveloped virions are present on the surface of the cell.

(B) Section showing aggregates of unenveloped C capsids in the cytoplasm. Cytoplasmic capsids (black arrowheads) are not seen in close proximity to membrane structures, but are surrounded by darker staining suggestive of the presence of tegument material.

Nuclear (n) and cytoplasmic (c) compartments are labeled. Bar = 1μm.

(A)

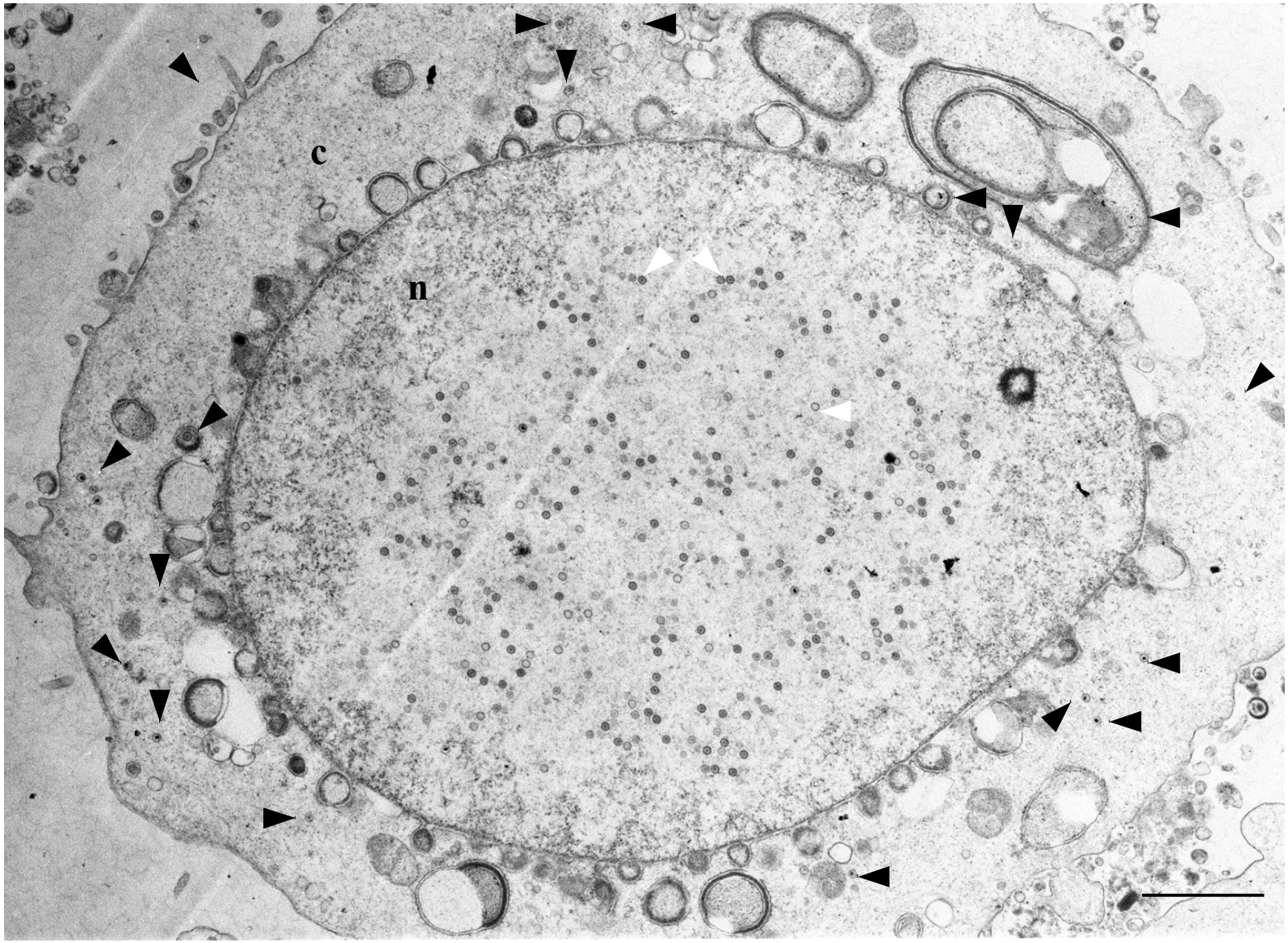

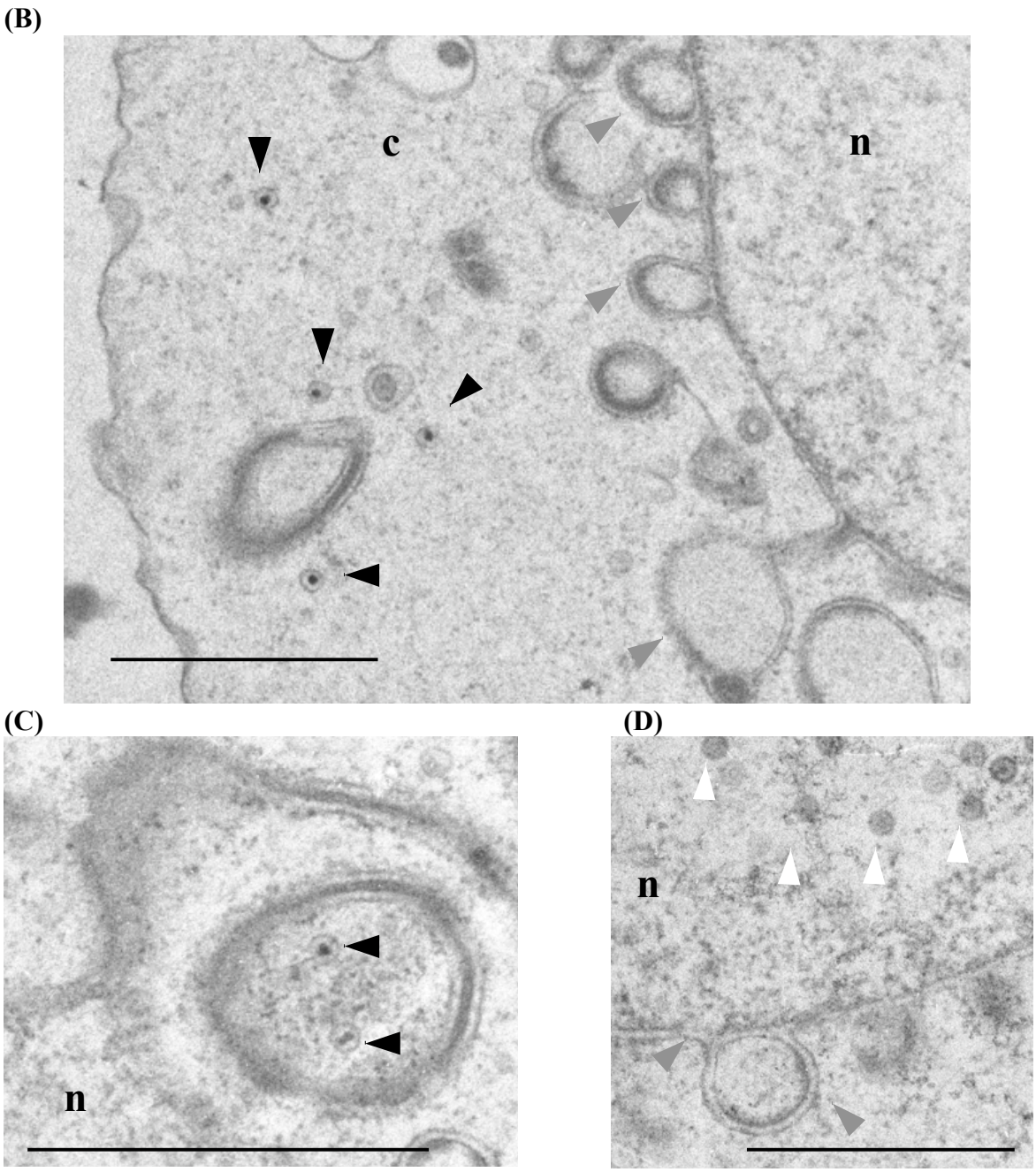

Figure 4.10: Electron microscopic analysis of $HFFF_2$ cells infected with ARΔUL36ΔUL37

A monolayer of $HFFF_2$ cells was infected with 5 pfu/cell of ARΔUL36ΔUL37 and prepared for EM as for Fig. 4.6.

(A) Electron micrograph of an ARΔUL36ΔUL37 infected cell. A,B and C capsids are present in the nucleus (white arrowheads) C capsids are dispersed throughout the cytoplasm (black arrow heads) as for ARΔUL36 (Fig 4.8). No enveloped virions are present on the surface of the cell.

(B-D) Enlarged sections showing unusual rearrangements of cellular membranes. Extensive alteration to the nuclear membrane is apparent with vesicles seeming to form between the membrane leaflets (B and D, grey arrowheads), while capsids are sometimes seen in membrane bound structures that may contain nucleoplasm (C).

Nuclear (n) and cytoplasmic (c) compartments are labeled. Bar = 1μm.

(A)

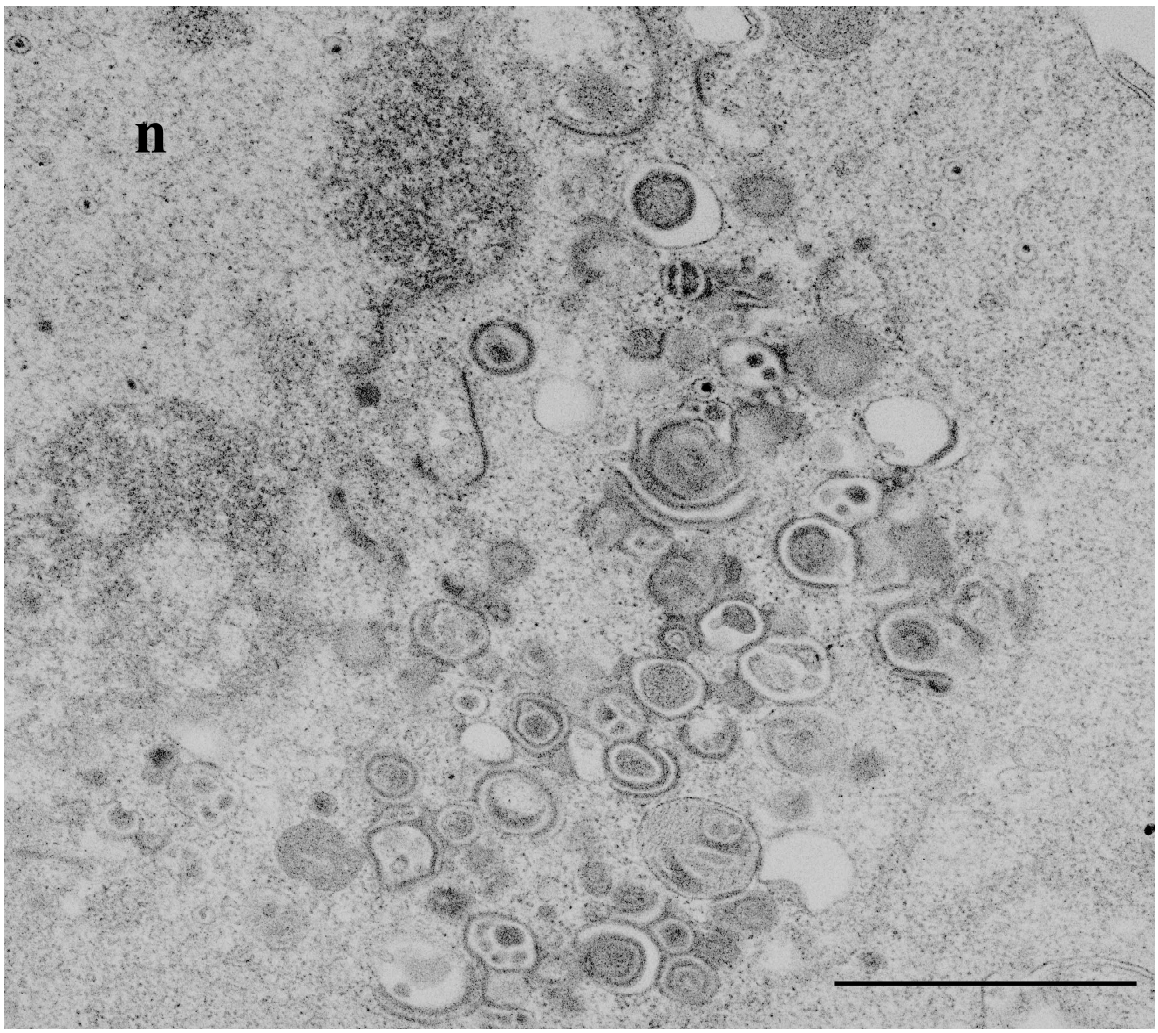

(B)

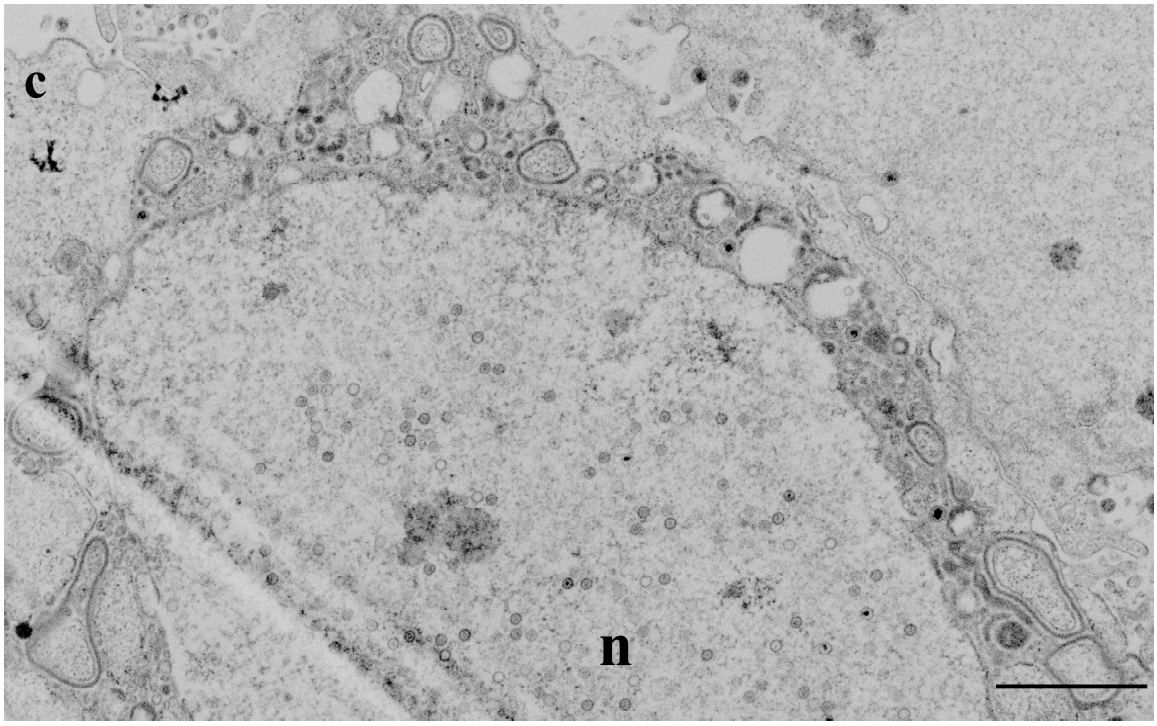

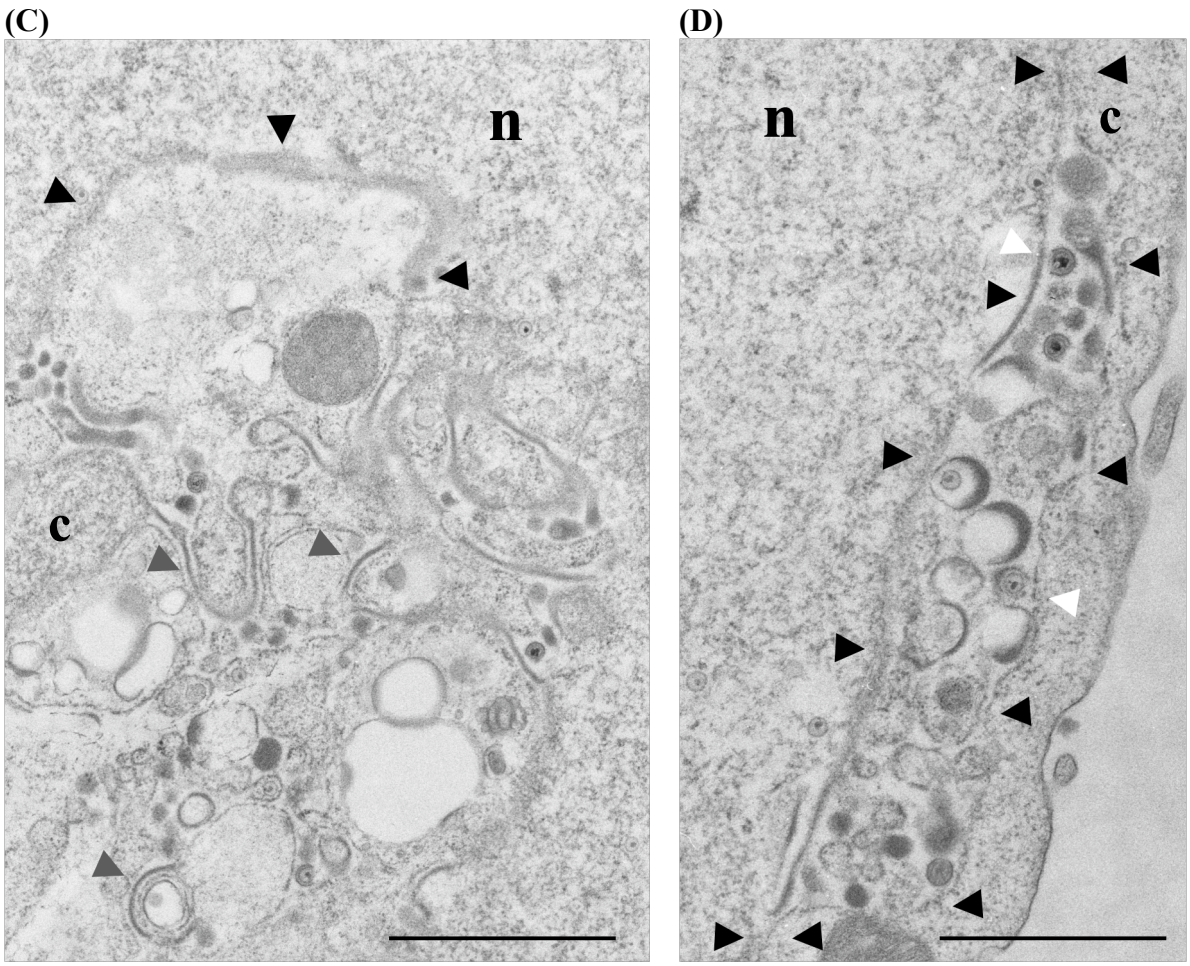

Figure 4.11: Electron microscopic analysis of BHK and RS cells infected with ARΔUL36ΔUL37; alterations to the nuclear membranes.

Monolayers of BHK (A-B) and RS (C-D) cells were infected with 5 pfu/cell of ARΔUL36ΔUL37 and prepared for EM as for Fig. 4.6.

(A) Electron micrograph of an infected BHK cell. This arrangement of cytoplasmic membranes is similar to that seen in cells infected with WT HSV-1 (Fig. 4.6) and there are no apparent changes to the nuclear membrane structure.

(B) Section from an infected BHK cell showing a rare example of extensive rearrangement of the nuclear membrane similar to those seen in $HFFF_2$ cells (Fig. 4.10).

(C) Section from an infected RS cell showing modest changes to the structure of cytoplasmic membranes (grey arrowheads) with no apparent changes to the nuclear membrane (black arrowheads).

(D) Section from an infected RS cell showing some rearrangement of the nuclear membrane similar to those seen in $HFFF_2$ cells (Fig. 4.10). Within the perinuclear space are capsids, some of which may be primary virions (white arrowheads). The nuclear membrane leaflets are highlighted with black arrowheads.

Nuclear (n) and cytoplasmic (c) compartments are labeled. Bar = 1μm.

capsids in small aggregates similar to that shown in Fig. 4.7. In contrast, examination of ARΔUL36 showed individual C capsids throughout the cytoplasm. This phenotype closely resembled that of the PrV mutant, PrV-ΔUL36F, which like ARΔUL36 has the entire UL36 ORF deleted (Fuchs *et al.*, 2004), and suggests that the accumulation of C capsids into aggregates in KΔUL36 is a specific phenotype of this mutant. To quantify this effect the cytoplasmic capsids in cells infected with WT HSV-1 and the three inner tegument mutants were classified as either free, or aggregated, and the number of enveloped capsids and extracellular virions in WT HSV-1 was also determined (Table 4.2). This confirmed that cytoplasmic ARΔUL36 capsids were dispersed, KΔUL36 capsids were predominantly found in aggregates and FRΔUL37 capsids were almost completely found in aggregates (Figs. 4.7-4.9). The most likely explanation of the clustering of KΔUL36 cytoplasmic capsids is that it is caused by the N terminal fragment of pUL36, expressed as a result of the incomplete deletion of the UL36 ORF (Fig. 4.4). This is further addressed in section 5.2.1.1.

4.5.2. Nuclear retention of nucleocapsids

The analysis of FRΔUL37 was in broad agreement with previously reported tegument mutants, in which absence of pUL37 leads to accumulation of large cytoplasmic aggregates of C capsids (Desai *et al.*, 2001; Klupp *et al.*, 2001b). However, there was a disparity with KΔUL37 where Desai *et al.*, (2001) reported that fractionation of ^{3}H-thymidine labelled KΔUL37-infected cells, showed that 75% of DNA filled capsids were associated with the nucleus. Despite the presence of aggregates of cytoplasmic C capsids in their EM images, they interpreted this as evidence for a defect in nuclear exit caused by deletion of UL37. In order to investigate trafficking of capsids in these mutants, electron micrographs of cells infected with WT HSV-1, KΔUL36, ARΔUL36 and FRΔUL37 were analysed to determine the number of capsids present in the nucleus and cytoplasm. The results are summarised in Table 4.2 (derived from data in Appendix A), and show no evidence for retention of capsids in the nucleus for KΔUL36, ARΔUL36 or FRΔUL37. Indeed, the ratio of A, B and C capsids in the nuclei of cells infected with these mutants is very similar to that in WT HSV-1-infected cells. This analysis also suggests no retention of capsids to the nuclei of cells infected with ARΔUL36 in agreement with Fuchs *et al.*, (2004) and contrasting with a report for another PrV mutant lacking pUL36. This report demonstrated a strong retention of capsids to the nucleus in the absence of pUL36 (Luxton *et al.*, 2006) which was not seen in any other analysis for equivalent PrV or HSV-1 mutants (Desai, 2000; Fuchs *et al.*, 2004).

		Nuclear		Cytoplasmic		
Virus	**Capsid**	**No. capsids**	**% total nuclear capsids**	**No. free capsids**	**No. aggregated capsids**	**% of total DNA containing capsids[b]**
WT HSV-1	A	154	17	2		
	B	691	76	2		
	C	63	7	40		12
	Virions [a]			217		68
FRΔUL37	A	227	13	2	3	
	B	1,380	77	4	21	
	C	177	10	39	425	72
KΔUL36	A	107	14	17	1	
	B	586	77	10	2	
	C	71	9	149	324	87
ARΔUL36	A	161	19	13		
	B	544	66	68		
	C	123	15	276		69

Table 4.2: Subcellular distribution of capsids in WT and mutant HSV-1 infected cells.

[a] Includes enveloped cytoplasmic and extracellular capsids.

[b] Percentage of total DNA containing capsids relates to the number of DNA containing capsids seen outside the nucleus compared to the total (nuclear + cytoplasmic) numbers of DNA containing capsids.

Source data in Appendix A.

To address the discrepancy between the results with FRΔUL37 and the published observations with KΔUL37 (Desai *et al.*, 2001), cells infected with FRΔUL37 were separated into nuclear and cytoplasmic fractions, and analysed by electron microscopy (Fig. 4.12). This revealed that very few C capsids were in the cytoplasmic fraction and that the majority were indeed present in the nuclear fraction, but located outside of the nuclei. It seems likely therefore, that the apparent block on nuclear exit reported by Desai *et al.*, (2001), was an incorrect interpretation caused by the large cytoplasmic capsid aggregates copelleting with the nuclei during fractionation of infected cells. The results presented here together with those of Klupp *et al.*, (2001b) on PrV-ΔUL37, suggest that the primary defect of UL37 deletion mutants is a block on secondary envelopment, and not on nuclear egress.

4.6. Analysis of the association of HSV-1 tegument proteins with capsids in infected cells

Association of tegument proteins with capsids in infected cells was probed using immunofluorescence and Immuno-EM techniques to understand the effect of inner tegument deletions on the association of capsid with other tegument components. The process of tegument assembly on capsids is poorly understood and mutants lacking inner tegument proteins provide a system by which the addition of these proteins to the capsid might be examined to understand the order of acquisition of such proteins by the capsid.

4.6.1. Immunofluorescence:

For immunofluorescence studies of capsid-tegument protein interactions $HFFF_2$ cells were infected at 5 pfu/cell for 24h before fixation and processing for immunofluorescence. Cells were probed with DM165 (anti-VP5) in combination with one of either αVP1-2NT1r (anti-pUL36), M780 (anti-pUL37) or AGV031 (anti-pUL49) or with 191A (anti-VP5) and VP16 (1-21) (anti-pUL48).

The cytoplasmic patterns of VP5 labelling in these infected cells (Figs. 4.13-4.15) correspond closely with the capsid distributions seen by EM (Figs. 4.6-4.9), and by fluorescence *in situ* DNA labelling (Fig. 6.4). Therefore, the VP5 labelling is assumed to indicate the presence of capsids.

(A)

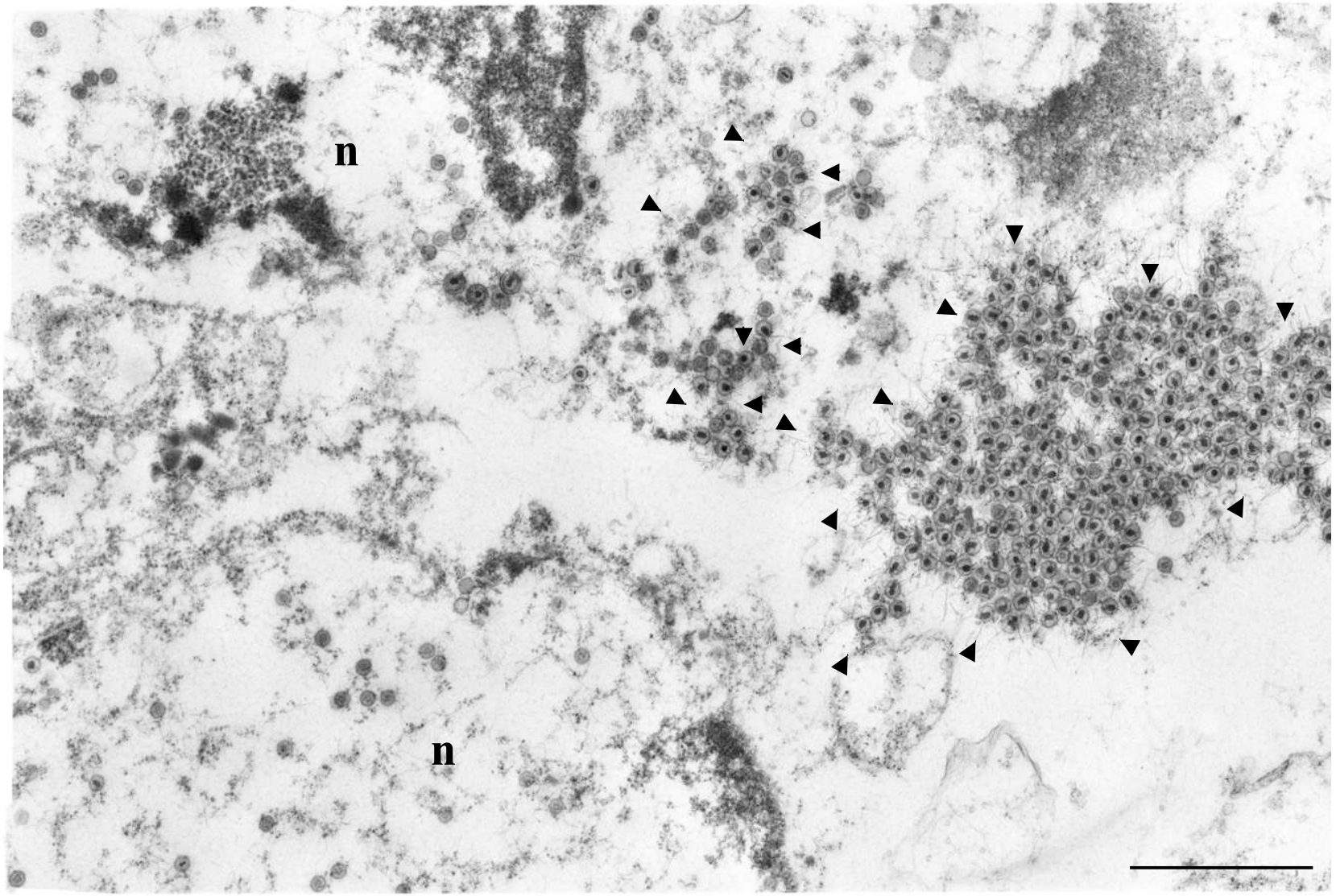

(B)

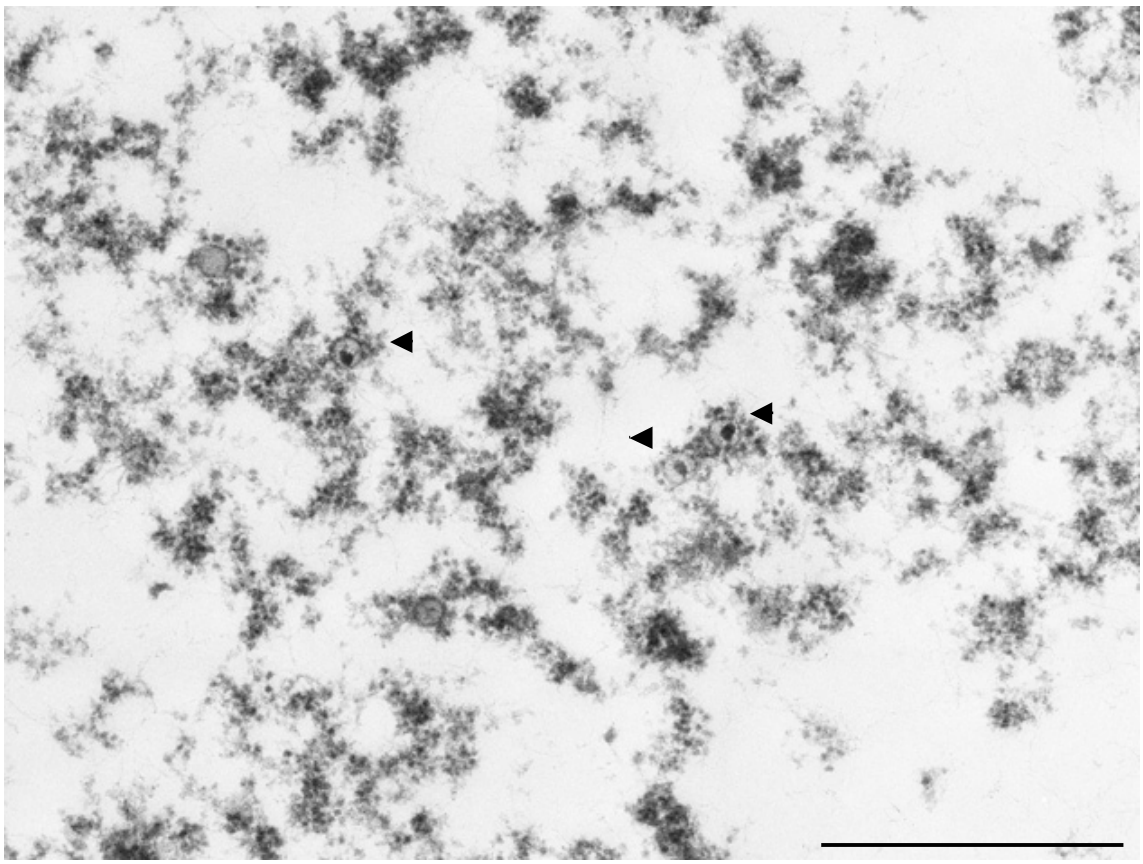

Figure 4.12: Association of FRΔUL37 cytoplasmic capsid aggregates with the nuclear fraction of infected cells.

BHK cells infected with 5 pfu/cell of FRΔUL37 were separated into nuclear and cytoplasmic fractions using the method described for preparation of capsids (section 2.2.9), and the fractions were then prepared for thin sectioning and EM (section 2.2.11).

(A) Electron micrograph of the nuclear fraction, showing aggregates of C capsids (black arrowheads) outside of the nuclei (marked n).

(B) Electron micrograph of the cytoplasmic fraction. No aggregates of capsids were appareant, with only a very few dispersed capsids seen (black arrowheads).

Bar = 1μm.

4.6.1.1. Association of pUL36 with capsids:

In WT HSV-1 infected cells there was strong labelling for VP5 throughout the nucleus, with punctate cytoplasmic labelling revealing the distribution of capsids and virions. pUL36 labelling (green) was much weaker and was largely confined to the cytoplasm in agreement with the findings of Möhl *et al*. (2009) in PrV. VP5 and pUL36 had similar distribution patterns in the cytoplasm with extensive colocalisation (yellow) as expected for WT HSV-1, where these two proteins must associate for the production of mature virions. In FRΔUL37 infection, the pattern of VP5 was different with large concentrations of cytoplasmic labelling corresponding to the capsid aggregations seen by EM (Fig. 4.9). As in WT HSV-1, pUL36 was confined to the cytoplasm where it showed extensive colocalisation with the capsid aggregates, suggesting that pUL36 is capable of associating with capsids in the absence of pUL37. In KΔUL36 infection the VP5 labelling again showed evidence of cytoplasmic capsid aggregates consistent with the EM pattern (Fig. 4.7). In this case, the N terminal fragment of pUL36 was detected throughout both the nucleus and the cytoplasm but was not preferentially associated with the cytoplasmic capsid aggregates. In ARΔUL36 infected cells no pUL36 was detected and capsids (red) were seen dispersed throughout the cell (Fig. 4.13).

4.6.1.2. Association of pUL37 with capsids:

Association of pUL37 with cytoplasmic capsids could not be established as the antibody (M780) failed to recognise pUL37 under the fixation and labelling conditions used.

4.6.1.3. Association of pUL48 with capsids

As expected, and unlike pUL36, pUL48 was found in the nucleus in all infections. In WT HSV-1 infection cytoplasmic pUL48 gave a punctate labelling pattern similar to, and largely colocalising with, that of VP5. Some structures, which were labelled solely with anti pUL48, either represent cases where tegument had obscured the VP5 epitope or marked the presence of pUL48 containing L particles. In contrast, in FRΔUL37, KΔUL36 and ARΔUL36 infections it was more uniformly dispersed throughout the cytoplasm. Cytoplasmic capsid aggregates of FRΔUL37 showed some, but not extensive colocalisation with pUL48 suggesting that pUL48 may bind to pUL36 decorated capsids in the absence of pUL37. In both ΔUL36 infections pUL48 was not observed to colocalise with capsids (Fig. 4.14).

4.6.1.4. Association of pUL49 with capsids:

In WT HSV-1 infection pUL49 was again found to colocalise with capsids as would be expected for the formation of mature virions. The extent of such colocalisation was more limited than might be expected presumably because the acquisition of tegument rendered the VP5 epitope inaccessible. As with pUL48 some structures were apparent which were labelled solely for pUL49. In FRΔUL37 infection pUL49 labelling was spread extensively throughout the cytoplasm but unlike pUL48 was largely punctate, presumably representing L particle formation. Interestingly, pUL49 was seen to colocalise with cytoplasmic capsid aggregates of this mutant. This observation requires confirmation by other means but suggests that acquisition of outer tegument might not be completely abolished in the absence of pUL37. In both ΔUL36 mutant infections, pUL49 was not found to colocalise with capsids, and was instead found as punctate structures likely corresponding to L particles (Fig. 4.15).

4.6.2. Immuno-EM:

For immuno-EM studies of capsid tegument protein interactions $HFFF_2$ cells were infected at 5 pfu/cell for 24 h, before fixation and processing for Immuno-EM. Sections were probed individually with the following antibodies, #E12-E3 (anti-pUL36), M780 (anti-pUL37) and VP16 (1-21) (anti-pUL48) with a goat secondary antibody conjugated to 10nm gold particles for visualisation.

4.6.2.1. Association of pUL36 with capsids:

In WT HSV-1 infection, pUL36 was detected in extracellular particles (Fig. 4.16). Similarly, cytoplasmic capsid aggregates of FRΔUL37 labelled with gold supporting the presence of pUL36 on these capsids, in agreement with immunofluorescence data (Figs. 4.13 and 4.16). This is in keeping with the close association of pUL36 and the capsid (Coller *et al.*, 2007; Luxton *et al.*, 2006) and particularly with the suggestion that pUL36 might form the innermost layer of the tegument and interact with the pentons (reviewed Mettenleiter, 2004; Zhou *et al.*, 1999). As would be expected no gold particles were associated with capsids in ARΔUL36 infections indicating that binding of the antibody was specific for pUL36 and that none was present on these capsids (Fig. 4.16). What cytoplasmic background labelling was seen in ARΔUL36 infection was similar to that for WT HSV-1 and FRΔUL37 infections. Cytoplasmic capsids of KΔUL36 were not as well

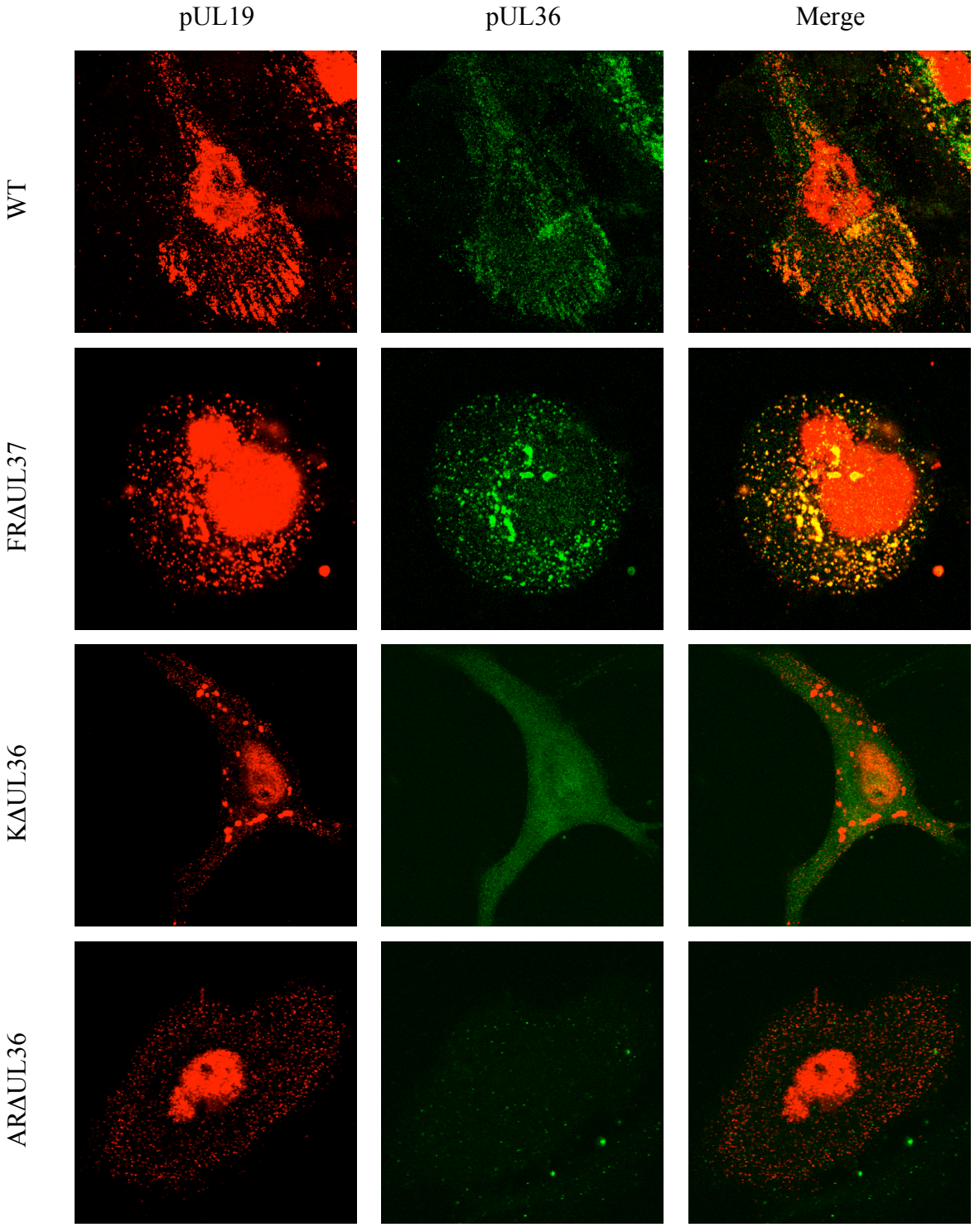
pUL19
pUL36
Merge
WT
FRΔUL37
KΔUL36
ARΔUL36

Figure 4.13: Analysis of pUL19 and pUL36 localisation in infected cells by immunofluorescence.

Replicate monolayers of $HFFF_2$ cells were infected with 5 pfu/cell of WT HSV-1 (WT), FRΔUL37, KΔUL36 or ARΔUL36. Cells were fixed and prepared for immunofluorescence at 24 h pi pUL19 (red) was detected using DM165 mouse antibody and Alexafluor 568-conjugated goat anti-mouse secondary antibody. pUL36 (green) was detected using αVP1-2NT1r rabbit antibody and Alexafluor 488-conjugated goat anti-rabbit secondary antibody.

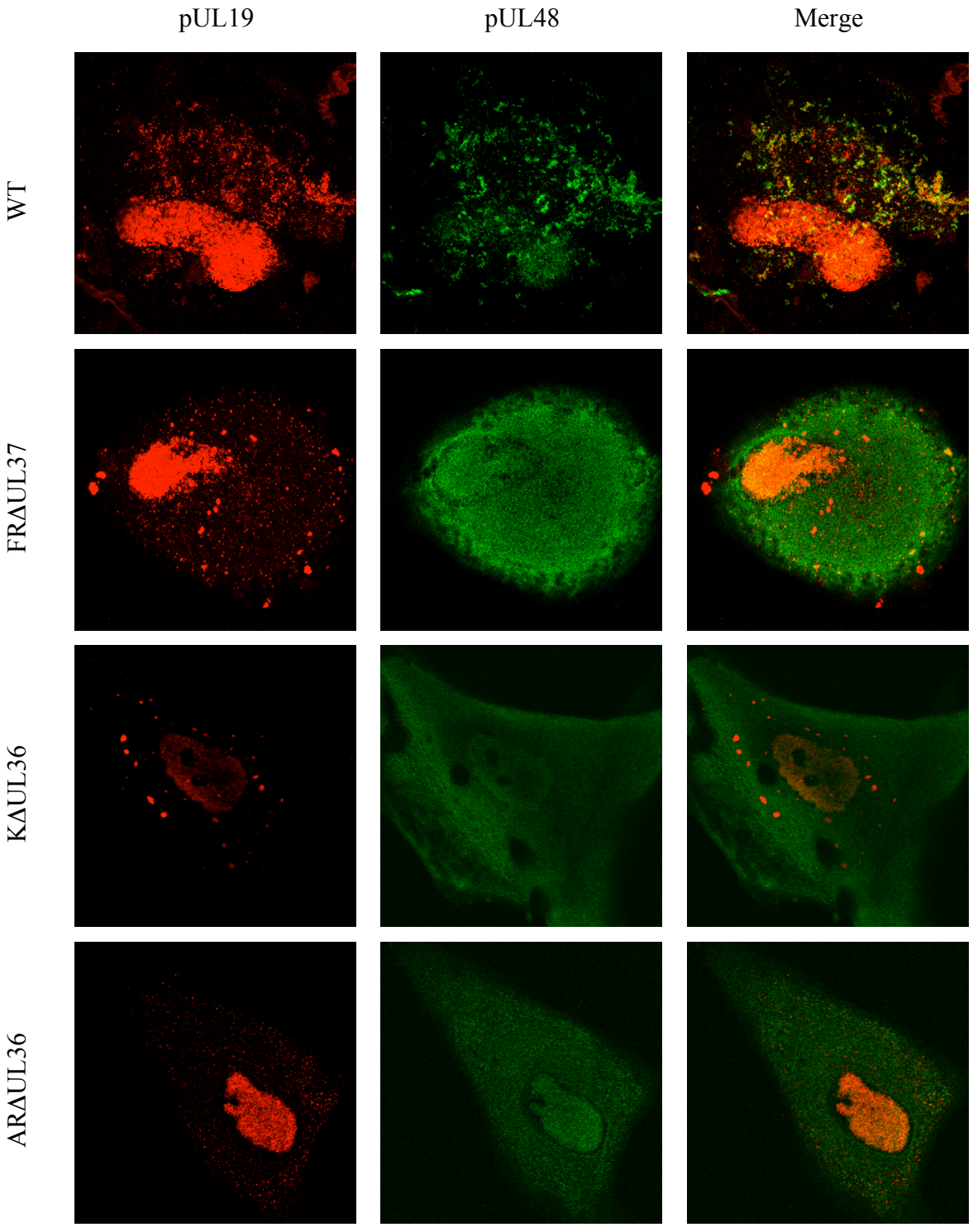
pUL19
pUL48
Merge
WT
FRΔUL37
KΔUL36
ARΔUL36

Figure 4.14: Analysis of pUL19 and pUL48 localisation in infected cells by immunofluorescence.

Replicate monolayers of $HFFF_2$ cells were infected and prepared for immunofluorescence as described for Fig 4.13. pUL19 (red) was detected using 191A rabbit antibody and Alexafluor 568-conjugated goat anti-rabbit secondary antibody and pUL48 (green) was detected using VP16 (1-21) mouse antibody and Alexafluor 488-conjugated goat anti-mouse secondary antibody.

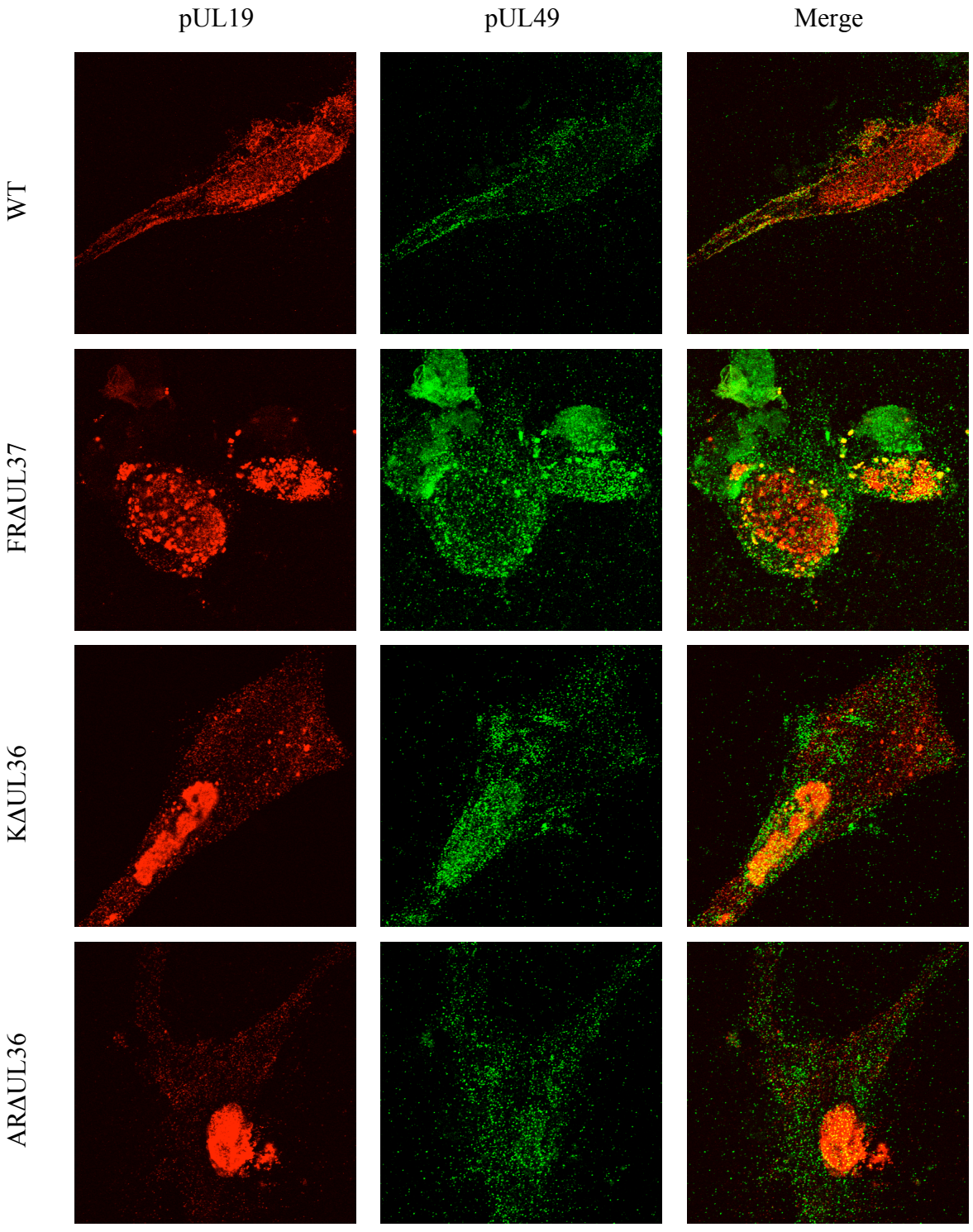
pUL19
pUL49
Merge
WT
FRΔUL37
KΔUL36
ARΔUL36

Figure 4.15: Analysis of pUL19 and pUL49 localisation in infected cells by immunofluorescence.

Replicate monolayers of $HFFF_2$ cells were infected and prepared for immunofluorescence as described for Fig 4.13. pUL19 (red) labelling was as before and pUL49 (green) was detected using AGV031 rabbit antibody and Alexafluor 488-conjugated goat anti-rabbit secondary antibody.

labelled with gold as those of FRΔUL37 but the association of gold with capsids was stronger than that with the bulk cytoplasm suggesting that the N-terminal pUL36 fragment might be present on these capsids. This is in contrast with data from immunofluorescence (Fig. 4.13) but agrees with the presence of this N terminal fragment of pUL36 on capsids as seen in western blots of purified capsids (Fig. 5.3).

4.6.2.2. Association of pUL37 with capsids:

Association of pUL37 with cytoplasmic capsids could not be established as the antibody (M780) failed to recognise pUL37 under the conditions used.

4.6.2.3. Association of pUL48 with capsids:

Extracellular virions and L particles of WT HSV-1 labelled strongly with gold confirming pUL48 was present as would be expected. Cytoplasmic aggregates of FRΔUL37 capsids labelled, although poorly, with gold indicating that some pUL48 might be present, in keeping with immunofluorescence studies. Cytoplasmic capsids of KΔUL36 were occasionally seen labelled with gold, suggesting that only minor amounts of pUL48 might be associated with these capsids. ARΔUL36 cytoplasmic capsids did not label with gold confirming that pUL48 did not associate with these capsids (Fig. 4.17).

From these IF and EM studies, it is clear that pUL36 is associated with cytoplasmic capsids in the absence of pUL37 (Figs. 4.13 and 4.16), indicating that pUL36 may be the first tegument protein recruited to the capsids. Further, the association of pUL36 with cytoplasmic capsids, potentially in combination with outer tegument proteins, is probably the cause of the aggregation seen in FRΔUL37. It is notable that some signal for both pUL48 and pUL49 was associated with pUL36 decorated capsids, by IF even in the absence of pUL37, although this result is not replicated for pUL49 by western blotting of purified cytoplasmic capsids (Fig. 5.7). Such association was not seen in PrV for pUL49 (Klupp *et al.*, 2001b) and as such must be treated carefully. Evidence from analysis of L particles suggests that both pUL36 and pUL37 are required for efficient interaction with other tegument proteins. The mapped binding site for pUL48 is present in pUL36 decorating cytoplasmic capsids of FRΔUL37 (Mijatov *et al.*, 2007), so the necessity for pUL37 in recruiting pUL48 to these capsids remains to be determined. In yeast-2-hybrid screening, interaction of pUL36 and pUL48 is possible independently of pUL37 (Mijatov *et al.*, 2007; Vittone *et al.*, 2005) but this is an artificial system in which to assess such

(A)

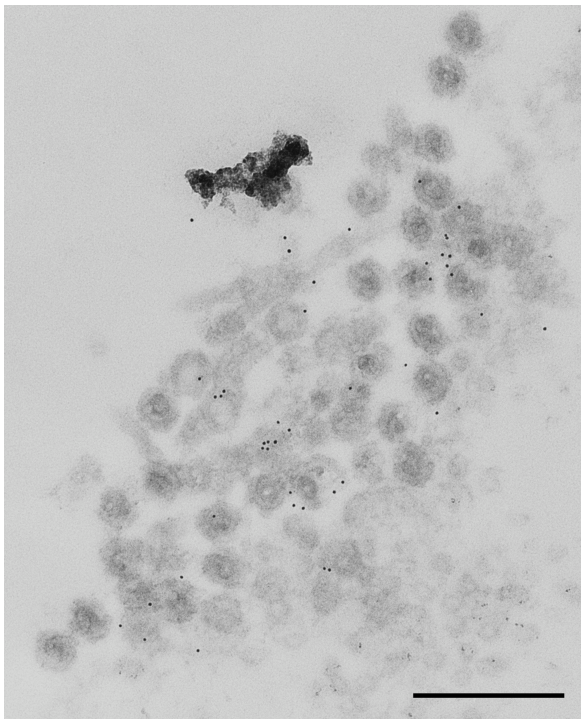

(B)

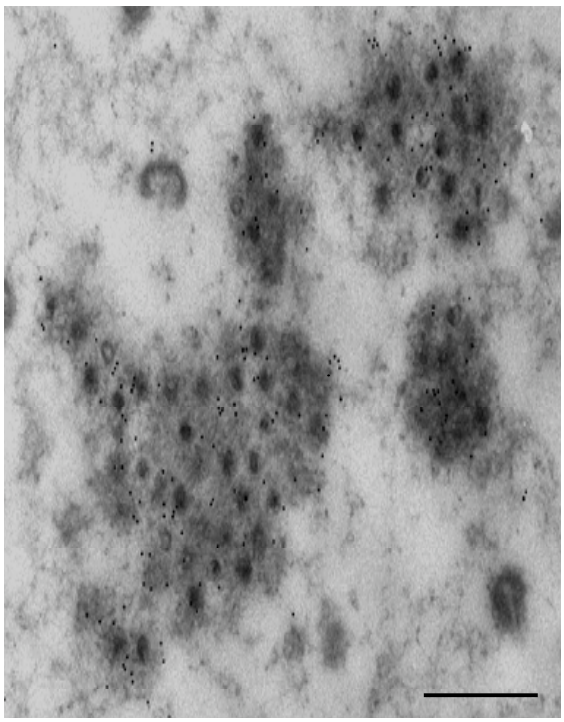

(C)

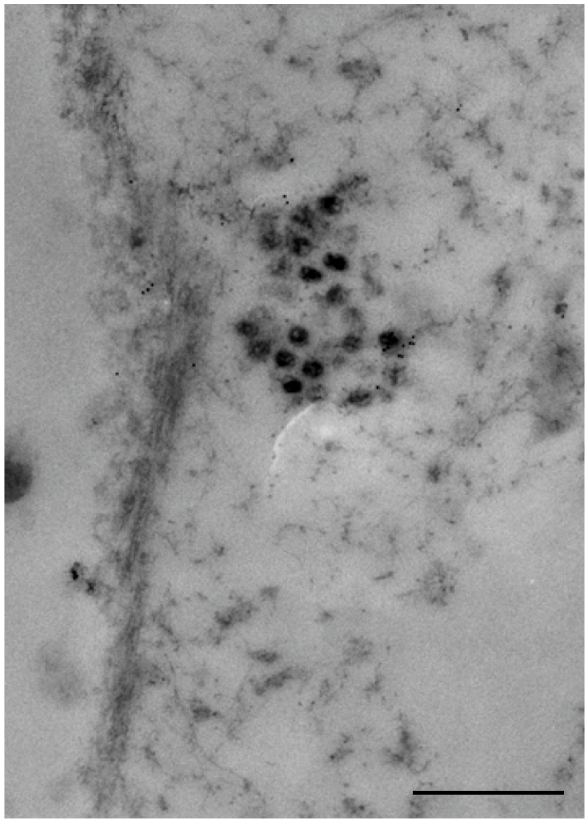

(D)

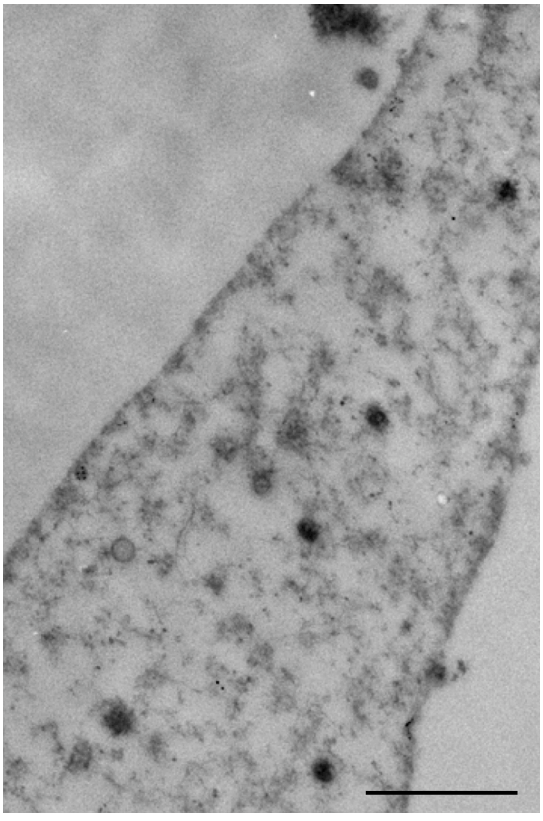

Figure 4.16: Analysis of capsid and pUL36 localisation in infected cells by immuno-EM. Replicate monolayers of $HFFF_2$ cells were infected with 5 pfu/cell of (A) WT HSV-1, (B) FRΔUL37, (C) KΔUL36 or (D) ARΔUL36. After incubation at 37^{o}C for 24 h they were fixed and prepared for immuno-EM. pUL36 was detected using mouse monoclonal serum #E12-E3 and 10nm gold conjugated goat anti mouse IgG secondary antibody. In each case the fields of view show areas of infected cell cytoplasm.
All scale bars 500nm.

(A)

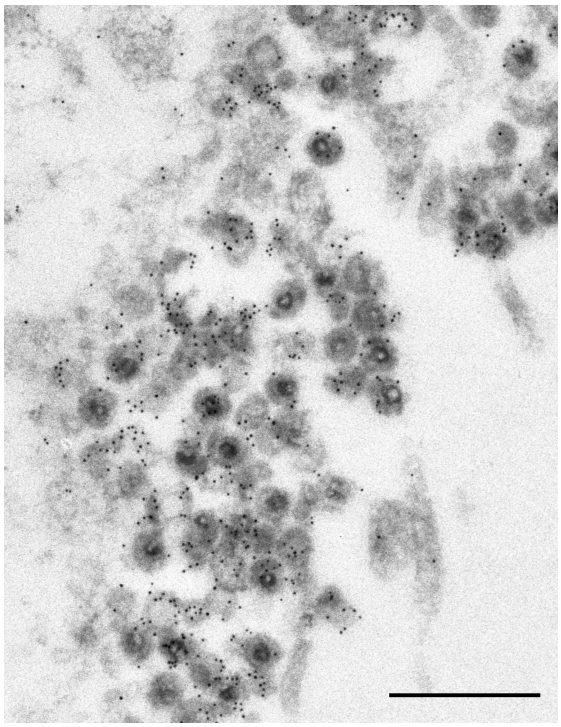

(B)

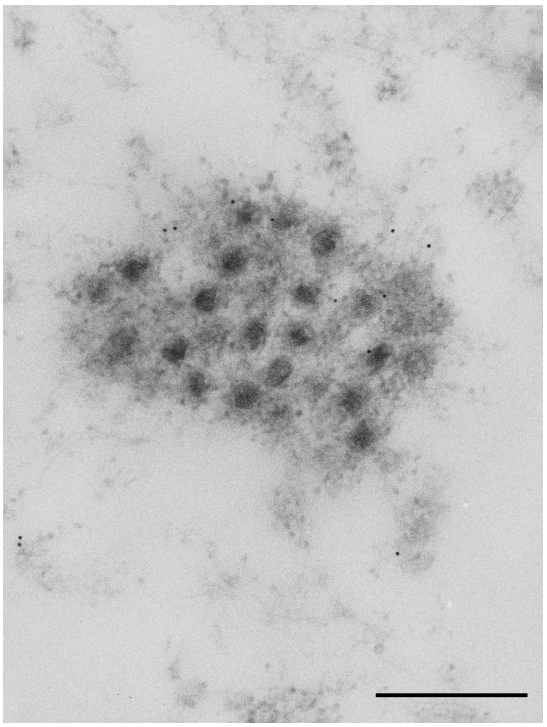

(C)

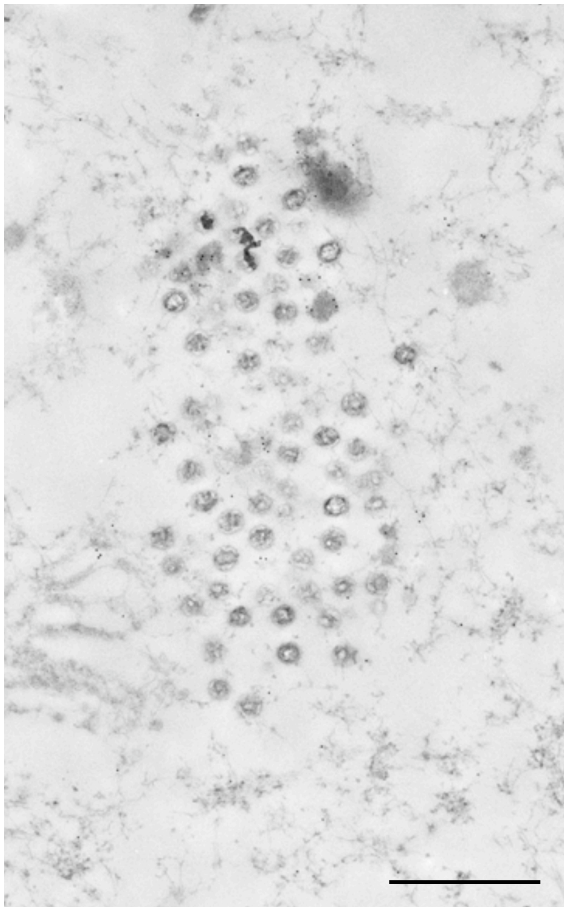

(D)

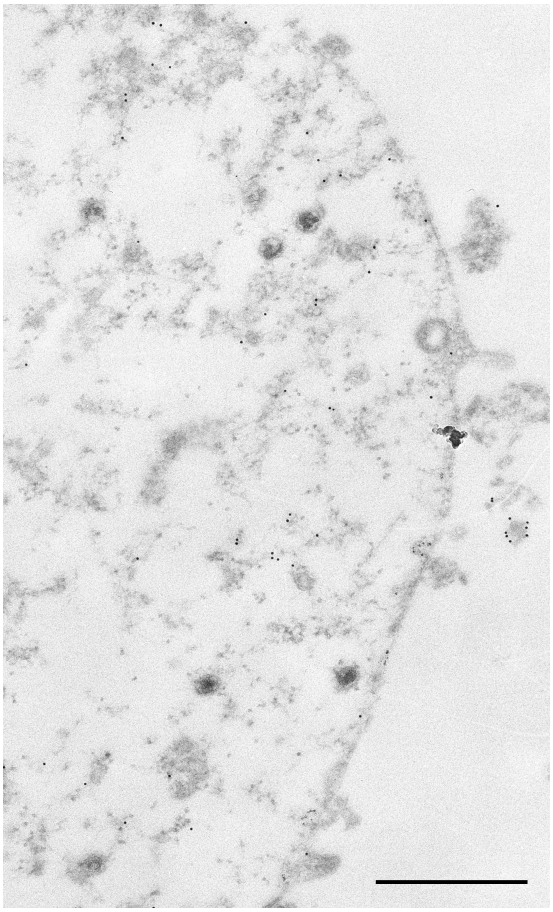

Figure 4.17: Analysis of capsid and pUL48 localisation in infected cells by immuno-EM. Replicate monolayers of $HFFF_2$ cells were infected with 5 pfu/cell of (A) WT HSV-1, (B) FRΔUL37, (C) KΔUL36 or (D) ARΔUL36 and prepared for immuno-EM as described in Fig. 4.16. pUL48 was detected using mouse monoclonal serum VP16 (1-21) and 10nm gold conjugated goat anti mouse IgG secondary antibody. In each case the fields of view show areas of infected cell cytoplasm.
All scale bars 500nm.

interactions. If pUL48 can bind pUL36 in the absence of pUL37 then this might explain the apparent association of pUL49, by IF, with capsid aggregates of FRΔUL37, as pUL48 has been shown to bind pUL49 (Vittone *et al.*, 2005). However, this would imply that pUL37 is not required for acquisition of some members of the outer tegument and that its essential role in secondary envelopment must involve some other function.

The analyses presented in this section suggest that the independent tegument mutants ARΔUL36 and FRΔUL37 behave much as expected based on previous reports (Desai *et al.*, 2001; Desai, 2000; Fuchs *et al.*, 2004; Klupp *et al.*, 2001b; Luxton *et al.*, 2006). The growth of tegument mutants was similar to that of WT HSV-1 on their respective complementing cells, and strains derived from pBAC SR27 contained no detrimental second site mutations. Loss of oriL sequences from pBAC SR27 derived strains did not seem to overly affect the growth of these strains in tissue culture (Table 4.1). Analysis of protein expression in these mutants confirmed the expected absence of either pUL36 and/or pUL37 in accordance with their genotypes (Fig. 4.4). Expression of the outer tegument proteins pUL48 and pUL49 was unaffected by the deletion of either or both inner tegument proteins (Fig. 4.4), and the expression of the N terminal fragment of pUL36 remaining in KΔUL36 was confirmed.

In addition, these analyses have provided data that clarify the effects of deletion of UL36 and UL37 in non-complementing cells. In contrast with the previously reported HSV-1 ΔUL36 mutant, KΔUL36, ARΔUL36 does not exhibit aggregated cytoplasmic capsids, suggesting that the nature of the deletion in KΔUL36 causes this particular phenotype, for which the 43 kDa N terminal fragment of pUL36 appears responsible. The analyses also confirmed previous reports that pUL37 is absolutely required for virion formation in HSV-1 (Desai *et al.*, 2001). However, it did not support a previous study of an HSV-1 mutant lacking pUL37, which reported that there was retention of capsids in the nucleus of infected cells giving rise to a suggestion that pUL37 is involved in nuclear egress (Desai *et al.*, 2001). No evidence for nuclear retention of capsids after deletion of pUL36 or pUL37 was seen in either ARΔUL36 or FRΔUL37, contrasting with reports in both HSV-1 and PrV (Desai *et al.*, 2001; Luxton *et al.*, 2006). Data presented here suggest that the association of C capsids with the nuclear fraction in cells infected with FRΔUL37 was due to copelleting of nuclei and large capsid aggregates during centrifugation (Fig. 4.7).

Analysis of the double deletion mutant ARΔUL36ΔUL37 showed that cytoplasmic C capsids of this mutant display the dispersed phenotype seen in ARΔUL36. This supports

the hypothesis that pUL36 may be added to capsids prior to pUL37 and that presence of pUL36 is necessary and sufficient to cause the formation of the aggregates seen in FRΔUL37 and KΔUL37 (Fig. 4.9; Fig. 4.13) (Desai *et al.*, 2001). Further this analysis has revealed an as yet unreported phenotype for inner tegument deletion mutants lacking both pUL36 and pUL37, involving rearrangement of the nuclear membrane and the formation of vesicles within the perinuclear space. This phenotype appears to be cell type dependent, being least common in BHK-21 cells, of intermediate severity in RS cells and most prominent in $HFFF_2$ cells (Fig. 4.8).

CHAPTER 5

ASSEMBLY OF HSV-1 IN THE ABSENCE OF pUL36 AND pUL37

5. Assembly of HSV-1 in the absence of pUL36 and pUL37

5.1. Acquisition and assembly of tegument

Previous investigations into the functions of pUL36 and pUL37 have highlighted the important roles of these two proteins in the maturation of capsids into virions. The analyses of pUL36 for both HSV-1 and PrV showed that this protein was essential to the formation of mature virions, with C capsids accumulating within the cytoplasm in its absence (Desai, 2000; Fuchs *et al.*, 2004). However, analyses of pUL37 showed differences between HSV-1 and PrV. While mutants of both viruses accumulated C capsids within the cytoplasm, in PrV, enveloped virions were also produced in small numbers. Therefore, pUL37 appeared important for the replication of PrV but not essential for virion assembly as had been reported for HSV-1 (Desai *et al.*, 2001; Klupp *et al.*, 2001b).

Infection with HSV-1 leads to the formation of two distinct extracellular structures, mature virions containing C capsids, tegument and envelope, and light (L) particles. L particles are composed of only tegument and envelope components (Szilagyi & Cunningham, 1991) and as they lack capsids are non-replicative. Their existence makes it clear that tegument components are competent to undergo envelopment in the absence of capsids. Nevertheless, interactions between the capsid and the tegument must presumably be necessary for the incorporation of the capsid into the mature virion.

The tegument has been suggested to have two subdivisions, the inner tegument, which comprises both pUL36 and pUL37, together with pUS3, and the outer tegument, which contains the remaining tegument proteins (Mettenleiter, 2006). Structural studies have suggested that pUL36 may bind directly to capsids and this is supported by studies which identified both pUL36 and pUL37 as present on nuclear capsids (Bucks *et al.*, 2007; Zhou *et al.*, 1999). Since pUL36 and pUL37 are also present in L particles, they represent good candidates to act as linking proteins to connect the capsid and tegument compartments.

The role of individual tegument proteins in L particle formation has not been extensively studied. For PrV it has been shown that L particles are still produced in the absence of pUL37 (Klupp *et al.*, 2001b) and that deletion of pUL48 abolishes inclusion of pUL36 and

pUL37 into these structures (Fuchs *et al.*, 2002a). However to date no such analysis of the requirement for pUL36 and pUL37 in HSV-1 L particles has been undertaken.

5.2. Purification and isolation of capsids and L particles from HSV-1 tegument mutant infections

5.2.1. Purification of capsids

EM analysis showed that infections with inner tegument mutants produce large numbers of nuclear and cytoplasmic capsids (Figs. 4.7 - 4.10). In order to determine their properties, capsid purification was carried out using the procedures described in Methods (section 2.2.9). $1x10^9$ BHK cells were infected with 5 pfu/cell of WT HSV-1, K5ΔZ, or the inner tegument mutants and incubated at 37^{o}C for 24 h. The cells were harvested, separated into nuclear and cytoplasmic fractions, and capsids were released by sonication before banding on sucrose gradients. Nuclear A, B and C capsids, were readily purified from cells infected with WT HSV-1, FRΔUL37, KΔUL36, ARΔUL36 and ARΔUL36ΔUL37 (Fig. 5.1). In all cases they gave a typical gradient pattern with B capsids as the predominant type observed. As expected, capsids were not isolated from the infection with the major capsid protein mutant, K5ΔZ. The mutant K5ΔZ provides a useful control, as any capsids recovered would have to be derived from input virus. The absence of capsids after infection with K5ΔZ demonstrates that the large amount of inoculum used in these infections was not contributing significantly to the capsid profiles shown here.

Relatively few attempts to purify cytoplasmic capsids have been described and there is little information on their structure or composition. Again, as expected, no cytoplasmic capsids were isolated from the K5ΔZ control sample. Interestingly, cytoplasmic capsids were not isolated from WT HSV-1 and FRΔUL37 infections either. In the case of WT HSV-1, most of the cytoplasmic capsids will exit the cell as mature virions and will not accumulate in the cytoplasm as was seen in the tegument mutant infections (Figs. 4.6 - 4.10). Alternatively, de-enveloped tegument is known to be sticky (McLauchlan & Rixon, 1992) and any partially tegumented capsids present in the WT HSV-1-infected cytoplasmic fraction might have aggregated and pelleted with the nuclei as is seen for FRΔUL37 (Fig. 4.12). As shown previously (section 4.5.2 Fig. 4.12), the reason why no capsids were seen on the FRΔUL37 gradient appears to be that during separation of the nuclear and cytoplasmic fractions the large cytoplasmic capsid aggregates co-pelleted with the nuclei.

(A) WT K5ΔZ FRΔUL37 KΔUL36 ARΔUL36

A

B

C

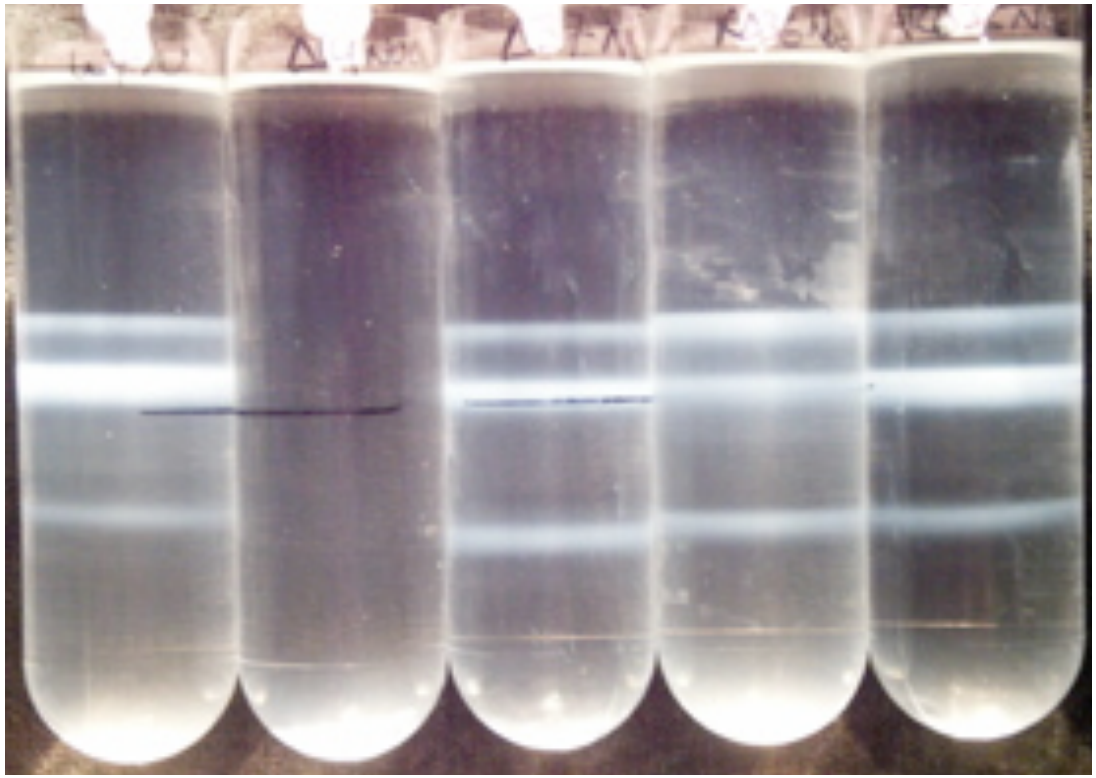

(B) WT ARΔUL36ΔUL37

A

B

C

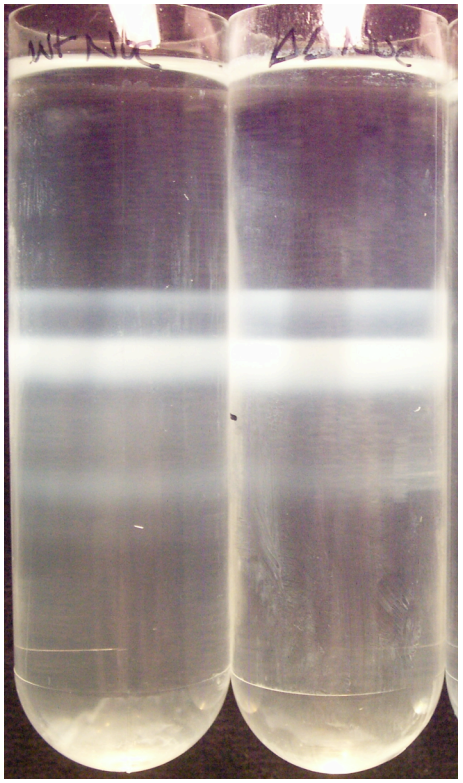

Figure 5.1: Isolation of viral nucleocapsids from the nuclei of infected cells.

Batches of $1x10^9$ BHK cells were infected with 5 pfu/cell of WT HSV-1, K5ΔZ, FRΔUL37, KΔUL36 ARΔUL36 or ARΔUL36ΔUL37. Nuclear and cytoplasmic (see Fig. 5.2) fractions were prepared (section 2.2.9). Viral nucleocapsids were released from the nuclei by sonication and individual capsid species (A, B and C) were separated on 20-50% w/v sucrose gradients.

These capsids were then absent from the cytoplasmic fraction in downstream manipulations. In contrast to WT HSV-1 and FRΔUL37, cytoplasmic A, B and C capsids of KΔUL36, ARΔUL36 and ARΔUL36ΔUL37 (Fig. 5.2) were readily recovered and separated on sucrose gradients, with C capsids being most abundant.

5.2.1.1. Analysis of KΔUL36 cytoplasmic capsids

KΔUL36 and ARΔUL36 show phenotypic differences in capsid distribution by EM, matching the differences reported between KΔUL36 and a ΔUL36 mutant of PrV (section 4.5.1) (Desai, 2000; Fuchs *et al.*, 2004). These viruses differ in the nature of their deletions. Thus, in ARΔUL36 the complete UL36 ORF is deleted (section 4.3) (Roberts *et al.*, 2009), while in KΔUL36 the N terminal 361 codons are retained (Desai, 2000). This raises the possibility that this N terminal 43 kDa fragment of pUL36, which is known to be expressed in KΔUL36 infected cells (section 4.3 Fig. 4.4) (Roberts *et al.*, 2009), might account for the differences in capsid distribution. For the 43 kDa fragment to be responsible it would need to be associated with these capsids. Immunofluorescence studies presented earlier did not detect this fragment of pUL36 in association with capsids (section 4.6.1.1 Fig. 4.13). To determine if this fragment was associated with capsids, and thus responsible for the aggregation of capsids seen in KΔUL36 infection, a 30 ml gradient of purified KΔUL36 cytoplasmic capsids was fractionated in 1ml steps and the capsids were recovered by pelleting at 50,000 rpm for 30 mins (section 2.2.9.1). The fractions were analysed by SDS PAGE and subsequent western blotting (Fig. 5.3). The blot was probed sequentially with antibodies DM165 (anti VP5), to locate the capsid peaks, and MCA406 (anti VP22a scaffolding protein) to differentiate A, B and C capsids. It was also probed with #E12-E3 (anti pUL36) to assess association of the 43 kDa N terminal fragment of pUL36 with the capsids.

The analysis of the gradient fractions revealed two peaks of VP5 corresponding to C (fractions 5-8) and B/A capsids (fractions 12-20) respectively (Fig. 5.3). B capsids were localised by MCA406 to fractions 13-16 and A capsids were assigned to fractions 17 to 18 reflecting the closeness of A and B capsids on the gradient. Analysis of the gradient for the presence of the 43 kDa fragment of pUL36 shows that the presence of this protein correlates with that of VP5. Thus there is a broad peak in the fractions containing the C capsids and a slightly stronger peak in the A- and B- capsid fractions. This sedimentation pattern for the 43 kDa band strongly suggests that it is associated with capsids. A capsid binding domain has not previously been reported in the N terminal region of pUL36, and

(A) WT K5ΔZ FRΔUL37 KΔUL36 ARΔUL36

A

B

C

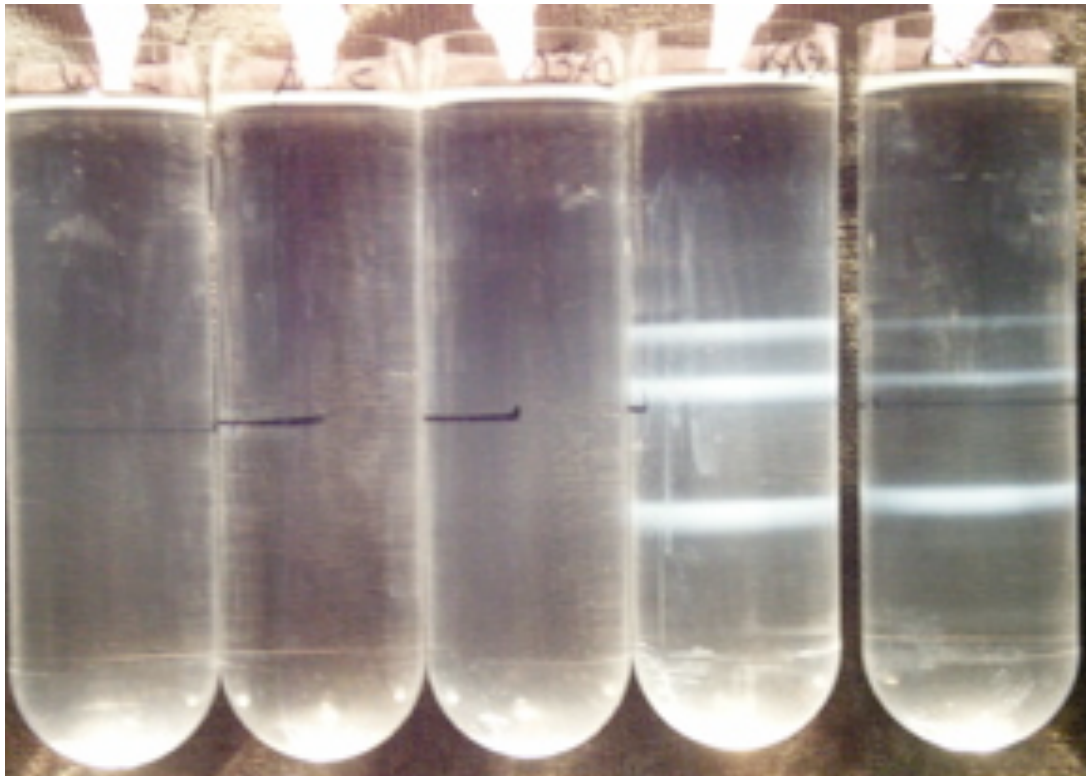

(B) WT ARΔUL36ΔUL37

A

B

C

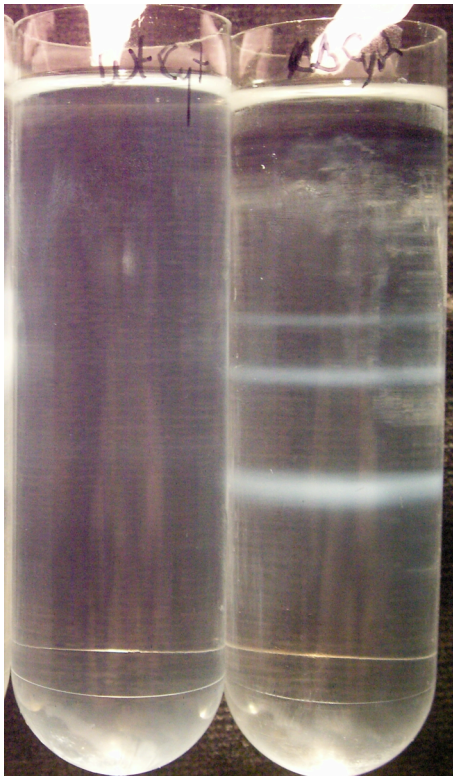

Figure 5.2: Isolation of viral nucleocapsids from the cytoplasm of infected cells.
Viral nucleocapsids were isolated by sonication from the cytoplasm of BHK cells infected as for Fig. 5.1. The individual capsid species (A, B and C) were separated on 20-50% w/v sucrose gradients.

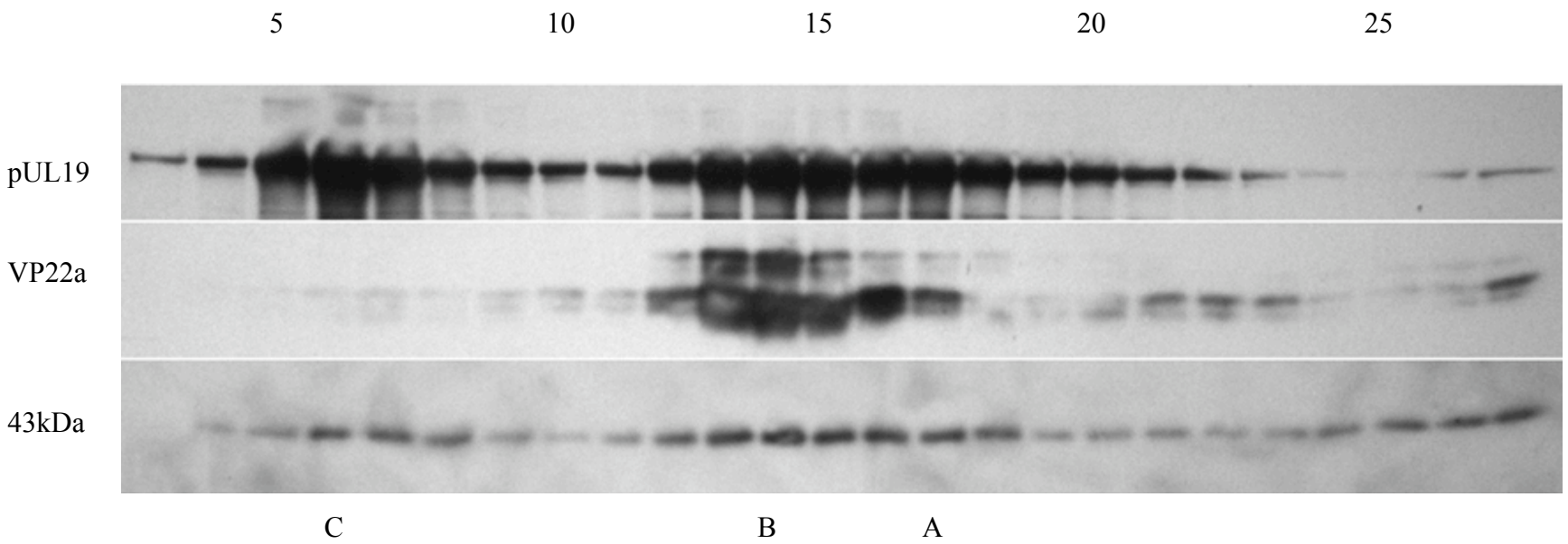
5
10
15
20
25
pUL19
VP22a
43kDa
C
B
A

Figure 5.3: Analysis of cytoplasmic KΔUL36 nucleocapsids.

Viral nucleocapsids isolated from the cytoplasm of KΔUL36 infected cells were separated on sucrose gradients as shown in Fig. 5.2. The gradient was collected from the bottom in 30 equal fractions and fractions 3 to 27 were subjected to SDS-PAGE and transferred to nitrocellulose membrane for western blotting. The membrane was probed sequentially with the anti-pUL36 mAb #E12-E3 (43 kDa), DM165 (pUL19) and MCA406 (VP22a). DM165 was used to show the distribution of all capsid types and MCA406 to localise B capsids. The positions at which A, B and C capsids migrated are indicated below the blot, while fractions 5, 10, 15, 20, and 25 are labelled above.

currently the only known interacting domain has been mapped to the C terminal 62 residues which interact with the minor capsid protein, pUL25 (Coller *et al.*, 2007). Therefore, these results with KΔUL36 appear to imply the presence of second capsid binding sequence in the N-terminal portion of this very large protein and suggest that both the N and C termini of pUL36 are capable of interacting with capsids.

5.2.2. Purification of L particles

Although the identification of L particles showed that tegument formation and envelopment do not require the presence of capsids, little use has been made of them to study other constraints on particle assembly. As mentioned above the production and composition of capsidless particles was investigated for a UL48 deletion mutant in PrV (Fuchs *et al.*, 2002a). In addition, studies on UL36 and UL37 deletion mutants of PrV reported the presence of capsidless particles (equivalent to HSV-1 L particles) on the surface of infected cell sections examined by EM, but did not examine purified L particles or analyse their composition (Klupp *et al.*, 2002; Klupp *et al.*, 2001b). However, even these limited analyses have not been done in HSV-1. Therefore, to study the roles of pUL36 and pUL37, L particles were prepared from the growth medium of the BHK cells infected for capsid preparation (section 5.2.1). Concentrated extracellular particles were separated on Ficol gradients and the resulting profiles were examined to visualise virions and L particles (Fig. 5.4). As expected, infection with WT HSV-1 produced both virions and L particles, with a sharp band corresponding to virions and an upper diffuse band of L particles evident on the gradient (Fig. 5.4). L particles were also produced by K5ΔZ infected cells in the absence of the major capsid protein, but, as expected, no virion band was seen (Fig. 5.4). Similarly, infections with the tegument mutants FRΔUL37, KΔUL36, ARΔUL36 and ARΔUL36ΔUL37 (Fig. 5.4) produced L particles but not extracellular virions. This shows that pUL36 or pUL37 are not necessary for the other tegument and envelope components to assemble and be exocytosed.

5.2.2.1. Analysis of L particles produced by HSV-1 tegument mutant infections

To examine the protein composition of the particles produced by WT HSV-1, K5ΔZ and the tegument mutants, 30 ml gradients were fractionated into 10 equal fractions of ~3ml and the particles were pelleted by centrifugation at 50,000 rpm for 30 mins. Proteins were then separated on 10% SDS PAGE gels and transferred to nitrocellulose membranes for

(A) WT K5ΔZ FRΔUL37 KΔUL36 ARΔUL36

LP

V

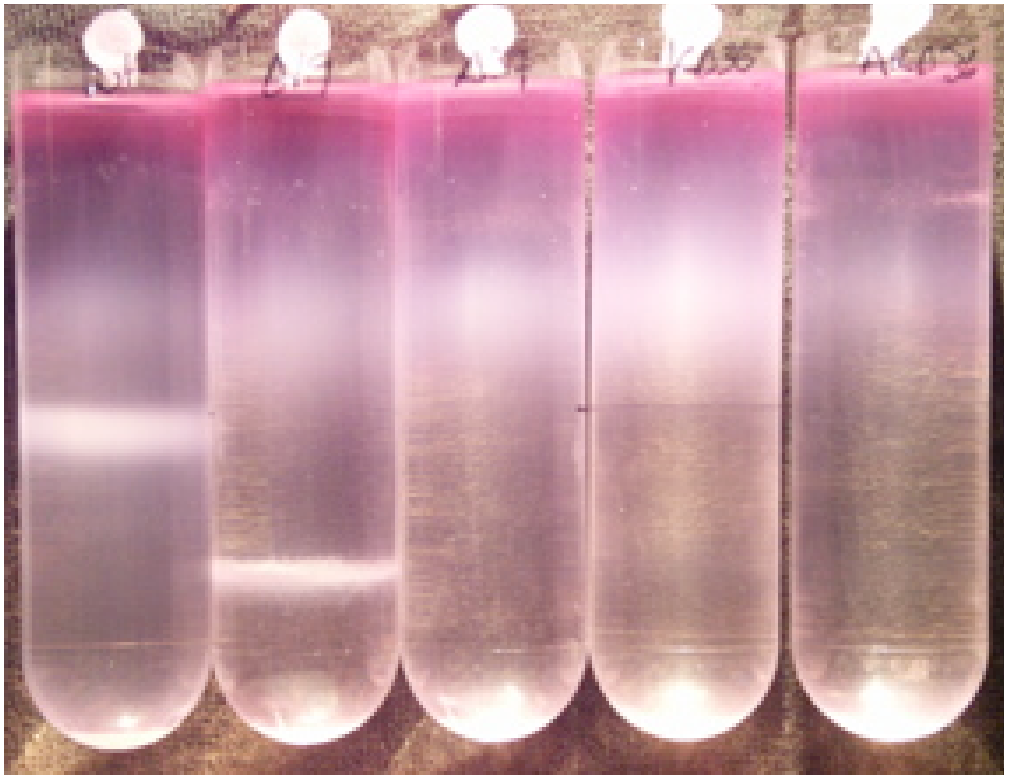

(B) WT ARΔUL36ΔUL37

LP

V

Figure 5.4: Isolation of virions and L particles from the extracellular medium of infected cells.

Batches of $1x10^9$ BHK cells were infected with 5 pfu/cell of WT HSV-1, K5ΔZ, FRΔUL37, KΔUL36, ARΔUL36 (A) or ARΔUL36ΔUL37 (B). Virions and L particles were prepared from the culture medium (section 2.2.10) and separated on 5-15% w/v Ficol gradients. The positions of virions (V) and L-particles (LP) are indicated.

western blotting. A sample of purified WT HSV-1 L particles was used as a control on each blot.

Blots were probed sequentially with either antibodies AGV031 (anti pUL49), E12-E3 (anti pUL36) and M780 (anti pUL37), or VP16 (1-21) (anti pUL48) and mAb4846 (anti gD). Analysis of gradient fractions from WT HSV-1, K5ΔZ, and the tegument mutants FRΔUL37, ARΔUL36 and KΔUL36 (Fig. 5.5) showed that incorporation of pUL49 (VP22) into L particles was unaffected by the presence or absence of pUL36 or pUL37 meaning that this protein could serve as a marker for the localisation of extracellular particles on the fractionated gradient. Incorporation of pUL48 was also assessed and found to mirror the results for pUL49 (Fig. 5.6). The envelope protein gD was widely distributed over the gradient but peaks were observed corresponding to the position of virions and L particles (Fig. 5.6). pUL36 was detected in fractions 1-6 of the WT HSV-1 gradient, which corresponds to the positions of virions and L particles, and in fractions 4-6 of the K5ΔZ gradient, which contained the L particle fractions. The distribution of pUL37 was similar with peaks coincident with those of pUL36 (Fig. 5.5). Unsurprisingly, pUL36 was absent from ARΔUL36 L particles. Unexpectedly, however, pUL37 was also missing from ARΔUL36 L particles (Fig. 5.5). Furthermore, FRΔUL37 L particles also lacked both pUL36 and pUL37 (Fig. 5.5). Such behaviour implies that pUL36 and pUL37 are mutually dependent for incorporation into L particles and suggests that they must form a complex for incorporation into tegument.

Analysis of KΔUL36 L particles revealed that full-length pUL36 was missing and, as might be inferred from the phenotype of ARΔUL36, pUL37 was also absent. However, the N terminal 43 kDa fragment of pUL36 that is expressed by this mutant was detected and showed a similar distribution across the gradient to pUL49 (Fig. 5.5). This suggests that this fragment (residues 1- 361) was being incorporated into the tegument. The interactions which might direct the incorporation of this fragment of pUL36 are not clear. One possibility could be an interaction with pUL48 (Lee *et al.*, 2008; Vittone *et al.*, 2005). The binding site of pUL48 has been mapped by yeast-2-hybrid screening to the N terminal half of pUL36 (residues 1-1874) (Lee *et al.*, 2008; Vittone *et al.*, 2005), with further data suggesting that the binding site lies between residues 124-511 (Mijatov *et al.*, 2007). If the pUL48 binding site does indeed lie between residues 124-511 of pUL36 then it would not be fully contained in the 43 kDa fragment of pUL36. However, interaction with pUL48 cannot be ruled out as the precise limits of the interaction domain have not been determined. The only other interaction shown by yeast-2-hybrid, for pUL36, is with

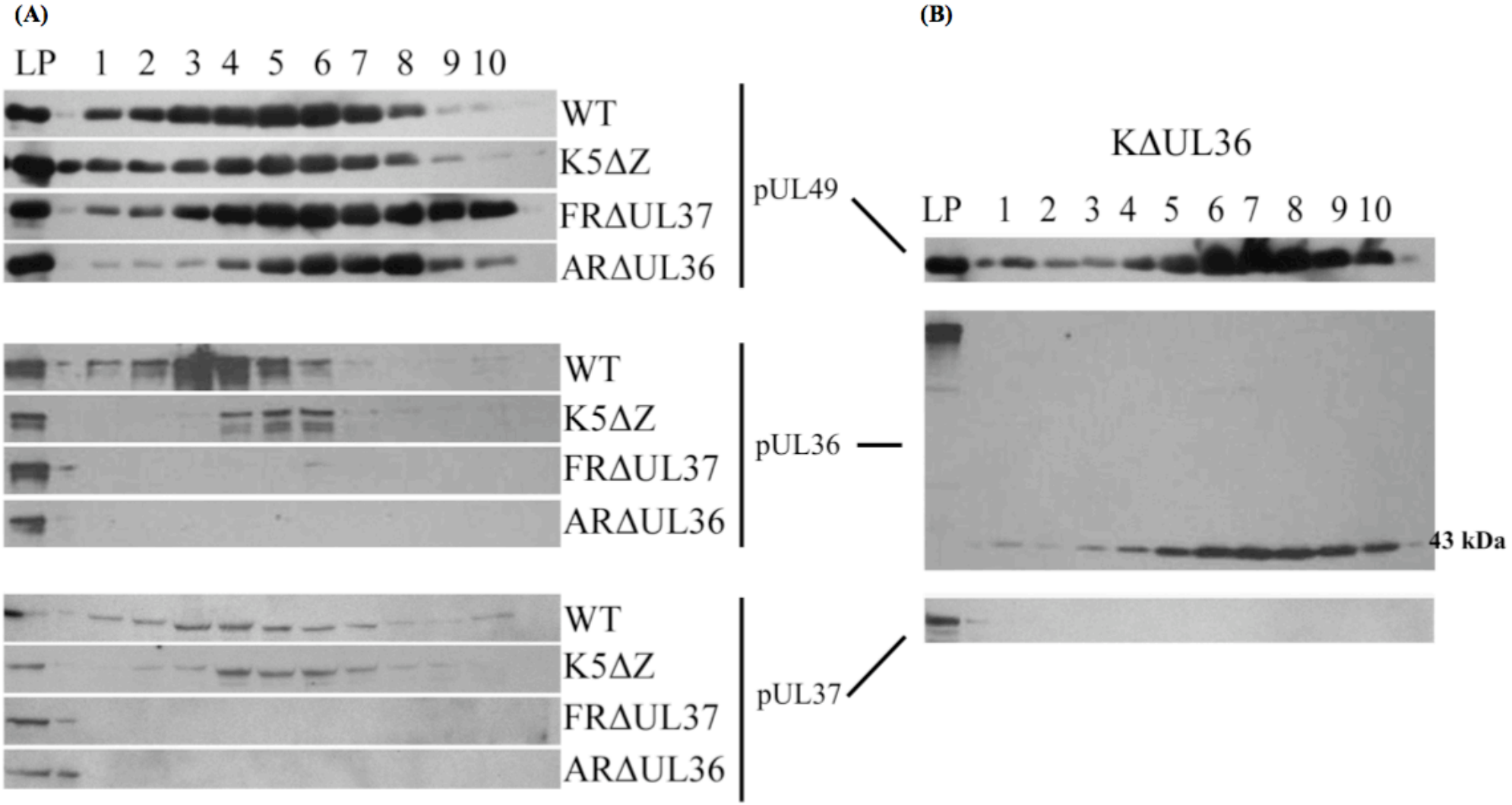
(A)
LP 1 2 3 4 5 6 7 8 9 10
WT
K5ΔZ
FRΔUL37
ARΔUL36
pUL49
WT
K5ΔZ
FRΔUL37
ARΔUL36
pUL36
WT
K5ΔZ
FRΔUL37
ARΔUL36
pUL37
(B)
KΔUL36
LP 1 2 3 4 5 6 7 8 9 10
43 kDa

Figure 5.5: Protein content of extracellular particles from cells infected with HSV-1 inner tegument mutant viruses.

Virions and L particles from cells infected with WT HSV-1, K5ΔZ, FRΔUL37, KΔUL36, or ARΔUL36 were separated on 5-15% w/v Ficol gradients as shown in Fig. 5.4. Gradients were collected from the bottom in 10 equal fractions, subjected to SDS-PAGE and transferred to nitrocellulose membranes for western blotting. The membranes were probed sequentially with #E12-E3 (pUL36), M780 (pUL37) and AGV031 (pUL49). A control sample of HSV-1 strain 17+ L particles (LP) was run on each gel. Fraction numbers are given above the blots.

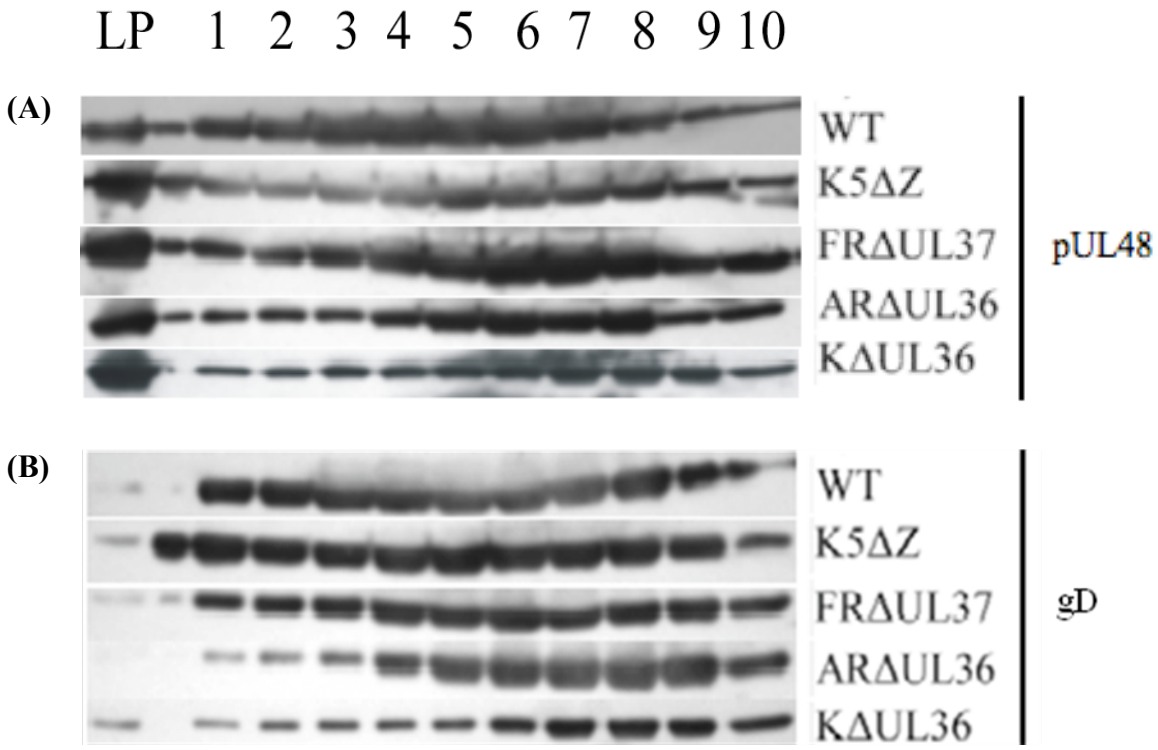
LP 1 2 3 4 5 6 7 8 9 10
(A)
WT
K5ΔZ
FRΔUL37
ARΔUL36
KΔUL36
pUL48
(B)
WT
K5ΔZ
FRΔUL37
ARΔUL36
KΔUL36
gD

Figure 5.6: Further examination of the protein content of extracellular particles from cells infected with HSV-1 inner tegument mutant viruses.

Gradient fractions of WT HSV-1, K5ΔZ, FRΔUL37, KΔUL36, or ARΔUL36 virions and L particles were analysed by western blotting as shown in Fig 5.5. The membranes were probed sequentially with VP16 (1-21) (pUL48) and mAb4846 (gD). A control sample of HSV-1 strain 17+ L particles (LP) was run on each gel. Fraction numbers are given above the blots.

pUL37, and pUL37 is absent from these L particles. This confirms the 43 kDa fragment lacks the domain that interacts with pUL37, which has been mapped to residues 512 to 767 (Vittone *et al.*, 2005) and shown to involve F593 and E596 (Mijatov *et al.*, 2007). Therefore the incorporation of this fragment is not reliant on interaction with pUL37, but it may be incorporated through an interaction with pUL48. Alternatively, residues 1-361 may contain a previously unreported interaction with other tegument components.

Interestingly, the pUL48 and pUL49 immunoblots appear to show that L particles produced by the ΔUL36 and ΔUL37 mutants extended higher up the gradients than those of WT or K5ΔZ. The reason for this is not known but it suggests that the presence of these inner tegument proteins may have some effect on the size or structure of L particles.

5.3. Capsid-tegument interaction: reconstruction of cytoplasmic capsids isolated from HSV-1 tegument mutant infections

Interaction between the capsid and tegument is important for the formation of mature virions, however the nature of this interaction currently remains the subject of intense speculation. Since the reconstruction of intact HSV-1 virions by Zhou *et al*. (1999) many have interpreted the additional tegument density seen at the penton vertices as definitive evidence of the interaction of pUL36 with capsids. However, it is important to note that the authors stated that their proposal that this additional density was pUL36 was speculative, and was based on the estimated mass of the tegument density seen in the reconstruction and previous biochemical data regarding pUL36. More recently, Trus *et al*., (2007) performed reconstruction of nuclear capsids of WT HSV-1 and a UL25 minus mutant (KUL25NS) and proposed that the inner part of the density seen by Zhou *et al*. (1999) is formed by a heterodimer of pUL25 and pUL17. This interpretation was based on the observation that pUL25 and pUL17 were found on WT HSV-1 nuclear A and B capsids at lower levels than on nuclear C capsids and this correlated with the absence of a "C capsid specific component (CCSC)" from nuclear A capsids of WT HSV-1. Unfortunately, no C capsids are recovered from infections in the absence of pUL25 or pUL17 preventing direct comparison of C capsids with and without pUL25 and pUL17 (McNab *et al.*, 1998; Thurlow *et al.*, 2006). The authors suggest that the absence of the CCSC from WT nuclear A and B capsids may be due to low occupancy resulting in poor resolution of the CCSC or

from disorder of pUL25 and pUL17 obscuring their contribution to the density map once symmetry is imposed.

In a direct attempt to determine whether pUL36 (or pUL37) was responsible for some or all of the penton-associated density, cytoplasmic capsids produced by the inner tegument mutants were examined. The aim of identifying the penton associated tegument material was dependent on being able to purify and compare cytoplasmic C capsids from cells infected with the inner tegument mutants. As shown in Figure 5.2, cytoplasmic capsids of ARΔUL36 could be readily purified. However, this was not the case with FRΔUL37. Their tendency to aggregate meant that they were not amenable to sucrose gradient separation and they also proved recalcitrant to alternative attempts at isolation. However, after repeated attempts, small amounts of purified FRΔUL37 capsids were obtained from infection of HeLa cells which had been observed to produce fewer and smaller capsid aggregates (D. Pasdeloup pers. comm.). Capsids produced in this manner were used for cryo-EM imaging and icosahedral reconstruction.

To determine the identity of specific structures identified by cryo-EM reconstruction, it is necessary to know the protein compositions of the capsids being examined. This was complicated by the difficulty in preparing FRΔUL37 cytoplasmic capsids. However, immunofluorescence and immuno-EM studies on the mutants ARΔUL36 and FRΔUL37 confirmed that cytoplasmic capsids of FRΔUL37 were associated with pUL36 and potentially with pUL48, whilst capsids of ARΔUL36 did not associate with either protein (section 4.6). Further analysis of capsid composition by western blotting confirmed the presence of pUL36 in the FRΔUL37 cytoplasmic capsid sample and its absence from ARΔUL36 cytoplasmic capsids. Neither pUL37 nor pUL49 were detected with the FRΔUL37 cytoplasmic capsids, whilst some pUL49 was present in the ARΔUL36 cytoplasmic capsid sample, in contrast to previous immunofluorescence data (Fig. 5.7, Fig. 4.15). Interestingly, pUL48 was present in the cytoplasmic capsid samples of both FRΔUL37 and ARΔUL36 (Fig. 5.7). In order to confirm the presence of these proteins on the capsids, it would be desirable to perform such analyses across a fractionated gradient rather than on the pooled capsid pellets as this would assess their distribution with respect to the capsids. This was not possible due to the low recovery of FRΔUL37 cytoplasmic capsids. Both pUL25 and pUL17 were found to be present on ARΔUL36 cytoplasmic capsids (Fig. 5.8.) the presence of these proteins on FRΔUL37 cytoplasmic capsids was not verified due to the small quantities recovered.

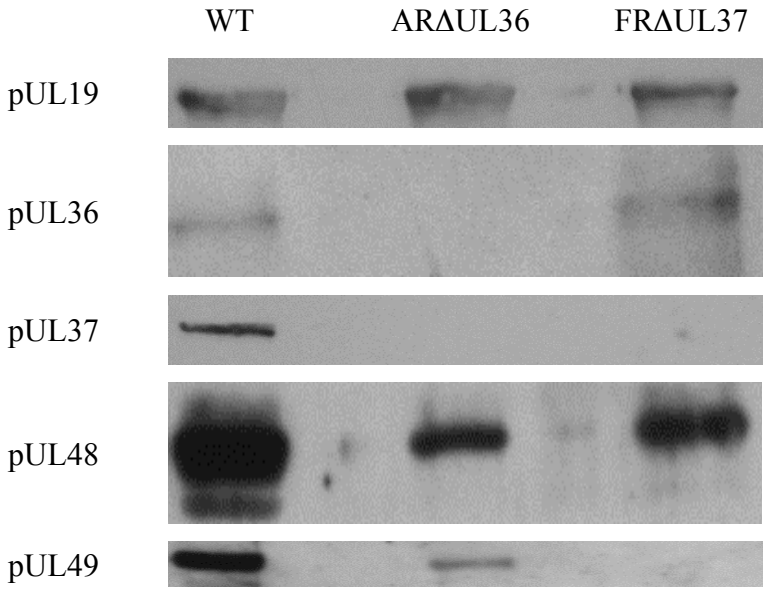

Figure 5.7: Protein composition of cytoplasmic C capsids purified from ARΔUL36 and FRΔUL37 infections

Cytoplasmic C capsids, of ARΔUL36 and FRΔUL37, purified from infected cells were subjected to western blotting. WT HSV-1 virions (WT) were used as a control, The membranes were probed sequentially with DM165 (pUL19), M780 (pUL37), AGV031 (pUL49), #E12-E3 (pUL36), and VP16 (1-21) (pUL48). Because of the difficulty in purifying FRΔUL37 capsids, the samples were equalised for pUL19 content.

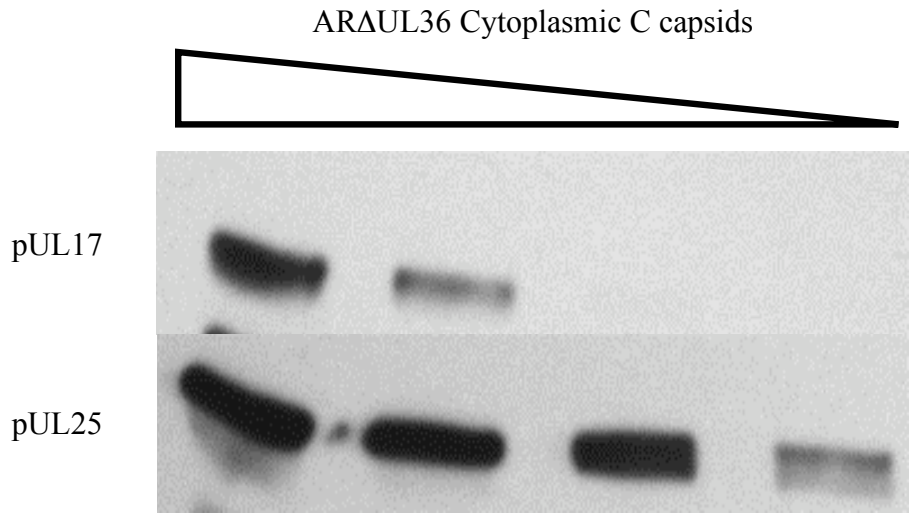

Figure 5.8: Association of the minor capsid proteins pUL17 and pUL25 with purified cytoplasmic C capsids of ARΔUL36

Sequential two fold dilutions of purified cytoplasmic C capsids of ARΔUL36 (Fig. 5.2) were separated by SDS-PAGE and subjected to western blotting to establish the presence of the minor capsid proteins pUL17 and pUL25. The membrane was probed sequentially with UL17 (pUL17) and UL25 (pUL25). The left most lane contains the highest volume of capsid sample decreasing in each subsequent lane to the right.

Cryo-EM imaging and icosahedral reconstruction of HSV-1 WT nuclear B capsids, and ARΔUL36 and FRΔUL37 cytoplasmic C capsids were carried out by Rebecca Pink, Walt Adamson and David Bhella. The structure of WT nuclear B capsids has been well characterised and these were included to allow comparison with the capsid structures determined for the inner tegument mutants. In line with previous studies, reconstruction of WT HSV-1 B capsids revealed the characteristic T = 16 symmetry of angular mature herpesvirus capsids and confirmed that there was no obvious 'extra' density associated with the pentons (Newcomb *et al.*, 1993; Zhou *et al.*, 1999; Zhou *et al.*, 1994) (Fig. 5.9). The reconstructed ARΔUL36 and FRΔUL37 cytoplasmic C capsids also had the characteristic shape and symmetry of mature angular HSV-1 capsids (Figs. 5.10 and 5.11). Close examination of the ARΔUL36 capsid reconstruction shows that it has no notable differences from the WT B capsid structure apart from a small amount of extra density associated with the Ta and Tc triplexes (nomenclature of Zhou *et al.*, 1994) (Fig 5.10). This density is in the approximate position previously ascribed to the CCSC but is somewhat smaller (Trus *et al.*, 2007). The large amount of extra density present on virion vertices was not seen on these ARΔUL36 cytoplasmic capsids. In contrast, the reconstruction of the FRΔUL37 cytoplasmic C capsids was markedly different in appearance from that of the WT B capsids and revealed the clear presence of a penton associated density extending from the Tc triplex via the peripentonal hexon and Ta triplex, before reaching the penton crown. This density is essentially identical to the extra density seen at the capsid vertices in the reconstruction of intact virions (Zhou *et al.*, 1999). Furthermore, unlike the CCSC (Trus *et al.*, 2007), it extends to the upper part of the penton (Figs. 5.11 and 5.12).

The extra density seen on the ARΔUL36 cytoplasmic C capsids demonstrates that at least this portion of the vertex-associated additional densities seen in virion reconstructions is not composed of pUL36 as originally suggested by Zhou *et al*. (1999). It therefore supports the claim by Trus *et al*. (2007) that the inner portions of this density, which they designated as the CCSC, could represent a heterodimer of the minor capsid proteins pUL25 and pUL17. The presence of pUL17 and pUL25 on purified ARΔUL36 cytoplasmic C capsids has been verified by western blotting (Fig. 5.8), thereby increasing the likelihood that these proteins account for the density seen here. However, the amount of additional density on the ARΔUL36 capsids was smaller than the CCSC and corresponded closely to that part which was suggested to represent pUL25 (Trus *et al.*, 2007). The reason for this difference is not clear. It may reflect differences in the abundance or stability of these minor capsid proteins on the different types of capsids used in the two studies. Indeed, Trus *et al*. (2007) reported that pUL25 was present in a higher copy number than pUL17 in their capsid

(A)

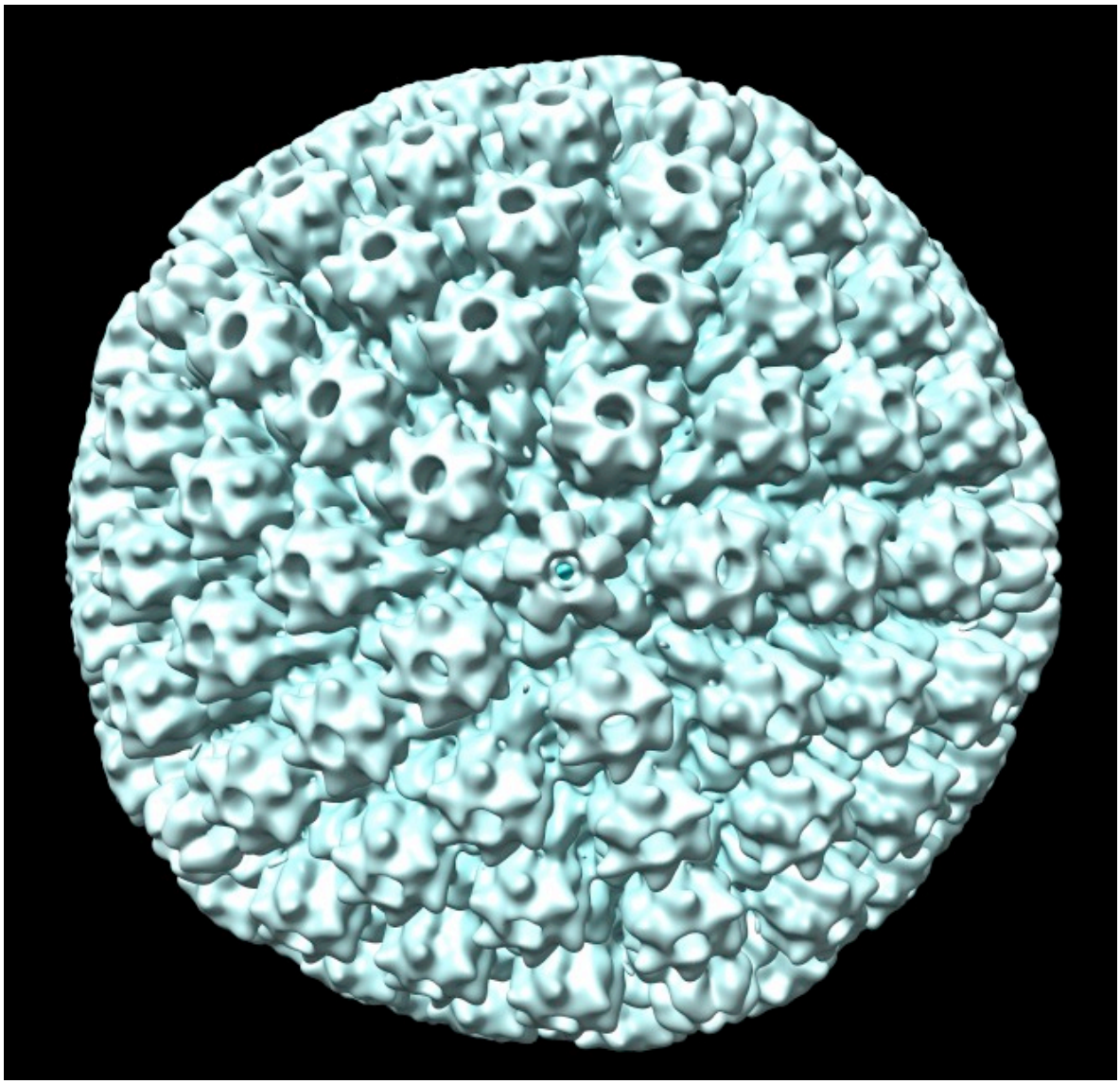

(B)

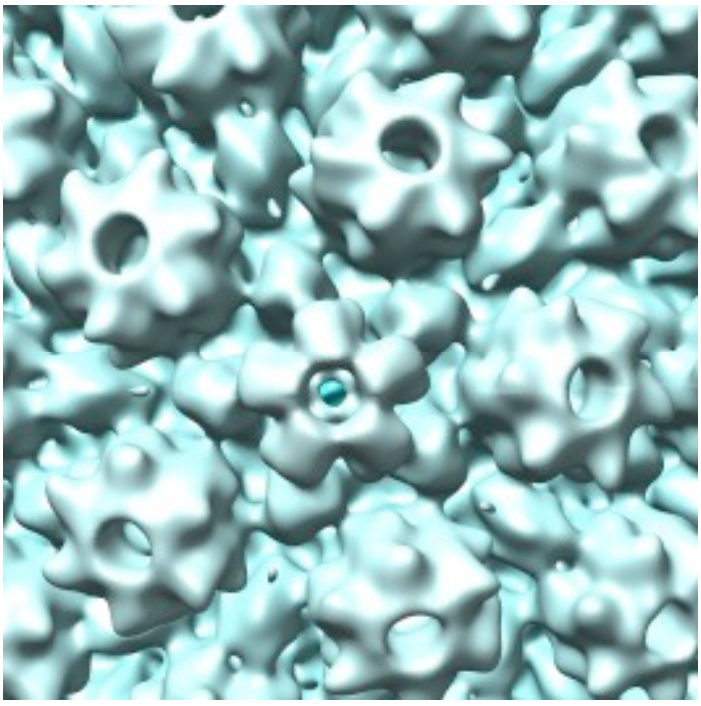

Figure 5.9: Reconstruction of nuclear WT HSV-1 B capsids.

B capsids were prepared from the nuclei of BHK cells infected with 5 pfu/cell of WT HSV-1 and purified on 20-50% w/v sucrose gradients as described in section 2.2.9. They were vitrified and visualised in a JEOL 2200 cryo-electron microscope at liquid nitrogen temperature.

(A) A ~24Å resolution reconstruction of the WT HSV-1 nuclear B capsid viewed looking down a 5 fold axis, from 146 particles.

(B) Enlargement of the area immediately surrounding the vertex showing the absence of density linking the peripentonal hexons to the penton crown.

(A)

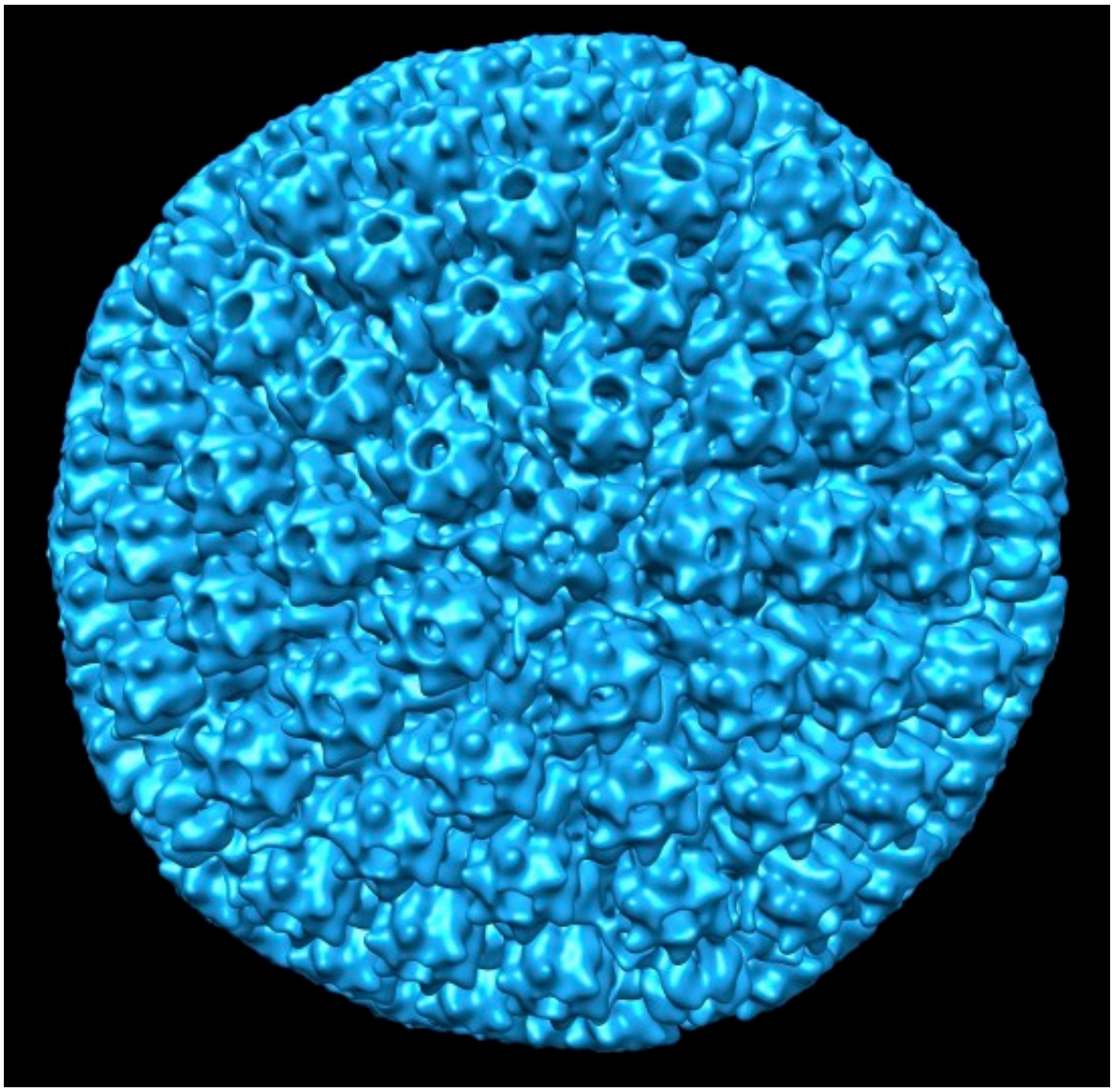

(B)

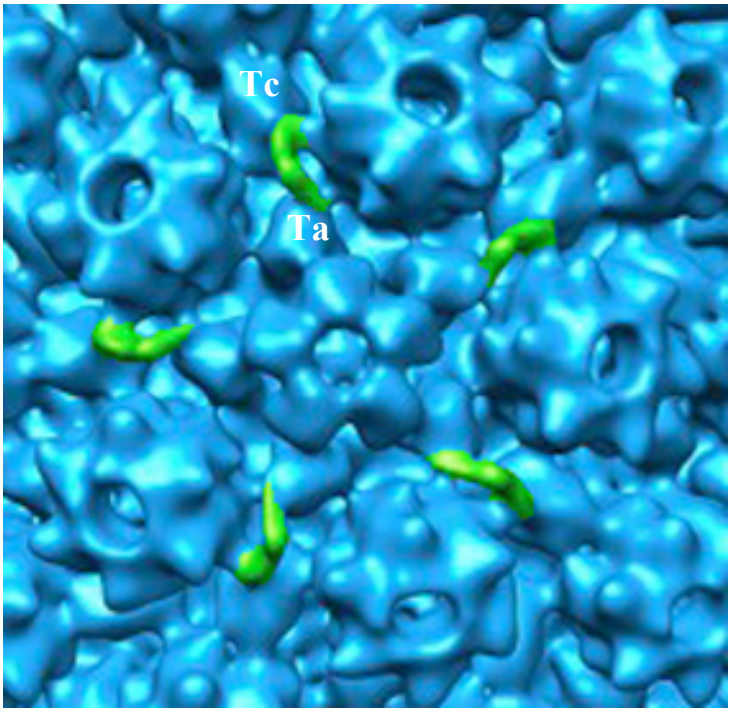

Figure 5.10: Reconstruction of ARΔUL36 cytoplasmic C capsids.

C capsids were isolated from the cytoplasm of BHK cells infected with 5 pfu/cell of ARΔUL36 and purified on 20-50% w/v sucrose gradients as described in section 2.2.9. They were vitrified and visualised in a JEOL 2200 cryo-electron microscope at liquid nitrogen temperature.

(A) A ~24Å resolution reconstruction of the ARΔUL36 cytoplasmic C capsid viewed looking down a 5 fold axis, from 834 particles.

(B) Enlargement of the area immediately surrounding the vertex. The vertex associated densities not seen in the WT HSV-1 B capsid reconstruction (Fig. 5.9) are coloured in green. Ta and Tc mark the triplexes between the penton and the P hexon, and between the C and P hexons respectively from the nomenclature of Zhou *et al*. (1994)

(A)

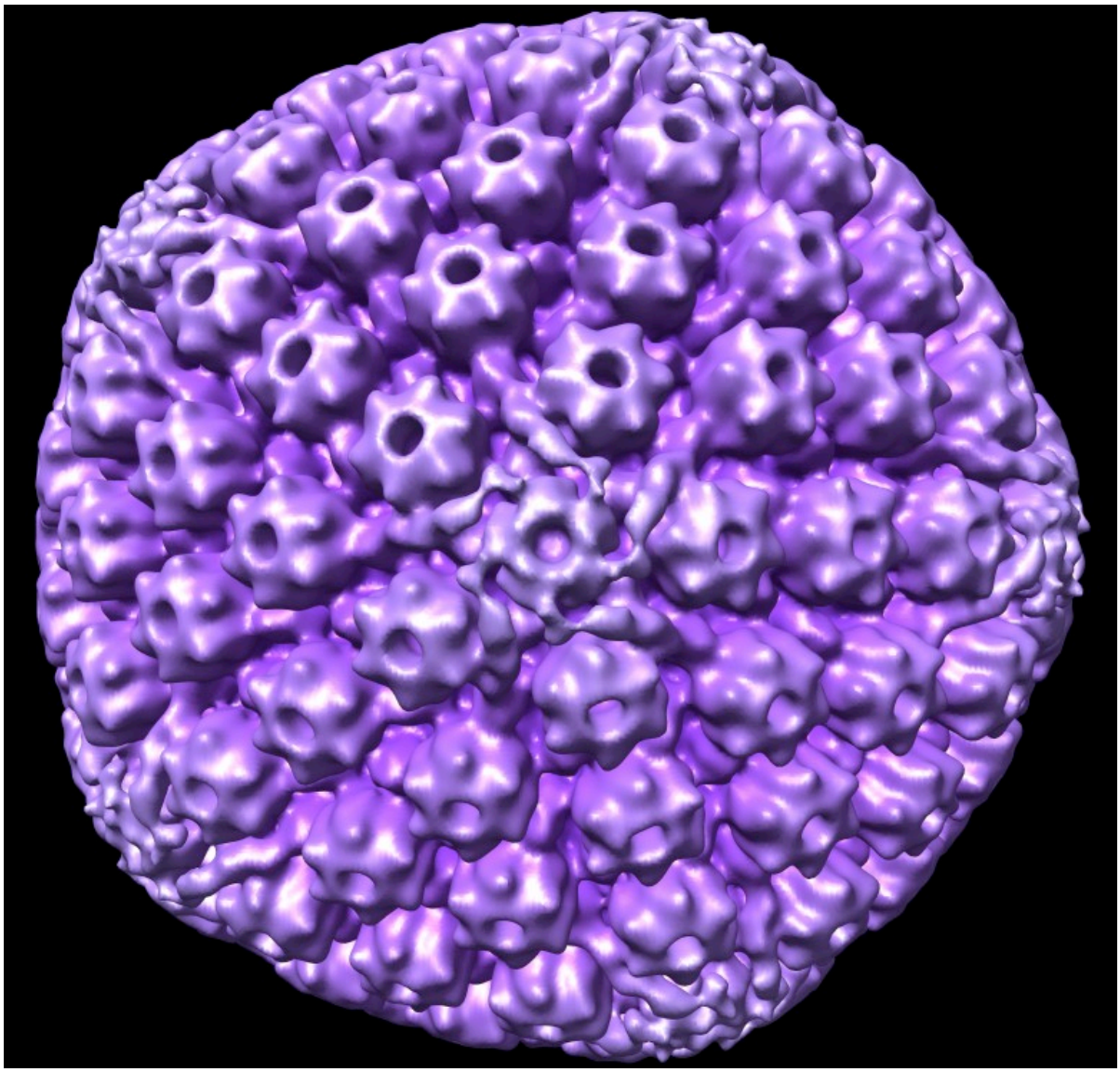

(B)

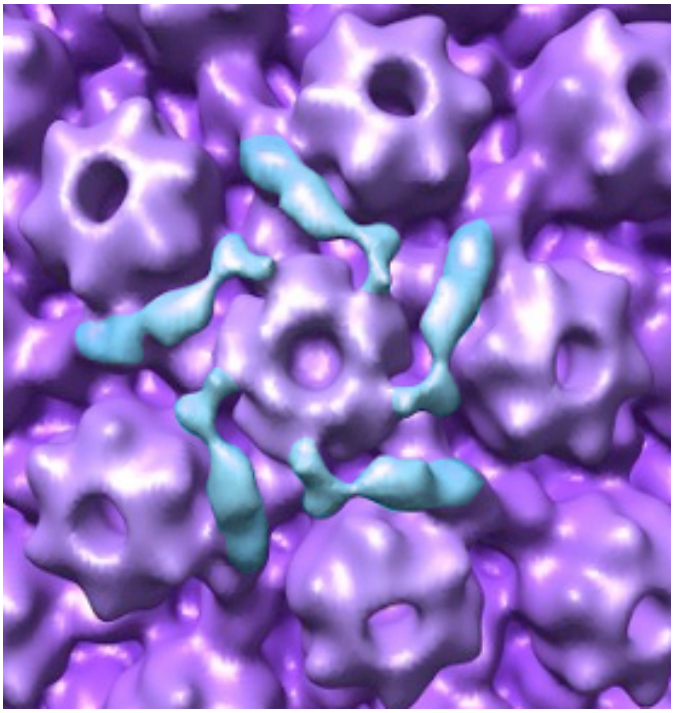

Figure 5.11: Reconstruction of FRΔUL37 cytoplasmic C capsids.

FRΔUL37 cytoplasmic C capsids were purified and imaged as for Fig. 5.10.

(A): A ~31Å resolution reconstruction of the FRΔUL37 cytoplasmic C capsid viewed looking down a 5 fold axis, from 110 particles.

(B): Enlargement of the area immediately surrounding the vertex. The vertex associated densities not seen in the WT HSV-1 B capsid reconstruction (Fig. 5.9) are coloured in light blue.

(A)

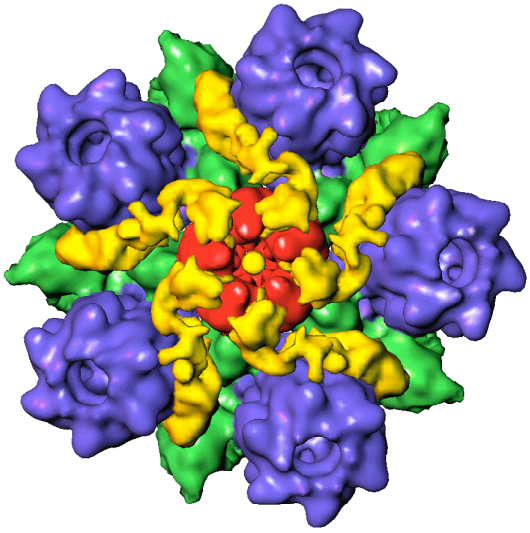

(B)

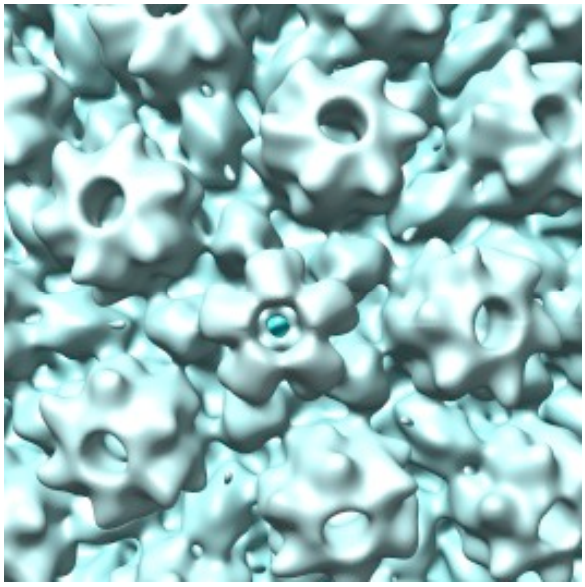

(C)

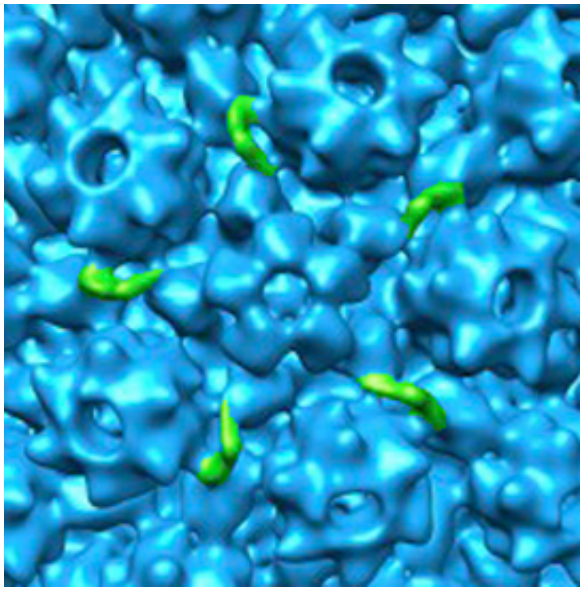

(D)

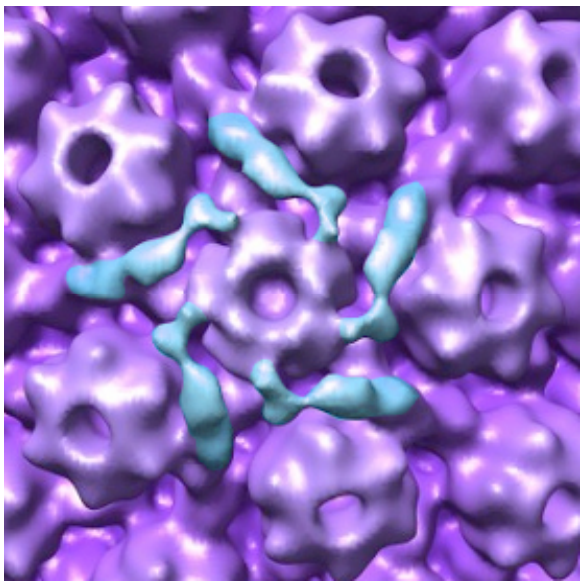

Figure 5.12: Comparison of penton vertices.

(A) Penton view from an intact WT HSV-1 virion with P hexons (blue), Triplexes (green) and the penton (red) with the penton associated tegument density highlighted (yellow). Reproduced from Zhou *et al*. (1999).

(B) Penton view from a WT HSV-1 nuclear B capsid (Fig. 5.9).

(C) Penton view from an ARΔUL36 cytoplasmic C capsid (Fig. 5.10).

(D) Penton view from an FRΔUL37 cytoplasmic C capsid (Fig. 5.11).

preparations implying that they might not always occur in a 1:1 ratio. Alternatively, the pUL17 on ARΔUL36 capsids might not be as stably positioned as pUL25, in which case it would not appear in the reconstructions. Differences in resolution and thresholding would also affect the reconstructed images (the threshold value for the reconstructions of Trus *et al*. (2007) was not reported, while those presented here are set to a standard of mean + 1 SD). As such the absence of this probable pUL17 density from ARΔUL36 cytoplasmic C capsids cannot be interpreted in a definitive manner.

In contrast to the situation with ARΔUL36, it is clear that a density similar to that reported by Zhou *et al*. (1999) in reconstructions of intact virions is present on cytoplasmic C capsids of the mutant FRΔUL37. Therefore, it is possible to exclude pUL37 as a candidate for contributing to this density. Based on the models presented in the literature for the assembly and structure of herpes virions the most probable candidate for that part of this density not accounted for by the CCSC, is pUL36. The presence of pUL36 on FRΔUL37 capsids, as shown by immunofluorescence, immuno-EM and western blot, supports the case for pUL36 being a component of this extra density. The absence of the outer tegument protein, pUL49, from the FRΔUL37 capsids examined by western blotting provides indirect evidence that the additional density is likely contributed by the inner tegument, although the apparent presence of at least some pUL48, as determined by both IF and western blotting, weakens this interpretation. Unfortunately, due to the difficulty in preparing FRΔUL37 capsids there was not time during this project to confirm the location of pUL36 by carrying out gold labelling. If we accept that pUL36 is present at the vertices of these capsids, it provides support for the idea that pUL36 is added to capsids before pUL37 which agrees with the current models of virion assembly (Mettenleiter, 2006).

Data presented here has confirmed that capsids of HSV-1 can be purified from both nuclear and cytoplasmic fractions of mutant-infected cells (Figs. 5.1 and 5.2). However, cytoplasmic capsids could only be routinely isolated from ΔUL36 mutants, while those of FRΔUL37 could be isolated with difficulty and yields were low. The poor recovery of FRΔUL37 capsids is due to the copelleting of nuclei and capsid aggregates as shown here (section 4.5.2 Fig. 4.12). The accumulation of capsid aggregates in FRΔUL37 infection seems likely to be due to the presence of pUL36 on these capsids as shown by Immunofluorescence and Immuno-EM (section 4.6). This suggestion is supported by the different behaviours of KΔUL36 and ARΔUL36, where the presence of the N terminal fragment of pUL36 on the KΔUL36 capsids (Fig. 5.3) is sufficient to cause them to aggregate. To date the only report of capsid binding activity for pUL36 is with pUL25.

Two binding sites have been identified, one in the 62 extreme C terminal residues (Coller *et al.*, 2007) and the other between residues 2037 and 2353 (Pasdeloup *et al.*, 2009). However, the binding by the N-terminal KΔUL36 fragment, indicates that it may contain a previously unreported capsid binding activity. This would then suggest that there may be capsid binding domains present at both termini of pUL36, although the interaction partner of the N terminal domain has yet to be identified. To characterise the capsid binding activity within the N terminal 361 residues of pUL36, generation of defined mutants expressing subregions from residues 1-361 would be required to map the binding domain and to exclude the possibility that the capsid binding activity is conferred by the fusion codons present in KΔUL36.

The interaction of pUL36 with pUL25 is interesting when considered together with their possible locations on the capsids. Trus *et al*. (2007) proposed the orientation of the pUL25/pUL17 heterodimer is such that pUL25 forms in the lowest (capsid floor proximal) domain of the CCSC density, while pUL17 was inferred to occupy a position closer to the penton structure. The demonstrated interaction between pUL25 and the extreme C terminal end of pUL36 (Coller *et al.*, 2007) may suggest that the C-terminus of pUL36 extends over this region of the capsid to make contact with pUL25. From the reconstruction of Zhou *et al*. (1999), it is clear that, unlike the CCSC, the penton-associated density in the virion contacts the penton crown. It is notable that this penton crown contact is recapitulated in the reconstruction of FRΔUL37 cytoplasmic C capsids, suggesting that this is a feature created by pUL36. Therefore, it is reasonable to propose that pUL36 extends over the top of the CCSC, making contact with pUL25, and probably with pUL17, and reaching to the top of the penton. One possible explanation for the weakness of the CCSC like density in the reconstruction of ARΔUL36 cytoplasmic C capsids is that pUL36 by contacting the penton crown, and via interactions with pUL25 and pUL17 is capable of stabilising an otherwise disordered feature leading to the resolution of this structure in FRΔUL37. Whether this explanation is correct or not, it is clear that the penton associated density on virions and FRΔUL37 capsids is larger than can be accounted for by pUL25 and pUL17 and the lack of this material from ARΔUL36 capsids makes pUL36 a very strong candidate to contribute the extra mass.

The cytoplasmic C capsids made by ARΔUL36 and FRΔUL37 are, in most respects, ideally suited to answer the question of which proteins are responsible for the penton coordinated density as they have the potential to correlate the presence or absence of pUL36 and pUL37 to any changes in penton associated density in either case. To some

extent this has proven to be the case. Thus, reconstructions of ARΔUL36 capsids lacking pUL36 inform us that the small additional density equivalent to the CCSC cannot be due to pUL36. Conversely, the absence of the more extensive penton associated density, suggest that this density may be due to UL36, or alternatively, that pUL36 functions in the pathway leading to loading of the molecule responsible for the density. Similarly, the presence of the penton associated density on the reconstruction of the FRΔUL37 capsids informs us that it cannot be formed by pUL37. It also provides the strongest evidence to date that pUL36 is a component of this structure. Unfortunately, the difficulty in purifying FRΔUL37 cytoplasmic capsids meant that their precise protein composition could not be unambiguously determined. Thus, although all available evidence supports the presence of pUL36, other proteins, notably pUL48, cannot be ruled out, leaving open the question of whether pUL36 is the sole tegument protein that contributes to this structure. Nevertheless, the combined analysis of ARΔUL36 and FRΔUL37 by cryo-EM reconstruction provides strong support for the speculation of Zhou *et al.* (1999) that pUL36 contributes to the penton associated tegument density seen in reconstructions of whole virions.

The ideal means by which to resolve the potential contributions of pUL25 and pUL17 to this density would be the perform reconstructions of capsids derived from mutants lacking these proteins. However, the absence of either pUL25 or pUL17 results in a failure to package viral DNA meaning analysis of cytoplasmic capsids derived from these mutants is not possible (McNab *et al.*, 1998; Salmon *et al.*, 1998; Stow, 2001). An alternative approach would be to use an antibody labelling strategy to attempt to localise both pUL25 and pUL17 to this density, however the success of such a strategy is dependent on the accessibility of the epitope recognised by the antibody for binding.

KΔUL36 cytoplasmic C capsids may also provide an interesting target for reconstruction given the apparent association of the 43 kDa N terminal fragment of pUL36 with capsids by western blotting (section 5.2.1.1). The nature of this association is unknown and may become more apparent using cryo-EM reconstruction techniques. A further target for reconstruction would be to use cytoplasmic capsids derived from a mutant expressing the extreme C terminal end of pUL36 (Coller *et al.*, 2007), which might allow the contribution of pUL36 to the penton density to be established on the assumption that the interaction of pUL25 and pUL36 occurs in this structure.

L particles were readily isolated from infections with the tegument mutants (Fig. 5.4), which confirms findings from PrV. Examination of their protein composition suggested

that the presence of pUL48, pUL49 and gD in L particles did not require of either inner tegument protein. Interestingly, the absence of either inner tegument protein resulted in the simultaneous absence of the other. Thus, L particles produced by ARΔUL36 lacked both pUL36 and pUL37, as was the case for FRΔUL37 L particles. This would suggest that for incorporation into the tegument that pUL36 and pUL37 must form a complex, which is in agreement with other data which showed that pUL37 fails to localise to the Golgi in the absence of pUL36 (Desai *et al.*, 2008). Unexpectedly, the 43 kDa N terminal fragment of pUL36 expressed by KΔUL36 was found to be present in L particles produced by this mutant in the absence of pUL37. The interactions which direct this incorporation remain unclear although an interaction with pUL48 cannot be discounted (Lee *et al.*, 2008; Mijatov *et al.*, 2007; Vittone *et al.*, 2005).

From the data presented here it is possible to begin to draw some inferences concerning the assembly of HSV-1. Evidence from FRΔUL37 indicates that pUL36 may be added to capsids in the absence of pUL37, suggesting that pUL36 might be the first of these inner tegument components recruited to the capsid. Previous analyses and those presented here (section 4.5) show that the absence of pUL36 prevents secondary envelopment, as does the absence of pUL37. Evidence suggests that localisation of pUL37 to the Golgi (and by presumption incorporation into virions) requires pUL36 (Desai *et al.*, 2008). In addition, data presented here demonstrates the need of pUL36 and pUL37 to form a complex for incorporation into L particles and this requirement can be assumed to extend to virions, given the essential nature of pUL37 in virion formation (section 4.5). As such it is possible that recruitment of pUL37 to pUL36 decorated capsids is the signal for targeting of capsids to the Golgi (or TGN) for secondary envelopment. In both HSV-1 and PrV formation of L particles, and hence assembly of the outer tegument, can occur in the absence of the inner tegument proteins (Fuchs *et al.*, 2002a; Fuchs *et al.*, 2004; Klupp *et al.*, 2001b). Thus, the outer tegument is able to form independently and is competent to undergo envelopment supporting the idea that tegumentation may initiate at two distinct sites. Several outer tegument proteins are known to interact with the cytoplasmic tails of envelope glycoproteins and therefore could form candidates capable of nucleating the assembly of the outer tegument at the site of secondary envelopment. Crump *et al.* (2007) have speculated that late domain signals in pUL36 may be important for interaction with components of the ESCRT pathway suggesting that pUL36 may be directly involved in envelopment. Data from PrV shows that L particles are formed and released from cells in the absence of pUL36 (Fuchs *et al.*, 2002a) as well as in HSV-1 infections lacking pUL36 (section 5..2.2.1). This suggests that pUL36 may not be the only viral protein interacting

with the ESCRT pathway, assuming that L particles and virions are produced by the same mechanism. However, pUL36 is a very large protein which is likely to be involved in multiple processes and is certainly essential for envelopment of the nucleocapsid in complex with pUL37. One question this model raises is the interface between the inner and outer tegument. A possible candidate has been identified in PrV, where deletion of UL48 prevented envelopment of capsids, resulting in cytoplasmic aggregates of pUL36 and pUL37 decorated capsids (Fuchs *et al.*, 2002a). Furthermore, this mutant produced L particles which lacked pUL48 and both inner tegument proteins, whilst representative members of the outer tegument (pUL46, pUL47 and pUL49) were present (Fuchs *et al.*, 2002a). Thus it is possible that an interaction between the complex of pUL36/pUL37 and pUL48 is required for secondary envelopment.

Interestingly, in PrV the necessity for pUL37 to complete secondary envelopment is not as strict as in HSV-1 (Klupp *et al.*, 2001b), suggesting that pUL36 alone might be able to contact pUL48 and thus proceed to secondary envelopment, albeit at much lower levels than WT. Immunofluorescence and immuno-EM data presented earlier (section 4.6) suggests that pUL48 may be associated with cytoplasmic capsid aggregates of FRΔUL37 indicating that pUL37 may not be required for these interactions in HSV-1 either. However, unlike in PrV these interactions appear insufficient to overcome the deficit of pUL37 and suggest that the functions of pUL37 in HSV-1 and PrV may be subtly different. In support of this interface role for pUL48 is yeast-2-hybrid data that suggest it is able to interact with a number of other outer tegument proteins (Lee *et al.*, 2008; Vittone *et al.*, 2005), although the assembly of these components into L particles is possible in the absence of pUL48 (Fuchs *et al.*, 2002a). This suggests that pUL48 may form a nexus for interactions that unite the inner tegument decorated nucleocapsid with the outer tegument assembled at the site of secondary envelopment resulting in the production of mature virus. Such a model leaves questions about the site to which pUL48 is recruited, being either the inner tegument decorated capsid or the membrane site of secondary envelopment. In essence, either or both are possible. As with the pUL36/pUL37 complex, direct recruitment to the site of secondary envelopment would presumably result in incorporation into L particles, whilst recruitment to capsids might be responsible for targeting them to sites of secondary envelopment.

CHAPTER 6

DIFFERING ROLES OF pUL36 AND pUL37 IN THE INITIATION OF INFECTION

6. Differing Roles of pUL36 and pUL37 in the initiation of infection

6.1. Role of the inner tegument proteins in the initiation of infection

Studies in PrV suggest that pUL36 and pUL37 remain closely associated with the incoming capsid after disassembly of the outer tegument and transport to the nucleus (Luxton *et al.*, 2006). This raises the possibility that pUL36 and pUL37 have roles in capsid transport, NPC targeting, DNA release or some other early event in infection. This is supported by studies on the temperature-sensitive mutant *ts*B7 (Batterson *et al.*, 1983), which suggested a role for pUL36 in genome uncoating, as DNA filled C capsids are seen to bind at, or close to, nuclear pores at the non-permissive temperature. Recent data suggests that a cleavage of pUL36 is required for release of the viral genome at the nuclear pore (Jovasevic *et al.*, 2008). Thus, inhibition of serine or cysteine proteases with L-(Tosylamido-2-phenyl) ethyl chloromethyl ketone (TPCK) prevented processing of pUL36 and blocked viral DNA release from capsids. This proteolytic processing event was also blocked in tsB7 at the non-permissive temperature providing further support for the idea that it is required for release of the viral genome. The absence of a ts mutant for pUL37 meant that there was effectively no data for the role of this protein in the initiation of infection. The inability of HSV-1 mutants deleted for UL36 or UL37 to produce virions means that cells cannot be infected with such deficient viruses in order to study the requirement for these proteins at early times post infection. This has hindered the study of their functions and highlighted the need for a different approach whereby the deletion mutants ARΔUL36 and FRΔUL37 could be used to study the initial stages of infection.

In order to do this, a method was required to circumvent the need for HSV-1 capsids to envelope and cross the plasma membrane, while still exposing naïve nuclei to progeny particles. Such a state is sometimes achieved in natural HSV-1 infections by the formation of a syncytium (Keller *et al.*, 1970; Manservigi *et al.*, 1977; Ruyechan *et al.*, 1979). A syncytium is formed when many cells fuse to produce a single giant cell where multiple nuclei share a common cytoplasm. As well as occurring naturally, such fusion can be induced by exposing cells to fusogenic agents such as polyethylene glycol (PEG) (Lewis & Albrechtbuehler, 1987). Therefore, to assess the effect of tegument mutations on initiation of infection, the experimental approach adopted was to infect cells at a low MOI and

induce fusion at early times post infection. This exposes naïve nuclei to the cytoplasmic capsids produced by the nucleus from the initially infected cell allowing the competence of these capsids to be assessed by monitoring the spread of infection (as shown by the engagement of nuclei in viral replication) throughout the syncytium (Fig. 6.1). The method employed to monitor the spread of viral replication is important. Viral protein markers such as ICP8 or late proteins such as VP5 would not specifically highlight the "infected" nuclei, as viral proteins have free access to all nuclei in a syncytium. However, viral DNA should be present in nuclei only if capsids have bound to their pores and released their genomes. Therefore, the spread of infection was assessed by detecting the presence of HSV-1 DNA using fluorescence *in situ* hybridization (FISH) (Everett *et al.*, 2007).

6.2. Initiation of infection in the absence of pUL36 and pUL37

To elucidate the roles of pUL36 and pUL37 in the initiation of infection, monolayers of $HFFF_2$ cells on coverslips were infected at a low MOI (0.01 pfu/cell) and at 1 h post infection were induced to form syncytia by treatment with PEG and DMSO (section 2.2.7). Typically syncytia obtained using this method contained fewer than 20 nuclei. As such, infection at 0.01 pfu/cell meant that few syncytia contained more than one initially infected cell. At 24h post infection the coverslips were fixed, and the distribution of HSV-1 DNA was determined by FISH using a viral DNA specific Cy3 labelled probe. Cells were counterstained with DAPI and CellMask deep red to highlight nuclei and cytoplasm, respectively. The cells were infected with HSV-1 strain 17 (WT) or with K5ΔZ, ARΔUL36, KΔUL36, or FRΔUL37 mutant virus. WT HSV-1 was used as a positive control for spread within syncytia, and the capsid minus mutant, K5ΔZ, was used as a negative control. Infection of unfused $HFFF_2$ cells produced the expected pattern of infection. Thus, infection with WT HSV-1 resulted in the spread of viral DNA to many cells in the monolayer, while, with the mutants K5ΔZ, FRΔUL37, KΔUL36 and ARΔUL36, viral DNA remained restricted to the nucleus of the initially infected cell, with no spread of infection to surrounding cells (Fig. 6.2). This failure to spread to adjacent cells reflected the inability of these mutants to produce infectious virus particles.

Infection of cells that were subsequently induced to form syncytia, assays the ability of the particles produced by the UL36 and UL37 mutants to establish a new cycle of replication. As with unfused cells, the controls gave the expected patterns of spread. Thus, WT virus had spread between nuclei, generating labeling patterns within syncytia similar to those

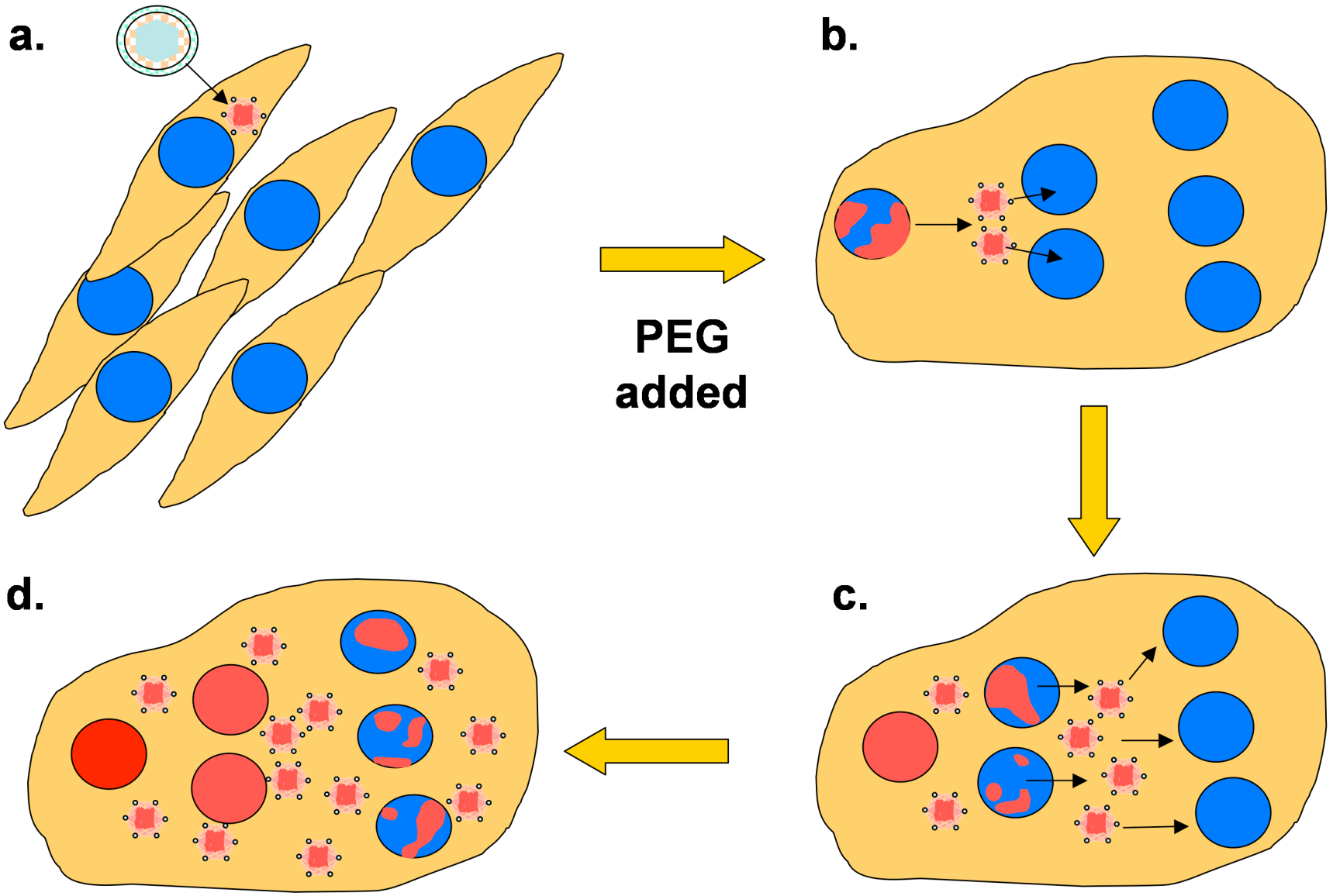
a.
b.
PEG
added
c.
d.

Figure 6.1: Principle of the syncitial model of infection.

Infection of a monolayer at low MOI (0.01 pfu/cell) resulted in isolated infected cells surrounded by uninfected cells (a). These cells were induced to fuse by addition of PEG at 1 h post-infection, before the start of DNA replication or virion assembly (b). The resulting syncytia typically contained less than 20 nuclei, meaning that most contained no more than one infected nucleus (shown in red). In such cases DNA filled capsids produced by the initially infected nucleus can gain direct access to the other, naïve nuclei (shown in blue). The spread of infection to new nuclei was assessed after 24 h at 37˚C (c and d) by Fluorescence In Situ Hybridisation (FISH) using a viral DNA specific probe. This detects both replicating viral DNA in infected nuclei and packaged DNA in cytoplasmic capsids.

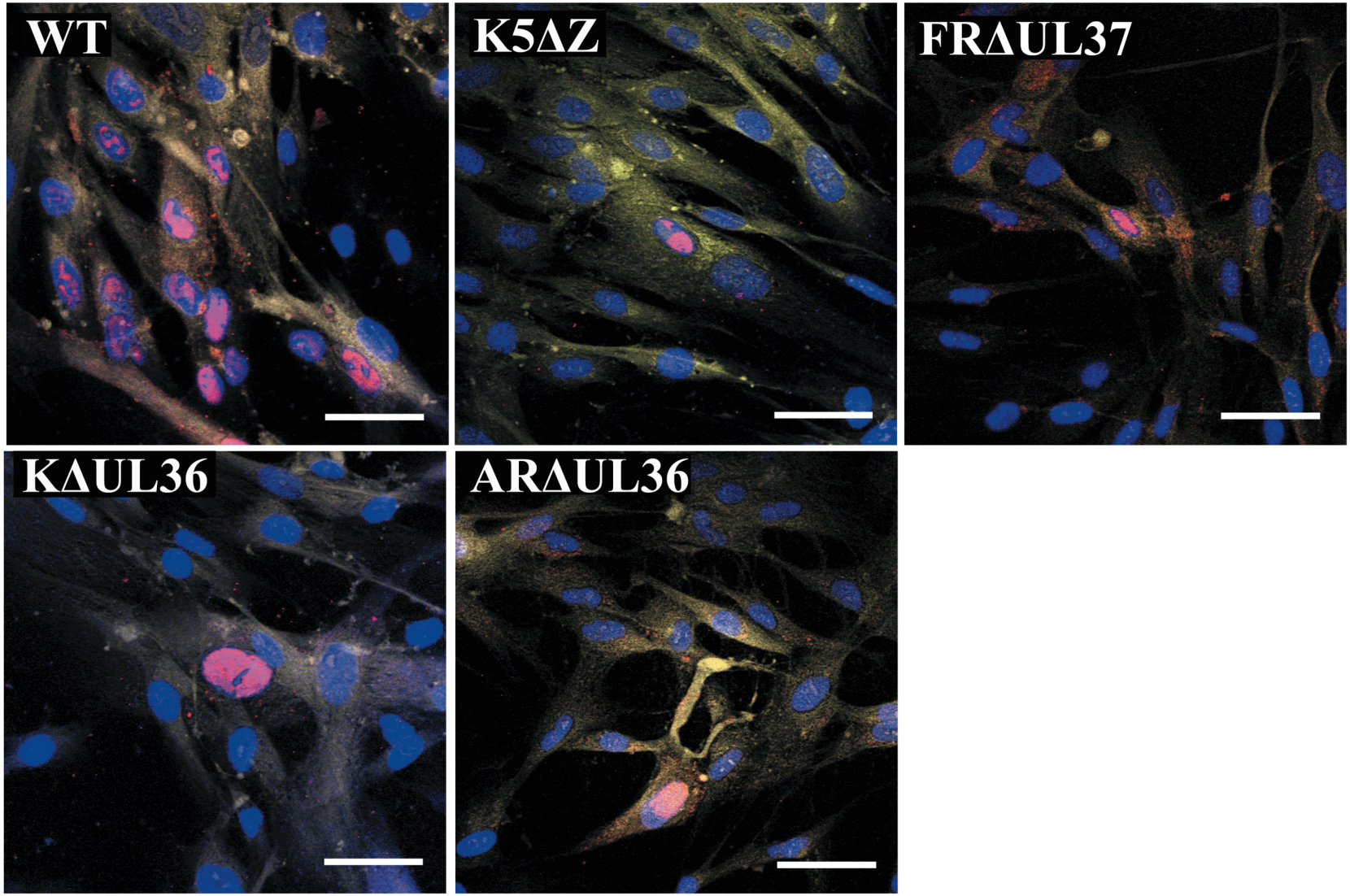
WT
K5ΔZ
FRΔUL37
KΔUL36
ARΔUL36

Figure 6.2: Distribution of viral DNA in infected monolayers

Replicate monolayers of $HFFF_2$ cells were infected with 0.01 pfu/cell of WT HSV-1 (WT) K5ΔZ, FRΔUL37, KΔUL36 or ARΔUL36 mutant virus. Cells were fixed and probed at 24 h post infection. Viral DNA was visualised by FISH usisng Cy3- labelled probe (red), nuclei were stained with DAPI (blue) and the cytoplasm was stained with CellMask deep red (yellow). Bars, 50μm in all panels.

seen in unfused cells (Fig. 6.3), whereas in K5ΔZ-infected samples, viral DNA was confined to individual nuclei within syncytia.

Infection with KΔUL36 and ARΔUL36, like K5ΔZ, showed the presence of viral DNA in only the initially infected nucleus. In contrast, infection with FRΔUL37 led to viral DNA being detected in multiple nuclei, in patterns reminiscent of those seen in the WT infection. This indicates the capacity of FRΔUL37 cytoplasmic C capsids to interact with the nuclear pore, transfer their DNA to naïve nuclei and initiate a new cycle of replication (Fig. 6.3).

From the data presented here it is apparent that formation of intact virions is not required for spread of infection in syncytia, and that new cycles of replication can potentially be established by unenveloped cytoplasmic C capsids. However, not all C capsids are equally competent as in the absence of WT pUL36 the cytoplasmic C capsids of both KΔUL36 and ARΔUL36 were unable to initiate a new cycle of replication in naïve nuclei. In contrast, the cytoplasmic C capsids of FRΔUL37, which were shown to be associated with pUL36 (section 4.6.1.1), are fully capable of interacting with nuclear pores and are competent to uncoat the viral genome leading to initiation of replication in a previously naïve nucleus. Data from Batterson *et al*., (1983) concerning the temperature sensitive defect of tsB7 correlates well with this observation, with both suggesting a critical role for pUL36 in processes leading to uncoating of the viral genome.

Examination of these infections in the absence of a cytoplasmic stain confirmed that the pattern of viral DNA staining in the cytoplasm replicates the distribution of viral capsids seen by electron microscopy. The mutant K5ΔZ showed no labelling within the cytoplasm, confirming that viral DNA is retained in the nucleus when capsids cannot be formed, and since viral DNA remained restricted to the initially infected nucleus this showed that unpackaged viral DNA could not spread between nuclei. Aggregates of cytoplasmic viral DNA labelling were seen in both KΔUL36 and FRΔUL37, and are distinct from one another with capsid aggregates of KΔUL36 characteristically smaller than those of FRΔUL37. Viral DNA was also detected as discrete fluorescent spots distributed throughout the entire cytoplasm of WT HSV-1 and ARΔUL36 infected syncytia. This suggested that the failure of ARΔUL36 to initiate infection of naïve nuclei is not due to limitations on the movement of these capsids throughout the cell (Fig. 6.4).

The specificity of the viral DNA probe was confirmed by performing FISH on cells treated with the viral DNA polymerase inhibitor, phosphonoacetic acid (PAA) (Honess & Watson,

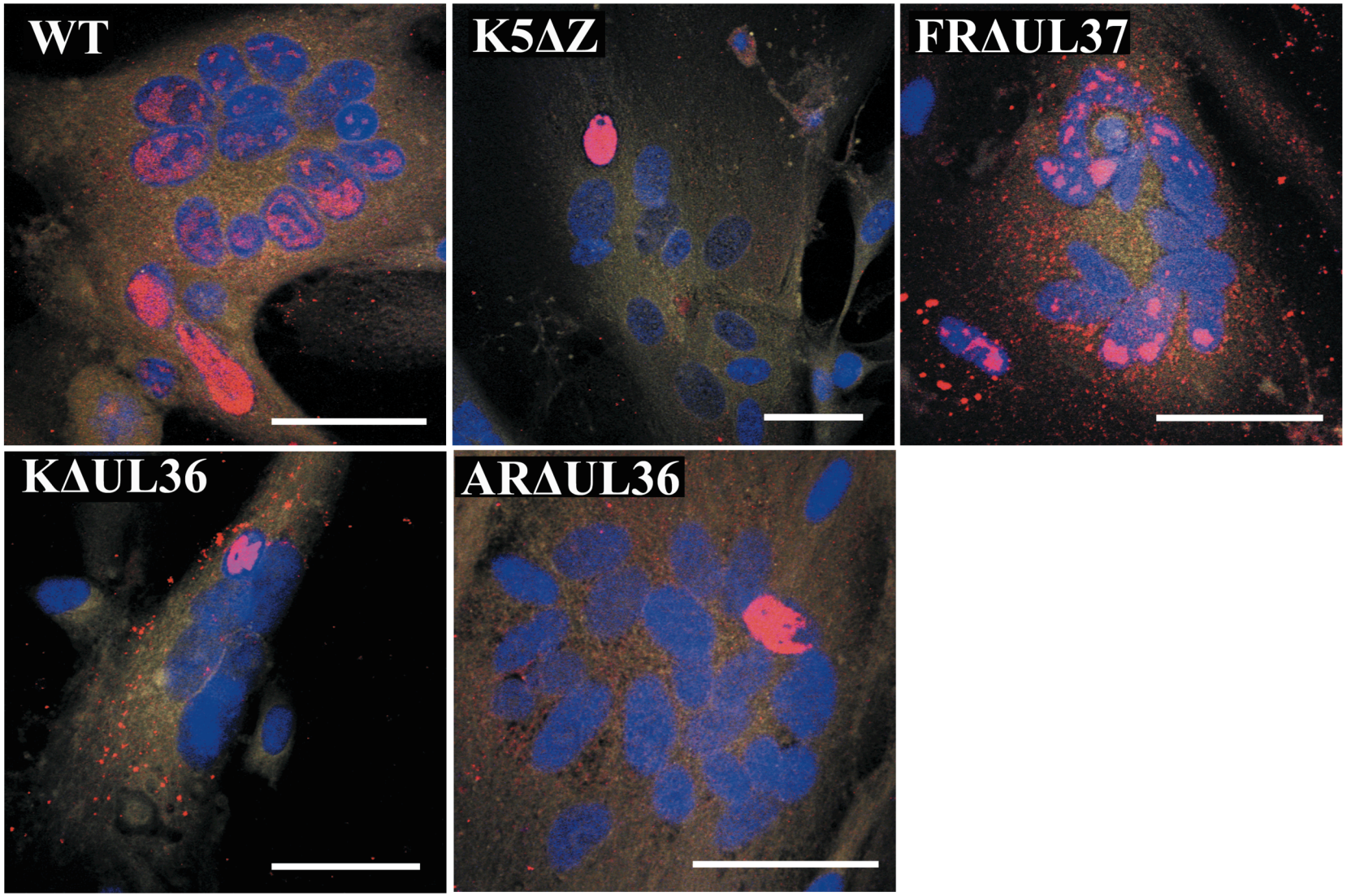
WT
K5ΔZ
FRΔUL37
KΔUL36
ARΔUL36

Figure 6.3: Distribution of viral DNA in infected syncytia

Replicate monolayers of $HFFF_2$ cells were infected with 0.01 pfu/cell of WT HSV-1 (WT), K5ΔZ, FRΔUL37, KΔUL36 or ARΔUL36 virus. Cells were induced to form syncytia at 1 h post infection and fixed and probed at 24 h post infection. Viral DNA was visualised by FISH using Cy3- labelled probe (red), nuclei were stained with DAPI (blue) and the cytoplasm was stained with CellMask deep red (yellow). Bars, 50μm in all panels.

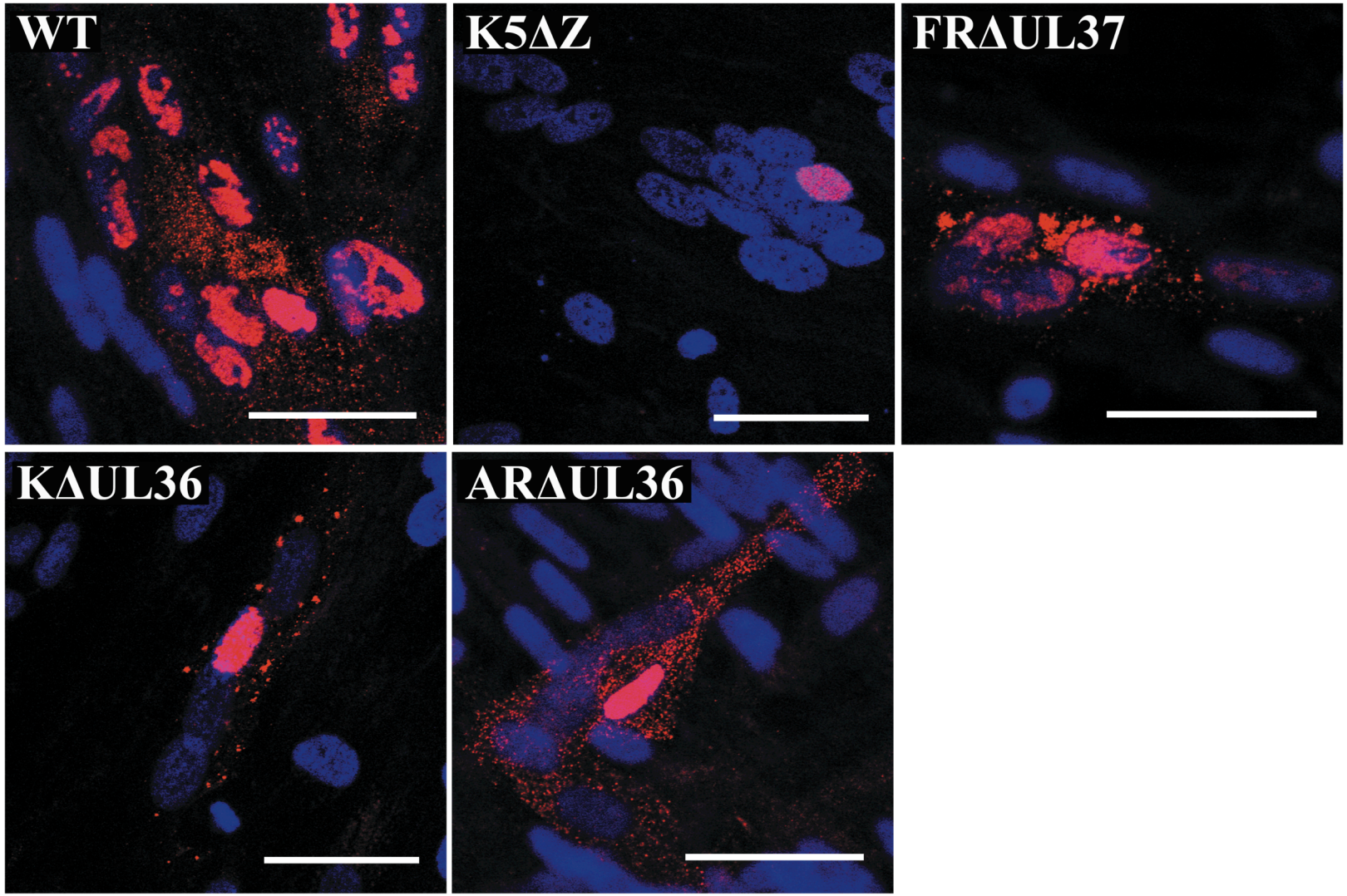
WT
K5ΔZ
FRΔUL37
KΔUL36
ARΔUL36

Figure 6.4: Distribution of viral DNA in infected syncytia

Replicate monolayers of $HFFF_2$ cells were infected and induced to form syncytia as described for Fig. 6.3. Viral DNA was visualised by FISH using Cy3- labelled probe (red), nuclei were stained with DAPI (blue) and the cytoplasmic stain CellMask deep red was omitted. Bars, 50μm in all panels.

1977). PAA treatment prevents HSV DNA replication and examination of the FISH treated samples revealed that there was no label in any infected PAA treated syncytia (Fig. 6.5).

The distribution of capsids in the infected syncytia was confirmed using immunofluorescent detection of the major capsid protein VP5 (Fig. 6.6). As expected in the mutant K5ΔZ where the UL19 ORF is disrupted, no VP5 antigen was detected. In infections with WT HSV-1, FRΔUL37, KΔUL36 and ARΔUL36, VP5 was detected in all the nuclei in infected syncytia confirming their accessibility to cytoplasmic proteins. For each mutant the distribution of label within the cytoplasm mirrored that seen by FISH detection of viral DNA (Fig. 6.4). However, detection of VP5 in the WT HSV-1 infection was less effective with fewer particles being detected than by FISH and their labelling intensity being lower than for the inner tegument mutants. Since many of the WT HSV-1 particles would be undergoing maturation or would already be enveloped, this presumably reflected masking of the VP5 epitope under the gentler fixation conditions used for immunofluorescence compared to FISH. Immunodetection of VP5 showed that the pattern of viral DNA labelling within the cytoplasm correlates well with the presence of cytoplasmic C capsids.

6.3. Effect of Nocodazole treatment on infection with the ΔUL37 mutant FRΔUL37

Previous studies on incoming particles released from the virion after fusion at the plasma membrane have demonstrated an important but not essential role for microtubules in the establishment of infection (Sodeik *et al.*, 1997). Therefore, to assess the contribution of microtubule mediated capsid transport to the spread of infection, FRΔUL37 infected syncytia were treated with nocodazole to depolymerise the microtubule network (Debrabander *et al.*, 1976). Duplicate coverslips of $HFFF_2$ cells were infected and fused to form syncytia as previously described. At 3 h post infection they were treated with Nocodazole (0.5μg/ml) and then incubated at 37°C for a further 21h. One coverslip was then fixed and processed for immunofluorescence and the other for FISH. Depolymerisation of the microtubule network was confirmed by comparing the α tubulin staining in Nocodazole treated and untreated syncytia (Fig. 6.7 upper panel). The FISH labelled samples showed that in the presence of Nocodazole (+ noc) both WT HSV-1 and FRΔUL37 exhibited reduced numbers of viral DNA containing nuclei compared to untreated syncytia, suggesting a retardation in the spread of infection (Fig. 6.7). Nocodazole has been previously reported to delay onset of infection in unfused cells,

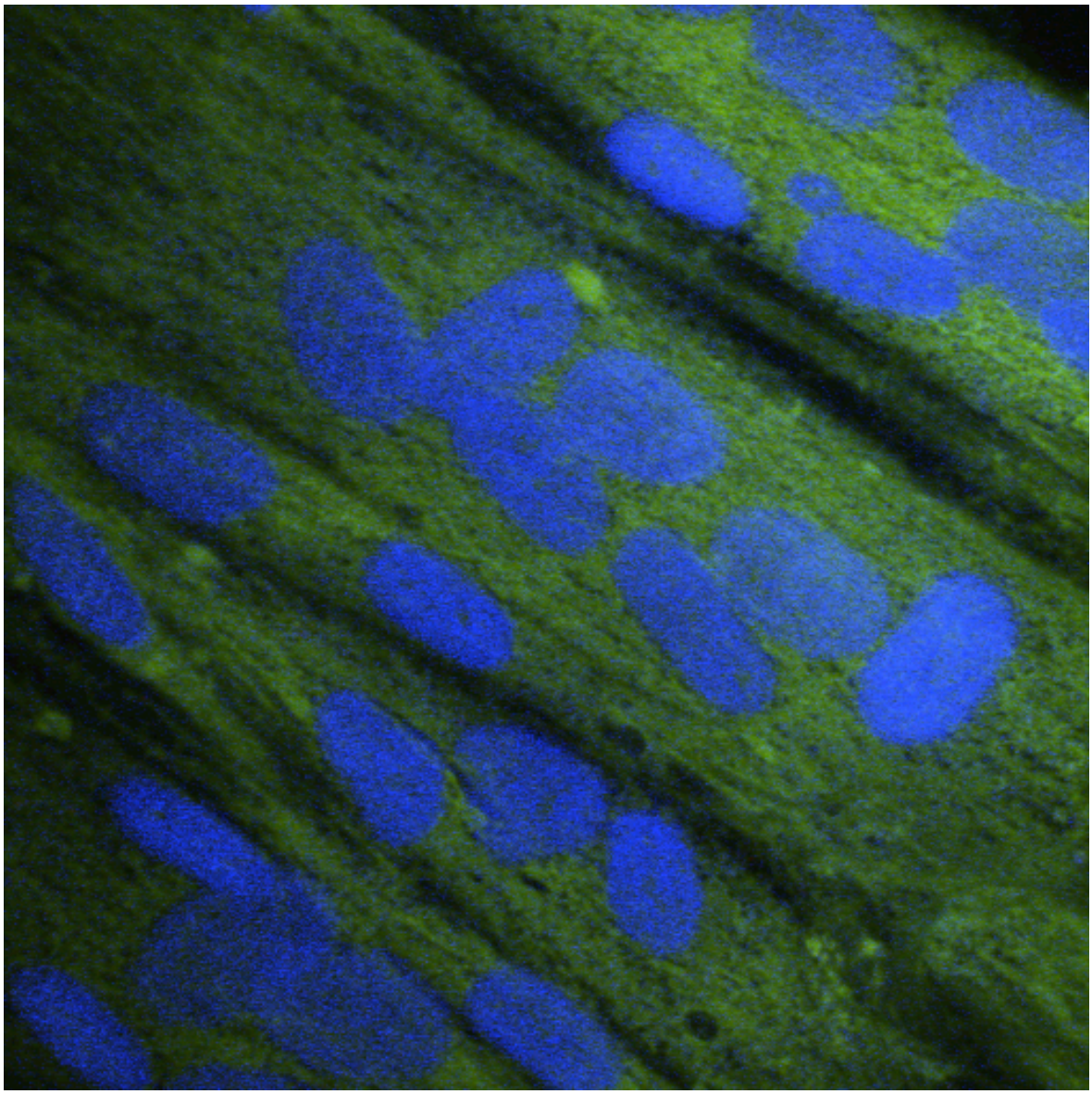

Figure 6.5: Effect of PAA on FISH labelling of WT infected syncytia.

A monolayer of $HFFF_2$ cells was infected with 0.01 pfu/cell of WT HSV-1 and induced to form syncytia as described for Fig. 6.3. PAA (200 μg/ml) was added at 1 h pi and the cells were incubated for a further 23 h. The samples were analysed for HSV DNA by FISH using Cy3- labelled probe (red). Nuclei were stained with DAPI (blue) and the cytoplasm was stained with CellMask deep red (yellow).

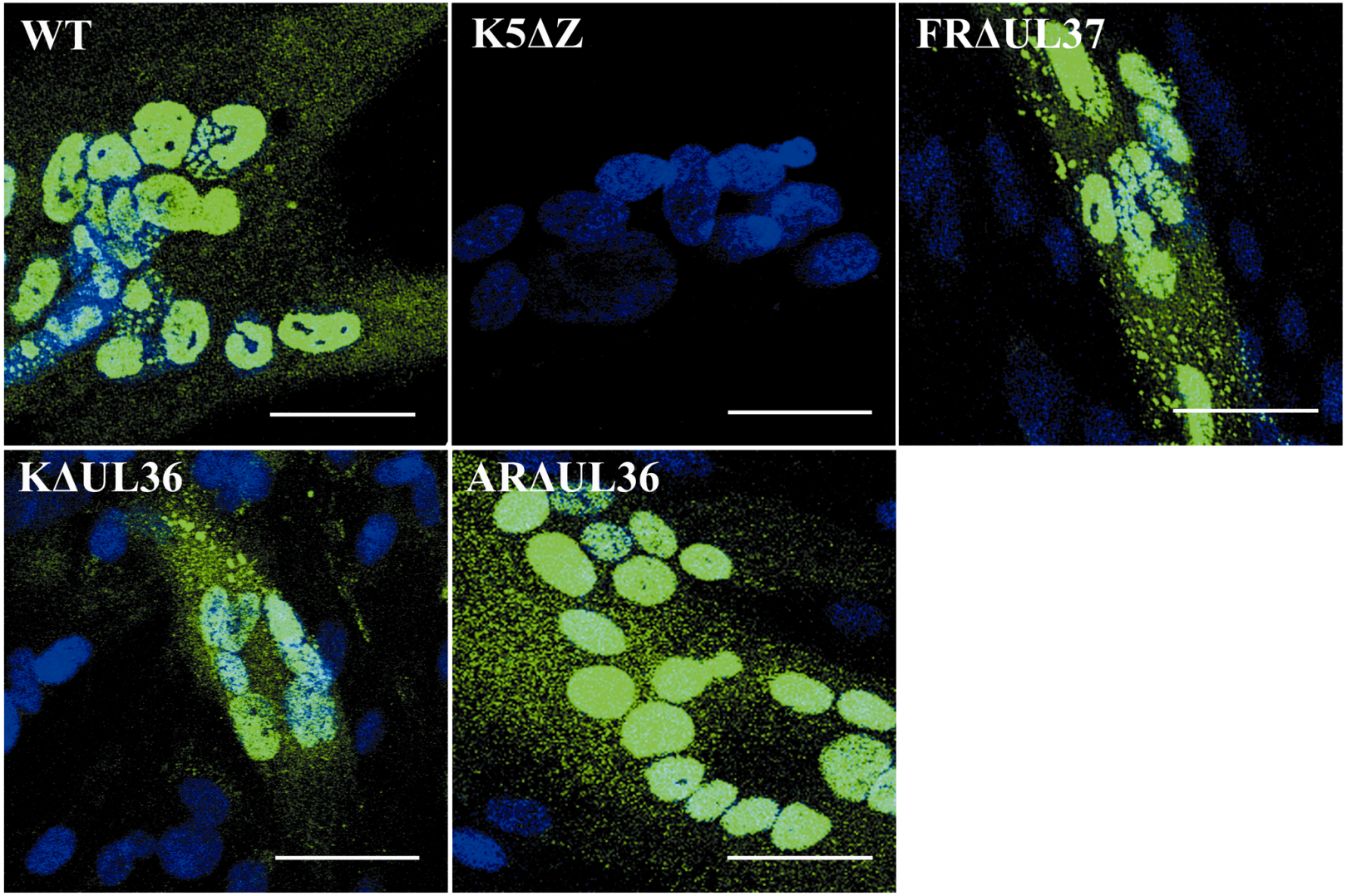
WT
K5ΔZ
FRΔUL37
KΔUL36
ARΔUL36

Figure 6.6: Distribution of the major capsid protein in infected syncytia

Replicate monolayers of $HFFF_2$ cells were infected and induced to form syncytia as described for Fig. 6.3. At 24 h post infection the cells were fixed and the major capsid protein (VP5, pUL19) was visualised by immunofluorescence using mAb DM165 and GAM_{488} secondary antibody (green). Nuclei were stained with DAPI (blue). Scale bars represent 50 μm in all panels.

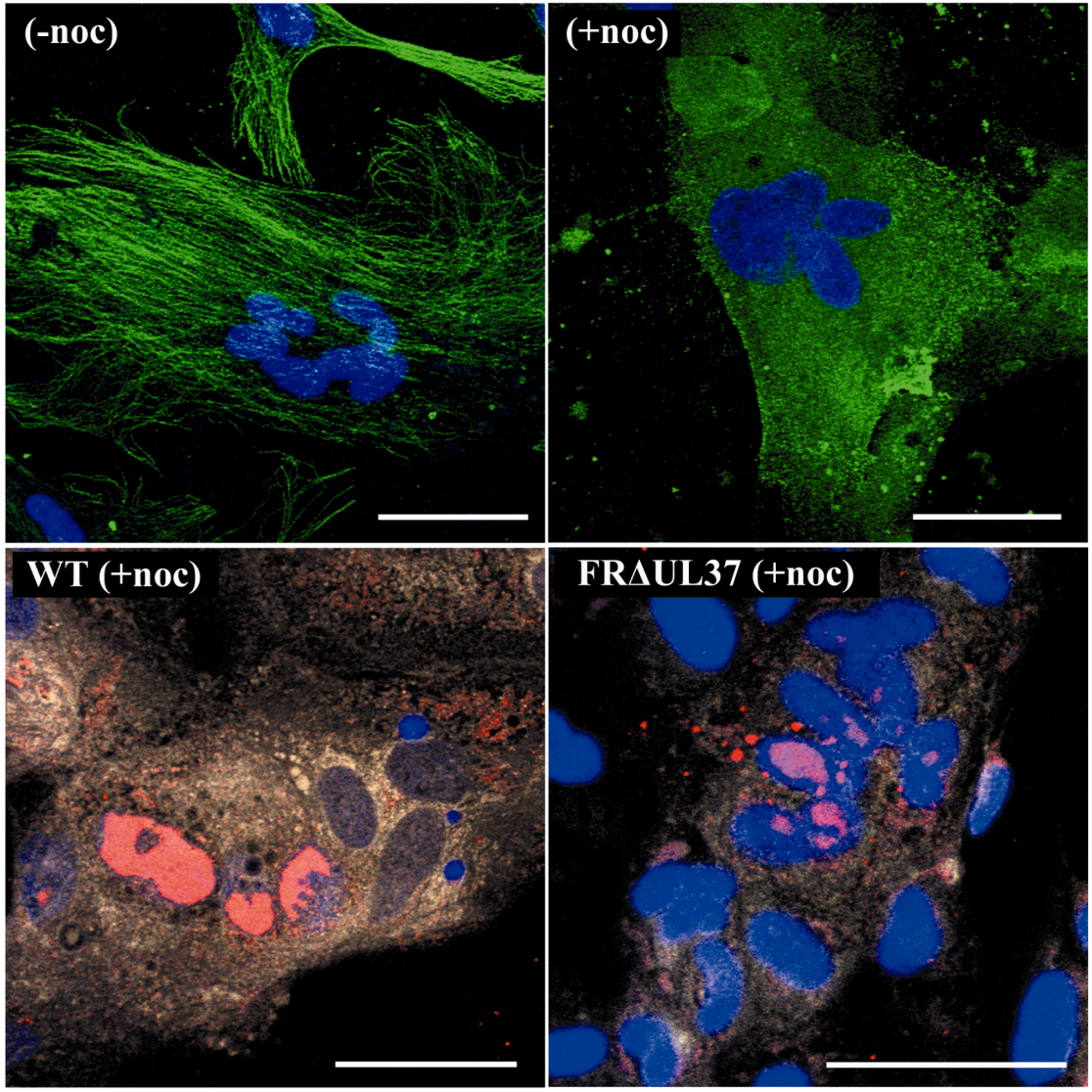
(-noc)
(+noc)
WT (+noc)
FRΔUL37 (+noc)

Figure 6.7: Effect of Nocodazole treatment on spread of infection in syncytia

Replicate monolayers of $HFFF_2$ cells were infected with 0.01 pfu/cell of WT HSV-1 (WT) or FRΔUL37 and induced to form syncytia as described for Fig. 6.3. Cells were left untreated (-noc) or exposed to Nocodazole (0.5 μg/ml) at 3 h pi (+noc). Cells were fixed at 24 h pi. One sample (top panels) for each condition was fixed to preserve the microtubule network (section 2.2.6) while the second sample (bottom panels) was prepared for FISH using Cy3- labelled probe (red). Tubulin was visualised by immunofluorescence using mAb DM1A and GAM_{488} secondary antibody (green). Nuclei were stained with DAPI (blue) and the cytoplasm was stained (lower panels only) with CellMask deep red (yellow). Scale bars represent 50 μm in all panels.

suggesting that HSV-1 infection does not require an intact microtubule network but is more efficient in its presence (Sodeik *et al.*, 1997). From this analysis it was clear that the transport of FRΔUL37 capsids is affected similarly to WT HSV-1 (Table 6.1) providing further evidence that cytoplasmic capsids generated by this mutant are broadly equivalent to incoming viral capsids after membrane fusion and tegument disassembly.

Infection of naïve nuclei by FRΔUL37 cytoplasmic capsids in the presence of Nocodazole is in agreement with previous data regarding the ability of WT HSV-1 to infect cells in the presence of Nocodazole (Sodeik *et al.*, 1997) and suggests that pUL37 is not essential for interactions between the incoming capsid and non-MT motor proteins. It has been shown that WT PrV (and presumably by extrapolation WT HSV-1) cytoplasmic nucleocapsids are able to utilise the alternative transport system of the actin cytoskeleton, with transport effectively abolished by the combined effect of both nocodazole and cytochalasin D (Luxton *et al.*, 2006). This suggests that cytoplasmic nucleocapsids of FRΔUL37 may retain the ability to contact the actin transport systems. Although FRΔUL37 cytoplasmic capsids appeared almost as effective as WT HSV-1 capsids at infecting naïve nuclei in the presence of Nocodazole, a recent report suggested that pUL37 might have some role in cytoplasmic nucleocapsid transport. Krautwald *et al*. (2009) showed a delay in the initiation of infection by PrV virions lacking pUL37 and suggested that this results from a function of pUL37 in nucleocapsid transport. Although pUL37 is absent from FRΔUL37 capsids, the presence of pUL36 has been shown by immunofluorescence colocalisation of capsid and pUL36 and the association of immunogold label against pUL36 with capsid aggregates of FRΔUL37 (section 4.6) similar to reports from PrV (Luxton *et al.*, 2006). Thus, pUL36 appears to be necessary and possibly sufficient for both non-MT and MT based cytoplasmic capsid transport. However, cytoplasmic C capsids of ARΔUL36 were not restricted in their ability to traverse the cell, suggesting that the binding of motor proteins or accessory proteins is not necessarily restricted to pUL36 but that specificity for certain types of accessory or motor protein might be conferred by its presence.

Taken together, these data suggest that pUL37 is not essential for transport of the nucleocapsid through the cytoplasm. From the experiments described here it is not possible to state with certainty the contribution of pUL36 to capsid transport. However, its is noteworthy that Luxton *et al*. (2006) reported that in the absence of pUL36, capsids are not transported in a curvilinear manner which is characteristic of engaging active transport systems, but undergo random non processive motion (by passive diffusion), which may be consistent with the distribution of nucleocapsids throughout the cytoplasm as seen in

Virus	% labelled nuclei	
	- Noc	+Noc
WT HSV-1	98	46
FRΔUL37	76	32
ARΔUL36	10	13

Table 6.1: Effect of Nocodazole treatment on spread of infection in syncytia.

ARΔUL36 infected syncytia. The importance of pUL36 to microtubule mediated transport was also highlighted, although the complete abrogation of transport was only seen after treatment with both nocodazole and cytochalasin D (Luxton *et al.*, 2006). Whilst the experiments presented here do not directly address the role of pUL36 in microtubule mediated transport it is notable that infection of naïve nuclei is affected by depolymeration of the microtubule network, and that in FRΔUL37, pUL36 is associated with the nucleocapsid (section 4.6). Taken with the data of Wolfstein *et al*. (2006) showing the requirement of pUL36 and pUL37 on capsids for microtubule transport using purified microtubules and Luxton *et al*. (2006) with similar requirements in cell based assays, a role of pUL36 in capsid transport becomes most compelling.

The results presented here show that there is a difference in the ability of cytoplasmic capsids produced by the UL36 mutants, KΔUL36 and ARΔUL36, and the UL37 mutant FRΔUL37 to initiate infection of naïve nuclei. The major reason for this difference presumably relates to the presence of pUL36. Thus, FRΔUL37 lacks pUL37, but is capable of expressing pUL36, which it is suggested forms the innermost layer of the tegument, which is retained on capsids after transport to the nucleus (Luxton *et al.*, 2006), and is present on aggregated cytoplasmic capsids of FRΔUL37. Furthermore, the mutant tsB7 shows that pUL36 functions in the process of, or processes leading to, binding of the capsid to the nuclear pore and release of viral DNA (Batterson *et al.*, 1983). Therefore, since the cytoplasmic capsids produced by FRΔUL37 are as effective as those of WT HSV-1 at initiating infection of naïve nuclei, they presumably possess all the necessary functions and information to fulfil these roles. Whilst the experiments presented here are not sufficient to dissect the potential roles of pUL36 in nucleus directed transport, nuclear pore recognition, nuclear pore binding or genome release a growing body of data has implicated pUL36 in all of these functions (Batterson *et al.*, 1983; Jovasevic *et al.*, 2008; Luxton *et al.*, 2006; Ojala *et al.*, 2000; Wolfstein *et al.*, 2006). Given the size of pUL36 and its essential nature in both model alphaherpesviruses (HSV-1 and PrV) as well as it's wider conservation in other herpesviruses, there is no reason why all these important functions and more should not be accomplished by this protein, either alone or as part of functional complexes with other virion components.

CHAPTER 7

ROLES OF THE INNER TEGUMENT IN HSV-1 INFECTION - DISCUSSION

7. Discussion

The tegument is a characteristic feature of herpes virions. It contains several proteins that function to bring about subversion of the host cell in order to facilitate the viral gene expression programme, and most early studies concentrated on these functions. However, our understanding of tegument structure and assembly is now increasing and more effort is being directed against this aspect of herpes virology, particularly with respect to the largest tegument protein, pUL36. Despite this increasing attention the tegument remains a complex structure containing in excess of 15-20 viral proteins, mRNAs and some cellular proteins, which has proved difficult to unravel and understand. Work with various systems, including yeast-2-hybrid interaction studies, deletion mutants and targeted mutagenesis has begun to develop our understanding of the complexity of the tegument. Data from these studies highlight the role that protein-protein interactions play in the assembly of the tegument and suggest that it is this complex network of interactions that drives virion formation through multiple interactions of individual tegument proteins (Fig. 7.1).

7.1. Tegument and assembly of HSV-1 virions

The tegument is believed to consist of two subdivisions, the inner and outer tegument, which seem to be involved in different aspects of infection. The sequence of tegument acquisition by nucleocapsids remains contentious and there are conflicting reports of tegument being added to capsids in both the nucleus and cytoplasm (Bucks *et al.*, 2007; Desai *et al.*, 2008; Fuchs *et al.*, 2002a; reviewed Mettenleiter, 2002; Naldinho-Souto *et al.*, 2006). The question of where the inner tegument is added remains unresolved. However, given the cytoplasmic accumulation of nucleocapsids exhibited by mutants lacking the inner tegument proteins, pUL36 or pUL37, it is increasingly apparent that neither of these proteins has a definitive role in nuclear exit but that both have their principal function in the cytoplasmic stages of secondary envelopment.

Increasingly, it is becoming apparent that tegument assembly (or acquisition) occurs at two separate sites, with inner tegument assembling on the capsid and outer tegument on the envelope. It is possible that pUL36 is the first protein acquired by nucleocapsids following completion of DNA packaging, although it may be that in a WT HSV-1 infection, pUL36 is added to capsids in complex with pUL37. The examination of FRΔUL37 cytoplasmic nucleocapsids described in this thesis showed that interaction of pUL36 with capsids can occur independently of interaction with pUL37. pUL36 bound to capsids also appears able

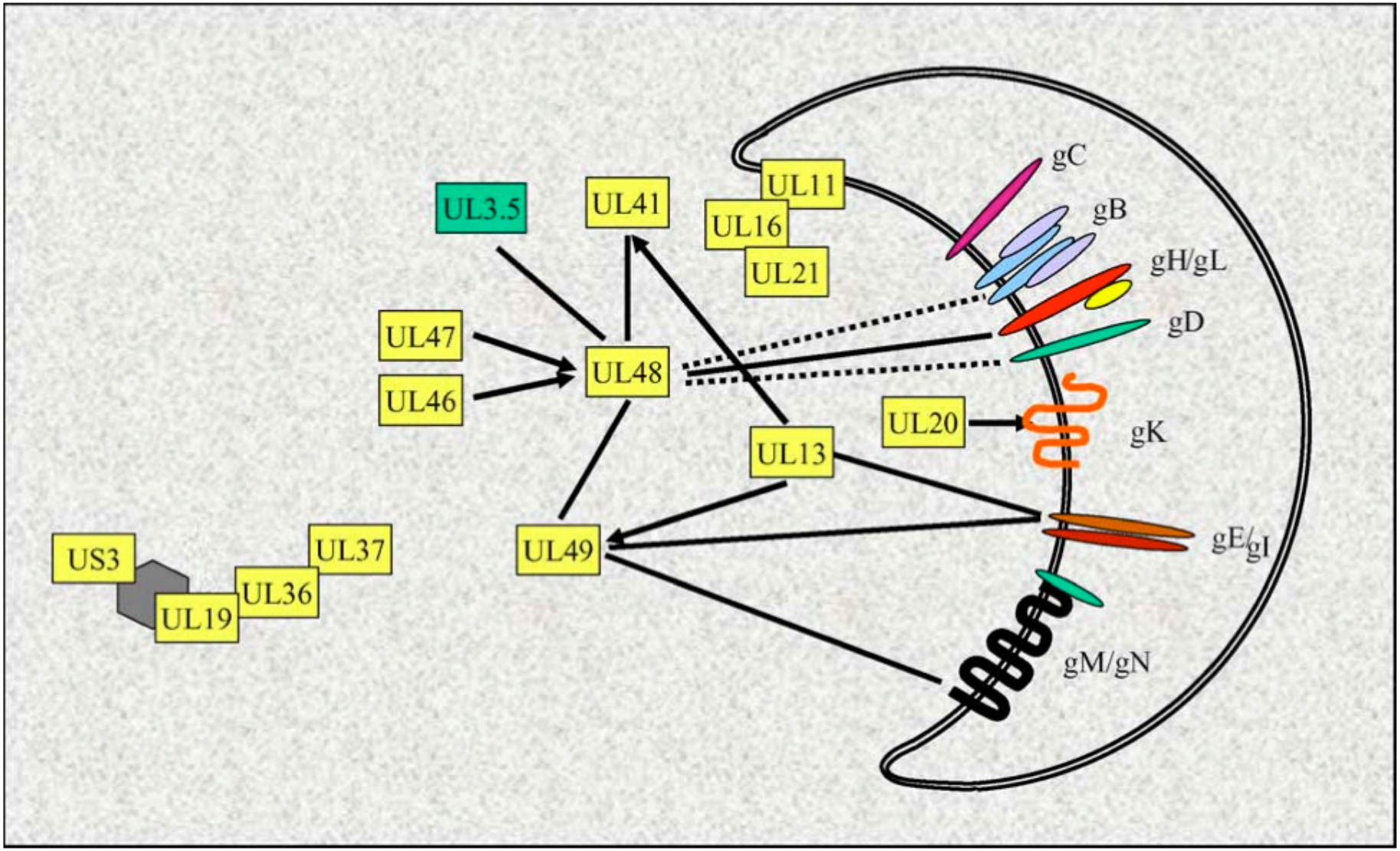
UL3.5
UL41
UL11
UL16
UL21
gC
gB
gH/gL
gD
UL47
UL46
UL48
UL20
gK
UL13
US3
UL19
UL36
UL37
UL49
gE/gI
gM/gN

Figure 7.1: Protein interactions driving the assembly of HSV-1

Model of interactions underlying the assembly of HSV-1 (and PrV), showing the two current divisions of the tegument. The inner tegument is shown assembled on the capsid (left) while the outer tegument is shown to assemble independently at the membrane system by interaction with glycoprotein cytoplasmic tails.

Within this network pUL48 forms a natural nexus of interactions with both outer tegument and glycoprotein tails. Data (Fuchs *et al*., 2002) also suggest an interaction between pUL48 and pUL36/pUL37 linking the inner and outer teguments.

Solid lines or direct contacts are representative of physical contacts, while dashed lines represent potential interactions and arrows indicate functional effects. UL3.5 is absent from HSV-1 and PrV, but is present in the BHV-1 virion.

Reproduced from Mettenleiter (2004).

to interact with other tegument components, such as pUL48, in the absence of pUL37. However, unlike in HSV, pUL37 is not absolutely essential for PrV virion formation, suggesting that in PrV there is a mechanism which can circumvent the essential role of pUL37 in HSV-1 virion assembly. This implies that pUL37 in PrV and HSV-1 fulfil subtly different functions in virion formation.

One area of significant uncertainty is the identity of the proteins interacting with the capsid at the penton vertex, which form the link between the capsid and tegument compartments of the virion. To date the proteins implicated are the minor capsid proteins pUL17 and pUL25 and the inner tegument protein pUL36 (Trus *et al.*, 2007; Zhou *et al.*, 1999), with current data providing conclusive proof for neither proposal. The initial suggestion that pUL36 could be responsible (Zhou *et al.*, 1999) was based solely on the known properties of pUL36 and its large mass. This appeared to be at least partially refuted by Trus *et al*. (2007), who showed a correlation between the presence of vertex associated density on C capsids, and pUL17 and pUL25. One limitation to the analysis of Trus *et al*. (2007) is that the contributions of pUL17 or pUL25 to the vertex density observed in their analysis could not be formally established by examining mutants deleted for these functions, since DNA filled nucleocapsids are not formed by these mutants and they were unable to visualise any extra density on WT HSV-1 B capsids despite the presence of the proteins. A further caveat is that the potential nuclear addition of pUL36 and pUL37 (Bucks *et al.*, 2007) to capsids, if confirmed, might account for some, or all of the extra density, although Trus *et al*. (2007) did not detect pUL36 on their capsids. It is interesting that the cytoplasmic C capsids of ARΔUL36 have only a weak density signature in the position reported for pUL17 and pUL25, despite the presence of these proteins in the capsid preparation. However, more careful analysis of ARΔUL36 cytoplasmic C capsids should provide a definitive answer to whether the density reported by Trus *et al*. (2007) can be attributed to pUL36 and this work is being continued. Indeed the structural analysis of FRΔUL37 cytoplasmic C capsids presented in this thesis, although not proving the involvement of pUL36, recapitulates its potential contribution to the density observed at the penton vertex, while excluding any role for pUL37. The density observed in virions (Zhou *et al.*, 1999) and in reconstructions of FRΔUL37 cytoplasmic capsids was more extensive than that seen by Trus *et al*. (2007) and extended further towards the top of the penton. It is possible, therefore, to speculate that a heterotrimeric complex of all three proteins, pUL25, pUL17 and pUL36, may account for the penton associated density. An interaction between pUL25 and the extreme C terminus of pUL36 has been documented in both PrV (Coller *et al.*, 2007) and HSV-1 (Pasdeloup *et al.*, 2009). Trus *et al*. (2007) assigned pUL25 to the capsid

floor-proximal portion of their vertex-associated density. Therefore, an interaction with pUL36 would suggest that the protein might lie on top of pUL25 and pUL17 and extend to the top of the penton, thereby forming a link between these components and the rest of the tegument, and may potentially stabilise the pUL25-pUL17 heterodimer. Final identification of the nature of this density will require a means to separate the contributions of each individual protein from the others and structures of higher resolution than are currently available.

A further point of interest will likely be the interaction of tegument, if any, with the portal vertex given the roles of pUL25 and pUL36 in viral DNA release and the replacement of a penton vertex with the portal structure. Currently, the analysis of the portal within the capsid shell tests the limits of contemporary cyro EM and cryo ET techniques (Cardone *et al.*, 2007; Chang *et al.*, 2007). Resolution of tegument portal interactions will firstly require an increased understanding of the association of portal with capsids, before analysis of capsids produced by mutants such as ARΔUL36 and FRΔUL37 to determine the patterns of tegument interaction at the portal vertex if this unique vertex can be robustly identified.

Current data support the proposition that the outer tegument assembles at the membrane system from which the virion envelope is derived by interaction with the tails of membrane embedded virion glycoproteins, particularly gD, gE and gH (Chi *et al.*, 2005; Farnsworth *et al.*, 2007; Gross *et al.*, 2003). Such assembly of the outer tegument at the membrane presumably accounts for the production of L particles. The formation of a site containing outer tegument and viral envelope proteins would result in a preformed site of secondary envelopment (PSSE) requiring association with an inner tegument decorated nucleocapsid for virion formation. Data from both PrV and HSV-1 mutants show that these PSSEs are competent to bud from the membrane system (currently thought to be the TGN) and be released from the host cell as L particles. That these PSSEs can form and bud in the absence of a wide variety of viral proteins suggests that there are multiple redundant interactions that drive the assembly of these structures and that no one protein is required to engage the ESCRT machinery component Vps4, which has been shown to have a role in facilitating viral envelopment (Crump *et al.*, 2007).

Studies reported here showing the exclusion of pUL36 or pUL37 from L particles derived from ΔUL37 or ΔUL36 infections respectively, indicate that PSSEs can incorporate pUL36 and pUL37 only when they are complexed together (Roberts *et al.*, 2009) and this is

supported by reports that pUL37 fails to localise to the TGN in the absence of pUL36 (Desai *et al.*, 2008). Their presence in L particles suggests that pUL36 and pUL37 can form a complex even in the absence of capsids. Data presented in this thesis suggests that envelopment of capsids also requires a complex of pUL36 and pUL37 as shown by the accumulation of pUL36 decorated capsids within the cytoplasm of FRΔUL37 infected cells and in keeping with the phenotypes of other ΔUL36 and ΔUL37 mutants (Desai *et al.*, 2001; Desai, 2000; Fuchs *et al.*, 2004; Klupp *et al.*, 2001b). A related study using ARΔUL36 and a fluorescently tagged version of FRΔUL37 showed that in the absence of pUL36 or pUL37, capsids did not associate with TGN-derived vesicles but remained distributed throughout the cytoplasm. This was in sharp contrast to WT HSV-1 capsids, which accumulated at the TGN and to capsids from another envelopment defective (gD-gE minus) mutant, which accumulated in the vicinity of TGN vesicles but did not undergo envelopment. From this it can be concluded that pUL36 and pUL37 are required for correct addressing of capsids to the TGN (D. Pasdeloup pers. comm.).

A study with a PrV mutant lacking pUL48 highlighted the accumulation of inner tegument decorated nucleocapsids within the cytoplasm of infected cells and the absence of these components from L particles whilst those same L particles contained representative outer tegument proteins (pUL46, pUL47, pUL49) (Fuchs *et al.*, 2002a). This suggests that pUL48 forms a bridge between the inner tegument and outer tegument and as such represents a critical nexus of interactions within virion formation. Therefore, the current definition of pUL48 as an outer tegument protein may need to be re-examined. Certainly increased attention on the localisation of pUL48 during infection would help to establish whether the function of pUL48 in assembly is exerted by primary recruitment to the inner tegument decorated capsid or to the PSSE, and answer the question of whether initial pUL48 association with capsid or PSSE is required for envelopment of virions. A recent report suggests that pUL48 may be recruited to the capsid early in virion assembly. pUL48 was found in primary virions of HSV-1 (Naldinho-Souto *et al.*, 2006), but this has not been seen in PrV (Fuchs *et al.*, 2002a) and the functional significance of this observation remains uncertain.

Thus, virion assembly is based on a complex set of protein interaction that are necessary and seemingly sufficient to achieve virion formation and release. Interactions that link each compartment are essential in this process and it would appear that tegument is assembled at two distinct sites, the inner tegument at the nucleocapsid, and the outer tegument at the membrane from which the viral envelope will be derived (summarised Fig.7.2). Within this

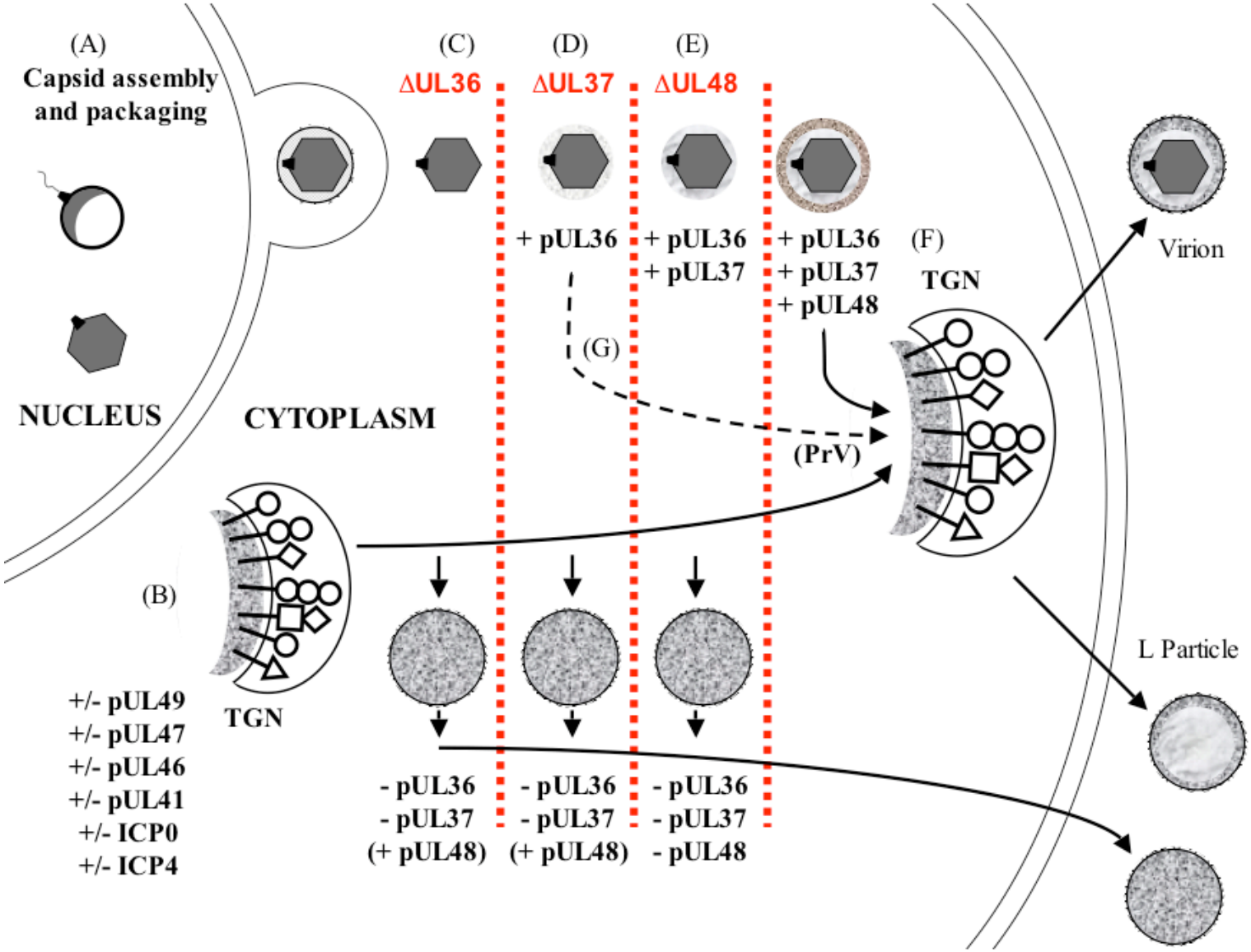
(A)
Capsid assembly
and packaging
NUCLEUS
CYTOPLASM
(B)
+/- pUL49
+/- pUL47
+/- pUL46
+/- pUL41
+/- ICP0
+/- ICP4
TGN
(C)
ΔUL36
(D)
ΔUL37
(E)
ΔUL48
+ pUL36
+ pUL36
+ pUL37
+ pUL36
+ pUL37
+ pUL48
(G)
(PrV)
(F)
TGN
Virion
L Particle
- pUL36
- pUL37
(+ pUL48)
- pUL36
- pUL37
(+ pUL48)
- pUL36
- pUL37
- pUL48

Figure 7.2: Model for the assembly of virions and L particles

(A) Assembly and packaging of the nucleocapsid takes place in the nucleus with subsequent release of the progeny nucleocapsid into the cytoplasm after budding through the nuclear membrane.

(B) Viral glycoproteins accumulate in the TGN and interact through their cytoplasmic tails with a range of tegument proteins to assemble a preformed site of secondary envelopment (PSSE).

(C) In the absence of pUL36 capsids accumulate within the cytoplasm and are not enveloped, while L particles are formed which lack pUL36 and pUL37.

(D) In the absence of pUL37 capsids decorated with pUL36 accumulate in cytoplasmic aggregates, L particles are formed and once more lack both pUL36 and pUL37.

(E) In the absence of pUL48 capsids decorated with pUL36 and pUL37 accumulate in cytoplasmic aggregates, L particles are formed and lack pUL36 and pUL37 in addition to lacking pUL48.

(F) In the presence of pUL36, pUL37 and pUL48 capsids are directed to the PSSE and acquire outer tegument and envelope components before exocytosis. Notably, pUL36, pUL37 and pUL48 are capable of interacting with the PSSE in the absence of capsid and this interaction produces an L particle.

(G) In PrV a mechanism exists by which capsids can proceed to secondary envelopment in the absence of pUL37. This mechanism is unknown and the requirement for other tegument proteins is uncertain (broken line).

network, pUL36, pUL37 and pUL48 are essential for envelopment. Seemingly, for the nucleocapsid to acquire a full tegument complement and final envelope a complex of pUL36 and pUL37 is required which must subsequently interact with pUL48 to direct acquisition of outer tegument. Likewise interaction of tegument with the cytoplasmic tails of gD, gE, gH and the presence of gI and gM are important for final envelopment.

7.2. Roles of the inner tegument in initiating infection

Our understanding of the roles of the inner tegument proteins in initiating infection was considerably less advanced than that of their roles in the later stages of viral infection. This deficit has recently begun to shrink as data emerge on the role of these proteins. Our understanding to date has been limited by the essential nature of these proteins in virion formation preventing their roles in the initiation of infection being studied in their absence.

The main tool available to assess the role of any inner tegument protein in initiating infection was a ts mutant tsB7 encoding a ts variant of pUL36 (Batterson *et al.*, 1983; Knipe *et al.*, 1981). No similar mutant of pUL37 has been available however limiting our understanding of the role of this protein. Analyses with tsB7 have suggested a role for pUL36 in genome uncoating (Batterson *et al.*, 1983), while other studies using WT HSV-1 have implicated pUL36 in recognition of the nuclear pore and potentially with genome uncoating in keeping with data from tsB7 (Copeland *et al.*, 2009; Ojala *et al.*, 2000; Pasdeloup *et al.*, 2009). Furthermore, pUL36 has been shown to be retained on capsids transported toward the nucleus in PrV and is important for microtubule based transport, presumably towards the nucleus, in HSV-1 (Luxton *et al.*, 2006; Morrison *et al.*, 1998a; Wolfstein *et al.*, 2006). Thus pUL36 appeared integral to the initiation of infection, while our knowledge of pUL37 functions at this stage of the life cycle was negligible.

It would seem likely that pUL36 functions at multiple stages in the initiation of infection, although to date this has yet to be formally proven. It could be suggested that pUL36 may have no function in recognising the nuclear pore or in genome uncoating and that these apparent functions result from transport towards the nucleus mediated by pUL36. However, analysis of tsB7 and WT HSV-1 suggests that pUL36 does indeed have a role in genome uncoating (Batterson *et al.*, 1983; Jovasevic *et al.*, 2008). Data presented within this thesis support the idea that pUL36 might also function in recognition of the nuclear pore, in that capsids lacking pUL36 (ARΔUL36) are widely distributed throughout the cytoplasm of infected syncytia, but no new cycles of viral DNA replication are initiated in

the naïve nuclei present within the same syncytium, nor are viral genomes seen in close proximity to the nuclear rim. This, in addition to the data from FRΔUL37 where new cycles of replication are established in initially naïve nuclei, suggests that pUL36 is required to recognise and interact with the nuclear pore complex.

Dissecting the contribution of pUL36 to each of these individual roles will be challenging. Use of targeted deletion or substitution mutagenesis has the potential to define the domains responsible for each activity but would need to show that any modification did not impair pUL36 folding, recruitment or functions other than those targeted. A more amenable approach might be to use complete deletion mutants, such as those described here, to analyse the contribution of inner tegument proteins to each individual function in minimal in vitro models, similar to the approaches of Wolfstein *et al*. (2006) and Ojala *et al*. (2000).

The contributions of pUL36 and pUL37 to transport might be further examined using a methodology similar to that of Wolfstein *et al*. (2006), but replacing stripped virions with more defined purified cytoplasmic C capsids. This would offer the possibility of assigning pUL36 function in the absence of pUL37 and then supplementing purified pUL37 to those same capsids to understand the direct effect of pUL37. Potentially, these purified cytoplasmic capsids could also be used to screen soluble components of the NPC for interaction or induction of genome uncoating. Likewise, such cytoplasmic capsids of tegument deletion mutants might be productively used in assays binding purified nuclei, whereby the structure of NPC bound and NPC free capsids could be established using cryo-ET methods.

Perhaps a most useful mutant would be a tsB7 lacking UL37 which could be locked into the NPC bound but genome retained state, with controlled genome release upon temperature shift as desired. If used in the syncytial model of infection demonstrated within this thesis, this would permit capsids bound to nuclear pores in the absence of pUL37 to be examined structurally, by cryo-ET, after purification of the nuclei.

Our understanding of the function of pUL37 in initiating infection lags behind that of pUL36. Evidence from PrV suggests that pUL37 may be involved in capsid transport (Krautwald *et al.*, 2009), but this data must be regarded carefully in light of the essential need for pUL37 in HSV-1 versus its non-essential, but enhancing role in PrV virion formation. Other data from PrV also suggests a role in capsid transport (Luxton *et al.*, 2006), which would make studies using HSV-1 mutants lacking pUL37 or with mutated

pUL37 in systems like that of Wolfstein *et al*. (2006) highly informative as to the role pUL37 may play in this stage of infection.

The apparent multifunctional nature of pUL36 and its essential role in virion production and in mediating infection may present a viable drug target. Should analysis of pUL36 function continue and yield mechanistic and structural data about pUL36 in capsid transport (motor protein binding), NPC binding and genome release it may be possible to target these activities selectively with novel small molecule inhibitors to block infection.

Recognition and binding of the nuclear pore complex is likely to be a feature of pUL36 conserved from ancestral herpesviruses. Herpesviruses are increasingly thought to be derived from an ancestor shared with bacteriophage, which would likewise require a function to recognise and bind the surface of the host cell. If the ancestral relationship between herpesviruses and bacteriophage is considered, and the proposition that structural features of the capsid are most likely to be retained (such as that seen in the major capsid protein fold (Baker *et al.*, 2005)) and passed to progeny generations, then it is not a giant leap to consider that a protein capable of recognising and binding the surface of the ancestral host might be retained and evolve through time. The origin of the nucleus itself is uncertain, and indeed an area of particular controversy (Cavalier-Smith, 2009; Dolan *et al.*, 2002; Forterre, 2006; Lake & Rivera, 1994; Martin, 2005), but one contention is that it is derived from the symbiosis of an archae with a eubacterium (Dolan *et al.*, 2002; Horiike *et al.*, 2001; Horiike *et al.*, 2004; Horiike *et al.*, 2002). If this was the case, it suggests that the bacteriophage lineage that gave rise to the herpesvirus lineage was able to adapt to the new situation of its host and adopt the necessary functions to traverse the eubacterium (equivalent to a modern eukaryotic cytoplasm) and to recognise the surface of the original host (precursor to the nucleus). This leads to the highly speculative proposition that pUL36 may be a descendent of one of the original phage attachment proteins and that its role in binding to the nuclear pore reflects an original role in phage attachment and penetration. Such an ancient root to the advent of herpesviruses would explain their apparent ubiquity in mammals, birds, fish and amphibians as well as their presence in invertebrates. It would, potentially, further explain the bacteriophage like nuclear assembly of capsids, and their release by envelopment at the nuclear membrane into the cytoplasm prior to mature virion formation through secondary envelopment and the probable cytoplasmic acquisition of tegument.

REFERENCES

Abaitua, F. & O'Hare, P. (2008). Identification of a highly conserve functional nuclear localization signal within the N-terminal region of herpes simplex virus type 1 VP1-2 tegument protein. *Journal of Virology* **82**, 5234-5244.

Adamson, W. E., McNab, D., Preston, V. G. & Rixon, F. J. (2006). Mutational analysis of the herpes simplex virus triplex protein VP19C. *Journal of Virology* **80**, 1537-1548.

Albright, A. G. & Jenkins, F. J. (1993). The herpes-simplex virus UL37-protein is phosphorylated in infected-cells. *Journal of Virology* **67**, 4842-4847.

Alwine, J. C., Steinhar.Wl & Hill, C. W. (1974). Transcription of herpes-simplex type-1 DNA in nuclei isolated from infected Hep-2 and KB-cells. *Virology* **60**, 302-307.

Antinone, S. E., Shubeita, G. T., Coller, K. E., Lee, J. I., Haverlock-Moyns, S., Gross, S. P. & Smith, G. A. (2006). The herpesvirus capsid surface protein, VP26, and the majority of the tegument proteins are dispensable for capsid transport toward the nucleus. *Journal of Virology* **80**, 5494-5498.

Arii, J., Uema, M., Morimoto, T., Sagara, H., Akashi, H., Ono, E., Arase, H. & Kawaguchi, Y. (2009). Entry of Herpes Simplex Virus 1 and Other Alphaherpesviruses via the Paired Immunoglobulin-Like Type 2 Receptor alpha. *Journal of Virology* **83**, 4520-4527.

Arzul, I., Renault, T., Lipart, C. & Davison, A. J. (2001). Evidence for interspecies transmission of oyster herpesvirus in marine bivalves. *Journal of General Virology* **82**, 865-870.

Babst, M., Wendland, B., Estepa, E. J. & Emr, S. D. (1998). The Vps4p AAA ATPase regulates membrane association of a Vps protein complex required for normal endosome function. *Embo Journal* **17**, 2982-2993.

Baines, J. D. & Roizman, B. (1991). The open reading frames UL3, UL4, UL10, and UL16 are dispensable for the replication of herpes-simplex virus 1 in cell-culture. *Journal of Virology* **65**, 938-944.

Baker, M. L., Jiang, W., Bowman, B. R., Zhou, Z. H., Quiocho, F. A., Rixon, F. J. & Chiu, W. (2003). Architecture of the herpes simplex virus major capsid protein derived from structural bioinformatics. *Journal of Molecular Biology* **331**, 447-456.

Baker, M. L., Jiang, W., Rixon, F. J. & Chiu, W. (2005). Common ancestry of herpesviruses and tailed DNA bacteriophages. *Journal of Virology* **79**, 14967-14970.

Balliet, J. W. & Schaffer, P. A. (2006). Point mutations in herpes simplex virus type 1 oriL, but not in oriS, reduce pathogenesis during acute infection of mice and impair reactivation from latency. *Journal of Virology* **80**, 440-450.

Bamford, D. H., Burnett, R. M. & Stuart, D. I. (2002). Evolution of viral structure. *Theor Popul Biol* **61**, 461-470.

Batterson, W., Furlong, D. & Roizman, B. (1983). Molecular-genetics of herpes-simplex virus 8. Further characterization of a temperature-sensitive mutant defective in release of viral-DNA and in other stages of the viral reproductive-cycle. *Journal of Virology* **45**, 397-407.

Belnap, D. M. & Steven, A. C. (2000). 'Deja vu all over again': the similar structures of bacteriophage PRD1 and adenovirus. *Trends in Microbiology* **8**, 91-93.

Benetti, L., Munger, J. & Roizman, B. (2003). The herpes simplex virus 1 U(s)3 protein kinase blocks caspase-dependent double cleavage and activation of the proapoptotic protein BAD. *Journal of Virology* **77**, 6567-6573.

Benson, S. D., Bamford, J. K. H., Bamford, D. H. & Burnett, R. M. (1999). Viral evolution revealed by bacteriophage PRD1 and human adenovirus coat protein structures. *Cell* **98**, 825-833.

Benson, S. D., Bamford, J. K. H., Bamford, D. H. & Burnett, R. M. (2004). Does common architecture reveal a viral lineage spanning all three domains of life? *Mol Cell* **16**, 673-685.

Bernard, J. & Mercier, A. (1993). Sequence of 2 EcoRI fragments from salmonis herpesvirus-2 and comparison with ictalurid herpesvirus-1. *Arch Virol* **132**, 437-442.

Bhella, D., Rixon, F. J. & Dargan, D. J. (2000). Cryomicroscopy of human cytomegalovirus virions reveals move densely packed genomic DNA than in herpes simplex virus type 1. *Journal of Molecular Biology* **295**, 155-161.

Bieniasz, P. D. (2006). Late budding domains and host proteins in enveloped virus release. *Virology* **344**, 55-63.

Bishop, N. & Woodman, P. (2000). ATPase-defective mammalian VPS4 localizes to aberrant endosomes and impairs cholesterol trafficking. *Molecular Biology of the Cell* **11**, 227-239.

Boehmer, P. E. & Lehman, I. R. (1997). Herpes simplex virus DNA replication. *Annual Review of Biochemistry* **66**, 347-384.

Booy, F. P., Newcomb, W. W., Trus, B. L., Brown, J. C., Baker, T. S. & Steven, A. C. (1991). Liquid-crystalline, phage-like packing of encapsidated DNA in herpes-simplex virus. *Cell* **64**, 1007-1015.

Booy, F. P., Trus, B. L., Newcomb, W. W., Brown, J. C., Conway, J. F. & Steven, A. C. (1994). Localisation of the 12kDa protein, VP26, in the capsid of herpes simplex virus type 1. In *13th International Congress on Electron Microscopy*, pp. 27-28. Edited by B. Jouffrey & C. Colliex. Paris, France: Editions Physique.

Boutell, C., Sadis, S. & Everett, R. D. (2002). Herpes simplex virus type 1 immediate-early protein ICP0 and is isolated RING finger domain act as ubiquitin E3 ligases in vitro. *Journal of Virology* **76**, 10.

Bowman, B. R., Baker, M. L., Rixon, F. J., Chiu, W. & Quiocho, F. A. (2003). Structure of the herpesvirus major capsid protein. *Embo Journal* **22**, 757-765.

Brack, A. R., Dijkstra, J. M., Granzow, H., Klupp, B. G. & Mettenleiter, T. C. (1999). Inhibition of virion maturation by simultaneous deletion of glycoproteins E, I, and M of pseudorabies virus. *Journal of Virology* **73**, 5364-5372.

Brown, S. M., Ritchie, D. A. & Subak-Sharpe, J. H. (1973). Genetic studies with herpes-simplex virus type-1 - isolation of temperature-sensitive mutants, their arrangement into complementation groups and recombination analysis leading to a linkage map. *Journal of General Virology* **18**, 329-346.

Bruckner, R. C., Crute, J. J., Dodson, M. S. & Lehman, I. R. (1991). The herpes-simplex virus-1 origin binding-protein - a DNA helicase. *Journal of Biological Chemistry* **266**, 2669-2674.

Buckmaster, A. E., Scott, S. D., Sanderson, M. J., Boursnell, M. E. G., Ross, N. L. J. & Binns, M. M. (1988). Gene sequence and mapping data from Mareks-disease virus and herpesvirus of turkeys - implications for herpesvirus classification. *Journal of General Virology* **69**, 2033-2042.

Bucks, M. A., O'Regan, K. J., Murphy, M. A., Wills, J. W. & Courtney, R. J. (2007). Herpes simplex virus type 1 tegument proteins VP1/2 and UL37 are associated with intranuclear capsids. *Virology* **361**, 316-324.

Cai, W., Gu, B. & Person, S. (1988). Role of glycoprotein B of herpes simplex virus type 1 in viral entry and cell fusion. *Journal of Virology* **62**, 2596-2604.

Cai, W. H., Astor, T. L., Liptak, L. M., Cho, C., Coen, D. M. & Schaffer, P. A. (1993). The herpes-simplex virus type-1 regulatory protein ICP0 enhances virus-replication during acute infection and reactivation from latency. *Journal of Virology* **67**, 7501-7512.

Campadelli, G., Brandimarti, R., Dilazzaro, C., Ward, P. L., Roizman, B. & Torrisi, M. R. (1993). Fragmentation and dispersal of Golgi proteins and redistribution of glycoproteins and glycolipids processed through the Golgi-apparatus after infection with herpes-simplex virus-1. *Proceedings of the National Academy of Sciences of the United States of America* **90**, 2798-2802.

Campbell, M. E. M., Palfreyman, J. W. & Preston, C. M. (1984). Identification of herpes-simplex virus-DNA sequences which encode a trans-acting polypeptide responsible for stimulation of immediate early transcription. *Journal of Molecular Biology* **180**, 1-19.

Cardone, G., Winkler, D. C., Trus, B. L., Cheng, N. Q., Heuser, J. E., Newcomb, W. W., Brown, J. C. & Steven, A. C. (2007). Visualization of the herpes simplex virus portal in situ by cryo-electron tomography. *Virology* **361**, 426-434.

Carfi, A., Willis, S. H., Whitbeck, J. C., Krummenacher, C., Cohen, G. H., Eisenberg, R. J. & Wiley, D. C. (2001). Herpes simplex virus glycoprotein D bound to the human receptor HveA. *Mol Cell* **8**, 169-179.

Cartier, A., Komai, T. & Masucci, M. G. (2003). The Us3 protein kinase of herpes simplex virus 1 blocks apoptosis and induces phosporylation of the Bcl-2 family member Bad. *Experimental Cell Research* **291**, 242-250.

Cavalier-Smith, T. (2009). Predation and eukaryote cell origins: A coevolutionary perspective. *International Journal of Biochemistry & Cell Biology* **41**, 307-322.

Cerritelli, M. E., Cheng, N. Q., Rosenberg, A. H., McPherson, C. E., Booy, F. P. & Steven, A. C. (1997). Encapsidated conformation of bacteriophage T7 DNA. *Cell* **91**, 271-280.

Ch'ng, T. H. & Enquist, L. W. (2005). Neuron-to-cell spread of pseudorabies virus in a compartmented neuronal culture system. *Journal of Virology* **79**, 10875-10889.

Chang, J. T., Schmid, M. F., Rixon, F. J. & Chiu, W. (2007). Electron cryotomography reveals the portal in the herpesvirus capsid. *Journal of Virology* **81**, 2065-2068.

Chee, M. S., Bankier, A. T., Beck, S., Bohni, R., Brown, C. M., Cerny, R., Horsnell, T., Hutchison, C. A., Kouzarides, T., Martignetti, J. A., Preddie, E., Satchwell, S. C., Tomlinson, P., Weston, K. M. & Barrell, B. G. (1990). Analysis of the protein-coding content of the sequence of human cytomegalovirus strain AD169. *Current Topics in Microbiology and Immunology* **154**, 125-169.

Chen, D. H., Jakana, J., McNab, D., Mitchell, J., Zhou, Z. H., Dougherty, M., Chiu, W. & Rixon, F. J. (2001). The pattern of tegument-capsid interaction in the herpes simplex virus type 1 virion is not influenced by the small hexon-associated protein VP26. *Journal of Virology* **75**, 11863-11867.

Chen, D. H., Jiang, H., Lee, M., Liu, F. Y. & Zhou, Z. H. (1999). Three-dimensional visualization of tegument/capsid interactions in the intact human cytomegalovirus. *Virology* **260**, 10-16.

Cheung, P., Banfield, B. W. & Tufaro, F. (1991). Brefeldin-A arrests the maturation and egress of herpes-simplex virus-particles during infection. *Journal of Virology* **65**, 1893-1904.

Chi, J. H. I., Harley, C. A., Mukhopadhyay, A. & Wilson, D. W. (2005). The cytoplasmic tall of herpes simplex virus envelope glycoprotein D binds to the tegument protein VP22 and to capsids. *Journal of General Virology* **86**, 253-261.

Chou, J. & Roizman, B. (1989). Characterization of DNA sequence-common and sequence-specific proteins binding to cis-acting sites for cleavage of the terminal a-sequence of the herpes-simplex virus-1 genome. *Journal of Virology* **63**, 1059-1068.

Clarke, R. W., Monnier, N., Li, H. T., Zhou, D. J., Browne, H. & Klenerman, D. (2007). Two-color fluorescence analysis of individual virions determines the distribution of the copy number of proteins in herpes simplex virus particles. *Biophysical Journal* **93**, 1329-1337.

Cohen, J. I., Straus, S. E. & Arvin, A. M. (2007). Varicella-Zoster virus replication, pathogenesis and management. In *Fields Virology 5th ed*. Edited by D. M. Knipe & P. M. Howley: Lippincott Williams & Wilkins

Coleman, H. M., Connor, V., Cheng, Z. S. C., Grey, F., Preston, C. M. & Efstathiou, S. (2008). Histone modifications associated with herpes simplex virus type 1

genomes during quiescence and following ICP0-mediated de-repression. *Journal of General Virology* **89**, 68-77.

Coller, K. E., Lee, J. I. H., Ueda, A. & Smith, G. A. (2007). The capsid and tegument of the alphaherpesviruses are linked by an interaction between the UL25 and VP1/2 proteins. *Journal of Virology* **81**, 11790-11797.

Coller, K. E. & Smith, G. A. (2008). Two viral kinases are required for sustained long distance axon transport of a neuroinvasive herpesvirus. *Traffic* **9**, 1458-1470.

Collins, J. (1981). Instability of palindromic DNA in Escherichia-coli. In *Cold Spring Harbor Laboratory Cold Spring Harbor Symposia on Quantitative Biology, Vol 45 Parts 1 and 2 Movable Genetic Elements; Xxi+445p(Part 1); Xiii+578p(Part 2) Cold Spring Harbor Laboratory: Cold Spring Harbor, NY, USA Illus*, pp. P409-416.

Conley, A. J., Knipe, D. M., Jones, P. C. & Roizman, B. (1981). Molecular-genetics of herpes-simplex virus 7. Characterization of a temperature-sensitive mutant produced by in vitro mutagenesis and defective in DNA-synthesis and accumulation of gamma-polypeptides. *Journal of Virology* **37**, 191-206.

Copeland, A. M., Newcomb, W. W. & Brown, J. C. (2009). Herpes Simplex Virus Replication: Roles of Viral Proteins and Nucleoporins in Capsid-Nucleus Attachment. *Journal of Virology* **83**, 1660-1668.

Correnti, J., Munster, V., Chan, T. & van der Woude, M. (2002). Dam-dependent phase variation of Ag43 in Escherichia coli is altered in a seqA mutant. *Molecular Microbiology* **44**, 521-532.

Costanzo, F., Campadellifiume, G., Foatomasi, L. & Cassai, E. (1977). Evidence that herpes-simplex virus-DNA is transcribed by cellular RNA polymerase-B. *Journal of Virology* **21**, 996-1001.

Crump, C. A., Yates, C. & Minson, T. (2007). Herpes simplex virus type 1 cytoplasmic envelopment requires functional Vps4. *Journal of Virology* **81**, 7380-7387.

Crute, J. J., Mocarski, E. S. & Lehman, I. R. (1988). A DNA helicase induced by herpes-simplex virus type-1. *Nucleic Acids Res* **16**, 6585-6596.

Crute, J. J., Tsurumi, T., Zhu, L., Weller, S. K., Olivo, P. D., Challberg, M. D., Mocarski, E. S. & Lehman, I. R. (1989). Herpes-simplex virus-1 helicase primase - a complex of 3 herpes-encoded gene-products. *Proceedings of the National Academy of Sciences of the United States of America* **86**, 2186-2189.

Cunningham, C. & Davison, A. J. (1993). A cosmid-based system for constructing mutants of herpes-simplex virus type-1. *Virology* **197**, 116-124.

Dai, W., Jia, Q. M., Bortz, E., Shah, S., Liu, J., Atanasov, I., Li, X. D., Taylor, K. A., Sun, R. & Zhou, Z. H. (2008). Unique structures in a tumor herpesvirus revealed by cryo-electron tomography and microscopy. *Journal of Structural Biology* **161**, 11.

Daikoku, T., Yamashita, Y., Tsurumi, T., Maeno, K. & Nishiyama, Y. (1993). Purification and biochemical-characterization of the protein-kinase encoded by the US3 gene of herpes-simplex virus type-2. *Virology* **197**, 685-694.

Daikoku, T., Yamashita, Y., Tsurumi, T. & Nishiyama, Y. (1995). The US3 protein-kinase of herpes-simplex virus type-2 is associated with phosphorylation of the UL12 alkaline nuclease in vitro. *Arch Virol* **140**, 1637-1644.

Dalrymple, M. A., McGeoch, D. J., Davison, A. J. & Preston, C. M. (1985). DNA-sequence of the herpes-simplex virus type-1 gene whose product is responsible for transcriptional activation of immediate early promoters. *Nucleic Acids Res* **13**, 7865-7879.

Dargan, D. J. (1986). The structure and assembly of herpesviruses. In *Electron Microscopy of Proteins*, pp. 359-437. London: Academic Press.

Dargan, D. J., Patel, A. H. & Subak-Sharpe, J. H. (1995). PREPS - herpes-simplex virus type 1-specific particles produced by infected-cells when viral-DNA replication is blocked. *Journal of Virology* **69**, 4924-4932.

Dargan, D. J. & Subak-Sharpe, J. H. (1997). The effect of herpes simplex virus type 1 L-particles on virus entry, replication, and the infectivity of naked herpesvirus DNA. *Virology* **239**, 378-388.

Dasgupta, A. & Wilson, D. W. (1999). ATP depletion blocks herpes simplex virus DNA packaging acid capsid maturation. *Journal of Virology* **73**, 2006-2015.

Dasgupta, A. & Wilson, D. W. (2001). Evaluation of the primary effect of brefeldin A treatment upon herpes simplex virus assembly. *Journal of General Virology* **82**, 1561-1567.

Davison, A. J. (1992). Channel catfish virus - a new type of herpesvirus. *Virology* **186**, 9-14.

Davison, A. J. (1998). The genome of salmonid herpesvirus 1. *Journal of Virology* **72**, 1974-1982.

Davison, A. J. (2002). Evolution of the herpesviruses. *Veterinary Microbiology* **86**, 20.

Davison, A. J. & Davison, M. D. (1995). Identification of structural proteins of Channel catfish virus by mass-spectrometry. *Virology* **206**, 1035-1043.

Davison, A. J., Eberle, R., Ehlers, B., Hayward, G. S., McGeoch, D. J., Minson, A. C., Pellett, P. E., Roizman, B., Studdert, M. J. & Thiry, E. (2009). The order Herpesvirales. *Arch Virol* **154**, 171-177.

Davison, A. J., Eberle, R., Hayward, G. S., McGeoch, D. J., Minson, A. C., Pellett, P. E., Roizman, B., Studdert, M. J. & Thiry, E. (2005a). Herpesviridae. In *Virus Taxonomy: VIIIth Report of the International Committee on Taxonomy of viruses*, pp. 193-212. Edited by C. M. Fauquet, M. A. Mayo, J. Maniloff, U. Desselberger & L. A. Ball. London, UK: Elsevier Academic Press.

Davison, A. J., Trus, B. L., Cheng, N. Q., Steven, A. C., Watson, M. S., Cunningham, C., Le Deuff, R. M. & Renault, T. (2005b). A novel class of herpesvirus with bivalve hosts. *Journal of General Virology* **86**, 41-53.

de Bruyn Kops, A., Uprichard, S. L., Chen, M. & Knipe, D. M. (1998). Comparison of the intranuclear distributions of herpes simplex virus proteins involved in various viral functions. *Virology* **252**, 162-178.

Debrabander, M. J., Vandeveire, R. M. L., Aerts, F. E. M., Borgers, M. & Janssen, P. A. J. (1976). Effects of methyl 5-(2-thienylcarbonyl)-1H-benzimidazol-2-yl carbamate, (R-17934-NSC-238159), a new synthetic antitumoral drug interfering with microtubules, on mammalian-cells cultured in vitro. *Cancer Research* **36**, 905-916.

del Rio, T., Ch'ng, T. H., Flood, E. A., Gross, S. P. & Enquist, L. W. (2005). Heterogeneity of a fluorescent tegument component in single pseudorabies virus virions and enveloped axonal assemblies. *Journal of Virology* **79**, 3903-3919.

del Rio, T., Werner, H. C. & Enquist, L. W. (2002). The pseudorabies virus VP22 homologue (UL49) is dispensable for virus growth in vitro and has no effect on virulence and neuronal spread in rodents. *Journal of Virology* **76**, 774-782.

Demirov, D. G. & Freed, E. O. (2004). Retrovirus budding. *Virus Research* **106**, 87-102.

Desai, P., Deluca, N. A., Glorioso, J. C. & Person, S. (1993). Mutations in herpes-simplex virus type-1 genes encoding VP5 and VP23 abrogate capsid formation and cleavage of replicated DNA. *Journal of Virology* **67**, 1357-1364.

Desai, P., DeLuca, N. A. & Person, S. (1998). Herpes simplex virus type 1 VP26 is not essential for replication in cell culture but influences production of infectious virus in the nervous system of infected mice. *Virology* **247**, 115-124.

Desai, P. & Person, S. (1999). Second site mutations in the N-terminus of the major capsid protein (VP5) overcome a block at the maturation cleavage site of the capsid scaffold proteins of herpes simplex virus type 1. *Virology* **261**, 357-366.

Desai, P., Sexton, G. L., Huang, E. & Person, S. (2008). Localization of Herpes Simplex Virus Type 1 UL37 in the Golgi Complex Requires UL36 but Not Capsid Structures. *Journal of Virology* **82**, 11354-11361.

Desai, P., Sexton, G. L., McCaffery, J. M. & Person, S. (2001). A null mutation in the gene encoding the herpes simplex virus type 1 UL37 polypeptide abrogates virus maturation. *Journal of Virology* **75**, 10259-10271.

Desai, P. J. (2000). A null mutation in the UL36 gene of herpes simplex virus type 1 results in accumulation of unenveloped DNA-filled capsids in the cytoplasm of infected cells. *Journal of Virology* **74**, 11608-11618.

Diefenbach, R. J., Miranda-Saksena, M., Douglas, M. W. & Cunningham, A. L. (2008). Transport and egress of herpes simplex virus in neurons. *Reviews in Medical Virology* **18**, 35-51.

Dohner, K., Nagel, C. H. & Sodeik, B. (2005). Viral stop-and-go along microtubules: taking a ride with dynein and kinesins. *Trends in Microbiology* **13**, 320-327.

Dohner, K., Radtke, K., Schmidt, S. & Sodeik, B. (2006). Eclipse phase of herpes simplex virus type 1 infection: Efficient dynein-mediated capsid transport without the small capsid protein VP26. *Journal of Virology* **80**, 8211-8224.

Dohner, K., Wolfstein, A., Prank, U., Echeverri, C., Dujardin, D., Vallee, R. & Sodeik, B. (2002). Function of dynein and dynactin in herpes simplex virus capsid transport. *Molecular Biology of the Cell* **13**, 2795-2809.

Dolan, M. F., Melnitsky, H., Margulis, L. & Kolnicki, R. (2002). Motility proteins and the origin of the nucleus. *Anatomical Record* **268**, 290-301.

Douglas, M. W., Diefenbach, R. J., Homa, F. L., Miranda-Saksena, M., Rixon, F. J., Vittone, V., Byth, K. & Cunningham, A. L. (2004). Herpes simplex virus type 1 capsid protein VP26 interacts with dynein light chains RP3 and Tctex1 and plays a role in retrograde cellular transport. *Journal of Biological Chemistry* **279**, 28522-28530.

Duffy, C., LaVail, J. H., Tauscher, A. N., Wills, E. G., Blaho, J. A. & Baines, J. D. (2006). Characterization of a U(L)49-null mutant: VP22 of herpes simplex virus type 1 facilitates viral spread in cultured cells and the mouse cornea. *Journal of Virology* **80**, 8664-8675.

Efstathiou, S. & Preston, C. M. (2005). Towards an understanding of the molecular basis of herpes simplex virus latency. *Virus Research* **111**, 108-119.

Elias, P. & Lehman, I. R. (1988). Interaction of origin binding-protein with an origin of replication of herpes-simplex virus-1. *Proceedings of the National Academy of Sciences of the United States of America* **85**, 2959-2963.

Elias, P., Odonnell, M. E., Mocarski, E. S. & Lehman, I. R. (1986). A DNA-binding protein-specific for an origin of replication of herpes-simplex virus type-1. *Proceedings of the National Academy of Sciences of the United States of America* **83**, 6322-6326.

Elliott, G., Hafezi, W., Whiteley, A. & Bernard, E. (2005). Deletion of the herpes simplex virus VP22-encoding gene (UL49) alters the expression, localization, and virion incorporation of ICP0. *Journal of Virology* **79**, 9735-9745.

Elliott, G. & O'Hare, P. (1997). Intercellular trafficking and protein delivery by a herpesvirus structural protein. *Cell* **88**, 223-233.

Elliott, G. & O'Hare, P. (1998). Herpes simplex virus type 1 tegument protein VP22 induces the stabilization and hyperacetylation of microtubules. *Journal of Virology* **72**, 6448-6455.

Elliott, G., O'Reilly, D. & O'Hare, P. (1996). Phosphorylation of the herpes simplex virus type I tegument protein VP22. *Virology* **226**, 140-145.

Elliott, G. D. & Meredith, D. M. (1992). The herpes-simplex virus type-1 tegument protein VP22 is encoded by gene UL49. *Journal of General Virology* **73**, 723-726.

Everett, R. D. & Murray, J. (2005). ND10 components relocate to sites associated with herpes simplex virus type 1 nucleoprotein complexes during virus infection. *Journal of Virology* **79**, 5078-5089.

Everett, R. D., Murray, J., Orr, A. & Preston, C. M. (2007). Herpes simplex virus type 1 genomes are associated with ND10 nuclear substructures in quiescently infected human fibroblasts. *Journal of Virology* **81**, 10991-11004.

Everett, R. D., Parada, C., Gripon, P., Sirma, H. & Orr, A. (2008). Replication of ICP0-Null mutant herpes simplex virus type 1 is restricted by both PML and Sp100. *Journal of Virology* **82**, 2661-2672.

Everett, R. D., Parsy, M. L. & Orr, A. (2009). Analysis of the Functions of Herpes Simplex Virus Type 1 Regulatory Protein ICP0 That Are Critical for Lytic Infection and Derepression of Quiescent Viral Genomes. *Journal of Virology* **83**, 4963-4977.

Everett, R. D., Rechter, S., Papior, P., Tavalai, N., Stamminger, T. & Orr, A. (2006). PML contributes to a cellular mechanism of repression of herpes simplex virus type 1 infection that is inactivated by ICP0. *Journal of Virology* **80**, 7995-8005.

Everly, D. N., Feng, P. H., Mian, I. S. & Read, G. S. (2002). mRNA degradation by the virion host shutoff (Vhs) protein of herpes simplex virus: Genetic and biochemical evidence that Vhs is a nuclease. *Journal of Virology* **76**, 8560-8571.

Farnsworth, A., Goldsmith, K. & Johnson, D. C. (2003). Herpes simplex virus glycoproteins gD and gE/gI serve essential but redundant functions during acquisition of the virion envelope in the cytoplasm. *Journal of Virology* **77**, 8481-8494.

Farnsworth, A. & Johnson, D. C. (2006). Herpes simplex virus gE/gI must accumulate in the trans-golgi network at early times and then redistribute to cell junctions to promote cell-cell spread. *Journal of Virology* **80**, 3167-3179.

Farnsworth, A., Wisner, T. W. & Johnson, D. C. (2007). Cytoplasmic residues of herpes simplex virus glycoprotein gE required for secondary envelopment and binding of tegument proteins VP22 and UL11 to gE and gD. *Journal of Virology* **81**, 319-331.

Farrell, M. J., Dobson, A. T. & Feldman, L. T. (1991). Herpes-simplex virus latency-associated transcript is a stable intron. *Proceedings of the National Academy of Sciences of the United States of America* **88**, 790-794.

Feng, P. H., Everly, D. N. & Read, G. S. (2001). mRNA decay during herpesvirus infections: Interaction between a putative viral nuclease and a cellular translation factor. *Journal of Virology* **75**, 10272-10280.

Fenwick, M. L. & Everett, R. D. (1990). Inactivation of the shutoff gene (UL41) of herpes-simplex virus type-1 and type-2. *Journal of General Virology* **71**, 2961-2967.

Fenwick, M. L. & McMenamin, M. M. (1984). Early virion-associated suppression of cellular protein-synthesis by herpes-simplex virus is accompanied by inactivation of messenger-RNA. *Journal of General Virology* **65**, 1225-1228.

Fierer, D. S. & Challberg, M. D. (1992). Purification and characterization of UL9, the herpes-simplex virus type-1 origin-binding protein. *Journal of Virology* **66**, 3986-3995.

Forrester, A., Farrell, H., Wilkinson, G., Kaye, J., Davispoynter, N. & Minson, T. (1992). Construction and properties of a mutant of herpes-simplex virus type-1 with glycoprotein-H coding sequences deleted. *Journal of Virology* **66**, 341-348.

Forterre, P. (2006). The origin of viruses and their possible roles in major evolutionary transitions. *Virus Research* **117**, 5-16.

Fraile-Ramos, A., Pelchen-Matthews, A., Kledal, T. N., Browne, H., Schwartz, T. W. & Marsh, M. (2002). Localization of HCMV UL33 and US27 in Endocytic compartments and viral membranes. *Traffic* **3**, 218-232.

Frame, M. C., Purves, F. C., McGeoch, D. J., Marsden, H. S. & Leader, D. P. (1987). Identification of the herpes-simplex virus protein-kinase as the product of viral gene US3. *Journal of General Virology* **68**, 2699-2704.

Fuchs, W., Granzow, H., Klupp, B. G., Kopp, M. & Mettenleiter, T. C. (2002a). The UL48 tegument protein of pseudorabies virus is critical for intracytoplasmic assembly of infectious virions. *Journal of Virology* **76**, 6729-6742.

Fuchs, W., Klupp, B. G., Granzow, H., Hengartner, C., Brack, A., Mundt, A., Enquist, L. W. & Mettenleiter, T. C. (2002b). Physical interaction between envelope glycoproteins E and M of pseudorabies virus and the major tegument protein UL49. *Journal of Virology* **76**, 8208-8217.

Fuchs, W., Klupp, B. G., Granzow, H. & Mettenleiter, T. C. (2004). Essential function of the pseudorabies virus UL36 gene product is independent of its interaction with the UL37 protein. *Journal of Virology* **78**, 11879-11889.

Fuchs, W., Klupp, B. G., Granzow, H., Osterrieder, N. & Mettenleiter, T. C. (2002c). The interacting UL31 and UL34 gene products of pseudorabies virus are involved in egress from the host-cell nucleus and represent components of primary enveloped but not mature virions. *Journal of Virology* **76**, 364-378.

Gao, M., Matusickkumar, L., Hurlburt, W., Ditusa, S. F., Newcomb, W. W., Brown, J. C., McCann, P. J., Deckman, I. & Colonno, R. J. (1994). The protease of herpes-simplex virus type-1 is essential for functional capsid formation and viral growth. *Journal of Virology* **68**, 3702-3712.

Ghoshchoudhury, N., Graham, A. & Ghosh, H. P. (1987). Herpes-simplex virus type-2 glycoprotein biogenesis - effect of monensin on glycoprotein maturation, intracellular-transport and virus infectivity. *Journal of General Virology* **68**, 1939-1949.

Gibbs, J. S., Chiou, H. C., Hall, J. D., Mount, D. W., Retondo, M. J., Weller, S. K. & Coen, D. M. (1985). Sequence and mapping analyses of the herpes-simplex virus-DNA polymerase gene predict a C-terminal substrate binding domain. *Proceedings of the National Academy of Sciences of the United States of America* **82**, 7969-7973.

Goding, C. R. & O'Hare, P. (1989). Herpes-simplex virus Vmw65 octamer binding-protein interaction - a paradigm for combinatorial control of transcription. *Virology* **173**, 363-367.

Granzow, H., Klupp, B. G., Fuchs, W., Veits, J., Osterrieder, N. & Mettenleiter, T. C. (2001). Egress of alphaherpesviruses: Comparative ultrastructural study. *Journal of Virology* **75**, 3675-3684.

Granzow, H., Klupp, B. G. & Mettenleiter, T. C. (2004). The pseudorabies virus US3 protein is a component of primary and of mature virions. *Journal of Virology* **78**, 1314-1323.

Greber, U. F. & Fassati, A. (2003). Nuclear import of viral DNA genomes. *Traffic* **4**, 136-143.

Greber, U. F. & Way, M. (2006). A superhighway to virus infection. *Cell* **124**, 741-754.

Grey, F., Hook, L. & Nelson, J. (2008). The functions of herpesvirus-encoded microRNAs. *Medical Microbiology and Immunology* **197**, 261-267.

Gross, S. T., Harley, C. A. & Wilson, D. W. (2003). The cytoplasmic tail of Herpes simplex virus glycoprotein H binds to the tegument protein VP16 in vitro and in vivo. *Virology* **317**, 1-12.

Grunewald, K., Desai, P., Winkler, D. C., Heymann, J. B., Belnap, D. M., Baumeister, W. & Steven, A. C. (2003). Three-dimensional structure of herpes simplex virus from cryo-electron tomography. *Science* **302**, 1396-1398.

Gu, H. D. & Roizman, B. (2009). The Two Functions of Herpes Simplex Virus 1 ICP0, Inhibition of Silencing by the CoREST/REST/HDAC Complex and Degradation of PML, Are Executed in Tandem. *Journal of Virology* **83**, 181-187.

Guzman, L. M., Belin, D., Carson, M. J. & Beckwith, J. (1995). Tight regulation, modulation, and high-level expression by vectors containing the arabinose P-BAD promoter. *Journal of Bacteriology* **177**, 4121-4130.

Hafezi, W., Bernard, E., Cook, R. & Elliott, G. (2005). Herpes simplex virus tegument protein VP22 contains an internal VP16 interaction domain and a C-terminal domain that are both required for VP22 assembly into the virus particle. *Journal of Virology* **79**, 13082-13093.

Hancock, M. H., Corcoran, J. A. & Smiley, J. R. (2006). Herpes simplex virus regulatory proteins VP16 and ICP0 counteract an innate intranuclear barrier to viral gene expression. *Virology* **352**, 237-252.

Handler, C. G., Cohen, G. H. & Eisenberg, R. J. (1996a). Cross-linking of glycoprotein oligomers during herpes simplex virus type 1 entry. *Journal of Virology* **70**, 6076-6082.

Handler, C. G., Eisenberg, R. J. & Cohen, G. H. (1996b). Oligomeric structure of glycoproteins in herpes simplex virus type 1. *Journal of Virology* **70**, 6067-6075.

Harley, C. A., Dasgupta, A. & Wilson, D. W. (2001). Characterization of herpes simplex virus-containing organelles by subcellular fractionation: Role for organelle acidification in assembly of infectious particles. *Journal of Virology* **75**, 1236-1251.

Heldwein, E. E., Lou, H., Bender, F. C., Cohen, G. H., Eisenberg, R. J. & Harrison, S. C. (2006). Crystal structure of glycoprotein B from herpes simplex virus 1. *Science* **313**, 217-220.

Hernandez, T. R. & Lehman, I. R. (1990). Functional interaction between the herpes simplex-1 DNA-polymerase and UL42 protein. *Journal of Biological Chemistry* **265**, 11227-11232.

Herold, B. C., Visalli, R. J., Susmarski, N., Brandt, C. R. & Spear, P. G. (1994). Glycoprotein-C-independent binding of herpes-simplex virus to cells requires cell-surface heparan-sulfate and glycoprotein-B. *Journal of General Virology* **75**, 1211-1222.

Herold, B. C., Wudunn, D., Soltys, N. & Spear, P. G. (1991). Glycoprotein-C of herpes-simplex virus type-1 plays a principal role in the adsorption of virus to cells and in infectivity. *Journal of Virology* **65**, 1090-1098.

Heymann, J. B., Cheng, N. Q., Newcomb, W. W., Trus, B. L., Brown, J. C. & Steven, A. C. (2003). Dynamics of herpes simplex virus capsid maturation visualized by time-lapse cryo-electron microscopy. *Nat Struct Biol* **10**, 334-341.

Hirokawa, N. (1998). Kinesin and dynein superfamily proteins and the mechanism of organelle transport. *Science* **279**, 519-526.

Hofemeister, H. & O'Hare, P. (2008). Nuclear pore composition and gating in herpes simplex virus-infected cells. *Journal of Virology* **82**, 8392-8399.

Holland, D. J., Miranda-Saksena, M., Boadle, R. A., Armati, P. & Cunningham, A. L. (1999). Anterograde transport of herpes simplex virus proteins in axons of peripheral human fetal neurons: an immunoelectron microscopy study. *Journal of Virology* **73**, 8503-8511.

Homa, F. L. & Brown, J. C. (1997). Capsid assembly and DNA packaging in herpes simplex virus. *Reviews in Medical Virology* **7**, 107-122.

Honess, R. W. & Roizman, B. (1974). Regulation of herpesvirus macromolecular-synthesis 1. Cascade regulation of synthesis of 3 groups of viral proteins. *Journal of Virology* **14**, 8-19.

Honess, R. W. & Roizman, B. (1975). Regulation of herpesvirus macromolecular-synthesis - sequential transition of polypeptide-synthesis requires functional viral polypeptides 3. *Proceedings of the National Academy of Sciences of the United States of America* **72**, 1276-1280.

Honess, R. W. & Watson, D. H. (1977). Herpes-simplex virus-resistance and sensitivity to Phosphonoacetic acid. *Journal of Virology* **21**, 584-600.

Horiike, T., Hamada, K., Kanaya, S. & Shinozawa, T. (2001). Origin of eukaryotic cell nuclei by symbiosis of Archaea in Bacteria is revealed by homology-hit analysis. *Nature Cell Biology* **3**, 210-214.

Horiike, T., Hamada, K., Miyata, D. & Shinozawa, T. (2004). The origin of eukaryotes is suggested as the symbiosis of pyrococcus into gamma-proteobacteria by phylogenetic tree based on gene content. *Journal of Molecular Evolution* **59**, 606-619.

Horiike, T., Hamada, K. & Shinozawa, T. (2002). Origin of Eukaryotic Cell Nuclei by Symbiosis of Archaea in Bacteria supported by the newly clarified origin of functional genes. *Genes & Genetic Systems* **77**, 369-376.

Hugel, T., Michaelis, J., Hetherington, C. L., Jardine, P. J., Grimes, S., Walter, J. M., Faik, W., Anderson, D. L. & Bustamante, C. (2007). Experimental test of connector rotation during DNA packaging into bacteriophage phi 29 capsids. *Plos Biology* **5**, 558-567.

Hurley, J. H. & Emr, S. D. (2006). The ESCRT complexes: Structure and mechanism of a membrane-trafficking network. *Annual Review of Biophysics and Biomolecular Structure* **35**, 277-298.

Igarashi, K., Fawl, R., Roller, R. J. & Roizman, B. (1993). Construction and properties of a recombinant herpes-simplex virus-1 lacking both S-component origins of DNA-synthesis. *Journal of Virology* **67**, 2123-2132.

Izaurralde, E., Kann, M., Pante, N., Sodeik, B. & Hohn, T. (1999). Viruses, microorganisms and scientists meet the nuclear pore (Leysin, Switzerland; February 26-March 1, 1998; European Molecular Biology Organization). *EMBO (European Molecular Biology Organization) Journal* **18**, 289-296.

Jackson, S. A. & DeLuca, N. A. (2003). Relationship of herpes simplex virus genome configuration to productive and persistent infections. *Proceedings of the National Academy of Sciences of the United States of America* **100**, 7871-7876.

Jerome, K. R., Fox, R., Chen, Z., Sears, A. E., Lee, H. Y. & Corey, L. (1999). Herpes simplex virus inhibits apoptosis through the action of two genes, Us5 and Us3. *Journal of Virology* **73**, 8950-8957.

Johnson, D. C. & Ligas, M. W. (1988). Herpes-simplex viruses lacking glycoprotein-D are unable to inhibit virus penetration - quantitative evidence for virus-specific cell-surface receptors. *Journal of Virology* **62**, 4605-4612.

Jones, C. (2003). Herpes simplex virus type 1 and bovine herpesvirus 1 latency. *Clinical Microbiology Reviews* **16**, 79-+.

Jones, P. C. & Roizman, B. (1979). Regulation of herpesvirus macromolecular-synthesis 8. Transcription program consists of 3 phases during which both extent of transcription and accumulation of RNA in the cytoplasm are regulated. *Journal of Virology* **31**, 299-314.

Jonker, H. R. A., Wechselberger, R. W., Boelens, R., Folkers, G. E. & Kaptein, R. (2005). Structural properties of the promiscuous VP16 activation domain. *Biochemistry* **44**, 827-839.

Jovasevic, V., Liang, L. & Roizman, B. (2008). Proteolytic cleavage of VP1-2 is required for release of herpes simplex virus 1 DNA into the nucleus. *Journal of Virology* **82**, 3311-3319.

Kato, K., Daikoku, T., Goshima, F., Kume, H., Yamaki, K. & Nishiyama, Y. (2000). Synthesis, subcellular localization and VP16 interaction of the herpes simplex virus type 2 UL46 gene product. *Arch Virol* **145**, 2149-2162.

Kattenhorn, L. M., Korbel, G. A., Kessler, B. M., Spooner, E. & Ploegh, H. L. (2005). A deubiquitinating enzyme encoded by HSV-1 belongs to a family of cysteine proteases that is conserved across the family Herpesviridae. *Mol Cell* **19**, 547-557.

Keller, J. M., Spear, P. G. & Roizman, B. (1970). Proteins specified by herpes simplex virus 3. Viruses differing in their effects on social behavior of infected cells specify different membrane glycoproteins. *Proceedings of the National Academy of Sciences of the United States of America* **65**, 865-&.

Kieff, E. D. & Rickinson, A. B. (2007). Epstein-Barr virus and its replication. In *Fields Virology 5th ed*. Edited by D. M. Knipe & P. M. Howley: Lippincott Williams & Wilkins

Klopfleisch, R., Klupp, B. G., Fuchs, W., Kopp, M., Teifke, J. P. & Mettenleiter, T. C. (2006). Influence of pseudorabies virus proteins on neuroinvasion and neurovirulence in mice. *Journal of Virology* **80**, 5571-5576.

Klopfleisch, R., Teifke, J. P., Fuchs, W., Kopp, M., Klupp, B. G. & Mettenleiter, T. C. (2004). Influence of tegument proteins of pseudorabies virus on neuroinvasion and transneuronal spread in the nervous system of adult mice after intranasal inoculation. *Journal of Virology* **78**, 2956-2966.

Klupp, B., Altenschmidt, J., Granzow, H., Fuchs, W. & Mettenleiter, T. C. (2008). Glycoproteins required for entry are not necessary for egress of pseudorabies virus. *Journal of Virology* **82**, 6299-6309.

Klupp, B. G., Fuchs, W., Granzow, H., Nixdorf, R. & Mettenleiter, T. C. (2002). Pseudorabies virus UL36 tegument protein physically interacts with the UL37 protein. *Journal of Virology* **76**, 3065-3071.

Klupp, B. G., Fuchs, W., Weiland, E. & Mettenleiter, T. C. (1997). Pseudorabies virus glycoprotein L is necessary for virus infectivity but dispensable for virion localization of glycoprotein H. *Journal of Virology* **71**, 7687-7695.

Klupp, B. G., Granzow, H., Karger, A. & Mettenleiter, T. C. (2005). Identification, subviral localization, and functional characterization of the pseudorabies virus UL17 protein. *Journal of Virology* **79**, 13442-13453.

Klupp, B. G., Granzow, H. & Mettenleiter, T. C. (2000). Primary envelopment of pseudorabies virus at the nuclear membrane requires the UL34 gene product. *Journal of Virology* **74**, 10063-10073.

Klupp, B. G., Granzow, H. & Mettenleiter, T. C. (2001a). Effect of the pseudorabies virus US3 protein on nuclear membrane localization of the UL34 protein and virus egress from the nucleus. *Journal of General Virology* **82**, 2363-2371.

Klupp, B. G., Granzow, H., Mundt, E. & Mettenleiter, T. C. (2001b). Pseudorabies virus UL37 gene product is involved in secondary envelopment. *Journal of Virology* **75**, 8927-8936.

Knipe, D. M., Batterson, W., Nosal, C., Roizman, B. & Buchan, A. (1981). Molecular-genetics of herpes-simplex virus 6. Characterization of a temperature-sensitive mutant defective in the expression of all early viral gene-products. *Journal of Virology* **38**, 539-547.

Kopp, M., Klupp, B. G., Granzow, H., Fuchs, W. & Mettenleiter, T. C. (2002). Identification and characterization of the pseudorabies virus tegument proteins UL46 and UL47: Role for UL47 in virion morphogenesis in the cytoplasm. *Journal of Virology* **76**, 8820-8833.

Krautwald, M., Fuchs, W., Klupp, B. G. & Mettenleiter, T. C. (2009). Translocation of Incoming Pseudorabies Virus Capsids to the Cell Nucleus Is Delayed in the Absence of Tegument Protein pUL37. *Journal of Virology* **83**, 3389-3396.

Krautwald, M., Maresch, C., Klupp, B. G., Fuchs, W. & Mettenleiter, T. C. (2008). Deletion or green fluorescent protein tagging of the pUL35 capsid component of pseudorabies virus impairs virus replication in cell culture and neuroinvasion in mice. *Journal of General Virology* **89**, 1346-1351.

Krikorian, C. R. & Read, G. S. (1991). In vitro messenger-RNA degradation system to study the virion host shutoff function of herpes-simplex virus. *Journal of Virology* **65**, 112-122.

Kristie, T. M., Vogel, J. L. & Sears, A. E. (1999). Nuclear localization of the C1 factor (host cell factor) in sensory neurons correlates with reactivation of herpes simplex virus from latency. *Proceedings of the National Academy of Sciences of the United States of America* **96**, 1229-1233.

Krummenacher, C., Nicola, A. V., Whitbeck, J. C., Lou, H., Hou, W. F., Lambris, J. D., Geraghty, R. J., Spear, P. G., Cohen, G. H. & Eisenberg, R. J. (1998). Herpes simplex virus glycoprotein D can bind to poliovirus receptor-related protein 1 or herpesvirus entry mediator, two structurally unrelated mediators of virus entry. *Journal of Virology* **72**, 7064-7074.

Krupovic, M. & Bamford, D. H. (2008a). Archaeal proviruses TKV4 and MVV extend the PRD1-adenovirus lineage to the phylum Euryarchaeota. *Virology* **375**, 292-300.

Krupovic, M. & Bamford, D. H. (2008b). OPINION Virus evolution: how far does the double beta-barrel viral lineage extend? *Nat Rev Microbiol* **6**, 941-948.

Kubat, N. J., Amelio, A. L., Giordani, N. V. & Bloom, D. C. (2004a). The herpes simplex virus type 1 latency-associated transcript (LAT) enhancer/rcr is hyperacetylated during latency independently of LAT transcription. *Journal of Virology* **78**, 12508-12518.

Kubat, N. J., Tran, R. K., McAnany, P. & Bloom, D. C. (2004b). Specific histone tail modification and not DNA methylation is a determinant of herpes simplex virus type 1 latent gene expression. *Journal of Virology* **78**, 1139-1149.

Kumar, S. & Hedges, S. B. (1998). A molecular timescale for vertebrate evolution. *Nature* **392**, 917-920.

Kwong, A. D. & Frenkel, N. (1987). Herpes-simplex virus-infected cells contain a function(s) that destabilizes both host and viral messenger-RNAs. *Proceedings of the National Academy of Sciences of the United States of America* **84**, 1926-1930.

Kwong, A. D., Kruper, J. A. & Frenkel, N. (1988). Herpes-simplex virus virion host shutoff function. *Journal of Virology* **62**, 912-921.

La Boissiere, S., Izeta, A., Malcomber, S. & O'Hare, P. (2004). Compartmentalization of VP16 in cells infected with recombinant herpes simplex virus expressing VP16-green fluorescent protein fusion proteins. *Journal of Virology* **78**, 8002-8014.

Laemmli, U. K. (1970). Cleavage of structural proteins during assembly of head of bacteriophage-T4. *Nature* **227**, 680-&.

Lake, J. A. & Rivera, M. C. (1994). Was the nucleus the 1st endosymbiont. *Proceedings of the National Academy of Sciences of the United States of America* **91**, 2880-2881.

Lam, Q., Smibert, C. A., Koop, K. E., Lavery, C., Capone, J. P., Weinheimer, S. P. & Smiley, J. R. (1996). Herpes simplex virus VP16 rescues viral mRNA from destruction by the virion host shutoff function. *Embo Journal* **15**, 2575-2581.

Lamberti, C. & Weller, S. K. (1996). The Herpes simplex virus type 1 UL6 protein is essential for cleavage and packaging but not for genomic inversion. *Virology* **226**, 403-407.

Lamberti, C. & Weller, S. K. (1998). The herpes simplex virus type 1 cleavage/packaging protein, UL32, is involved in efficient localization of capsids to replication compartments. *Journal of Virology* **72**, 2463-2473.

Langlois, C., Mas, C., Di Lello, P., Jenkins, L. M. M., Legault, P. & Omichinski, J. G. (2008). NMR structure of the complex between the Tfb1 subunit of TFIIH and the activation domain of VP16: Structural similarities between VP16 and p53. *Journal of the American Chemical Society* **130**, 10596-10604.

Leach, N., Bjerke, S. L., Christensen, D. K., Bouchard, J. M., Mou, F., Park, R., Baines, J., Haraguchi, T. & Roller, R. J. (2007). Emerin is hyperphosphorylated and redistributed in herpes simplex virus type 1-Infected cells in a manner dependent on both UL34 and US3. *Journal of Virology* **81**, 10792-10803.

Lee, C. K. & Knipe, D. M. (1985). An immunoassay for the study of DNA-binding activities of herpes-simplex virus protein-ICP8. *Journal of Virology* **54**, 731-738.

Lee, J. H., Vittone, V., Diefenbach, E., Cunningham, A. L. & Diefenbach, R. J. (2008). Identification of structural protein-protein interactions of herpes simplex virus type 1. *Virology* **378**, 347-354.

Leslie, J., Rixon, F. J. & McLauchlan, J. (1996). Overexpression of the herpes simplex virus type 1 tegument protein VP22 increases its incorporation into virus particles. *Virology* **220**, 60-68.

Levy, J. A. (1997). Three new human herpesviruses (HHV6, 7, and 8). *Lancet* **349**, 558-563.

Lewis, L. & Albrechtbuehler, G. (1987). Distribution of multiple centrospheres determines migration of BHK syncitia. *Cell Motility and the Cytoskeleton* **7**, 282-290.

Liashkovich, I., Hafezi, W., Kuhn, J. E., Oberleithner, H., Kramer, A. & Shahin, V. (2008). Exceptional mechanical and structural stability of HSV-1 unveiled with fluid atomic force microscopy. *J Cell Sci* **121**, 2287-2292.

Ling, P. D., Tan, J., Sewatanon, J. & Peng, R. S. (2008). Murine gammaherpesvirus 68 open reading frame 75c tegument protein induces the degradation of PML and is essential for production of infectious virus. *Journal of Virology* **82**, 8000-8012.

Liptak, L. M., Uprichard, S. L. & Knipe, D. M. (1996). Functional order of assembly of herpes simplex virus DNA replication proteins into prereplicative site structures. *Journal of Virology* **70**, 1759-1767.

Liu, M., Tang, J., Wang, X. D., Yang, T. Z. & Geller, A. I. (2005). Enhanced long-term expression from helper virus-free HSV-1 vectors packaged in the presence of deletions in genes that modulate the function of VP16, U(L)46 and U(L)47. *Journal of Neuroscience Methods* **145**, 1-9.

Liu, W. W., Goodhouse, J., Jeon, N. L. & Enquist, L. W. (2008). A microfluidic chamber for analysis of neuron-to-cell spread and axonal transport of an alpha-herpesvirus. *PLoS One* **3**, e2382.

Loret, S., Guay, G. & Lippe, R. (2008). Comprehensive characterization of extracellular herpes simplex virus type 1 virions. *Journal of Virology* **82**, 8605-8618.

Lu, R. & Misra, V. (2000a). Potential role for luman, the cellular homologue of herpes simplex virus VP16 (alpha gene trans-inducing factor), in herpesvirus latency. *Journal of Virology* **74**, 934-943.

Lu, R. & Misra, V. (2000b). Zhangfei: a second cellular protein interacts with herpes simplex virus accessory factor HCF in a manner similar to Luman and VP16. *Nucleic Acids Res* **28**, 2446-2454.

Lukashchuk, V., McFarlane, S., Everett, R. D. & Preston, C. M. (2008). Human Cytomegalovirus Protein pp71 Displaces the Chromatin-Associated Factor ATRX from Nuclear Domain 10 at Early Stages of Infection. *Journal of Virology* **82**, 12543-12554.

Lukonis, C. J., Burkham, J. & Weller, S. K. (1997). Herpes simplex virus type 1 prereplicative sites are a heterogeneous population: Only a subset are likely to be precursors to replication compartments. *Journal of Virology* **71**, 4771-4781.

Luxton, G. W. G., Haverlock, S., Coller, K. E., Antinone, S. E., Pincetic, A. & Smith, G. A. (2005). Targeting of herpesvirus capsid transport in axons is coupled to association with specific sets of tegument proteins. *Proceedings of the National Academy of Sciences of the United States of America* **102**, 5832-5837.

Luxton, G. W. G., Lee, J. I. H., Haverlock-Moyns, S., Schober, J. M. & Smith, G. A. (2006). The pseudorabies virus VP1/2 tegument protein is required for intracellular capsid transport. *Journal of Virology* **80**, 201-209.

Lyman, M. G. & Enquist, L. W. (2009). Herpesvirus Interactions with the Host Cytoskeleton. *Journal of Virology* **83**, 2058-2066.

Mabit, H., Nakano, M. Y., Prank, U., Sam, B., Dohner, K., Sodeik, B. & Greber, U. F. (2002). Intact microtubules support adenovirus and herpes simplex virus infections. *Journal of Virology* **76**, 9962-9971.

Macpherson, I. & Stoker, M. (1962). Polyoma transformation of hamster cell clones - investigation of genetic factors affecting cell competence. *Virology* **16**, 147-&.

Manservigi, R., Spear, P. G. & Buchan, A. (1977). Membrane proteins specified by herpes-simplex viruses 2. Cell-fusion induced by herpes-simplex virus is promoted and suppressed by different viral glycoproteins - (membranes). *Proceedings of the National Academy of Sciences of the United States of America* **74**, 3913-3917.

Marsh, M. & Helenius, A. (2006). Virus entry: Open sesame. *Cell* **124**, 729-740.

Marshall, K. R., Lachmann, R. H., Efstathiou, S., Rinaldi, A. & Preston, C. M. (2000). Long-term transgene expression in mice infected with a herpes simplex virus type 1 mutant severely impaired for immediate-early gene expression. *Journal of Virology* **74**, 956-964.

Martin, A., O'Hare, P., McLauchlan, J. & Elliott, G. (2002). Herpes simplex virus tegument protein VP22 contains overlapping domains for cytoplasmic localization, microtubule interaction, and chromatin binding. *Journal of Virology* **76**, 4961-4970.

Martin, W. (2005). Archaebacteria (Archaea) and the origin of the eukaryotic nucleus. *Current Opinion in Microbiology* **8**, 630-637.

Martinez, R., Shao, L. & Weller, S. K. (1992). The conserved helicase motifs of the herpes-simplex virus type-1 origin-binding protein UL9 are important for function. *Journal of Virology* **66**, 6735-6746.

Matsuzaki, A., Yamauchi, Y., Kato, A., Goshima, F., Kawaguchi, Y., Yoshikawa, T. & Nishiyama, Y. (2005). US3 protein kinase of herpes simplex virus type 2 is required for the stability of the UL46-encoded tegument protein and its association with virus particles. *Journal of General Virology* **86**, 1979-1985.

Maul, G. G., Ishov, A. M. & Everett, R. D. (1996). Nuclear domain 10 as preexisting potential replication start sites of herpes simplex virus type-1. *Virology* **217**, 67-75.

Maurer, U. E., Sodeik, B. & Grunewald, K. (2008). Native 3D intermediates of membrane fusion in herpes simplex virus 1 entry. *Proceedings of the National Academy of Sciences of the United States of America* **105**, 10559-10564.

McClelland, D. A., Aitken, J. D., Bhella, D., McNab, D., Mitchell, J., Kelly, S. M., Price, N. C. & Rixon, F. J. (2002). pH reduction as a trigger for dissociation of herpes simplex virus type 1 scaffolds. *Journal of Virology* **76**, 7407-7417.

McDonald, D., Vodicka, M. A., Lucero, G., Svitkina, T. M., Borisy, G. G., Emerman, M. & Hope, T. J. (2002). Visualization of the intracellular behavior of HIV in living cells. *Journal of Cell Biology* **159**, 441-452.

McGeoch, D. J., Dalrymple, M. A., Davison, A. J., Dolan, A., Frame, M. C., McNab, D., Perry, L. J., Scott, J. E. & Taylor, P. (1988). The complete DNA-sequence of the long unique region in the genome of herpes-simplex virus type-1. *Journal of General Virology* **69**, 1531-1574.

McLauchlan, J. (1997). The abundance of the herpes simplex virus type 1 UL37 tegument protein in virus particles is closely controlled. *Journal of General Virology* **78**, 189-194.

McLauchlan, J., Addison, C., Craigie, M. C. & Rixon, F. J. (1992). Noninfectious L-particles supply functions which can facilitate infection by HSV-1. *Virology* **190**, 682-688.

McLauchlan, J., Liefkens, K. & Stow, N. D. (1994). The herpes-simplex virus type-1 UL37 gene-product is a component of virus-particles. *Journal of General Virology* **75**, 2047-2052.

McLauchlan, J. & Rixon, F. J. (1992). Characterization of enveloped tegument structures (L-particles) produced by alphaherpesviruses - integrity of the tegument does not depend on the presence of capsid or envelope. *Journal of General Virology* **73**, 269-276.

McMahon, R. & Walsh, D. (2008). Efficient Quiescent Infection of Normal Human Diploid Fibroblasts with Wild-Type Herpes Simplex Virus Type 1. *Journal of Virology* **82**, 10218-10230.

McNab, A. R., Desai, P., Person, S., Roof, L. L., Thomsen, D. R., Newcomb, W. W., Brown, J. C. & Homa, F. L. (1998). The product of the herpes simplex virus type 1 UL25 gene is required for encapsidation but not for cleavage of replicated viral DNA. *Journal of Virology* **72**, 1060-1070.

McNabb, D. S. & Courtney, R. J. (1992a). Analysis of the UL36 open reading frame encoding the large tegument protein (ICP1/2) of herpes-simplex virus type-1. *Journal of Virology* **66**, 7581-7584.

McNabb, D. S. & Courtney, R. J. (1992b). Characterization of the large tegument protein (ICP1/2) of herpes-simplex virus type-1. *Virology* **190**, 221-232.

Meijer, W. J. J., Horcajadas, J. A. & Salas, M. (2001). phi 29 family of phages. *Microbiol Mol Biol Rev* **65**, 261-+.

Mettenleiter, T. C. (2002). Herpesvirus assembly and egress. *Journal of Virology* **76**, 1537-1547.

Mettenleiter, T. C. (2004). Budding events in herpesvirus morphogenesis. *Virus Research* **106**, 14.

Mettenleiter, T. C. (2006). Intriguing interplay between viral proteins during herpesvirus assembly or: The herpesvirus assembly puzzle. *Veterinary Microbiology* **113**, 7.

Mettenleiter, T. C., Klupp, B. G. & Granzow, H. (2006). Herpesvirus assembly: a tale of two membranes. *Current Opinion in Microbiology* **9**, 423-429.

Michael, K., Klupp, B. G., Mettenleiter, T. C. & Karger, A. (2006). Composition of pseudorabies virus particles lacking tegument protein US3, UL47, or UL49 or envelope glycoprotein E. *Journal of Virology* **80**, 1332-1339.

Mijatov, B., Cunningham, A. L. & Diefenbach, R. J. (2007). Residues F593 and E596 of HSV-1 tegument protein pUL36 (VP1/2) mediate binding of tegument protein pUL37. *Virology* **368**, 26-31.

Miranda-Saksena, M., Boadle, R. A., Aggarwal, A., Tijono, B., Rixon, F. J., Diefenbach, R. J. & Cunningham, A. L. (2009). Herpes Simplex Virus Utilizes the Large Secretory Vesicle Pathway for Anterograde Transport of Tegument and Envelope Proteins and for Viral Exocytosis from Growth Cones of Human Fetal Axons. *Journal of Virology* **83**, 3187-3199.

Mocarski, E. S., Shenk, T. & Pass, R. F. (2007). Cytomegaloviruses. In *Fields Virology 5th ed*. Edited by D. M. Knipe & P. M. Howley: Lippincott Williams & Wilkins

Möhl, B. S., Böttcher, S., Granzow, H., Kuhn, J., Klupp, B. G. & T.C., M. (2009). Intracellular Localization of the Pseudorabies Virus Large Tegument Protein pUL36. *Journal of Virology*

Monier, K., Armas, J. C. G., Etteldorf, S., Ghazal, P. & Sullivan, K. F. (2000). Annexation of the interchromosomal space during viral infection. *Nature Cell Biology* **2**, 661-665.

Morita, E. & Sundquist, W. I. (2004). Retrovirus budding. *Annual Review of Cell and Developmental Biology* **20**, 395-425.

Morris, J. B., Hofemeister, H. & O'Hare, P. (2007). Herpes simplex virus infection induces phosphorylation and delocalization of emerin, a key inner nuclear membrane protein. *Journal of Virology* **81**, 4429-4437.

Morrison, E. E., Stevenson, A. J., Wang, Y. F. & Meredith, D. M. (1998a). Differences in the intracellular localization and fate of herpes simplex virus tegument proteins early in the infection of Vero cells. *Journal of General Virology* **79**, 2517-2528.

Morrison, E. E., Wang, Y. F. & Meredith, D. M. (1998b). Phosphorylation of structural components promotes dissociation of the herpes simplex virus type 1 tegument. *Journal of Virology* **72**, 7108-7114.

Mossman, K. L., Sherburne, R., Lavery, C., Duncan, J. & Smiley, J. R. (2000). Evidence that herpes simplex virus VP16 is required for viral egress downstream of the initial envelopment event. *Journal of Virology* **74**, 13.

Mou, F., Wills, E. & Baines, J. D. (2009). Phosphorylation of the U(L)31 Protein of Herpes Simplex Virus 1 by the U(S)3-Encoded Kinase Regulates Localization of

the Nuclear Envelopment Complex and Egress of Nucleocapsids. *Journal of Virology* **83**, 5181-5191.

Mou, F., Wills, E. G., Park, R. & Baines, J. D. (2008). Effects of lamin A/C, lamin B1, and viral U(s)3 kinase activity on viral infectivity, virion egress, and the targeting of herpes simplex virus U(L)34-Encoded protein to the inner nuclear membrane. *Journal of Virology* **82**, 8094-8104.

Mouzakitis, G., McLauchlan, J., Barreca, C., Kueltzo, L. & O'Hare, P. (2005). Characterization of VP22 in herpes simplex virus-infected cells. *Journal of Virology* **79**, 12185-12198.

Mukhopadhyay, S., Kuhn, R. J. & Rossmann, M. G. (2005). A structural perspective of the Flavivirus life cycle. *Nat Rev Microbiol* **3**, 13-22.

Muranyi, W., Haas, J., Wagner, M., Krohne, G. & Koszinowski, U. H. (2002). Cytomegalovirus recruitment of cellular kinases to dissolve the nuclear lamina. *Science* **297**, 854-857.

Murphy, M. A., Bucks, M. A., O'Regan, K. J. & Courtney, R. J. (2008). The HSV-1 tegument protein pUL46 associates with cellular membranes and viral capsids. *Virology* **376**, 279-289.

Nagel, C. H., Dohner, K., Fathollahy, M., Strive, T., Borst, E. M., Messerle, M. & Sodeik, B. (2008). Nuclear egress and envelopment of herpes simplex virus capsids analyzed with dual-color fluorescence HSV1(17(+)). *Journal of Virology* **82**, 3109-3124.

Naldinho-Souto, R., Browne, H. & Minson, T. (2006). Herpes simplex virus tegument protein VP16 is a component of primary enveloped virions. *Journal of Virology* **80**, 2582-2584.

Nevins, J. R. (1991). Transcriptional activation by viral regulatory proteins. *Trends in Biochemical Sciences* **16**, 435-439.

Newcomb, W. W. & Brown, J. C. (1991). Structure of the herpes-simplex virus capsid - effects of extraction with guanidine-hydrochloride and partial reconstitution of extracted capsids. *Journal of Virology* **65**, 613-620.

Newcomb, W. W. & Brown, J. C. (1994). Induced extrusion of DNA from the capsid of herpes-simplex virus type-1. *Journal of Virology* **68**, 433-440.

Newcomb, W. W. & Brown, J. C. (2002). Inhibition of herpes simplex virus replication by WAY-150138: Assembly of capsids depleted of the portal and terminase proteins involved in DNA encapsidation. *Journal of Virology* **76**, 10084-10088.

Newcomb, W. W., Homa, F. L., Thomsen, D. R., Booy, F. P., Trus, B. L., Steven, A. C., Spencer, J. V. & Brown, J. C. (1996). Assembly of the herpes simplex virus capsid: Characterization of intermediates observed during cell-free capsid formation. *Journal of Molecular Biology* **263**, 432-446.

Newcomb, W. W., Homa, F. L., Thomsen, D. R. & Brown, J. C. (2001a). In vitro assembly of the herpes simplex virus procapsid: Formation of small procapsids at reduced scaffolding protein concentration. *Journal of Structural Biology* **133**, 23-31.

Newcomb, W. W., Homa, F. L., Thomsen, D. R., Trus, B. L., Cheng, N. Q., Steven, A., Booy, F. & Brown, J. C. (1999). Assembly of the herpes simplex virus procapsid from purified components and identification of small complexes containing the major capsid and scaffolding proteins. *Journal of Virology* **73**, 4239-4250.

Newcomb, W. W., Homa, F. L., Thomsen, D. R., Ye, Z. P. & Brown, J. C. (1994). Cell-free assembly of the herpes-simplex virus capsid. *Journal of Virology* **68**, 6059-6063.

Newcomb, W. W., Juhas, R. M., Thomsen, D. R., Homa, F. L., Burch, A. D., Weller, S. K. & Brown, J. C. (2001b). The UL6 gene product forms the portal for entry of DNA into the herpes simplex virus capsid. *Journal of Virology* **75**, 10923-10932.

Newcomb, W. W., Thomsen, D. R., Homa, F. L. & Brown, J. C. (2003). Assembly of the herpes simplex virus capsid: Identification of soluble scaffold-portal complexes

and their role in formation of portal-containing capsids. *Journal of Virology* **77**, 9862-9871.

Newcomb, W. W., Trus, B. L., Booy, F. P., Steven, A. C., Wall, J. S. & Brown, J. C. (1993). Structure of the herpes-simplex virus capsid - molecular composition of the pentons and the triplexes. *Journal of Molecular Biology* **232**, 499-511.

Newcomb, W. W., Trus, B. L., Cheng, N. Q., Steven, A. C., Sheaffer, A. K., Tenney, D. J., Weller, S. K. & Brown, J. C. (2000). Isolation of herpes simplex virus procapsids from cells infected with a protease-deficient mutant virus. *Journal of Virology* **74**, 1663-1673.

Nicholson, P., Addison, C., Cross, A. M., Kennard, J., Preston, V. G. & Rixon, F. J. (1994). Localization of the herpes-simplex virus type-1 major capsid protein VP5 to the cell-nucleus requires the abundant scaffolding protein VP22a. *Journal of General Virology* **75**, 1091-1099.

Nishiyama, Y., Yamada, Y., Kurachi, R. & Daikoku, T. (1992). Construction of a US3 Lacz insertion mutant of herpes-simplex virus type-2 and characterization of its phenotype in vitro and in vivo. *Virology* **190**, 256-268.

Nozawa, N., Yamauchi, Y., Ohtsuka, K., Kawaguchi, Y. & Nishiyama, Y. (2004). Formation of aggresome-like structures in herpes simplex virus type 2-infected cells and a potential role in virus assembly. *Experimental Cell Research* **299**, 486-497.

O'Hare, P. (1993). The virion transactivator of herpes simplex virus. *Seminars in Virology* **4**, 145-155.

O'Regan, K. J., Murphy, M. A., Bucks, M. A., Wills, J. W. & Courtney, R. J. (2007). Incorporation of the herpes simplex virus type 1 tegument protein VP22 into the virus particle is independent of interaction with VP16. *Virology* **369**, 263-280.

Ogasawara, M., Suzutani, T., Yoshida, I. & Azuma, M. (2001). Role of the UL25 gene product in packaging DNA into the herpes simplex virus capsid: Location of UL25 product in the capsid and demonstration that it binds DNA. *Journal of Virology* **75**, 1427-1436.

Ogawa-Goto, K., Tanaka, K., Gibson, W., Moriishi, E., Miura, Y., Kurata, T., Irie, S. & Sata, T. (2003). Microtubule network facilitates nuclear targeting of human cytomegalovirus capsid. *Journal of Virology* **77**, 8541-8547.

Ohka, S., Sakai, M., Bohnert, S., Igarashi, H., Deinhardt, K., Schiavo, G. & Nomoto, A. (2009). Receptor-Dependent and -Independent Axonal Retrograde Transport of Poliovirus in Motor Neurons. *Journal of Virology* **83**, 4995-5004.

Ojala, P. M., Sodeik, B., Ebersold, M. W., Kutay, U. & Helenius, A. (2000). Herpes simplex virus type 1 entry into host cells: Reconstitution of capsid binding and uncoating at the nuclear pore complex in vitro. *Molecular and Cellular Biology* **20**, 4922-4931.

Okoye, M. E., Sexton, G. L., Huang, E., McCaffery, J. M. & Desai, P. (2006). Functional analysis of the triplex proteins (VP19C and VP23) of herpes simplex virus type 1. *Journal of Virology* **80**, 929-940.

Olivo, P. D., Nelson, N. J. & Challberg, M. D. (1988). Herpes-simplex virus-DNA replication - the UL9 gene encodes an origin-binding protein. *Proceedings of the National Academy of Sciences of the United States of America* **85**, 5414-5418.

Oroskar, A. A. & Read, G. S. (1987). A mutant of herpes-simplex virus type-1 exhibits increased stability of immediate-early (alpha) messenger-RNAs. *Journal of Virology* **61**, 604-606.

Oroskar, A. A. & Read, G. S. (1989). Control of messenger-RNA stability by the virion host shutoff function of herpes-simplex virus. *Journal of Virology* **63**, 1897-1906.

Padula, M. E., Sydnor, M. L. & Wilson, D. W. (2009). Isolation and Preliminary Characterization of Herpes Simplex Virus 1 Primary Enveloped Virions from the Perinuclear Space. *Journal of Virology* **83**, 4757-4765.

Parris, D. S., Cross, A., Haarr, L., Orr, A., Frame, M. C., Murphy, M., McGeoch, D. J. & Marsden, H. S. (1988). Identification of the gene encoding the 65-kilodalton DNA-binding protein of herpes-simplex virus type-1. *Journal of Virology* **62**, 818-825.

Pasdeloup, D., Blondel, D., Isidro, A. L. & Rixon, F. J. (2009). Herpesvirus Capsid Association with the Nuclear Pore Complex and Viral DNA Release Involve the Nucleoporin CAN/Nup214 and the Capsid Protein pUL25. *Journal of Virology* **83**, 6610-6623.

Patel, A. H. & Maclean, J. B. (1995). The product of the UL6 gene of herpes-simplex virus type-1 is associated with virus capsids. *Virology* **206**, 465-478.

Patel, A. H., Rixon, F. J., Cunningham, C. & Davison, A. J. (1996). Isolation and characterization of herpes simplex virus type 1 mutants defective in the UL6 gene. *Virology* **217**, 111-123.

Pellett, P. E. & Roizman, B. (2007). The Family Herpesviridae: A brief introduction. In *Fields Virology 5th ed*. Edited by D. M. Knipe & P. M. Howley: Lippincott Williams & Wilkins

Penfold, M. E. T., Armati, P. & Cunningham, A. L. (1994). Axonal-transport of herpes-simplex virions to epidermal-cells - evidence for a specialized mode of virus transport and assembly. *Proceedings of the National Academy of Sciences of the United States of America* **91**, 6529-6533.

Pertel, P. E., Fridberg, A., Parish, M. L. & Spear, P. G. (2001). Cell fusion induced by herpes simplex virus glycoproteins gB, gD, and gH-gL requires a gD receptor but not necessarily heparan sulfate. *Virology* **279**, 313-324.

Polvinobodnar, M., Orberg, P. K. & Schaffer, P. A. (1987). Herpes-simplex virus type-1 oriL is not required for virus-replication or for the establishment and reactivation of latent infection in mice. *Journal of Virology* **61**, 3528-3535.

Pomeranz, L. E. & Blaho, J. A. (2000). Assembly of infectious herpes simplex virus type 1 virions in the absence of full-length VP22. *Journal of Virology* **74**, 10041-10054.

Poranen, M. M., Daugelavicius, R. & Bamford, D. H. (2002). Common principles in viral entry. *Annual Review of Microbiology* **56**, 521-538.

Potel, C. & Elliott, G. (2005). Phosphorylation of the herpes simplex virus tegument protein VP22 has no effect on incorporation of VP22 into the virus but is involved in optimal expression and virion packaging of ICP0. *Journal of Virology* **79**, 14057-14068.

Preston, C. M. & Nicholl, M. J. (1997). Repression of gene expression upon infection of cells with herpes simplex virus type 1 mutants impaired for immediate-early protein synthesis. *Journal of Virology* **71**, 7807-7813.

Preston, V. G., Coates, J. A. V. & Rixon, F. J. (1983). Identification and characterization of a herpes-simplex virus gene-product required for encapsidation of virus-DNA. *Journal of Virology* **45**, 1056-1064.

Preston, V. G., Murray, J., Preston, C. M., McDougall, I. M. & Stow, N. D. (2008). The UL25 gene product of herpes simplex virus type 1 is involved in uncoating of the viral genome. *Journal of Virology* **82**, 6654-6666.

Preston, V. G., Rixon, F. J., McDougall, I. M., McGregor, M. & Alkobaisi, M. F. (1992). Processing of the herpes-simplex virus assembly protein-ICP35 near its carboxy terminal end requires the product of the whole of the UL26 reading frame. *Virology* **186**, 87-98.

Radtke, K., Dohner, K. & Sodeik, B. (2006). Viral interactions with the cytoskeleton: a hitchhiker's guide to the cell. *Cellular Microbiology* **8**, 387-400.

Raiborg, C., Rusten, T. E. & Stenmark, H. (2003). Protein sorting into multivesicular endosomes. *Current Opinion in Cell Biology* **15**, 446-455.

Read, G. S. & Frenkel, N. (1983). Herpes-simplex virus mutants defective in the virion-associated shutoff of host polypeptide-synthesis and exhibiting abnormal synthesis of alpha-(immediate early) viral polypeptides. *Journal of Virology* **46**, 498-512.

Reynolds, A. E., Liang, L. & Baines, J. D. (2004). Conformational changes in the nuclear lamina induced by herpes simplex virus type 1 require genes U(L)31 and U(L)34. *Journal of Virology* **78**, 5564-5575.

Reynolds, A. E., Ryckman, B. J., Baines, J. D., Zhou, Y. P., Liang, L. & Roller, R. J. (2001). U(L)31 and U(L)34 proteins of herpes simplex virus type 1 form a complex that accumulates at the nuclear rim and is required for envelopment of nucleocapsids. *Journal of Virology* **75**, 8803-8817.

Reynolds, A. E., Wills, E. G., Roller, R. J., Ryckman, B. J. & Baines, J. D. (2002). Ultrastructural localization of the herpes simplex virus type 1 U(L)31, U(L)34, and U(S)3 proteins suggests specific roles in primary envelopment and egress of nucleocapsids. *Journal of Virology* **76**, 8939-8952.

Reynolds, E. S. (1963). Use of lead citrate at high pH as an electron-opaque stain in electron microscopy. *Journal of Cell Biology* **17**, 208-&.

Rixon, F. J., Addison, C. & McLauchlan, J. (1992). Assembly of enveloped tegument structures (L-particles) can occur independently of virion maturation in herpes-simplex virus type-1-infected cells. *Journal of General Virology* **73**, 277-284.

Rixon, F. J. & Chiu, W. (2003). Studying large viruses. *Virus Structure* **64**, 379-+.

Rixon, F. J. & McNab, D. (1999). Packaging-competent capsids of a herpes simplex virus temperature-sensitive mutant have properties similar to those of in vitro-assembled procapsids. *Journal of Virology* **73**, 5714-5721.

Roberts, A. P. E., Abaitua, F., O'Hare, P., McNab, D., Rixon, F. J. & Pasdeloup, D. (2009). Differing Roles of Inner Tegument Proteins pUL36 and pUL37 during Entry of Herpes Simplex Virus Type 1. *Journal of Virology* **83**, 105-116.

Roizman, B., Desrosier, R. C., Fleckenstein, B., Lopez, C., Minson, A. C. & Studdert, M. J. (1992). The family herpesviridae: an update. *Arch Virol* **123**, 24.

Roizman, B., Knipe, D. M. & Whitley, R. J. (2007). Herpes Simplex Viruses. In *Fields Virology 5th ed*. Edited by D. M. Knipe & P. M. Howley: Lippincott Williams & Wilkins.

Roizman, B., Roane, P. R. & Aurelian, L. (1963). Multiplication of herpes simplex virus 1. Programming of viral DNA duplication in Hep-2 cells. *Virology* **21**, 482-&.

Roop, C., Hutchinson, L. & Johnson, D. C. (1993). A mutant herpes-simplex virus type-1 unable to express glycoprotein-L cannot enter cells, and its particles lack glycoprotein-H. *Journal of Virology* **67**, 2285-2297.

Ruyechan, W. T., Morse, L. S., Knipe, D. M. & Roizman, B. (1979). Molecular genetics of herpes-simplex virus 2. Mapping of the major viral glycoproteins and of the genetic loci specifying the social-behavior of infected-cells. *Journal of Virology* **29**, 677-697.

Saad, A., Zhou, Z. H., Jakana, J., Chiu, W. & Rixon, F. J. (1999). Roles of triplex and scaffolding proteins in herpes simplex virus type 1 capsid formation suggested by structures of recombinant particles. *Journal of Virology* **73**, 6821-6830.

Saksena, M. M., Wakisaka, H., Tijono, B., Boadle, R. A., Rixon, F., Takahashi, H. & Cunningham, A. L. (2006). Herpes simplex virus type 1 accumulation, envelopment, and exit in growth cones and varicosities in mid-distal regions of axons. *Journal of Virology* **80**, 3592-3606.

Salmon, B., Cunningham, C., Davison, A. J., Harris, W. J. & Baines, J. D. (1998). The herpes simplex virus type 1 U(L)17 gene encodes virion tegument proteins that are required for cleavage and packaging of viral DNA. *Journal of Virology* **72**, 3779-3788.

Schlieker, C., Korbel, G. A., Kattenhorn, L. M. & Ploegh, H. L. (2005). A deubiquitinating activity is conserved in the large tegument protein of the Herpesviridae. *Journal of Virology* **79**, 15582-15585.

Schlieker, C., Weihofen, W. A., Frijns, E., Kattenhorn, L. M., Gaudet, R. & Ploegh, H. L. (2007). Structure of a herpesvirus-encoded cysteine protease reveals a unique class of deubiquitinating enzymes. *Mol Cell* **25**, 677-687.

Sciortino, M. T., Suzuki, M., Taddeo, B. & Roizman, B. (2001). RNAs extracted from herpes simplex virus 1 virions: Apparent selectivity of viral but not cellular RNAs packaged in virions. *Journal of Virology* **75**, 8105-8116.

Sciortino, M. T., Taddeo, B., Giuffre-Cuculletto, M., Medici, M. A., Mastino, A. & Roizman, B. (2007). Replication-competent herpes simplex virus 1 isolates selected from cells transfected with a bacterial artificial chromosome DNA lacking only the U(L)49 gene vary with respect to the defect in the U(L)41 gene encoding host shutoff RNase. *Journal of Virology* **81**, 10924-10932.

Sciortino, M. T., Taddeo, B., Poon, A. P. W., Mastino, A. & Roizman, B. (2002). Of the three tegument proteins that package mRNA in herpes simplex virions, one (VP22) transports the mRNA to uninfected cells for expression prior to viral infection. *Proceedings of the National Academy of Sciences of the United States of America* **99**, 8318-8323.

Scott, E. S. & O'Hare, P. (2001). Fate of the inner nuclear membrane protein lamin B receptor and nuclear lamins in herpes simplex virus type 1 infection. *Journal of Virology* **75**, 8818-8830.

Shahin, V., Hafezi, W., Oberleithner, H., Ludwig, Y., Windoffer, B., Schillers, H. & Kuhn, J. E. (2006). The genome of HSV-1 translocates through the nuclear pore as a condensed rod-like structure. *J Cell Sci* **119**, 23-30.

Shanda, S. K. & Wilson, D. W. (2008). UL36p is required for efficient transport of membrane-associated herpes simplex virus type 1 along microtubules. *Journal of Virology* **82**, 7388-7394.

Shelton, L. S. G., Albright, A. G., Ruyechan, W. T. & Jenkins, F. J. (1994). Retention of the herpes-simplex virus type-1 (HSV-1) UL37 protein on single-stranded-DNA columns requires the HSV-1 ICP8 protein. *Journal of Virology* **68**, 521-525.

Shukla, D. & Spear, P. G. (2001). Herpesviruses and heparan sulfate: an intimate relationship in aid of viral entry. *Journal of Clinical Investigation* **108**, 503-510.

Siegel, R. W., Jain, R. & Bradbury, A. (2001). Using an in vivo phagemid system to identify non-compatible loxP sequences. *FEBS Lett* **499**, 147-153.

Simpson-Holley, M., Baines, J., Roller, R. & Knipe, D. M. (2004). Herpes simplex virus 1 U(L)31 and U(L)34 gene products promote the late maturation of viral replication compartments to the nuclear periphery. *Journal of Virology* **78**, 5591-5600.

Simpson-Holley, M., Colgrove, R. C., Nalepa, G., Harper, J. W. & Knipe, D. M. (2005). Identification and functional evaluation of cellular and viral factors involved in the alteration of nuclear architecture during herpes simplex virus 1 infection. *Journal of Virology* **79**, 12840-12851.

Skepper, J. N., Whiteley, A., Browne, H. & Minson, A. (2001). Herpes simplex virus nucleocapsids mature to progeny virions by an envelopment -> deenvelopment -> reenvelopment pathway. *Journal of Virology* **75**, 5697-5702.

Slagsvold, T., Pattni, K., Malerod, L. & Stenmark, H. (2006). Endosomal and non-endosomal functions of ESCRT proteins. *Trends in Cell Biology* **16**, 317-326.

Smibert, C. A., Popova, B., Xiao, P., Capone, J. P. & Smiley, J. R. (1994). Herpes-simplex virus VP16 forms a complex with the virion host shutoff protein vhs. *Journal of Virology* **68**, 2339-2346.

Smiley, J. R. (2004). Herpes simplex virus virion host shutoff protein: Immune evasion mediated by a viral RNase? *Journal of Virology* **78**, 1063-1068.

Smith, G. A. & Enquist, L. W. (2000). A self-recombining bacterial artificial chromosome and its application for analysis of herpesvirus pathogenesis. *Proceedings of the National Academy of Sciences of the United States of America* **97**, 4873-4878.

Sodeik, B. (2000). Mechanisms of viral transport in the cytoplasm. *Trends in Microbiology* **8**, 465-472.

Sodeik, B. (2002). Unchain my heart, baby let me go - the entry and intracellular transport of HIV. *Journal of Cell Biology* **159**, 393-395.

Sodeik, B., Ebersold, M. W. & Helenius, A. (1997). Microtubule-mediated transport of incoming herpes simplex virus 1 capsids to the nucleus. *Journal of Cell Biology* **136**, 1007-1021.

Sourvinos, G. & Everett, R. D. (2002). Visualization of parental HSV-1 genomes and replication compartments in association with ND10 in live infected cells. *EMBO Journal* **21**, 4989-4997.

Spear, P. G. (2004). Herpes simplex virus: receptors and ligands for cell entry. *Cellular Microbiology* **6**, 401-410.

Spear, P. G. & Longnecker, R. (2003). Herpesvirus entry: an update. *Journal of Virology* **77**, 10179-10185.

Stabell, E. C. & Olivo, P. D. (1993). A truncated herpes-simplex virus origin-binding protein which contains the carboxyl-terminal origin-binding domain binds to the origin of replication but does not alter its conformation. *Nucleic Acids Res* **21**, 5203-5211.

Stannard, L. M., Fuller, A. O. & Spear, P. G. (1987). Herpes-simplex virus glycoproteins associated with different morphological entities projecting from the virion envelope. *Journal of General Virology* **68**, 715-725.

Stow, N. D. (1982). Localization of an origin of DNA-replication within the TRs/IRs repeated region of the herpes-simplex virus type-1 genome. *Embo Journal* **1**, 863-867.

Stow, N. D. (2001). Packaging of genomic and amplicon DNA by the herpes simplex virus type 1 UL25-null mutant KUL25NS. *Journal of Virology* **75**, 10755-10765.

Stow, N. D. & Wilkie, N. M. (1976). Improved technique for obtaining enhanced infectivity with herpes-simplex virus type-1 DNA. *Journal of General Virology* **33**, 447-458.

Strang, B. L. & Stow, N. D. (2005). Circularization of the herpes simplex virus type 1 genome upon lytic infection. *Journal of Virology* **79**, 12487-12494.

Subak-Sharpe, J. H. & Dargan, D. J. (1998). HSV molecular biology: General aspects of herpes simplex virus molecular biology. *Virus Genes* **16**, 239-251.

Sugimoto, K., Uema, M., Sagara, H., Tanaka, M., Sata, T., Hashimoto, Y. & Kawaguchi, Y. (2008). Simultaneous tracking of capsid, tegument, and envelope protein localization in living cells infected with triply fluorescent herpes simplex virus 1. *Journal of Virology* **82**, 5198-5211.

Suomalainen, M., Nakano, M. Y., Keller, S., Boucke, K., Stidwill, R. P. & Geber, U. F. (1999). Microtubule-dependent plus- and minus end-directed motilities are competing processes for nuclear targeting of adenovirus. *Journal of Cell Biology* **144**, 657-672.

Szilagyi, J. F. & Cunningham, C. (1991). Identification and characterization of a novel noninfectious herpes-simplex virus-related particle. *Journal of General Virology* **72**, 661-668.

Taddeo, B. & Roizman, B. (2006). The virion host shutoff protein (U(L)41) of herpes simplex virus 1 is an endoribonuclease with a substrate specificity similar to that of RNase A. *Journal of Virology* **80**, 9341-9345.

Taddeo, B., Sciortino, M. T., Zhang, W. & Roizman, B. (2007). Interaction of herpes simplex virus RNase with VP16 and VP22 is required for the accumulation of the protein but not for accumulation of mRNA. *Proceedings of the National Academy of Sciences of the United States of America* **104**, 12163-12168.

Taddeo, B., Zhang, W. R. & Roizman, B. (2006). The U(L)41 protein of herpes simplex virus 1 degrades RNA by endonucleolytic cleavage in absence of other cellular or viral proteins. *Proceedings of the National Academy of Sciences of the United States of America* **103**, 2827-2832.

Tang, J. H., Olson, N., Jardine, P. J., Girimes, S., Anderson, D. L. & Baker, T. S. (2008). DNA poised for release in bacteriophage phi 29. *Structure* **16**, 935-943.

Tatman, J. D., Preston, V. G., Nicholson, P., Elliott, R. M. & Rixon, F. J. (1994). Assembly of herpes-simplex virus type-1 capsids using a panel of recombinant baculoviruses. *Journal of General Virology* **75**, 1101-1113.

Tavalai, N., Papior, P., Rechter, S., Leis, M. & Stamminger, T. (2006). Evidence for a role of the cellular ND10 protein PML in mediating intrinsic immunity against human cytomegalovirus infections. *Journal of Virology* **80**, 8006-8018.

Taylor, T. J. & Knipe, D. M. (2004). Proteomics of herpes simplex virus replication compartments: Association of cellular DNA replication, repair, recombination, and chromatin remodeling proteins with ICP8. *Journal of Virology* **78**, 5856-5866.

Thomas, D. L., Lock, M., Zabolotny, J. M., Mohan, B. R. & Fraser, N. W. (2002). The 2-kilobase intron of the herpes simplex virus type 1 latency-associated transcript has a half-life of approximately 24 hours in SY5Y and COS-1 cells. *Journal of Virology* **76**, 532-540.

Thompson, R. L. & Sawtell, N. M. (2000). Replication of herpes simplex virus type 1 within trigeminal ganglia is required for high frequency but not high viral genome copy number latency. *Journal of Virology* **74**, 965-974.

Thomsen, D. R., Newcomb, W. W., Brown, J. C. & Homa, F. L. (1995). Assembly of the herpes-simplex virus capsid - requirement for the carboxyl-terminal 25 amino-acids of the proteins encoded by the UL26 and UL26.5 genes. *Journal of Virology* **69**, 3690-3703.

Thurlow, J. K., Murphy, M., Stow, N. D. & Preston, V. G. (2006). Herpes simplex virus type 1 DNA-packaging protein UL17 is required for efficient binding of UL25 to capsids. *Journal of Virology* **80**, 2118-2126.

Thurlow, J. K., Rixon, F. J., Murphy, M., Targett-Adams, P., Hughes, M. & Preston, V. G. (2005). The herpes simplex virus type 1 DNA packaging protein UL17 is a virion protein that is present in both the capsid and the tegument compartments. *Journal of Virology* **79**, 150-158.

Trus, B. L., Booy, F. P., Newcomb, W. W., Brown, J. C., Homa, F. L., Thomsen, D. R. & Steven, A. C. (1996). The herpes simplex virus procapsid: Structure, conformational changes upon maturation, and roles of the triplex proteins VP19c and VP23 in assembly. *Journal of Molecular Biology* **263**, 447-462.

Trus, B. L., Chen, N. Q., Newcomb, W. W., Homa, F. L., Brown, J. C. & Steven, A. C. (2004). Structure and polymorphism of the UL6 portal protein of herpes simplex virus type 1. *Journal of Virology* **78**, 12668-12671.

Trus, B. L., Heymann, J. B., Nealon, K., Cheng, N. Q., Newcomb, W. W., Brown, J. C., Kedes, D. H. & Steven, A. C. (2001). Capsid structure of Kaposi's sarcoma-associated herpesvirus, a gammaherpesvirus, compared to those of an alphaherpesvirus, herpes simplex virus type 1, and a betaherpesvirus, cytomegalovirus. *Journal of Virology* **75**, 2879-2890.

Trus, B. L., Newcomb, W. W., Cheng, N. Q., Cardone, G., Marekov, L., Horna, F. L., Brown, J. C. & Steven, A. C. (2007). Allosteric signaling and a nuclear exit strategy: Binding of UL25/UL17 heterodimers to DNA-filled HSV-1 capsids. *Mol Cell* **26**, 479-489.

Ullman, A. J. & Hearing, P. (2008). Cellular proteins PML and Daxx mediate an innate antiviral defense antagonized by the adenovirus E4 ORF3 protein. *Journal of Virology* **82**, 7325-7335.

Umbach, J. L., Kramer, M. F., Jurak, I., Karnowski, H. W., Coen, D. M. & Cullen, B. R. (2008). MicroRNAs expressed by herpes simplex virus 1 during latent infection regulate viral mRNAs. *Nature* **454**, 780-U108.

Uprichard, S. L. & Knipe, D. M. (1997). Assembly of herpes simplex virus replication proteins at two distinct intranuclear sites. *Virology* **229**, 113-125.

van Genderen, I. L., Brandimarti, R., Torrisi, M. R., Campadelli, G. & van Meer, G. (1994). The phospholipid-composition of extracellular herpes-simplex virions differs from that of host-cell nuclei. *Virology* **200**, 831-836.

van Zeijl, M., Fairhurst, J., Jones, T. R., Vernon, S. K., Morin, J., LaRocqe, J., Feld, B., O'Hara, B., Bloom, J. D. & Johann, S. V. (2000). Novel class of thiourea compounds that inhibit herpes simplex virus type 1 DNA cleavage and encapsidation: Resistance maps to the UL6 gene. *Journal of Virology* **74**, 9054-9061.

Vielkind, U. & Swierenga, S. H. (1989). A simple fixation procedure for immunofluorescent detection of different cytoskeletal components within the same cell. *Histochemistry* **91**, 81-88.

Vittone, V., Diefenbach, E., Triffett, D., Douglas, M. W., Cunningham, A. L. & Diefenbach, R. J. (2005). Determination of interactions between tegument proteins of herpes simplex virus type 1. *Journal of Virology* **79**, 9566-9571.

von Einem, J., Schumacher, D., O'Callaghan, D. J. & Osterrieder, N. (2006). The alpha t-TIF (VP16) homologue (ETIF) of equine herpesvirus 1 is essential for secondary envelopment and virus egress. *Journal of Virology* **80**, 2609-2620.

Walters, J. N., Sexton, G. L., McCaffery, J. M. & Desai, P. (2003). Mutation of single hydrophobic residue I27, L35, F39, L58, L65, L67, or L71 in the N terminus of VP5 abolishes interaction with the scaffold protein and prevents closure of herpes simplex virus type 1 capsid shells. *Journal of Virology* **77**, 4043-4059.

Wang, J. L., Loveland, A. N., Kattenhorn, L. M., Ploegh, H. L. & Gibson, W. (2006). High-molecular-weight protein (pUL48) of human cytomegalovirus is a competent deubiquitinating protease: Mutant viruses altered in its active-site cysteine or histidine are viable. *Journal of Virology* **80**, 6003-6012.

Warner, S. C., Chytrova, G., Desai, P. & Person, S. (2001). Mutations in the N-terminus of VP5 alter its interaction with the scaffold proteins of herpes simplex virus type 1. *Virology* **284**, 308-316.

Weinheimer, S. P., Boyd, B. A., Durham, S. K., Resnick, J. L. & Oboyle, D. R. (1992). Deletion of the VP16 open reading frame of herpes-simplex virus type-1. *Journal of Virology* **66**, 258-269.

Weir, J. P. (2001). Regulation of herpes simplex virus gene expression. *Gene* **271**, 117-130.

Whitbeck, J. C., Peng, C., Lou, H., Xu, R. L., Willis, S. H., DeLeon, M. P., Peng, T., Nicola, A. V., Montgomery, R. I., Warner, M. S., Soulika, A. M., Spruce, L. A., Moore, W. T., Lambris, J. D., Spear, P. G., Cohen, G. H. & Eisenberg, R. J. (1997). Glycoprotein D of herpes simplex virus (HSV) binds directly to HVEM, a member of the tumor necrosis factor receptor superfamily and a mediator of HSV entry. *Journal of Virology* **71**, 6083-6093.

Whiteley, A., Bruun, B., Minson, T. & Browne, H. (1999). Effects of targeting herpes simplex virus type 1 go to the endoplasmic reticulum and trans-golgi network. *Journal of Virology* **73**, 9515-9520.

Wild, P., Senn, C., Manera, C. L., Sutter, E., Schraner, E. M., Tobler, K., Ackermann, M., Ziegler, U., Lucas, M. S. & Kaech, A. (2009). Exploring the Nuclear Envelope of Herpes Simplex Virus 1-Infected Cells by High-Resolution Microscopy. *Journal of Virology* **83**, 408-419.

Wildy, P., Russell, W. C. & Horne, R. W. (1960). The morphology of herpes virus. *Virology* **12**, 204-222.

Wingfield, P. T., Stahl, S. J., Thomsen, D. R., Homa, F. L., Booy, F. P., Trus, B. L. & Steven, A. C. (1997). Hexon-only binding of VP26 reflects differences between the hexon and penton conformations of VP5, the major capsid protein of herpes simplex virus. *Journal of Virology* **71**, 8955-8961.

Wisner, T. W., Wright, C. C., Kato, A., Kawaguchi, Y., Mou, F., Baines, J. D., Roller, R. J. & Johnson, D. C. (2009). Herpesvirus gB-Induced Fusion between the Virion Envelope and Outer Nuclear Membrane during Virus Egress Is Regulated by the Viral US3 Kinase. *Journal of Virology* **83**, 3115-3126.

Wolfstein, A., Nagel, C. H., Radtke, K., Dohner, K., Allan, V. J. & Sodeik, B. (2006). The inner tegument promotes herpes simplex virus capsid motility along microtubules in vitro. *Traffic* **7**, 227-237.

Wray, G. A., Levinton, J. S. & Shapiro, L. H. (1996). Molecular evidence for deep precambrian divergences among metazoan phyla. *Science* **274**, 568-573.

Wu, C. A., Nelson, N. J., McGeoch, D. J. & Challberg, M. D. (1988). Identification of herpes-simplex virus type-1 genes required for origin-dependent DNA-synthesis. *Journal of Virology* **62**, 435-443.

Wudunn, D. & Spear, P. G. (1989). Initial interaction of herpes-simplex virus with cells is binding to heparan-sulfate. *Journal of Virology* **63**, 52-58.

Wysocka, J. & Herr, W. (2003). The herpes simplex virus VP16-induced complex: the makings of a regulatory switch. *Trends in Biochemical Sciences* **28**, 294-304.

Yu, X. K., O'Connor, C. M., Atanasov, V., Damania, B., Kedes, D. H. & Zhou, Z. H. (2003). Three-dimensional structures of the A, B, and C capsids of rhesus monkey rhadinovirus: Insights into gammaherpesvirus capsid assembly, maturation, and DNA packaging. *Journal of Virology* **77**, 13182-13193.

Zahariadis, G., Wagner, M. J., Doepker, R. C., Maciejko, J. M., Crider, C. M., Jerome, K. R. & Smiley, J. R. (2008). Cell-type-specific tyrosine phosphorylation of the herpes simplex virus tegument protein VP11/12 encoded by gene UL46. *Journal of Virology* **82**, 6098-6108.

Zelus, B. D., Stewart, R. S. & Ross, J. (1996). The virion host shutoff protein of herpes simplex virus type 1: Messenger ribonucleolytic activity in vitro. *Journal of Virology* **70**, 2411-2419.

Zhang, Y., Sirko, D. A. & McKnight, J. L. C. (1991). Role of herpes-simplex virus type-1 UL46 and UL47 in alpha-TIF-mediated transcriptional induction - characterization of 3 viral deletion mutants. *Journal of Virology* **65**, 829-841.

Zhang, Y. Z. & McKnight, J. L. C. (1993). Herpes-simplex virus type-1 UL46 and UL47 deletion mutants lack VP11 and VP12 or VP13 and VP14, respectively, and exhibit altered viral thymidine kinase expression. *Journal of Virology* **67**, 1482-1492.

Zhou, Z. H., Chen, D. H., Jakana, J., Rixon, F. J. & Chiu, W. (1999). Visualization of tegument-capsid interactions and DNA in intact herpes simplex virus type 1 virions. *Journal of Virology* **73**, 3210-3218.

Zhou, Z. H., Dougherty, M., Jakana, J., He, J., Rixon, F. J. & Chiu, W. (2000). Seeing the herpesvirus capsid at 8.5 angstrom. *Science* **288**, 877-880.

Zhou, Z. H., He, J., Jakana, J., Tatman, J. D., Rixon, F. J. & Chiu, W. (1995). Assembly of VP26 in herpes-simplex virus-1 inferred from structures of wild-type and recombinant capsids. *Nat Struct Biol* **2**, 1026-1030.

Zhou, Z. H., Prasad, B. V. V., Jakana, J., Rixon, F. J. & Chiu, W. (1994). Protein subunit structures in the herpes-simplex virus A-capsid determined from 400-kV spot-scan electron cryomicroscopy. *Journal of Molecular Biology* **242**, 456-469.

JOURNAL OF VIROLOGY, Jan. 2009, p. 105–116 Vol. 83, No. 1
0022-538X/09/$08.00+0 doi:10.1128/JVI.01032-08

Differing Roles of Inner Tegument Proteins pUL36 and pUL37 during Entry of Herpes Simplex Virus Type 1▽†

Ashley P. E. Roberts,[1] Fernando Abaitua,[2] Peter O'Hare,[2] David McNab,[1] Frazer J. Rixon,[1]* and David Pasdeloup[1]

MRC Virology Unit, Institute of Virology, University of Glasgow, Church Street, Glasgow G11 5JR, United Kingdom,[1] and Marie Curie Research Institute, The Chart, Oxted, Surrey RH8 0TL, United Kingdom[2]

Received 16 May 2008/Accepted 10 October 2008

Studies with herpes simplex virus type 1 (HSV-1) have shown that secondary envelopment and virus release are blocked in mutants deleted for the tegument protein gene UL36 or UL37, leading to the accumulation of DNA-containing capsids in the cytoplasm of infected cells. The failure to assemble infectious virions has meant that the roles of these genes in the initial stages of infection could not be investigated. To circumvent this, cells infected at a low multiplicity were fused to form syncytia, thereby allowing capsids released from infected nuclei access to uninfected nuclei without having to cross a plasma membrane. Visualization of virus DNA replication showed that a UL37-minus mutant was capable of transmitting infection to all the nuclei within a syncytium as efficiently as the wild-type HSV-1 strain 17$^+$ did, whereas infection by UL36-minus mutants failed to spread. Thus, these inner tegument proteins have differing functions, with pUL36 being essential during both the assembly and uptake stages of infection, while pUL37 is needed for the formation of virions but is not required during the initial stages of infection. Analysis of noninfectious enveloped particles (L-particles) further showed that pUL36 and pUL37 are dependent on each other for incorporation into tegument.

Herpesvirus virions have characteristic structures that combine symmetrical and nonsymmetrical components (22, 45, 58). The viral DNA genome is contained within an icosahedral capsid, a protein layer called the tegument surrounds the capsid, and the virion is bounded by a lipid envelope, which contains numerous glycoprotein spikes. Capsids are robust structures that can be readily purified from infected cells and studied in isolation from the other virion components. They are classified according to their internal composition as A-capsids (empty), B-capsids (containing scaffold), and C-capsids (containing DNA) (19, 23, 42, 50). The symmetry and uniformity of the capsid shell make it amenable to structural analysis, and its composition, structure, and morphogenesis have been studied extensively (23, 50, 59). In contrast, the bulk of the tegument appears to be highly variable, with the numbers of some component proteins differing widely among individual virus particles (7, 11). Compositionally, it is the most complex part of the virion, containing more than 15 viral gene products (23, 36, 50), many of which can be deleted without obviously affecting the virion structure. The tegument is usually described as amorphous, and its structure appears not to be correlated to that of the capsid, except at its inner boundary where a pattern of icosahedrally arranged elements interacting with capsid proteins is evident. These connections are distributed across the entire surface of the capsid in simian and human cytomegaloviruses (6, 53) but are confined to the vertices in herpes simplex virus type 1 (HSV-1) (22, 58).

Capsid assembly and DNA packaging take place in the nuclei of infected cells. The DNA-containing capsids (C-capsids) exit the nucleus by traversing the two layers of the nuclear membrane (36). They become enveloped at the inner leaflet but lose this primary envelope by fusion with the outer leaflet, which releases the capsid into the cytoplasm. Two viral gene products (genes UL31 and UL34) are required for this process (40, 44), but they do not form part of the mature virus particle (18). The US3-encoded protein kinase (pUS3), which is a constituent of tegument, is important for efficient nuclear exit (41, 56), but no tegument protein is known to be essential for capsid exit from the nucleus. The sequence and location of tegument assembly are still poorly understood. It has been reported that the HSV-1 tegument protein, pUL48 (VP16), and the HSV-1 and pseudorabies virus (PrV) pUS3 proteins are associated with primary enveloped capsids in the perinuclear space (21, 38, 41). However, the bulk of the tegument appears to be added in the cytoplasm, following which the mature virion is thought to be formed by envelopment at vesicles of the *trans*-Golgi network.

The products of HSV-1 genes UL36 and UL37 are tegument proteins which are believed to be closely associated with the capsid. The UL36 protein (pUL36) has been proposed as a possible candidate for the tegument protein attached to the vertices of capsids within virions (58), although recently it has been suggested that the proteins encoded by UL17 and UL25 form part of this material (53). There is no direct evidence for the location of the UL37 protein (pUL37) in the tegument, but it is known to interact with pUL36 (25, 37, 55) and has been described as an inner tegument protein. It is not clear where pUL36 and pUL37 become incorporated into virions, although both proteins have been reported as associating with capsids purified from the nuclei of infected cells (5). The putative interaction between pUL36 and the capsid may not entirely

* Corresponding author. Mailing address: MRC Virology Unit, Institute of Virology, University of Glasgow, Church Street, Glasgow G11 5JR, United Kingdom. Phone: 44 141 330 4025. Fax: 44 141 337 2236. E-mail: f.rixon@mrcvu.gla.ac.uk.

† Supplemental material for this article may be found at http://jvi.asm.org/.

▽ Published ahead of print on 29 October 2008.

account for its presence in the virion tegument, as it is also found in L-particles, which resemble virions in size and shape but lack capsids and therefore consist solely of enveloped tegument (52). L-particles are formed both in productive infections and in circumstances where virion assembly is blocked (43). Although pUL36 and pUL37 are components of L-particles (34, 52), studies with PrV mutants have shown that either one is dispensable for L-particle production (17, 26).

Mutational analysis has established that UL36 is essential for virus replication in both HSV-1 (3, 14) and PrV (17). However, although UL37 is essential in HSV-1 (13), deletion of this gene in PrV results in impairment but not abolition of growth (26). The phenotypes of HSV-1 mutants deleted for UL36 and UL37 are similar, and in both cases C-capsids accumulate in the cytoplasm of infected cells. This implies that the proteins are not required for capsid assembly, DNA packaging, or exit from the nucleus but are important for the further addition of tegument and envelope.

As well as being important in virus assembly and egress, UL36 plays a role during the initial phase of infection. Thus, infection of cells at nonpermissive temperatures with an HSV-1 temperature-sensitive mutant of UL36 (tsB7) prevents release of the viral DNA from capsids and causes them to accumulate in the vicinity of nuclear pores (3). No temperature-sensitive mutant has been reported for UL37, and its importance in initiation of infection is unknown. However, both pUL36 and pUL37 remain associated with capsids during transport to the nucleus (20, 29), indicating a possible role for pUL37 at this stage of infection.

In this paper we use deletion mutants with deletions of the UL36 and UL37 genes to study their roles during viral infection. Our studies confirm that neither protein is needed for formation of cytoplasmic C-capsids or for bulk tegument assembly, as evidenced by L-particle formation, making it likely that they act as the link between these two virion compartments. In addition, by examining the spread of infection within syncytia, we show that capsids lacking pUL36 are unable to transmit infection between nuclei, whereas initiating a new infectious cycle does not require pUL37.

MATERIALS AND METHODS

Cell culture. Human fetal foreskin fibroblasts ($HFFF_2$; European Collection of Cell Cultures) were grown in Dulbecco's modified Eagle medium (DMEM) supplemented with 10% fetal bovine serum (Gibco). Baby hamster kidney cells (BHK 21 clone 13; ATCC) were grown in Glasgow modified Eagle medium supplemented with 10% newborn bovine serum (Gibco) and tryptose phosphate broth. Rabbit skin (RS) cells (2) were grown in DMEM supplemented with 10% fetal bovine serum and 1% nonessential amino acids (Gibco).

Cell lines expressing HSV-1 genes. All complementing cell lines were derived from RS cells. Plasmids expressing the appropriate HSV-1 genes (see below) were mixed with pSV2Neo (Clontech) or with pC1-Neo (Promega) and cotransfected by calcium phosphate precipitation (51) into 35-mm dishes of RS cells. Transfected cells were incubated for 24 h at 37°C before subculture into 24-well plates. Cells were overlaid with medium containing 1 mg/ml G418 (Gibco). The selection medium was replaced every 3 days, until colony growth was evident. The drug-resistant colonies were then selected, expanded, and tested for their ability to support growth of the mutant viruses.

(i) UL19. UL19(1) cells were provided by V. Preston (MRC Virology Unit). Briefly, the open reading frame (ORF) of UL19 (residues 40,528 to 36,353 [32]) was isolated from pJN6 (39) as a BglII fragment and cloned into the BamHI site of pApV (27). G418-resistant cell lines produced as described above were tested for their ability to support growth of the UL19 deletion mutant K5ΔZ (12), and one line was selected for further use (V. Preston, personal communication).

(ii) UL36. The expression plasmid pApV (27) was modified using the double-stranded oligonucleotide pApVBstBI generated from the complementary sequences 5′-CTAGAACGGATCCGTCGACTTCGAAC and 5′-GATCGTTCG AAGTCGACGGATCCGTT. pApVBstBI was inserted between the unique XbaI and BamHI sites to produce pApVB. This creates a new BamHI site and introduces a BstBI site between the HSV-1 ICP6 (UL39) promoter and simian virus 40 polyadenylation sequence. The C-terminal ~8,000 nucleotides of the UL36 ORF were isolated from cosmid cos14 (9) as a BamHI fragment (see Fig. S1 in the supplemental material) and cloned into BamHI-digested pApVB to form pApVB36C. pApVB36C was digested with BstBI and religated to give plasmid pApVB36CBs, which has only 32 bp of HSV-1 sequence downstream of the UL36 ORF. The missing N-terminal region of UL36 was generated by PCR using primers UL36_HA_Nterm and UL36CTBamHIF (see Fig. S1 in the supplemental material) and cloned as an XbaI/BamHI fragment into XbaI/BamHI-digested pApVB36CBs to produce pHAUL36. This contains the full-length UL36 ORF (residues 80,540 to 71,016), fused to an influenza virus hemagglutinin (HA) epitope tag inserted at the N terminus. Cell lines generated using pHAUL36 and pSV2Neo (see above) were tested for their ability to complement the growth of the temperature-sensitive mutant tsB7 and the deletion mutant KΔUL36 (14). One line (HAUL36-1) was selected and used for all subsequent experiments.

(iii) UL37. Cell lines expressing UL37 were produced by two methods. Initially, the green fluorescent protein (GFP) vector, GFPemd (Packard), was modified to introduce SpeI sites at the N and C termini of the GFP ORF. The resulting SpeI fragment was cloned into the unique SpeI site located adjacent to the 3′ end of the UL37 ORF (see Fig. S1 in the supplemental material) in plasmid pGX336, which contains the BamHI O fragment (residues 79,441 to 86,980) cloned into pUC118. The resulting plasmid, pGX336GFP, which expresses a pUL37-GFP fusion protein was cotransfected with pSV2neo into RS cells. G418-resistant clones were screened for GFP expression following infection with wild-type (WT) HSV-1. One clone [1.40(2)] was selected and used in the production of the UL37 deletion mutant FRΔUL37 (see below). The plasmid, pGX336GFP, used to produce cell line 1.40(2) contains the UL37 ORF flanked by extensive HSV-1 sequences. To reduce the possibility that recombination with these sequences would rescue the FRΔUL37 mutation (see below), a second pUL37-expressing cell line was produced. The UL37 ORF (residues 84,171 to 80,707) was isolated from pUL373 (33) by BamHI digestion and cloned into BamHI-digested pApV to form pApV-UL373. pApV-UL373 was cotransfected into RS cells with pC1-Neo. G418-resistant clones were screened for their ability to complement the growth of FRΔUL37. One clone (80C02) was selected and used for all subsequent experiments.

Virus mutants. K5ΔZ (minus UL19) and KΔUL36 were provided by P. Desai (12, 14).

(i) UL36. Because the existing mutant, KΔUL36, contained only a partial deletion of the UL36 ORF, a second, complete deletion mutant was made using the HSV-1 bacterial artificial chromosome (BAC) pBAC SR27. In pBAC SR27 (supplied by C. Cunningham [MRC Virology Unit]), loxP recombination sites flank the bacterial maintenance sequences and a Cre recombinase gene, which are inserted between genes US1 and US2. The Cre recombinase is expressed following transfection into mammalian cells and results in the loss of the bacterial sequences (48). The UL36 ORF was removed from pBAC SR27 using a variation on the Lambda RED recombination system (Genebridges, GmbH). PCR was carried out on the supplied rpsL-neo template using primers UL36rm_loxFAS_F and UL36rm_loxFAS_R (see Fig. S1 in the supplemental material). The resulting PCR product contains the neomycin cassette flanked by nested FAS sites and sequences from upstream and downstream of the UL36 ORF. FAS sites are variant loxP sequences that will not undergo heterologous recombination with the archetypal loxP sites present in pBAC SR27 (47). The PCR fragment was recombined into pBAC SR27, and bacterial colonies were selected for neomycin resistance. The resulting BAC (pBAC SR27Δ36-1) has the UL36 ORF replaced by the neomycin cassette. Following transfection into HAUL36-1 cells, Cre recombinase is expressed, which excises both the FAS-flanked neomycin cassette and the loxP-flanked BAC maintenance sequences. Individual virus plaques were picked, and their ability to grow on HAUL36-1 and control RS cells was examined. Deletion of the UL36 ORF was confirmed by PCR and DNA sequencing, and one isolate (ARΔUL36) was selected for further use.

(ii) UL37. pGX336 was digested with ClaI and HpaI, which flank the UL37 ORF (see Fig. S1 in the supplemental material). The ClaI site was rendered blunt ended by treatment with T4 polymerase, and the plasmid was recircularized by ligation to generate pGX336-37minus. The red fluorescent protein (RFP) ORF from pDsRed-Monomer-N1 (Clontech) was isolated as an NheI/XbaI fragment and ligated into SpeI-digested pGX336-37minus to generate

pFRΔUL37. This removes the UL37 ORF apart from the three C-terminal amino acids and places the RFP ORF under the control of the UL37 promoter. pFRΔUL37 was cotransfected with HSV-1 strain 17^+ virion DNA into 1.40(2) cells (see above). Red fluorescent plaques were selected and screened for their differential ability to grow on 1.40(2) cells and parental RS cells. One isolate (FRΔUL37) was selected and grown for further use on 80C02 cells.

Rescuants. The NheI fragment (residues 68,662 to 85,304) containing the UL36 and UL37 sequences was cloned into the XbaI site of pUC19 to generate pUCNhe4. Noncomplementing RS cells transfected with pUCNhe4 were superinfected with 1 PFU of ARΔUL36 or FRΔUL37 per cell. Progeny virus was screened for the ability to grow on RS cells, and one virus from each rescue, designated ARΔUL36R and FRΔUL37R, was selected and grown for further use.

Cell fusion. $HFFF_2$ cells were seeded onto 22-mm square cover glasses in 35-mm culture dishes at 5×10^5 cells per dish and incubated at 37°C overnight. Duplicate plates of cells were infected for 1 h at 37°C with 0.01 PFU of the appropriate virus per cell. One plate from each pair was then overlaid with 2 ml of DMEM supplemented with 10% pooled human serum (Cellect). The second plate was washed twice in serum-free DMEM and then overlaid with 1 ml of 50% polyethylene glycol 1500 (PEG1500) in 75 mM HEPES (pH 8) (Roche) for 1 min at 37°C (28). The PEG solution was removed, and the cells were rinsed three times in DMEM containing 15% dimethyl sulfoxide and three times in DMEM and then overlaid with DMEM containing 10% pooled human serum. Both plates were maintained at 37°C for a further 23 h.

Preparation of fluorescent DNA probe. A pseudolibrary was produced by SacII digestion of a bacmid containing the entire HSV-1 genome and cloning 200- to 500-bp gel-purified fragments into pEGFP-C1 (Clontech). DNA from this pseudolibrary was used as a template for a PCR using Cy3-conjugated pEGFP-C1-specific primers (MWG). PCR products of suitable size (200 to 500 bp) were gel purified and used as a probe for fluorescent in situ hybridization (FISH).

FISH. Cells grown on cover glasses as described above were rinsed twice in phosphate-buffered saline (PBS) and fixed in 95% ethanol and 5% acetic acid at −20°C for 5 min. After fixation, the cells were air dried, rehydrated in PBS, and stored at 4°C until required. To carry out FISH (16), the cover glasses were incubated in hybridization buffer (50% formamide, 10% dextran sulfate, and 4× SSC [1× SSC is 0.15 M NaCl plus 0.015 M sodium citrate]) for 30 min at 37°C and then in probe solution (1 μl HSV-1 probe, 0.5 μl salmon testis DNA [10 mg/ml], 8.5 μl hybridization buffer) for 2 min at 95°C, before they were placed, cell side down, onto glass slides and incubated overnight at 37°C in a humidified hybridization chamber (Camlabs). They were washed twice at 65°C and once at room temperature with 2× SSC and overlaid with PBS before processing for immunofluorescence staining. If cytoplasmic labeling was required, they were then incubated for 30 min in PBS containing 0.5 μg/ml CellMask deep red (Invitrogen) and washed three times in PBS. All cover glasses were mounted in 2.5% 1,4-diazabicyclo[2.2.2]octane (Sigma) in Mowiol (Harco) containing 1 μg/ml 4′,6-diamidino-2-phenylindole dihydrochloride (DAPI) (Sigma). Samples were examined using a Zeiss LSM 510 meta confocal microscope.

Antibodies. The following antibodies were used: mouse monoclonal antibodies (MAbs) E12-E3 raised against the N-terminal 1 to 287 amino acids of pUL36 (1), DM165 against VP5 (31), VP16 (1-21) against pUL48 (Santa Cruz Biotechnology), MCA406 against VP22a (AbD Serotec), and DM1A against α-tubulin (Sigma); rabbit polyclonal antibody M780 against pUL37 (46); AGV031 against pUL49 (15); Alexa Fluor 488-conjugated goat anti-mouse antibody (Molecular Probes); and horseradish peroxidase-conjugated goat anti-mouse and goat anti-rabbit antibodies (Sigma).

Capsid and L-particle preparation. Ten 850-cm^2 roller bottles of BHK cells were infected at 5 PFU/cell with the appropriate virus. Three hours after infection, the cells were washed with 50 ml of PBS twice to remove unbound virus, then overlaid with 40 ml of fresh Glasgow modified Eagle medium supplemented with 10% newborn bovine serum and tryptose phosphate broth, and incubated for a further 21 h at 37°C. The culture medium was removed and retained for isolation of extracellular particles. Infected cells were removed, and nuclear and cytoplasmic fractions were separated by overlaying the monolayers with 25 ml of ice-cold PBS containing 1% IGEPAL [(octylphenoxy)polyethoxyethanol] CA-630 (Sigma) and protease inhibitors (complete, EDTA-free; Roche). Nuclei were harvested by centrifugation at 3,000 rpm for 10 min and resuspended in 30 ml of NTE buffer (0.5 M NaCl, 0.02 M Tris [ph 7.4], 0.01 M EDTA) containing 1% IGEPAL. Both the nuclear and cytoplasmic fractions were disrupted with a Branson sonifier 350 and clarified by centrifugation at 3,000 rpm for 10 min. The supernatants were transferred to fresh tubes, and the capsids were pelleted through 40% (wt/vol) sucrose cushions before being separated on 20 to 50% (wt/vol) sucrose gradients by centrifugation for 1 h at 25,000 rpm on an AH629 rotor (Sorvall).

TABLE 1. Growth of mutant viruses on complementing and noncomplementing cells

Virus	Growth of virus (titer) on:	
	Noncomplementing cells	Complementing cells
WT HSV-1	1.8×10^{10}	1.2×10^{10}
K5ΔZ	$<10^{4a}$	1.6×10^9
FRΔUL37	$<10^{4a}$	1.9×10^9
FRΔUL37R	6.2×10^{10}	9×10^{10}
KΔUL36	$<10^{4a}$	3.1×10^9
ARΔUL36	$<10^{4a}$	2.0×10^9
ARΔUL36R	2.5×10^{10}	2.4×10^{10}

[a] The input virus caused severe cytopathic effects at lower dilutions.

Extracellular particles were purified from the culture medium on 5 to 15% (wt/vol) Ficoll gradients as described previously (52).

Western blot analysis. Protein samples separated by electrophoresis on 10% sodium dodecyl sulfate (SDS)-polyacrylamide gels (SDS-polyacrylamide gel electrophoresis [SDS-PAGE]) were transferred electrophoretically to Hybond ECL membrane (Amersham). Blots were blocked for 30 min with 5% Marvel (Premium Brands) milk powder in 20 mM Tris (pH 8), 0.15 M NaCl, 1% Tween 20 (TBS-Tween) and incubated overnight at 4°C with appropriate antibodies diluted in 1% Marvel milk powder in TBS-Tween. Immunodetection was by enhanced chemiluminescence (ECL; Amersham). Before the blots were reprobed, the bound antibodies were stripped by incubating the membrane at 50°C in 62.5 mM Tris (pH 7), 2% SDS, and 100 mM β-mercaptoethanol for 30 min and washed two times in TBS-Tween.

Electron microscopy. Thirty-five-millimeter dishes of cells were fixed with 2.5% glutaraldehyde and 1% osmium tetroxide. Fixed cells were harvested and pelleted through 1% SeaPlaque agarose (Flowgen). The cell pellets were dehydrated through a graded alcohol series and embedded in Epon 812 resin. Thin sections were cut and examined in a JEOL 1200 EX II electron microscope.

RESULTS

Characterization of UL36 and UL37 mutants. The virus mutants studied in the following experiments were made using a variety of techniques, were generated from different parental strains, and include both complete (FRΔUL37 and ARΔUL36 [strain 17]) and partial (K5ΔZ and KΔUL36 [strain KOS]) gene deletions. Therefore, to compare their phenotypes, the growth characteristics and particle assembly pathways of the mutants were examined. Titration of virus stocks showed that the WT HSV-1 and the rescuants FRΔUL37R and ARΔUL36R grew equally well on complementing and noncomplementing cells and confirmed that all mutations were lethal for virus growth, with reductions in titer of $>10^5$ in each case (Table 1). Since each of the complementing cell lines was generated to contain only the relevant HSV-1 ORF, their ability to complement growth of the mutant viruses implies that no secondary mutations were contributing to the growth defects. This was confirmed by single-step growth analysis on complementing cells, which showed that all the mutant viruses exhibited similar growth patterns and grew to titers equivalent to that of wild-type HSV-1 (Fig. 1).

To determine the effects of the deletions on virus assembly, infected cells were examined by electron microscopy (Fig. 2). No enveloped virions were seen either on the cell surface or in cytoplasmic vacuoles of cells infected with any of the UL36 and UL37 mutants, while large numbers of nonenveloped C-capsids were present in the cytoplasm, confirming that these viruses are defective in envelopment and virus release. In

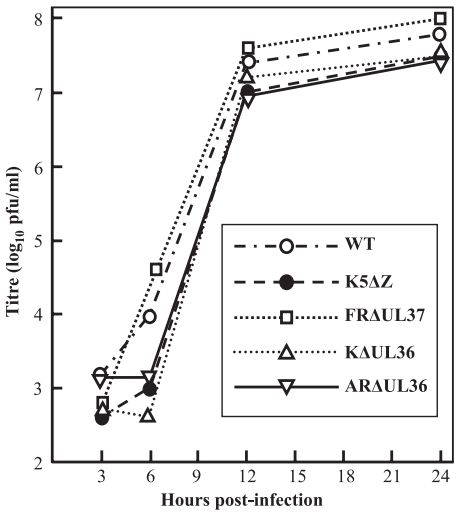

FIG. 1. Single-step virus growth. Replicate 35-mm dishes of complementing RS cells were infected with 10 PFU/cell of HSV-1 strain 17^+ (WT), K5ΔZ, FRΔUL37, KΔUL36, or ARΔUL36 mutant virus. After 1 h at 37°C, the cells were washed at low pH to remove residual input infectivity and overlaid with 2 ml of DMEM, and incubation was continued at 37°C. Wild-type HSV-1 was grown on RS cells in an identical fashion as a control. At 3, 6, 12, and 24 h after infection, the cells were harvested by scraping into the supernatant medium, and the progeny virus was titrated on complementing cells.

FRΔUL37-infected cells, the cytoplasmic C-capsids congregated in large aggregates similar to those seen with the independently derived mutant KΔUL37 (13) and their PrV counterpart, PrV-ΔUL37 (26). The tendency of these capsids to aggregate is indicative of the presence of tegument proteins, which are known to cause clumping of de-enveloped virions (35). However, they lack the densely staining tegument found associated with cytoplasmic PrV capsids when secondary envelopment was blocked by mutations in glycoproteins gE/gI and gM (4). Similar aggregations of cytoplasmic C-capsids were present in the KΔUL36-infected cells. In contrast, no aggregates were seen in ARΔUL36-infected cells with individual C-capsids being distributed throughout the cytoplasm, reproducing the pattern seen with the PrV mutant, PrV-ΔUL36F (17). The distribution of capsids in infected cells was quantified by counting the numbers present in electron microscopic images of randomly selected cell sections (Table 2). This confirmed that C-capsids accumulated in the cytoplasm of FRΔUL37-, KΔUL36-, and ARΔUL36-infected cells, with the majority of the FRΔUL37 and KΔUL36 C-capsids occurring in aggregates.

Sucrose gradient sedimentation was performed to analyze the properties of the mutant capsids. When nuclear extracts were sedimented through sucrose gradients, three bands corresponding to A-, B- and C-capsids were visible in all samples apart from K5ΔZ, which is deleted for the major capsid protein gene (12) and fails to assemble capsids (see Fig. S2A in the supplemental material). When cytoplasmic extracts from the same cells were analyzed, capsid bands were again present in KΔUL36 and ARΔUL36 gradients, but none were seen for WT HSV-1 or FRΔUL37 mutant virus (see Fig. S2B in the supplemental material). To determine the fate of the large number of cytoplasmic capsids present in FRΔUL37-infected cells, nuclear and cytoplasmic fractions from PBS-IGEPAL-treated cells were embedded, sectioned, and examined by electron microscopy (not shown). Very few capsids were found in the cytoplasmic fraction, while large numbers were present in the nuclear fraction, where the expected pattern of A-, B-, and C-capsids was observed inside nuclei. In addition, clusters of C-capsids were present outside the nuclear membrane, indicating that the large aggregations of cytoplasmic capsids seen in Fig. 2 had copelleted with the nuclei.

The differing distributions (aggregated and dispersed, respectively) of KΔUL36 and ARΔUL36 cytoplasmic C-capsids seen in Fig. 2, may reflect differences in the nature of their mutations. Thus, in ARΔUL36, the entire UL36 ORF has been deleted, whereas in KΔUL36 only the central portion has been removed (14), leaving 361 codons at the N terminus (plus a further 42 codons arising from a frameshift) that could encode a truncated form of pUL36. To determine whether this truncated form was expressed, the protein profiles of cells infected with WT HSV-1 or with FRΔUL37, KΔUL36, or ARΔUL36 mutant virus were probed with the pUL36-specific antibody, E12-E3. Western blotting confirmed that pUL36 bands of the expected sizes were present in the WT HSV-1- and FRΔUL37-infected cells, but not in the KΔUL36- or ARΔUL36-infected cells (Fig. 3A). However, the KΔUL36 sample did contain a strong band of the size expected for the residual N-terminal portion of pUL36 present in this mutant (predicted size of 43 kDa). Capsids were prepared from the cytoplasm of KΔUL36-infected cells and purified on sucrose gradients. Western blotting of gradient fractions showed that the 43-kDa protein fragment cosedimented with the capsid bands, confirming its association with KΔUL36 capsids (Fig. 3B). No signal was detected when these blots were probed with antibodies against pUL37 or the outer tegument protein, pUL48 (not shown).

Roles of UL36 and UL37 in the initial stages of virus infection. Since pUL36 and pUL37 are required for assembly of infectious virions, it is not possible to purify virions lacking these proteins in order to examine their behavior during the initial stages of infection. To overcome this limitation, we required a system in which virus could spread without needing to exit from and reenter cells. This is achieved naturally by syncytial viruses, in which the fusion of neighboring cell membranes exposes naïve cells to the contents of an infected cell's cytoplasm. To mimic this situation, we carried out studies in which cells, after infection, were induced to form syncytia by exposure to polyethylene glycol. Typical syncytia under these circumstances contained less than 20 nuclei. Therefore, infection at 0.01 PFU/cell ensured that few syncytia contained more than one initially infected cell. Following infection with the UL36 and UL37 mutants, the nuclear stages of assembly take place as normal, and capsids containing intact viral genomes are released into the cytoplasm. These progeny capsids have access to the other nuclei within the syncytium, and their ability to "infect" them can be determined by looking for replicating viral DNA.

Experiments in BHK and $HFFF_2$ cells gave similar results, and the $HFFF_2$ data are shown here as they produced more clearly delineated syncytia. To examine the spread of infection, monolayers of $HFFF_2$ cells were infected with HSV-1 strain 17^+ (WT) or with K5ΔZ, ARΔUL36, KΔUL36, or FRΔUL37

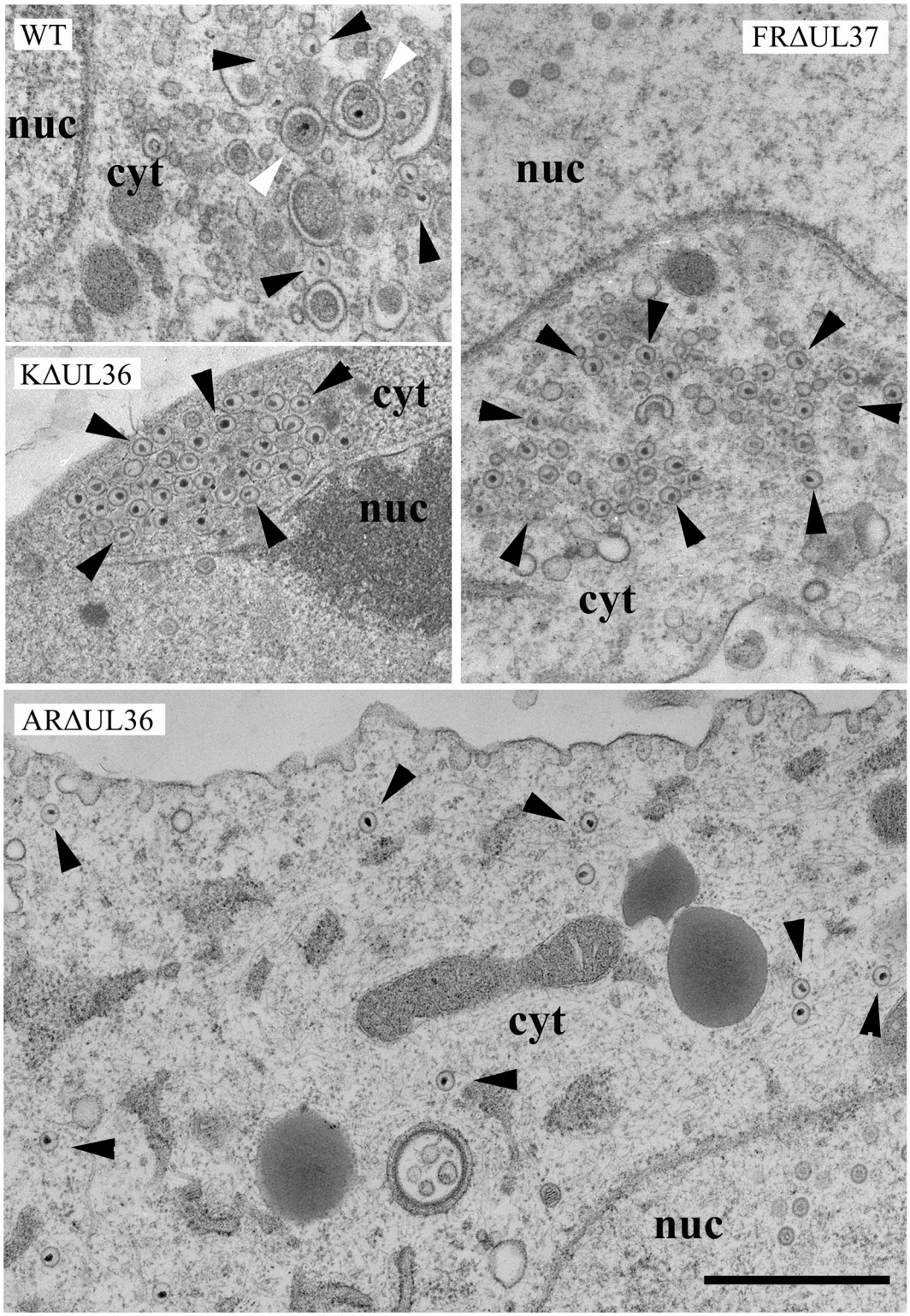

FIG. 2. Cytoplasmic capsids in infected cells. Replicate monolayers of $HFFF_2$ cells were infected with 5 PFU/cell of HSV-1 strain 17^+ (WT) or K5ΔZ, FRΔUL37, KΔUL36, or ARΔUL36 mutant virus. Cells were fixed and prepared for electron microscopy at 24 h postinfection. Both free capsids (black arrowheads) and enveloped virions (white arrowheads) were present in the cytoplasm of WT HSV-1-infected cells. In addition, large numbers of virions were present on the cell surfaces (not shown). KΔUL36 and FRΔUL37 cytoplasmic capsids accumulated in aggregates, while ARΔUL36 capsids were dispersed individually throughout the cytoplasm. No enveloped virions were seen with any of the mutant viruses. Nuclear (nuc) and cytoplasmic (cyt) compartments are labeled. Bar = 1 μm.

TABLE 2. Nuclear and cytoplasmic distribution of capsids in WT and mutant HSV-1-infected cells

Virus and capsid type	Nuclear		Cytoplasmic		
	No. of capids	% of total nuclear capsids	No. of free capids	No. of aggregated capsids	% of total DNA-containing capsids
WT HSV-1					
A	154	17	2		
B	691	76	2		
C	63	7	40		
Virions[a]			217		
FRΔUL37					
A	227	13	2	3	
B	1,380	77	4	21	
C	177	10	39	425	72
KΔUL36					
A	107	14	17	1	
B	586	77	10	2	
C	71	9	149	324	87
ARΔUL36					
A	161	19	13		
B	544	66	68		
C	123	15	276		69

[a] Includes enveloped cytoplasmic and extracellular capsids.

mutant virus (Fig. 4). WT HSV-1 was used as a positive control for spread within syncytia, and K5ΔZ was used as a negative control. After 1 h, the virus inoculum was removed, and the cells were either treated with PEG1500 (Roche) to induce fusion or left untreated. The cells were incubated for a further 23 h to allow time for infection to spread, then they were fixed, and the distribution of viral DNA was analyzed by fluorescent in situ hybridization. Infected nuclei were identified by the presence of fluorescent areas indicating replicating viral DNA. The addition of phosphonoacetic acid (an inhibitor of HSV-1 DNA polymerase) abolished labeling, confirming that the FISH probe was specifically recognizing newly synthesized virus DNA (not shown). Cells were counterstained with DAPI and CellMask deep red to highlight nuclei and cytoplasm, respectively.

Infection of unfused cells with WT virus gave rise to patches of cells with fluorescent nuclei, confirming that the virus was able to spread from an initially infected cell (Fig. 4A). As expected for a spreading infection, the pattern of labeling differed among individual cells, in some cases involving the entire nucleus and in others only localized patches. In contrast, infection of unfused cells with K5ΔZ, KΔUL36, ARΔUL36, or FRΔUL37 mutant virus resulted in only isolated fluorescing cells; the lack of spread to adjacent cells reflecting the inability of these mutants to produce infectious virus particles.

In PEG-treated cells, WT virus had also spread between nuclei, generating labeling patterns within syncytia similar to those seen in unfused cells (Fig. 4B). In contrast, the mutant viruses exhibited a range of labeling patterns. As would be predicted, in K5ΔZ-infected samples, viral DNA was confined to individual nuclei within syncytia, showing that unpackaged viral DNA could not spread between nuclei. In contrast, the FRΔUL37-infected samples contained multiple labeled nuclei. This demonstrates that formation of intact virions is not necessary for the spread of infection within syncytia but that this process can be mediated directly by cytoplasmic C-capsids. In both KΔUL36- and ARΔUL36-infected samples, replicating viral DNA was again confined to individual nuclei, indicating that not all cytoplasmic C-capsids are equally capable of transferring infection between nuclei and suggesting that, unlike pUL37, pUL36 plays an essential role in initiation of infection.

To determine the presence of cytoplasmic labeling, the experiment was repeated but without using CellMask deep red (Fig. 5). Cytoplasmic labeling clearly denoted the positions of extranuclear C-capsids or virions. Thus, fluorescent spots indicative of C-capsids were present in the cytoplasm of the WT HSV-1-, KΔUL36-, ARΔUL36-, and FRΔUL37-infected cells, but none were seen in cells infected with the major capsid protein mutant, K5ΔZ. Furthermore, the cytoplasmic fluorescence patterns confirmed the capsid distributions seen by electron microscopy. Thus, in FRΔUL37-infected cells, much of

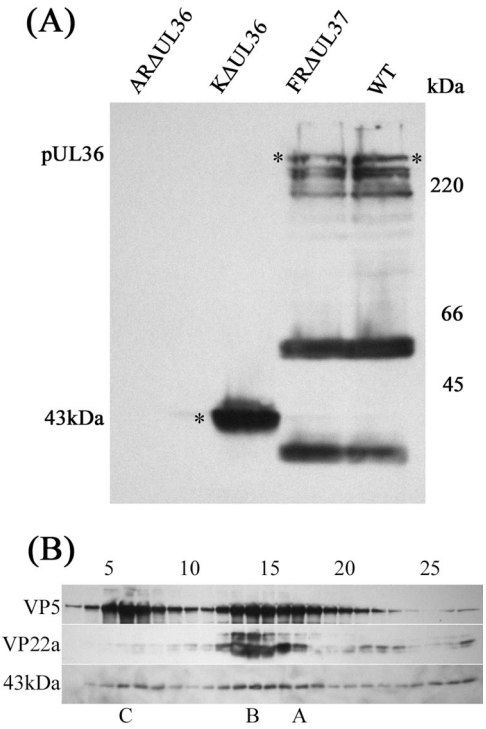

FIG. 3. KΔUL36 protein expression. (A) BHK cells were harvested 24 h after infection with 5 PFU/cell of HSV-1 strain 17^+ (WT) or FRΔUL37, KΔUL36, or ARΔUL36 mutant virus. Proteins were separated by SDS-PAGE, transferred to a nitrocellulose membrane, and probed with MAb E12-E3 directed against pUL36. The positions of full-length pUL36 and the 43-kDa N-terminal fragment (*) are indicated to the left of the gel and in the gel, and the positions of the protein size standards (in kilodaltons) are shown to the right of the gel. (B) Cytoplasmic capsids from KΔUL36-infected cells were separated by sucrose gradient sedimentation (see Fig. S2 in the supplemental material). The gradients were collected from the bottom in 30 equal fractions. Gradient fractions 3 to 27 were resolved by SDS-PAGE and analyzed by Western blotting. Blots were probed sequentially with MAb E12-E3 (anti-pUL36), DM165 (anti-VP5; to show the distribution of all capsid types), and MCA406 (anti-VP22a scaffolding protein; to show the location of B-capsids). The positions at which A-, B-, and C-capsids migrated are indicated below the blots. The positions of gradient fractions 5, 10, 15, 20, and 25 are shown above the blots.

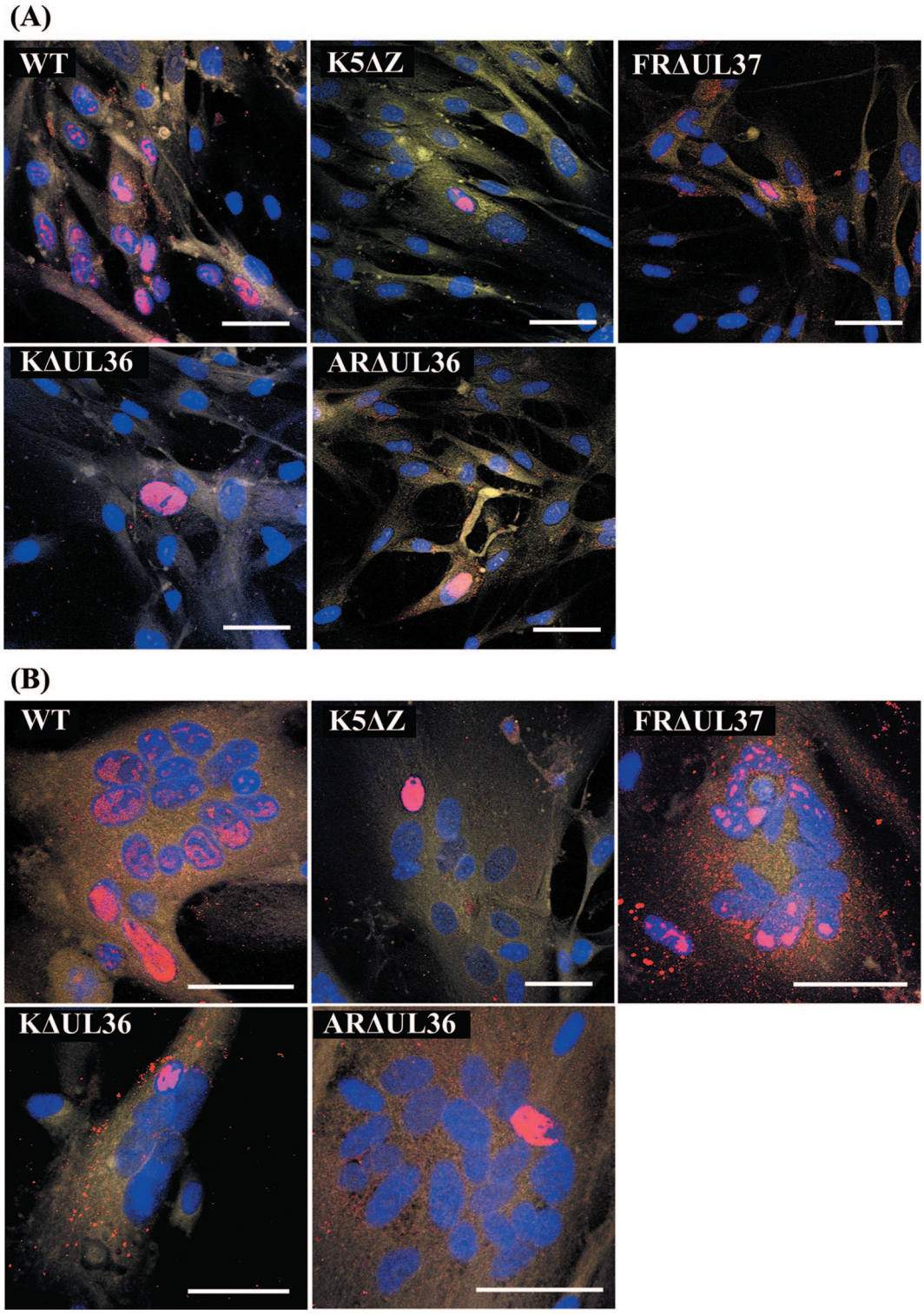

FIG. 4. Spread of virus infection. Replicate monolayers of $HFFF_2$ cells were infected with 0.01 PFU/cell of HSV-1 strain 17^+ (WT) or K5ΔZ, FRΔUL37, KΔUL36, or ARΔUL36 mutant virus. (A) Unfused cells; (B) cells after treatment with PEG and dimethyl sulfoxide at 1 h postinfection to induce syncytium formation. The cells were fixed and labeled at 24 h postinfection. Viral DNA was visualized by FISH using Cy3-labeled probe (red), nuclei were stained with DAPI (blue), and cell cytoplasm was stained with CellMask deep red (yellow). Bars, 50 μm in all panels.

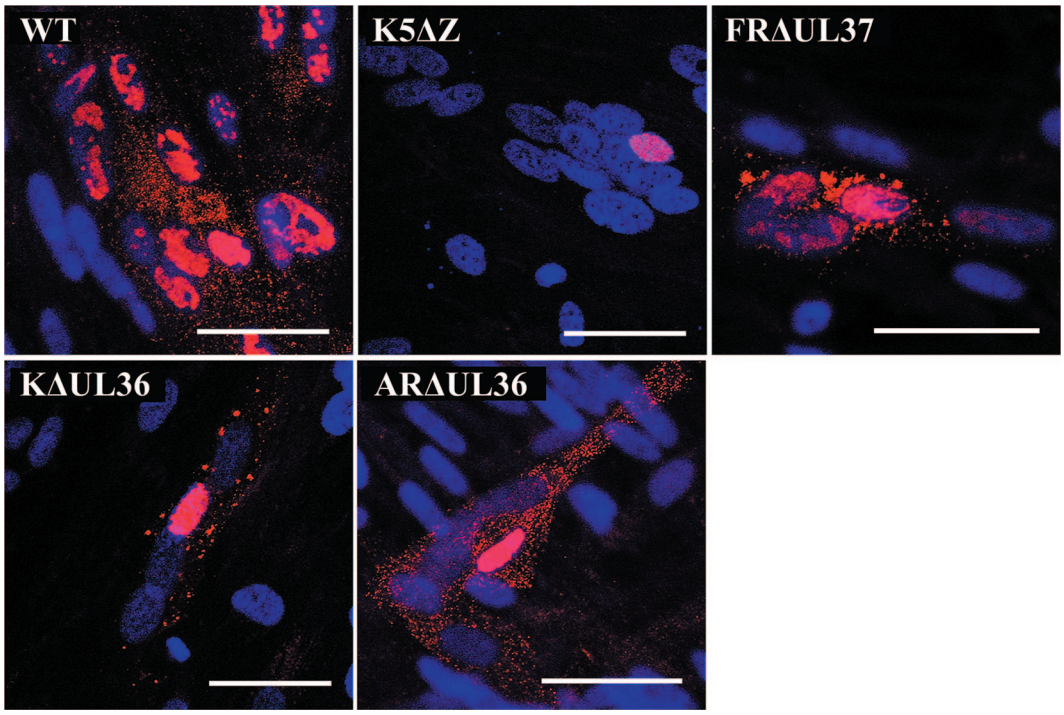

FIG. 5. Capsid distribution in infected syncytia. Replicate monolayers of $HFFF_2$ cells were infected and induced to form syncytia as described in the legend to Fig. 4. Viral DNA was visualized by FISH using Cy3-labeled probe (red), and nuclei were stained with DAPI (blue). Bars, 50 μm in all panels.

the labeling was in large irregular patches corresponding to the capsid aggregates shown in Fig. 2, although widely dispersed individual capsids were also evident. A similar pattern was seen in KΔUL36-infected cells, although the labeled patches were generally smaller than in FRΔUL37-infected cells. However, in ARΔUL36-infected cells, all cytoplasmic labeling was in uniformly distributed, discrete spots. That these patterns of cytoplasmic DNA labeling accurately reflected the distribution of cytoplasmic capsids was confirmed by immunofluorescent labeling using an antibody against the major capsid protein (see Fig. S3 in the supplemental material). The failure of KΔUL36 and ARΔUL36 to "infect" naïve nuclei within syncytia despite the evident ability of their capsids to spread throughout the cytoplasm suggests that the defect is not a result of reduced capsid mobility, while the divergent behaviors of the ΔUL36 and ΔUL37 mutants imply different roles for these two inner tegument proteins in capsid transport and DNA release during virus entry.

Role of microtubules in the spread of infection. To examine the role of microtubules in the spread of virus, cells were treated with nocodazole to depolymerize the microtubule network. Nocodazole was added 3 h after infection, and cells were incubated at 37°C for a further 21 h before being fixed and processed for FISH as before. Disruption of the microtubule network was confirmed by immunofluorescence (Fig. 6).

Nocodazole treatment had no obvious effect on the overall distribution of cytoplasmic capsids with the patterns of spread and aggregation in wild-type and mutant virus-infected syncytia resembling those seen in Fig. 4 and 5. Furthermore, nocodazole treatment of WT HSV-1-infected syncytia did not prevent the spread of infection but reduced its extent, with approximately half the number of labeled nuclei observed in nocodazole-treated syncytia (Fig. 6 and Table 3). This agrees with previous studies on unfused cells, which showed that disruption of microtubules delayed but did not prevent infection (49). A similar result was obtained with FRΔUL37, with nocodazole inhibiting but not abolishing spread within syncytia (Fig. 6 and Table 3). Unsurprisingly, nocodazole treatment had no effect on ARΔUL36 and KΔUL36 infections, which remained confined to individual nuclei (not shown). The disruption of the microtubule network did have any obvious effect on the gross distribution of capsids in infected syncytia, suggesting that extensive movement through the cytoplasm could occur by alternative mechanisms.

Incorporation of pUL36 and pUL37 into L-particles. pUL36 and pUL37 are components of virions and L-particles, and it has been shown for PrV that neither protein is required for L-particle assembly. To analyze tegument assembly in these virus mutants, particles released into infected-cell culture medium were collected and purified by Ficoll gradient sedimentation. All of the mutants gave similar sedimentation profiles with a broad light-scattering band in the position expected for L-particles and a complete absence of the prominent virion band found in WT HSV-1 (see Fig. S4 in the supplemental material). Gradient fractions were resolved by SDS-PAGE, and the distribution of virions and L-particles was determined using an antibody (AGV031) against the abundant tegument protein pUL49 (VP22; Fig. 7A). Interestingly, this appears to show that L-particles produced by the UL36 and UL37 mutants extended higher up the gradients than those of WT or K5ΔZ. The presence of pUL36 (Fig. 7B) and pUL37 (Fig. 7C) was determined by Western blotting with antibodies E12-E3

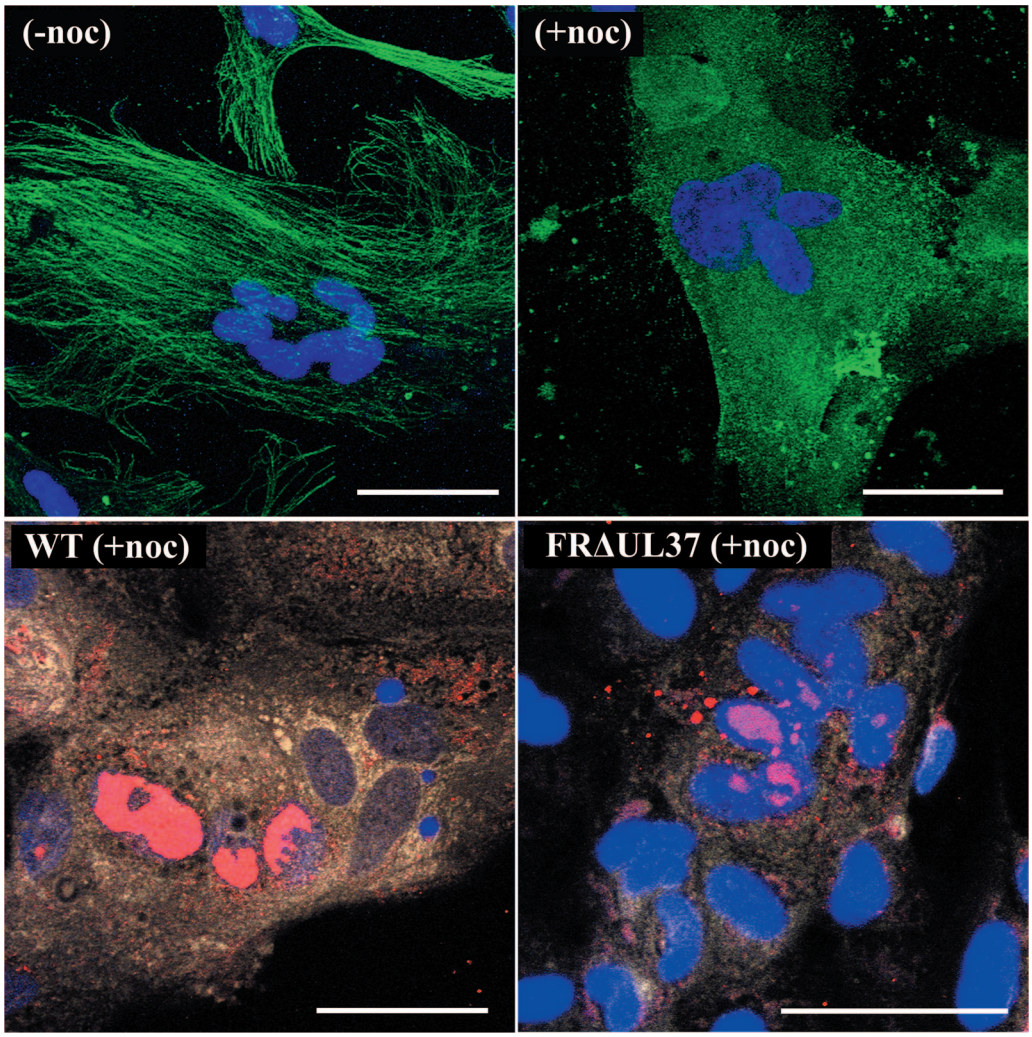

FIG. 6. Effect of nocodazole on spread of virus infection within syncytia. Replicate monolayers of $HFFF_2$ cells were infected with HSV-1 strain 17^+ (WT) or FRΔUL37 mutant virus and induced to form syncytia as described in the legend to Fig. 4. Nocodazole (0.5 μg/ml) was added at 3 h postinfection, and incubation was continued for a further 21 h. For immunofluorescence, cells were fixed (54), and microtubule proteins were identified with MAb DM1A and Alexa Fluor 488-conjugated goat anti-mouse secondary antibody (green). Viral DNA was visualized by FISH using Cy3-labeled probe (red). Nuclei were stained with DAPI (blue) The top panels show that the fibrillar microtubule network seen in uninfected syncytia [no nocodazole (−noc)] is disrupted by the addition of nocodazole (+noc). The bottom panels show the distribution of viral DNA in nocodazole-treated, WT HSV-1- and FRΔUL37-infected syncytia. Bars, 50 μm in all panels.

and M780, respectively. As expected, full-length pUL36 was detected in WT virions and L-particles and in K5ΔZ L-particles, but not in ARΔUL36 or KΔUL36 L-particles. However, the 43-kDa N-terminal fragment (Fig. 7B) of KΔUL36 had a sedimentation profile identical to that of pUL49, indicating that it had been incorporated into L-particles. Interestingly, only traces of pUL36 were detected in FRΔUL37 L-particles despite being present in normal amounts in the infected cells (Fig. 3A). Similarly, pUL37 was also present in WT HSV-1 and K5ΔZ particles and absent from FRΔUL37 L-particles (Fig. 7C). However, it was not detected in either ARΔUL36 or KΔUL36 L-particles, providing further evidence that pUL36 and pUL37 are dependent on one another for incorporation into tegument.

TABLE 3. Percentage of labeled nuclei in WT and mutant HSV-1-infected syncytia[a]

Virus	% of labeled nuclei	
	Not treated with nocodazole	Treated with nocodazole
WT HSV-1	98	46
FRΔUL37	76	32
ARΔUL36	10	13

[a] Only syncytia with at least one labeled nucleus were counted.

DISCUSSION

Previous studies to analyze the properties of HSV-1 and PrV mutants with deletions in the UL36 and UL37 genes have described the effects of the mutations on virion assembly and egress. Thus, UL36 and UL37 in HSV-1 (13, 14) and UL36 in

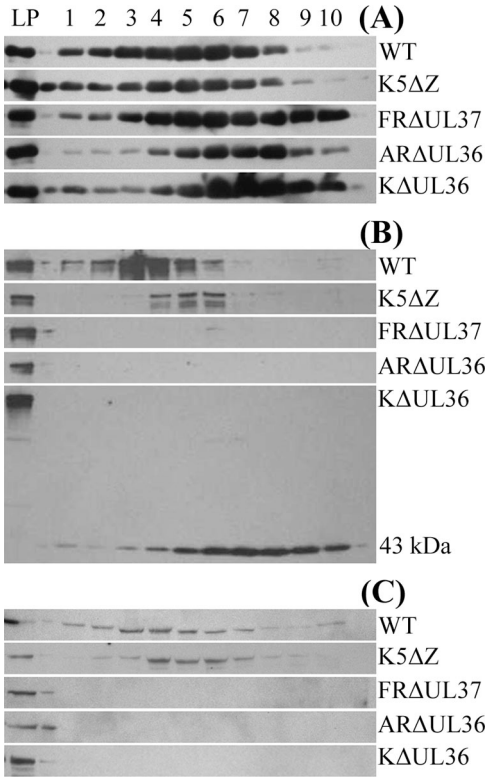

FIG. 7. Protein content of virions and L-particles. Extracellular virions and L-particles from cells infected with HSV-1 strain 17^+ (WT) and L-particles from cells infected with mutant virus K5ΔZ, FRΔUL37, KΔUL36, or ARΔUL36 were separated by Ficoll gradient sedimentation (see Fig. S4 in the supplemental material). The gradients were collected from the bottom in 10 equal fractions. A control sample of HSV-1 strain 17^+ L-particles (LP) was run on each gel. Gradient fractions were resolved by SDS-PAGE and analyzed by Western blotting. Blots were probed sequentially with E12-E3 (anti-pUL36) (B), M780 (anti-pUL37) (C), and AGV031 (anti-pUL49) (A). The position of the 43-kDa N-terminal fragment of pUL36 is indicated in panel B.

PrV (17, 30) are all essential for assembly of infectious virions, while studies in PrV showed that loss of UL37 reduced but did not abolish virus replication (26, 30). The results presented here using independently derived HSV-1 mutants support those of Desai et al. (13, 14) and confirm the phenotypic divergence between the HSV-1 and PrV UL37 mutants. A common feature of all the UL36 and UL37 deletion mutants described so far is that they produce large numbers of nonenveloped C-capsids when they infect noncomplementing cells. However, there are differing accounts of their effects on the nuclear and cytoplasmic distributions of these capsids. In UL37-minus mutants of both HSV-1 and PrV, the C-capsids form large aggregates in the cytoplasm (13, 26) (Fig. 2 and 5). Desai et al. (13) reported that their HSV-1 mutant, KΔUL37, also accumulated large numbers of capsids around the inner surface of the nuclear membrane, which they interpreted as indicating a block on nuclear exit. We did not see intranuclear accumulations with our independently derived HSV-1 mutant, FRΔUL37, although the total number of nuclear capsids was higher than found with WT HSV-1 or either UL36 mutant (Table 2). Furthermore, the ratio of A-, B-, and C-capsids in the nuclei suggested no specific accumulation of C-capsids. To quantify the effect of their mutation on capsid exit from the nucleus, Desai et al. (13) carried out gradient analysis of lysates prepared from nuclear and cytoplasmic fractions of KΔUL37-infected cells which showed that 75% of the DNA-containing capsids were associated with the nuclear fraction. This contrasted with data from our electron micrographs, which showed that the majority (72%) of the DNA-containing capsids were in the cytoplasm (Table 2). In an attempt to resolve this apparent contradiction, we repeated the separation of FRΔUL37-infected cells into nuclear and cytoplasmic fractions and analyzed their capsid content by electron microscopy. The electron microscopy images revealed that most C-capsids were indeed present in the nuclear pellet but were located outside nuclei. This suggests that the preferential association of C-capsids in the nuclear fraction is misleading and results from the large cytoplasmic capsid aggregates, which are a feature of the UL37 deletion mutants, copelleting with the nuclei. Inhibition of nuclear exit has also been reported for a UL37 mutant of PrV (30), although studies on a second PrV mutant (17, 26) produced no evidence of retention of capsids in the nucleus. The reasons for the differing behaviors of these mutations are unknown, but our studies and those of Klupp et al. (26) suggest that the major effect of deleting UL37 is to block secondary envelopment in the cytoplasm and that any role of pUL37 in nuclear exit is minor.

Differing behaviors have also been described for the UL36 mutants. Luxton et al. (30) reported that deletion of UL36 from PrV caused a dramatic reduction in capsid egress from nuclei. They suggested that the absence of such an effect in the HSV-1 mutant KΔUL36 could be due to the incomplete nature of its deletion. However, as shown here, removal of the entire UL36 ORF did not prevent efficient egress of capsids from the nucleus (Fig. 2 and 5; Table 2), nor was this effect observed with a different UL36 mutant of PrV (17). This phenotype therefore is not typical of other UL36 mutants. Another difference in the behavior of UL36 mutants is in their cytoplasmic distributions. Thus, KΔUL36 showed a tendency for capsids to accumulate in cytoplasmic clusters (14) in contrast to the PrV mutant, PrV-ΔUL36F, where capsids were dispersed evenly throughout the cytoplasm (17). However, the results described here for KΔUL36 and our independent HSV-1 mutant, ARΔUL36, show that this apparent difference does not reflect any biological distinction between HSV-1 and PrV but is most likely a consequence of the incomplete deletion in KΔUL36. Western blotting (Fig. 3) confirmed that the 43-kDa N-terminal truncation product of UL36 copurified with cytoplasmic KΔUL36 capsids, although they did not contain either pUL37 or pUL48. Therefore, it appears that this fragment is sufficient to cause their aggregation. The "stickiness" of UL36 has previously been suggested to account for the formation of large capsid aggregates by the UL37-minus mutants (17). Interestingly, the association of the 43-kDa fragment with capsids implies that capsid binding sequences map in this N-terminal region. Since a binding site for the minor capsid protein, pUL25, has recently been mapped to the C-terminal 62 residues of pUL36 (8), it appears that both N- and C-terminal regions of pUL36 interact with capsids.

Perhaps surprisingly in view of their close association with capsids, both pUL36 and pUL37 are found in L-particles, which lack capsids and consist solely of tegument and enve-

lope. It is likely that this reflects the probable function of these proteins as an interface between the capsid and outer tegument and that interaction with one or more of the outer tegument proteins accounts for their presence in L-particles. Indeed, L-particles from cells infected with a PrV, UL48-minus mutant did not contain either pUL36 or pUL37 (17). In view of this, it is interesting that pUL36 and pUL37 were dependent on one another for incorporation into L-particles (Fig. 7), suggesting that they enter L-particles as a complex. If these two proteins must form a complex before interacting with the outer tegument proteins, it would explain why tegument-like material is not detected around pUL36- or pUL37-minus cytoplasmic capsids (Fig. 2) (26). The occurrence of the 43-kDa N-terminal fragment of pUL36 in KΔUL36 L-particles is intriguing. This fragment does not include the region homologous to the pUL37 binding site in PrV (17), although it does overlap with a pUL48 interaction domain in HSV-1 (37). Its presence demonstrates that, unlike the full-length protein, this region of pUL36 can be incorporated into L-particles in the absence of pUL37.

Although the involvement of UL36 and UL37 in virus egress has been well documented, their role in virus entry is less easy to analyze. Studies with an HSV-1 temperature-sensitive mutant of UL36 (tsB7), which showed that capsids migrated to the vicinity of the nuclear pores but failed to release their DNA into the nucleus, provided the first indication that pUL36 functioned during the initial stages of infection (3). This is supported by recent work which showed that protease inhibitors prevented infection (10, 24) and linked their action to inhibition of cleavage of pUL36 on incoming capsids (24). Because UL36 deletion mutants do not form virions, they have not previously been used to study the role of pUL36 in entry. To circumvent this problem, we examined the behavior of the UL36 deletion mutants in artificially induced syncytia, since in the absence of plasma membranes separating neighboring cells, the virus capsids leaving an infected nucleus can gain direct access to uninfected nuclei without needing to undergo envelopment. Under these conditions, the environment of the capsids present in the cytoplasm of these syncytia was broadly equivalent to that of capsids from infecting virions that had undergone a normal fusion event. The failure of UL36 deletion mutants KΔUL36 and ARΔUL36 to infect new nuclei within syncytia despite having ready access to them confirms that pUL36 is involved in the initiation of infection and further strongly suggests that it must be present on the capsids. Therefore, the inhibition of infection seen with tsB7 or in the presence of protease inhibitors is not due to any failure to remove pUL36 from particles but reflects a positive requirement for pUL36 to ensure correct capsid transport and/or DNA release.

As with UL36, UL37 deletion mutants of HSV-1 fail to produce virions, and although UL37 mutants of PrV are viable, they are severely disabled, and it has not been possible to determine whether the small number of virions they produce have reduced specific infectivity (26, 30). Since no temperature-sensitive mutants in UL37 are available, essentially nothing was known of the role of this protein in virus entry. The observation that cytoplasmic capsids produced by FRΔUL37 were able to infect new nuclei clearly showed that pUL37 does not play an essential role in the initiation of infection and that its primary function is in the virion envelopment/release pathway, where it appears to act together with pUL36 as a template for assembly of outer tegument proteins.

The spread of infection within a syncytium will depend on the ability of the mutant virus particles to reach nuclear pores, to interact appropriately with them, and to release the virus genome into the nucleus. The retention of pUL36 and pUL37 on capsids during transport to the nucleus (29) would allow them to function at any or all of these stages. There is considerable evidence both from studies using an in vitro microtubule model (57) and from fluorescence microscopy of live cells (30) that the inner tegument proteins are important for capsid motility. In particular, studies of cells infected with PrV mutants showed that during virus egress pUL36 was absolutely required for processive capsid transport along microtubules, while pUL37 increased its efficiency (30). Furthermore, it was known that intact microtubules were needed to direct incoming capsids to the nuclear membrane (49), raising the possibility that failure of capsids to reach the nuclear pore could explain the block on infection by the UL36 deletion mutants. However, disrupting microtubules with nocodazole did not completely block HSV-1 infection of individual cells (49) and although the rate of spread was decreased, both WT HSV-1 and FRΔUL37 were able to infect naïve nuclei in nocodazole-treated syncytia. In addition, the widespread distribution of ARΔUL36 and KΔUL36 capsids throughout infected syncytia suggests that the uninfected nuclei were not physically inaccessible to them. Therefore, it is highly unlikely that the restriction of infection seen with the UL36 mutants is due solely to inefficient transport, and an additional role in nuclear pore recognition and/or DNA release seems probable.

In conclusion, we have shown that two inner tegument proteins that remain on capsids during the initial stages of infection have differing roles. One, pUL37, is dispensable during the initial stages of virus infection, while the second, pUL36, plays an essential, but as yet undefined, role in DNA release from the capsid and entry into the nucleus. The syncytial infection model should allow further investigation of the role of UL36 in the initial stages of infection.

ACKNOWLEDGMENTS

The HSV-1 bacterial artificial chromosome, pBAC SR27, was provided by C. Cunningham and A. J. Davison. Antibodies M780 and AGV031 were provided by F. Jenkins, (University of Pittsburgh) and G. Elliott (Imperial College), respectively. We thank M. McElwee for excellent technical support and V. Preston and D. McGeoch for critically reading the manuscript.

REFERENCES

1. **Abaitua, F., and P. O'Hare.** 2008. Identification of a highly conserved functional nuclear localization signal within the N-terminal region of herpes simplex virus type 1 VP1-2 tegument protein. J. Virol. **82:**5234–5244.
2. **Baines, J. D., and B. Roizman.** 1991. The open reading frames U_L3, U_L4, U_L10, and U_L16 are dispensable for the replication of herpes simplex virus 1 in cell culture. J. Virol. **65:**938–944.
3. **Batterson, W., D. Furlong, and B. Roizman.** 1983. Molecular genetics of herpes simplex virus. VIII. Further characterization of a temperature-sensitive mutant defective in release of viral DNA and in other stages of the viral reproductive cycle. J. Virol. **45:**397–407.
4. **Brack, A. R., J. M. Dijkstra, H. Granzow, B. G. Klupp, and T. C. Mettenleiter.** 1999. Inhibition of virion maturation by simultaneous deletion of glycoproteins E, I, and M of pseudorabies virus. J. Virol. **73:**5364–5372.
5. **Bucks, M. A., K. J. O'Regan, M. A. Murphy, J. W. Wills, and R. J. Courtney.** 2007. Herpes simplex virus type 1 tegument proteins VP1/2 and UL37 are associated with intranuclear capsids. Virology **361:**316–324.
6. **Chen, D. H., H. Jiang, M. Lee, F. Y. Liu, and Z. H. Zhou.** 1999. Three-

dimensional visualization of tegument/capsid interactions in the intact human cytomegalovirus. Virology **260:**10–16.
7. **Clarke, R. W., N. Monnier, H. T. Li, D. J. Zhou, H. Browne, and D. Klenerman.** 2007. Two-color fluorescence analysis of individual virions determines the distribution of the copy number of proteins in herpes simplex virus particles. Biophys. J. **93:**1329–1337.
8. **Coller, K. E., J. I.-H. Lee, A. Ueda, and G. A. Smith.** 2007. The capsid and tegument of the alphaherpesviruses are linked by an interaction between the UL25 and VP1/2 proteins. J. Virol. **81:**11790–11797.
9. **Cunningham, C., and A. J. Davison.** 1993. A cosmid-based system for constructing mutants of herpes simplex virus type 1. Virology **197:**116–124.
10. **Delboy, M. G., D. G. Roller, and A. V. Nicola.** 2008. Cellular proteasome activity facilitates herpes simplex virus entry at a postpenetration step. J. Virol. **82:**3381–3390.
11. **del Rio, T., T. H. Ch'ng, E. A. Flood, S. P. Gross, and L. W. Enquist.** 2005. Heterogeneity of a fluorescent tegument component in single pseudorabies virus virions and enveloped axonal assemblies. J. Virol. **79:**3903–3919.
12. **Desai, P., N. A. Deluca, J. C. Glorioso, and S. Person.** 1993. Mutations in herpes simplex virus type 1 genes encoding VP5 and VP23 abrogate capsid formation and cleavage of replicated DNA. J. Virol. **67:**1357–1364.
13. **Desai, P., G. L. Sexton, J. M. McCaffery, and S. Person.** 2001. A null mutation in the gene encoding the herpes simplex virus type 1 UL37 polypeptide abrogates virus maturation. J. Virol. **75:**10259–10271.
14. **Desai, P. J.** 2000. A null mutation in the UL36 gene of herpes simplex virus type 1 results in accumulation of unenveloped DNA-filled capsids in the cytoplasm of infected cells. J. Virol. **74:**11608–11618.
15. **Elliott, G., D. O'Reilly, and P. O'Hare.** 1996. Phosphorylation of the herpes simplex virus type-I tegument protein VP22. Virology **226:**140–145.
16. **Everett, R. D., J. Murray, A. Orr, and C. M. Preston.** 2007. Herpes simplex virus type 1 genomes are associated with ND10 nuclear substructures in quiescently infected human fibroblasts. J. Virol. **81:**10991–11004.
17. **Fuchs, W., B. G. Klupp, H. Granzow, and T. C. Mettenleiter.** 2004. Essential function of the pseudorabies virus UL36 gene product is independent of its interaction with the UL37 protein. J. Virol. **78:**11879–11889.
18. **Fuchs, W., B. G. Klupp, H. Granzow, N. Osterrieder, and T. C. Mettenleiter.** 2002. The interacting UL31 and UL34 gene products of pseudorabies virus are involved in egress from the host-cell nucleus and represent components of primary enveloped but not mature virions. J. Virol. **76:**364–378.
19. **Gibson, W., and B. Roizman.** 1972. Proteins specified by herpes simplex virus. VIII. Characterization and composition of multiple capsid forms of subtypes 1 and 2. J. Virol. **10:**1044–1052.
20. **Granzow, H., B. G. Klupp, and T. C. Mettenleiter.** 2005. Entry of pseudorabies virus: an immunogold-labeling study. J. Virol. **79:**3200–3205.
21. **Granzow, H., B. G. Klupp, and T. C. Mettenleiter.** 2004. The pseudorabies virus US3 protein is a component of primary and of mature virions. J. Virol. **78:**1314–1323.
22. **Grunewald, K., P. Desai, D. C. Winkler, J. B. Heymann, D. M. Belnap, W. Baumeister, and A. C. Steven.** 2003. Three-dimensional structure of herpes simplex virus from cryo-electron tomography. Science **302:**1396–1398.
23. **Homa, F. L., and J. C. Brown.** 1997. Capsid assembly and DNA packaging in herpes simplex virus. Rev. Med. Virol. **7:**107–122.
24. **Jovasevic, V., L. Liang, and B. Roizman.** 2008. Proteolytic cleavage of VP1-2 is required for release of herpes simplex virus 1 DNA into the nucleus. J. Virol. **82:**3311–3319.
25. **Klupp, B. G., W. Fuchs, H. Granzow, R. Nixdorf, and T. C. Mettenleiter.** 2002. Pseudorabies virus UL36 tegument protein physically interacts with the UL37 protein. J. Virol. **76:**3065–3071.
26. **Klupp, B. G., H. Granzow, E. Mundt, and T. C. Mettenleiter.** 2001. Pseudorabies virus UL37 gene product is involved in secondary envelopment. J. Virol. **75:**8927–8936.
27. **Lamberti, C., and S. K. Weller.** 1998. The herpes simplex virus type 1 cleavage/packaging protein, UL32, is involved in efficient localization of capsids to replication compartments. J. Virol. **72:**2463–2473.
28. **Lewis, L., and G. Albrechtbuehler.** 1987. Distribution of multiple centrospheres determines migration of BHK syncytia. Cell Motil. Cytoskelet. **7:**282–290.
29. **Luxton, G. W. G., S. Haverlock, K. E. Coller, S. E. Antinone, A. Pincetic, and G. A. Smith.** 2005. Targeting of herpesvirus capsid transport in axons is coupled to association with specific sets of tegument proteins. Proc. Natl. Acad. Sci. USA **102:**5832–5837.
30. **Luxton, G. W. G., J. I. H. Lee, S. Haverlock-Moyns, J. M. Schober, and G. A. Smith.** 2006. The pseudorabies virus VP1/2 tegument protein is required for intracellular capsid transport. J. Virol. **80:**201–209.
31. **McClelland, D. A., J. D. Aitken, D. Bhella, D. McNab, J. Mitchell, S. M. Kelly, N. C. Price, and F. J. Rixon.** 2002. pH reduction as a trigger for dissociation of herpes simplex virus type 1 scaffolds. J. Virol. **76:**7407–7417.
32. **McGeoch, D. J., M. A. Dalrymple, A. J. Davison, A. Dolan, M. C. Frame, D. McNab, L. J. Perry, J. E. Scott, and P. Taylor.** 1988. The complete DNA sequence of the long unique region in the genome of herpes simplex virus type 1. J. Gen. Virol. **69:**1531–1574.
33. **McLauchlan, J.** 1997. The abundance of the herpes simplex virus type 1 UL37 tegument protein in virus particles is closely controlled. J. Gen. Virol. **78:**189–194.
34. **McLauchlan, J., K. Liefkens, and N. D. Stow.** 1994. The herpes simplex virus type 1 UL37 gene-product is a component of virus particles. J. Gen. Virol. **75:**2047–2052.
35. **McLauchlan, J., and F. J. Rixon.** 1992. Characterization of enveloped tegument structures (L-particles) produced by alphaherpesviruses: integrity of the tegument does not depend on the presence of capsid or envelope. J. Gen. Virol. **73:**269–276.
36. **Mettenleiter, T. C.** 2002. Herpesvirus assembly and egress. J. Virol. **76:**1537–1547.
37. **Mijatov, B., A. L. Cunningham, and R. J. Diefenbach.** 2007. Residues F593 and E596 of HSV-1 tegument protein pUL36 (VP1/2) mediate binding of tegument protein pUL37. Virology **368:**26–31.
38. **Naldinho-Souto, R., H. Browne, and T. Minson.** 2006. Herpes simplex virus tegument protein VP16 is a component of primary enveloped virions. J. Virol. **80:**2582–2584.
39. **Nicholson, P., C. Addison, A. M. Cross, J. Kennard, V. G. Preston, and F. J. Rixon.** 1994. Localization of the herpes simplex virus type 1 major capsid protein VP5 to the cell nucleus requires the abundant scaffolding protein VP22a. J. Gen. Virol. **75:**1091–1099.
40. **Reynolds, A. E., B. J. Ryckman, J. D. Baines, Y. P. Zhou, L. Liang, and R. J. Roller.** 2001. U_L31 and U_L34 proteins of herpes simplex virus type 1 form a complex that accumulates at the nuclear rim and is required for envelopment of nucleocapsids. J. Virol. **75:**8803–8817.
41. **Reynolds, A. E., E. G. Wills, R. J. Roller, B. J. Ryckman, and J. D. Baines.** 2002. Ultrastructural localization of the herpes simplex virus type 1 UL31, UL34, and US3 proteins suggests specific roles in primary envelopment and egress of nucleocapsids. J. Virol. **76:**8939–8952.
42. **Rixon, F. J.** 1993. Structure and assembly of herpesviruses. Semin. Virol. **4:**135–144.
43. **Rixon, F. J., C. Addison, and J. McLauchlan.** 1992. Assembly of enveloped tegument structures (L-particles) can occur independently of virion maturation in herpes-simplex virus type 1-infected cells. J. Gen. Virol. **73:**277–284.
44. **Roller, R. J., Y. P. Zhou, R. Schnetzer, J. Ferguson, and D. DeSalvo.** 2000. Herpes simplex virus type 1 U_L34 gene product is required for viral envelopment. J. Virol. **74:**117–129.
45. **Schrag, J. D., B. V. V. Prasad, F. J. Rixon, and W. Chiu.** 1989. Three-dimensional structure of the HSV-1 nucleocapsid. Cell **56:**651–660.
46. **Shelton, L. S., A. G. Albright, W. T. Ruyechan, and F. J. Jenkins.** 1994. Retention of the herpes simplex virus type 1 (HSV-1) UL37 protein on single-stranded DNA columns requires the HSV-1 ICP8 protein. J. Virol. **68:**521–525.
47. **Siegel, R. W., R. Jain, and A. Bradbury.** 2001. Using an in vivo phagemid system to identify non-compatible loxP sequences. FEBS Lett. **499:**147–153.
48. **Smith, G. A., and L. W. Enquist.** 2000. A self-recombining bacterial artificial chromosome and its application for analysis of herpesvirus pathogenesis. Proc. Natl. Acad. Sci. USA **97:**4873–4878.
49. **Sodeik, B., M. W. Ebersold, and A. Helenius.** 1997. Microtubule-mediated transport of incoming herpes simplex virus 1 capsids to the nucleus. J. Cell Biol. **136:**1007–1021.
50. **Steven, A. C., and P. G. Spear.** 1997. Herpesvirus capsid assembly and envelopment, p. 312–351. *In* W. Chiu, R. M. Burnett, and R. Garcea (ed.), Structural biology of viruses. Oxford University Press, Oxford, United Kingdom.
51. **Stow, N. D., and N. M. Wilkie.** 1976. An improved technique for obtaining enhanced infectivity with herpes simplex virus type 1 DNA. J. Gen. Virol. **33:**447–458.
52. **Szilagyi, J. F., and C. Cunningham.** 1991. Identification and characterization of a novel non-infectious herpes simplex virus-related particle. J. Gen. Virol. **72:**661–668.
53. **Trus, B. L., W. W. Newcomb, N. Q. Cheng, G. Cardone, L. Marekov, F. L. Horna, J. C. Brown, and A. C. Steven.** 2007. Allosteric signaling and a nuclear exit strategy: binding of UL25/UL17 heterodimers to DNA-filled HSV-1 capsids. Mol. Cell **26:**479–489.
54. **Vielkind, U., and S. H. Swierenga.** 1989. A simple fixation procedure for immunofluorescent detection of different cytoskeletal components within the same cell. Histochemistry **91:**81–88.
55. **Vittone, V., E. Diefenbach, D. Triffett, M. W. Douglas, A. L. Cunningham, and R. J. Diefenbach.** 2005. Determination of interactions between tegument proteins of herpes simplex virus type 1. J. Virol. **79:**9566–9571.
56. **Wagenaar, F., J. M. A. Pol, B. Peeters, A. L. J. Gielkens, N. Dewind, and T. G. Kimman.** 1995. The US3-encoded protein kinase from pseudorabies virus affects egress of virions from the nucleus. J. Gen. Virol. **76:**1851–1859.
57. **Wolfstein, A., C. H. Nagel, K. Radtke, K. Dohner, V. J. Allan, and B. Sodeik.** 2006. The inner tegument promotes herpes simplex virus capsid motility along microtubules in vitro. Traffic **7:**227–237.
58. **Zhou, Z. H., D. H. Chen, J. Jakana, F. J. Rixon, and W. Chiu.** 1999. Visualization of tegument-capsid interactions and DNA in intact herpes simplex virus type 1 virions. J. Virol. **73:**3210–3218.
59. **Zhou, Z. H., M. Dougherty, J. Jakana, J. He, F. J. Rixon, and W. Chiu.** 2000. Seeing the herpesvirus capsid at 8.5 Å. Science **288:**877–880.

APPENDIX A

Supplementary data to Table 4.2

Micrographs 36-37033 – 42 (07-14) ARΔUL36

Micrographs 36-37043 – 52 (07-15) KΔUL36

Micrographs 36-37053 – 62 (07-16) FRΔUL37

Micrographs 36-37063 – 72 (07-17) WT HSV-1

36-37033

	Nuclear	perinuclear	Aggregate	Free	Extracellular	total
A	20	0	0	5	0	25
B	38	0	0	0	0	38
C	32	1	0	29	0	62
total	90	1	0	34	0	125

36-37034

	Nuclear	perinuclear	Aggregate	Free	Extracellular	total
A	9	0	0	0	0	9
B	22	0	0	0	0	22
C	4	0	0	41	0	45
total	35	0	0	41	0	76

36-37035

	Nuclear	perinuclear	Aggregate	Free	Extracellular	total
A	23	0	0	0	0	23
B	97	0	0	0	0	97
C	7	0	0	28	0	35
total	127	0	0	28	0	155

36-37036

	Nuclear	perinuclear	Aggregate	Free	Extracellular	total
A	9	0	0	1	0	10
B	24	0	0	8	0	32
C	7	0	0	26	0	33
total	40	0	0	35	0	75

36-3707 No nuclei in field

	Nuclear	perinuclear	Aggregate	Free	Extracellular	total
A	0	0	0	0	0	0
B	0	0	0	4	0	4
C	0	0	0	33	0	33
total	0	0	0	37	0	37

36-37038

	Nuclear	perinuclear	Aggregate	Free	Extracellular	total
A	25	0	0	1	0	26
B	113	0	0	3	0	116
C	31	0	0	11	0	42
total	169	0	0	15	0	184

36-37039

	Nuclear	perinuclear	Aggregate	Free	Extracellular	total
A	1	0	0	5	0	6
B	64	0	0	8	0	72
C	4	0	0	42	0	46
total	69	0	0	55	0	124

36-37040

	Nuclear	perinuclear	Aggregate	Free	Extracellular	total
A	52	0	0	0	0	52
B	131	0	0	3	0	134
C	28	0	0	17	0	45
total	211	0	0	20	0	231

36-37041 No Nuclei

	Nuclear	perinuclear	Aggregate	Free	Extracellular	total
A	0	0	0	1	0	1
B	0	0	0	29	0	29
C	0	0	0	28	0	28
total	0	0	0	58	0	58

36-3742

	Nuclear	perinuclear	Aggregate	Free	Extracellular	total
A	22	0	0	0	0	22
B	55	0	0	13	0	68
C	9	0	0	21	0	30
total	86	0	0	34	0	120

Summary 07-14 micrographs

	Nuclear	perinuclear	Aggregate	Free	Extracellular	total
A	161	0	0	13	0	174
B	544	0	0	68	0	612
C	122	1	0	276	0	399
total	827	1	0	357	0	1185

36-37043

	Nuclear	perinuclear	Aggregate	Free	Extracellular	total
A	10	0	0	0	0	10
B	63	0	0	0	0	63
C	7	1	4	11	0	23
total	80	1	4	11	0	96

36-37044 No Nuclei

	Nuclear	perinuclear	Aggregate	Free	Extracellular	total
A	0	0	0	0	0	0
B	0	0	0	0	0	0
C	0	0	67	31	0	98
total	0	0	67	31	0	98

36-37045

	Nuclear	perinuclear	Aggregate	Free	Extracellular	total
A	11	0	0	0	0	11
B	20	0	0	1	0	21
C	12	3	0	4	0	19
total	43	3	0	5	0	51

36-37046

	Nuclear	perinuclear	Aggregate	Free	Extracellular	total
A	15	0	0	0	0	15
B	96	0	1	0	0	97
C	5	2	7	17	0	31
total	116	2	8	17	0	143

36-37047

	Nuclear	perinuclear	Aggregate	Free	Extracellular	total
A	1	0	0	3	0	4
B	0	0	0	0	0	0
C	9	1	2	10	0	22
total	10	1	2	13	0	26

36-37048 enveloped C's in cytoplasm

	Nuclear	perinuclear	Aggregate	Free	Extracellular	total
A	10	0	0	0	0	10
B	113	0	0	1	0	114
C	7	0	4	19	0	30
total	130	0	4	20	0	154

36-37049

	Nuclear	perinuclear	Aggregate	Free	Extracellular	total
A	19	0	0	2	0	21
B	102	0	0	0	0	102
C	8	0	0	8	0	16
total	129	0	0	10	0	139

36-37050

	Nuclear	perinuclear	Aggregate	Free	Extracellular	total
A	9	0	1	0	0	10
B	71	0	1	1	0	73
C	2	2	19	9	0	32
total	82	2	21	10	0	115

36-37051 Some enveloped C's in cytoplasm, No nuclei

	Nuclear	perinuclear	Aggregate	Free	Extracellular	total
A	0	0	0	9	0	9
B	0	0	0	1	0	1
C	0	0	66	21	0	87
total	0	0	66	31	0	97

36-3752

	Nuclear	perinuclear	Aggregate	Free	Extracellular	total
A	32	0	0	3	0	35
B	121	0	0	6	0	127
C	7	5	155	19	0	186
total	160	5	155	28	0	348

Summary 07-15 micrographs

	Nuclear	perinuclear	Aggregate	Free	Extracellular	total
A	107	0	1	17	0	125
B	586	0	2	10	0	598
C	57	14	324	149	0	544
total	750	14	327	176	0	1267

36-37053

	Nuclear	perinuclear	Aggregate	Free	Extracellular	total
A	27	0	1	0	0	28
B	154	0	2	0	0	156
C	49	0	124	2	0	175
total	230	0	127	2	0	359

36-37054

	Nuclear	perinuclear	Aggregate	Free	Extracellular	total
A	0	0	0	0	0	0
B	3	0	0	0	0	3
C	2	0	84	5	0	91
total	5	0	84	5	0	94

36-37055

	Nuclear	perinuclear	Aggregate	Free	Extracellular	total
A	14	0	2	0	0	16
B	143	0	12	0	0	155
C	8	0	118	0	0	126
total	165	0	132	0	0	297

36-37056

	Nuclear	perinuclear	Aggregate	Free	Extracellular	total
A	33	0	0	0	0	33
B	305	0	1	0	0	306
C	14	0	40	12	0	66
total	352	0	41	12	0	405

36-37057

	Nuclear	perinuclear	Aggregate	Free	Extracellular	total
A	16	0	0	0	0	16
B	30	0	0	1	0	31
C	15	0	0	5	0	20
total	61	0	0	6	0	67

36-37058

	Nuclear	perinuclear	Aggregate	Free	Extracellular	total
A	36	0	0	2	0	38
B	184	0	0	2	0	186
C	13	0	0	7	0	20
total	233	0	0	11	0	244

36-37059

	Nuclear	perinuclear	Aggregate	Free	Extracellular	total
A	23	0	0	0	0	23
B	122	0	1	0	0	123
C	13	0	3	1	0	17
total	158	0	4	1	0	163

36-37060

	Nuclear	perinuclear	Aggregate	Free	Extracellular	total
A	17	0	0	0	0	17
B	34	0	0	0	0	34
C	19	0	3	0	0	22
total	70	0	3	0	0	73

36-37061

	Nuclear	perinuclear	Aggregate	Free	Extracellular	total
A	21	0	0	0	0	21
B	158	0	2	1	0	161
C	29	0	24	3	0	56
total	208	0	26	4	0	238

36-37062

	Nuclear	perinuclear	Aggregate	Free	Extracellular	total
A	40	0	0	0	0	40
B	247	0	3	0	0	250
C	15	0	29	4	0	48
total	302	0	32	4	0	338

Summary 07-16 micrographs

	Nuclear	perinuclear	Aggregate	Free	Extracellular	total
A	227	0	3	2	0	232
B	1380	0	21	4	0	1405
C	177	0	425	39	0	641
total	1784	0	449	45	0	2278

36-37063

	Nuclear	perinuclear	Aggregate	Free	Extracellular	total
A	0	0	0	0	0	0
B	0	0	0	0	2	2
C	0	0	0	7	59	66
total	0	0	0	7	61	68

36-37064

	Nuclear	perinuclear	Aggregate	Free	Extracellular	total
A	16	0	0	0	0	16
B	36	0	0	0	0	36
C	16	0	0	11	8	35
total	68	0	0	11	8	87

36-37065

	Nuclear	perinuclear	Aggregate	Free	Extracellular	total
A	20	0	0	0	0	20
B	28	0	0	0	0	28
C	5	0	0	5	15	25
total	53	0	0	5	15	73

36-37066

	Nuclear	perinuclear	Aggregate	Free	Extracellular	total
A	4	0	0	0	1	5
B	47	0	0	2	0	49
C	4	0	0	5	25	34
total	55	0	0	7	26	88

36-37067

	Nuclear	perinuclear	Aggregate	Free	Extracellular	total
A	26	0	0	0	0	26
B	45	0	0	0	0	45
C	16	0	0	1	10	27
total	87	0	0	1	10	98

36-37068

	Nuclear	perinuclear	Aggregate	Free	Extracellular	total
A	6	0	0	2	0	8
B	51	0	0	0	0	51
C	5	0	0	3	12	20
total	62	0	0	5	12	79

36-37069

	Nuclear	perinuclear	Aggregate	Free	Extracellular	total
A	0	0	0	0	0	0
B	0	0	0	0	0	0
C	1	0	0	4	2	7
total	1	0	0	4	2	7

36-37070

	Nuclear	perinuclear	Aggregate	Free	Extracellular	total
A	22	0	0	0	0	22
B	164	0	0	0	0	164
C	5	0	0	0	6	11
total	191	0	0	0	6	197

36-37071

	Nuclear	perinuclear	Aggregate	Free	Extracellular	total
A	0	0	0	0	0	0
B	11	0	0	0	0	11
C	0	0	0	4	31	35
total	11	0	0	4	31	46

36-37072

	Nuclear	perinuclear	Aggregate	Free	Extracellular	total
A	60	0	0	0	0	60
B	309	0	0	0	0	309
C	11	0	0	0	46	57
total	380	0	0	0	46	426

Summary 07-17 micrographs

	Nuclear	perinuclear	Aggregate	Free	Extracellular	total
A	154	0	0	2	1	157
B	691	0	0	2	2	695
C	63	0	0	40	214	317
total	908	0	0	44	217	1169